

Copyright is owned by the Author of the thesis. Permission is given for a copy to be downloaded by an individual for the purpose of research and private study only. The thesis may not be reproduced elsewhere without the permission of the Author.

A novel and environmentally friendly
method for preserving and depilating
sheepskin:
Comprehensive physical, biochemical and
molecular analyses

A thesis presented in partial fulfilment of the requirements
for the degree of

Doctor of Philosophy
in
Biochemistry

at Massey University, Manawatu, New Zealand.

Yi-Hsuan Tu

2021

Acknowledgements

First of all, sincere appreciation goes to my main supervisor Associate Professor Gill Norris for her utmost patience, guidance, time, and care she has graciously given. Her constant encouragement, support, and her belief in me has allowed me to carry on in difficult times. Without Gill, there would be no thesis. Thank you from the bottom of my heart, the best supervisor one can ever have, and my New Zealand Mum.

Secondly, thank you to all my past and present co-supervisors, Dr. Mark Patchett, Dr. Dragana Gagic, Associate Professor Jasna Rakonjac, and Dr. Meekyung Ahn, for all the invaluable advice, guidance, and patience with me throughout various parts of this project.

To Mr. Trevor Loo, your help and guidance with all laboratory equipment and for the collection of mass spectrometry data are greatly appreciated. To the team from LASRA, Geoff Holmes, Dr. Rafea Naffa, and Catherine Maidment, thank you for sharing your knowledge and experience of the leather industry, as well as providing technical support with leather sample processing. To Dinindu Senanayake from New Zealand eScience Infrastructure for all the computing technical support. To people in the X-lab, especially my lunch buddies - Fareeda, Tei, Brittany, Catherine, Sean, Shelley, Del, and Stuart, thank you for the friendship and encouragement. To my friends, Ethel, Eileen, Christine and many more I haven't mentioned, thank you for being there in various parts of this journey, short or long.

To my family, Mum, Dad, Rita, and Grandma, thank you for the unconditional love and support over the years. You are my constant when times are hard. To my New Zealand Mum and Dad, Gill and Robert Norris, a heartfelt thank you for taking me into your lovely home and looked after me just as I were your daughter. To Freddie and Dondon, thank you for being the silent support and the best writing buddies.

Lastly, all glory to God, the source of all knowledge, understanding, and wisdom, for His unfailing love and blessings throughout this research.

Abbreviations

ANCOM	Analysis of composition of microbes	PBS	Phosphate buffered saline
ANOVA	Analysis of variance	PCoA	Principal coordinate analysis
AQC	6-Aminoquinolyl-N-hydroxyseccinimidyl carbamate	PCR	Polymerase chain reaction
ASV	Amplicon sequence variant	PERMANOVA	Permutational multivariate analysis of variance
bp	Base pair	PG	Proteoglycan
CNBr	Cyanogen bromide	PSM	Peptide-spectrum match
DHLNL	Dihydroxylysine norleucine	QIIME2	Quantitative insights into microbial ecology
DNA	Deoxyribonucleic acid	rRNA	ribosomal ribonucleic acid
DTT	Dithiothreitol	SDS	Sodium dodecyl sulfate
ECM	Extracellular matrix	SEM	Scanning electron microscopy
FACIT	Fibril associated collagens with interrupted triple helices	TCA	Trichloroacetic acid
FDR	False discovery rate	TEM	Transmission electron microscopy
GAG	Glycosaminoglycan	TFA	Trifluoroacetic acid
HHL	Histidine hydroxylysine norleucine	TIC	Total ion current
HHMD	Histidine hydroxymerodesmosine	TSB	Tryptone soya broth
HLNL	Hydroxylysine norleucine	U.m.	Unclassified member
HPLC	High pressure liquid chromatography	µg	Microgram
IRS	Inner root sheath	µL	Microliter
ITS	Internal transcribed spacer		
kDa	Kilodalton		
LAB	Lactic acid bacteria		
LB	Luria broth		
LC-MS/MS	Liquid chromatography tandem mass spectrometry		
MeCN	Acetonitrile		
MeOH	Methanol		
mg	Milligram		
mL	Millilitre		
MS	Mass spectrometry		
MWt	Molecular weight		
OSP	Official sampling position		

Amino acid abbreviations

Amino acid	3-letter symbol	1-letter symbol
Alanine	Ala	A
Arginine	Arg	R
Asparagine	Asn	N
Aspartic acid	Asp	D
Cysteine	Cys	C
Glutamic acid	Glu	E
Glutamine	Gln	Q
Glycine	Gly	G
Histidine	His	H
Isoleucine	Ile	I
Leucine	Leu	L
Lysine	Lys	K
Methionine	Met	M
Phenylalanine	Phe	F
Proline	Pro	P
Serine	Ser	S
Threonine	Thr	T
Tryptophan	Trp	W
Tyrosine	Tyr	Y
Valine	Val	V
Hydroxylysine	Hyl	
Hydroxyproline	Hyp	
Norleucine	Nle	

Contents

Acknowledgements	i
Abbreviations	ii
List of Figures	ix
List of Tables	xiii
1 Introduction	1
1.1 Definition of the problem	2
1.2 Aims and objectives	3
1.3 Significance of this investigation	4
1.4 References	5
2 Literature review	9
2.1 Skin	10
2.2 Collagen	11
2.2.1 The collagen family and structure	11
2.2.2 Methods used in this study for the analysis of collagen	16
2.3 Collagen crosslinks	17
2.3.1 Collagen non-enzymatic crosslinks	17
2.3.2 Collagen enzymatic crosslinks	17
2.3.2.1 Immature collagen crosslinks	18
2.3.2.2 Mature collagen crosslinks found in skin	19
2.3.2.2.1 Pyrrolic crosslinks	20
2.3.2.2.2 Pyridinium crosslinks	20
2.3.2.2.3 Histidine-containing crosslinks	20
2.3.3 Methods used in this study to analyse collagen crosslinks	21
2.4 Glycosaminoglycans and proteoglycans	21
2.4.1 Proteoglycans	21
2.4.1.1 Basement membrane proteoglycans	22
2.4.1.2 Extracellular proteoglycans	22
2.4.1.2.1 Hyalectans	22
2.4.1.2.2 Small leucine-rich proteoglycans	23
2.4.2 Glycosaminoglycans	25
2.4.2.1 Chondroitin sulfate	25

2.4.2.2	Dermatan sulfate	28
2.4.2.3	Heparin and heparan sulfate	28
2.4.2.4	Keratan sulfate	28
2.4.2.5	Hyaluronic acid	29
2.4.3	Methods used in this study for the analysis of GAGs	29
2.5	Hair/wool	29
2.5.1	Hair follicle	30
2.5.2	Hair shaft	31
2.6	Overview of the conventional leather making process	31
2.6.1	Preservation	31
2.6.2	Depilation	31
2.6.3	Liming	32
2.6.4	Deliming and bating	32
2.6.5	Pickling	33
2.6.6	Degreasing	33
2.6.7	Tanning	33
2.6.8	Neutralising, dyeing and fat liquoring	34
2.6.9	Drying	34
2.7	Problems associated with conventional sulfide depilation	34
2.8	Other approaches to sulfide depilation	35
2.8.1	Plucking, shearing, and scalding	35
2.8.2	Cryogenic depilation	35
2.8.3	Chaotropic agents for depilation	35
2.8.4	Oxidative depilation	36
2.8.5	Organic sulfur compound depilation	36
2.8.6	Enzyme depilation	36
2.9	'Omics' methods used in this study	39
2.10	References	42
3	Physical analysis of sheepskin	61
3.1	Introduction	63
3.2	Materials and methods	65
3.2.1	Materials	65
3.2.2	Depilation trials using milk products and permeate solution	66
3.2.3	Scaled up trials using permeate	66
3.2.4	Scanning electron microscopy (SEM) evaluation of permeate-depilated sheepskin	68
3.2.5	Transmission electron microscopy (TEM) evaluation of the permeate-depilated sheepskin	68

3.2.6	Identification of the viable microorganisms in the milk media at the completion of depilation.	69
3.2.7	Tear strength analysis of depilated skins and the final leather product	70
3.2.8	Tensile strength analysis of depilated skins and final leather product	71
3.2.9	Leather shrinkage temperature measurements	72
3.3	Results and discussion	72
3.3.1	Sheepskin depilation using milk products and by-products. . .	72
3.3.2	Physical appearance of the permeate-depilated sheepskins. . .	74
3.3.3	Identification of microorganisms isolated from depilation trials with various milk products.	76
3.3.4	Tear and tensile strength analysis of permeate- depilated sheepskins	79
3.3.5	Leather shrinkage temperature	81
3.4	Conclusion	83
3.5	References	85
3.6	Supplementary information	90
4	Biochemical analysis of sheepskins	91
4.1	Introduction	93
4.2	Materials and Methods	96
4.2.1	Chemicals and materials	96
4.2.2	Preparation of skin samples and the permeate solution	97
4.2.3	Amino acid analysis of sheepskins	97
4.2.4	Collagen crosslink analysis of sheepskins	97
4.2.5	Glycosaminoglycan analysis of the sheepskins	98
4.2.6	Proteomic analysis of sheepskins	99
4.3	Results and Discussion	100
4.3.1	Amino acid composition of raw and permeate-depilated sheepskins	100
4.3.2	Collagen crosslink analysis of sheepskins	102
4.3.3	Glycosaminoglycan analysis of sheepskins	106
4.3.4	Proteomic analysis of sheepskins	107
4.4	References	118
4.5	Supplementary information - Methods	127
4.5.1	Amino acid analysis of sheepskin	127
4.5.2	Collagen crosslink analysis of sheepskin	129
4.5.3	Proteomic analysis of sheepskin	131

4.6	Supplementary information - Results	137
5	Microbial analysis of the depilation process	143
5.1	Introduction	145
5.2	Materials and Methods	148
5.2.1	Chemicals, materials, and kits	148
5.2.2	Metagenomic analysis of the microbial community throughout the permeate depilation of sheepskin.	149
5.2.2.1	Amplicon sequencing sample preparation	149
5.2.2.2	Bioinformatics and statistical analysis	149
5.2.3	Proteomic analysis of the permeate used to depilate sheepskin	151
5.2.4	Metabolomic analysis of the permeate used to depilate sheepskin	151
5.3	Results and discussion	152
5.3.1	The microbial diversity in permeate during sheepskin depilation	152
5.3.2	Relative abundance of microbial taxa during permeate depilation	154
5.4	References	164
5.5	Supplementary information - Methods	170
5.6	Supplementary information - Results	174
6	Final conclusions and future directions	189
6.1	Overall conclusions and future direction	190
6.2	References	192

List of Figures

Chapter 2

1	Diagram of the skin structure.	10
2	Schematic diagram of tropocollagen and an assembled collagen fibril.	16
3	Collagen crosslink chemical pathway.	19
4	Structure of the saccharide moieties of GAGs.	25
5	Diagram of the hair follicle structure.	30
6	Map of ribosomal DNA indicating variable regions as well as the primers used in this study.	41

Chapter 3

1	Image showing the instrument setup for the measurement of the tear and tensile strength of skin and leather samples.	71
2	Images of the sheepskin depilated with permeate and the final leather product.	74
3	SEM images of the sheepskin depilated with permeate and conventional sulfide method.	75
4	TEM images of a section of the corium of permeate-depilated sheepskins.	75
5	Comparison of tear and tensile strength of tanned leather and pre-tanned skins.	80
6	Representative stress-strain curves of sheepskin depilated using permeate and sulfide, and their respective final leather products.	82
7	Shrinkage temperature of leather made from sheepskin depilated using sulfide and permeate.	83

Chapter 3

S1	Examples of the different morphologies of microorganisms cultured from spent depilation liquid.	90
----	---	----

Chapter 4

1	Diagram of the skin structure.	93
---	--	----

LIST OF FIGURES

2	Total protein content in lyophilised sheepskins before and after permeate depilation.	101
3	Collagen crosslinks in raw sheepskins and sheepskins depilated using permeate.	104
4	Percentages of glycosaminoglycans in raw sheepskins and sheepskins depilated using permeate.	106
5	Volcano plot of the differentially abundant proteins found in sheepskins depilated using permeate and pickled sheepskins.	110
6	Schematic organisation of the collagens and proteoglycans in the ECM of skin.	112
7	Schematic longitudinal view of mammalian hair with key keratins and proteoglycans.	114

Chapter 4

S1	HPLC chromatogram of the separation of amino acid standards and hydrolysed permeate-depilated sheepskin.	128
S2	Diagram of the proteomic analysis workflow.	132
S3	4 - 15 % SDS-PAGE gels for sheepskin proteomic analysis.	142

Chapter 5

1	Alpha and beta diversity of bacteria from samples collected at different timepoints during permeate depilation of sheepskin.	154
2	Alpha and beta diversity of fungi from samples collected at different timepoints during permeate depilation of sheepskin.	155
3	Bar plot showing the distribution of microbial genera over the time course of permeate depilation of sheepskin.	158
4	Volcano plots of differentially expressed bacterial ASVs over the different timepoints of permeate depilation.	159

Chapter 5

S1	Average rarefaction curves obtained for each timepoint with the number of observed ASVs.	174
S2	Pielou's evenness index.	175
S3	Bar plot showing the microbial phyla distributions over the time course of permeate depilation.	176
S4	Bar plot showing the bacterial species distributions of permeate depilation.	177
S5	Bar plot showing the microbial genus distributions post permeate depilation at week 5, 8 and 14.	177

S6	ANCOM analysis of the differentially abundant 16S rRNA ASVs at the genus level.	178
S7	Volcano plots of differentially expressed fungal ASVs over the different timepoints of permeate depilation.	178

List of Tables

1	Collagen family characteristics and tissue distribution.	13
2	Collagen groups based on general structural similarities.	15
3	Repeating disaccharide units of glycosaminoglycans.	26
4	Enzymes used to depilate skin on a laboratory scale.	38
5	Examples of commercial depilation enzymes.	39

Chapter 3

1	Standard LASRA protocol for tanning sheepskins.	67
2	PCR primers used for the culturing of microorganisms at depilation.	70
3	Depilation trials with milk products and by-products.	73
4	Bacteria species identified in the sheepskin depilation trials using various milk products and by-products.	77
5	Fungal species identified in the sheepskin depilation trials using various milk products and by-products.	78
6	Comparison of tensile strength of tanned leather and pre-tanned skins.	80

Chapter 3

S1	PCR conditions.	90
----	-------------------------	----

Chapter 4

1	Components and concentrations of the protein extraction buffers.	100
2	Comparison of amino acid profile in ovine skin or collagen.	103
3	Top 50 abundant proteins identified in sheepskin depilated using permeate and pickled sheepskin.	108
4	Types of collagen identified in permeate-depilated with permeate and pickled sheepskin and their literature tissue distribution.	111
5	ECM proteins identified in sheepskin depilated with permeate and pickled sheepskin.	116

Chapter 4

S1	HPLC separation gradient for amino acid analysis	128
S2	Instrument configuration for collagen crosslink analysis	130
S3	Mass spectrometer source settings for collagen crosslink analysis	130

LIST OF TABLES

S4	Mass spectrometry settings for the detection of collagen crosslinks . . .	131
S5	Inclusion list for PRM analysis	131
S6	Solutions used for reduction, alkylation and proteolytic digestion . . .	134
S7	Mass spectrometer configuration used for proteomics analysis	135
S8	Parameter used for proteomic analysis	135
S9	Parameters used for proteomic data analysis	136
S10	Proteins identified in the proteomic analysis of sheepskin.	137

Chapter 5

1	Oligonucleotide primers used in this paper.	148
2	Bacteriocin peptides identified in the proteomic analysis of permeate upon completion of depilation.	162

Chapter 5

S1	PCR conditions.	170
S2	Mass spectrometer configuration used for proteomic analysis	170
S3	Parameter used for proteomic analysis	171
S4	Parameters used for proteomic data analysis	171
S5	List of bacterial and fungal species from the NCBI protein database. .	172
S6	Mass spectrometry instrument configuration for metabolomic analysis	173
S7	Mass spectrometer settings for metabolomic analysis	173
S8	Quality-filtering of the 16S rRNA sequencing samples.	179
S9	Quality-filtering of the ITS sequencing samples.	180
S10	Shannon's diversity index statistical tests of the 16S metagenome. . .	181
S11	Shannon's diversity index statistical tests of the ITS metagenome. . .	181
S12	'Others' genera list from the 16S rRNA genus level taxa bar plot. . .	182
S13	Bacteria proteins identified in the permeate solution after depilation.	183
S14	Bacterial proteins identified in the permeate solution after depilation.	184
S15	Fungi proteins identified in the permeate solution after depilation. . .	187
S16	List of potential antimicrobial secondary metabolites identified in the metabolomics analysis of permeate.	188

1 | Introduction

1.1 Definition of the problem

Leather products are manufactured from animal skins that have been subjected to various chemical procedures to form a product that has high tensile strength, resists tearing, has good temperature insulation and is water resistant. Because of these properties, leather has been used to make clothing, shelters, tools and other objects since ancient times. For instance, excavations of Neanderthal sites more than 40,000 years old uncovered leather making tools similar to those that are commonly used today^{1,2}. Furthermore, wall paintings and artefacts found in Egyptian tombs dating back to 5,000 BCE show that the ancient Egyptians knew how to make leather³. In those times, raw skin was turned into leather using organic reagents such as animal dung, urine and vegetable matter, with the whole process taking up to 60 days⁴. As technology advanced, chemicals were used instead of these natural products to expedite the process. However, with the convenience of chemical tanning, came concerns about pollution of the environment, as many of the chemicals used were, and still are corrosive and toxic⁵.

In 2018, New Zealand exports of raw skin, pickled skins and leather were worth \$375.72 million NZD⁶. Although this is not a large portion of total export earnings, skins are a by-product of the meat industry, and if not processed, must be destroyed, incurring a significant cost to the farmer. If processed, the environmental pollution that arises from the current processes poses a problem that will, because of changes in legislation, incur a significant cost to the manufacturer⁷. It is therefore necessary to find an environmentally friendly process for skin preservation and leather production. In order to understand the problem, current processes used for skin preservation and leather making will be described along with the environmental problems arising from them.

The first step of leather processing, depilation, in other words, removing hair from skins, accounts for one-third of the leather-making industrial waste due to the production of sulfide and alkaline water waste from the process^{8,9,10,11}. Conventional depilation of sheepskins requires painting a thick solution containing calcium or sodium hydroxide and sodium sulfide, on the flesh side of the pelt which allows the wool to be mechanically removed from the skin and opens up the collagen fibres¹². The chemicals are removed by washing the depilated skins with copious amounts of water that then must be treated to remove the sulfide and hydroxides before it can be fed into the waste stream. As environmental compliance becomes more demanding such processes will place significant financial burden on tanneries and the industry⁷.

To address this problem, research efforts have been aimed towards finding a method to depilate skins using enzymes, as these are recyclable and environmentally friendly. Various enzymes, such as keratinases, proteases and lipases have been shown to successfully remove hair from skin, but usually result in weakening and damage, especially to the skin surface, commonly called the grain by leather technologists^{13,14,15,16}. Furthermore, in some cases, the addition of sulfide to the enzyme mixture is necessary to provide depilation efficiency^{17,18}. Hence, at present, although significant advances have been made, the use of enzymes has not been effective on an industrial scale. This study describes an innovative method that preserves and depilates sheepskin using a milk by-product. It doesn't require the use of harsh chemicals or temperature control, and results in clean skin that is ready to be tanned.

In order to evaluate and understand the molecular mechanisms responsible for the depilation and preservation of sheepskins using this product, processed skins were evaluated on the basis of their physical and biochemical properties (including changes to the skin proteome) and compared to the same properties of pickled skins produced using the conventional process. Pickling is the stage in the conventional process that is most aligned to the state of the skin after depilation using this new process. Its success could be due to either a molecule(s) in the milk by-product, molecule(s) produced by the microorganisms in the milk by-product, microorganisms on the sheepskin, or through synergistic interactions of all of these. In order to identify these potential agents, metagenomic and proteomic analyses of the skins and their process solutions were carried out at specific times during depilation. A preliminary metabolomic analysis was also carried out on the depilating solution at the end of the process to detect the appearance of any small molecule(s) that might contribute to skin preservation.

1.2 Aims and objectives

This work aims to understand the molecular mechanisms of this new environmentally friendly process for preserving and depilating sheepskin. The first objective of this study, detailed in Chapter 3, was to answer the question “does it work and how does it work?” To answer these questions, skin was processed in a number of milk products in order to differentiate their effects and to understand why the skins are preserved. Once a standard process had been developed, the visual and physical properties of skins depilated using it were compared with those of conventionally depilated skins using scanning electron microscopy (SEM) and transmission electron microscopy

(TEM), then analysed for tear and tensile strength. The leather produced using this two-step process was also tested for tear and tensile strength as well as shrinkage temperature. At the same time the microorganisms in each of the products present at the completion of depilation were cultured and identified by 16S- and 18S rDNA sequencing.

The second objective was to ask if the building blocks of the skin are changed during the process and if so, how does this relate to changes in the physical properties of the resultant leather product. Chapter 4 presents the results of quantitative biochemical analyses of skins depilated with this new method and a comparison of the results with those from conventionally processed skins. Analyses included amino acids, collagen crosslinks, glycosaminoglycans (GAGs), and the proteomic profiles of the skins. The third objective was to investigate the role of microbes in this process. Microbes secrete enzymes and other compounds that may be responsible for both the preservation of the skins and their depilation. Chapter 5 explores the changes in the microbiome of the skins during depilation using metagenomics amplicon sequencing to identify bacteria and fungi present before, during and after depilation. Chapter 6 considers all the evidence from Chapters 3, 4 and 5, based on the prediction of the mechanisms involved in both the preservation and depilation of the sheepskin observed, suggests other experiments that should be done to validate the mechanism and its results.

1.3 Significance of this investigation

The aim of this project is to understand the molecular mechanism(s) of this new depilation process to both preserve and depilate sheepskins. This process of depilating skins currently contributes 60 - 70 % of the total pollution burden in the beamhouse process, and uses approximately 23 L of water per kg of skin to wash the both salt and other chemicals from the depilated skin¹⁹. As environmental controls for waste treatment and disposal become more stringent, and water shortages become more common due to climate change it is clear the current practices of the tanning industry will have to change, not only in New Zealand but worldwide. The development of an environmentally friendly process for depilation is therefore important. This thesis describes the initial steps to develop such a process. More importantly it shows that leather produced from sheepskin using the process on a laboratory scale does not display any damage to the grain, has a good appearance and its physical properties are the same as leather made using the conventional process. Investigations into how the process works are not yet

complete, although significant progress has been made. It is now ready to be taken to a pilot study. The findings will benefit the leather industry of New Zealand and could be adapted by other countries facing environmental issues caused by the leather manufacture.

1.4 References

- [1] M. Soressi, S. P. McPherron, M. Lenoir, T. Dogandžić, P. Goldberg, Z. Jacobs, Y. Maigrot, N. L. Martisius, C. E. Miller, W. Rendu, M. Richards, M. M. Skinner, T. E. Steele, S. Talamo, and J-P. Texier. Neandertals made the first specialized bone tools in Europe. *PNAS*, 110(35):14186, 2013. URL <http://www.pnas.org/content/110/35/14186.abstract>.
- [2] R. Thomson. Leather manufacture in the post-medieval period with special reference to Northamptonshire. *Post-Medieval Archaeol.*, 15(1):161–175, 1981. ISSN 0079-4236. doi: 10.1179/pma.1981.003. URL <https://doi.org/10.1179/pma.1981.003>.
- [3] A. J. Veldmeijer. *Leather work in ancient Egypt*, pages 2540–2550. Springer Netherlands, Dordrecht, 2016. ISBN 978-94-007-7747-7. doi: 10.1007/978-94-007-7747-7_9365. URL https://doi.org/10.1007/978-94-007-7747-7_9365.
- [4] A. Lucas and J. Harris. *Ancient Egyptian materials and industries*. Courier Corporation, New York, USA, 2012. ISBN 0486144941.
- [5] S. Dixit, A. Yadav, P. D. Dwivedi, and M. Das. Toxic hazards of leather industry and technologies to combat threat: a review. *J. Cleaner Prod.*, 87:39–49, 2015. ISSN 0959-6526. doi: <https://doi.org/10.1016/j.jclepro.2014.10.017>. URL <http://www.sciencedirect.com/science/article/pii/S0959652614010580>.
- [6] Statistics New Zealand. Group: Harmonised Trade - Export, 9 2019. URL <http://archive.stats.govt.nz/infoshare/>.
- [7] P. Thanikaivelan, J. R. Rao, B. U. Nair, and T. Ramasami. Progress and recent trends in biotechnological methods for leather processing. *Trends Biotechnol.*, 22(4): 181–188, 2004. ISSN 0167-7799. doi: <https://doi.org/10.1016/j.tibtech.2004.02.008>. URL <http://www.sciencedirect.com/science/article/pii/S0167779904000551>.
- [8] A. Cassano, E. Drioli, and R. Molinari. Recovery and reuse of chemicals in unhairing, degreasing and chromium tanning processes by membranes. *Desalination*, 113(2):251–261, 1997. ISSN 0011-9164. doi: [https://doi.org/10.1016/S0011-9164\(97\)00137-9](https://doi.org/10.1016/S0011-9164(97)00137-9). URL <http://www.sciencedirect.com/science/article/pii/S0011916497001379>.

- [9] A. Cassano, E. Drioli, R. Molinari, D. Grimaldi, F. La Cara, and M. Rossi. Enzymatic membrane reactor for eco-friendly goat skin unhairing. *J. Soc. Leather Technol. Chem.*, 84(5):205–11, 2000. ISSN 0144-0322.
- [10] N. R. Kamini, C. Hemachander, J. G. S. Mala, and R. Puvanakrishnan. Microbial enzyme technology as an alternative to conventional chemicals in leather industry. *Curr. Sci. India*, 77(1):80–86, 1999. ISSN 00113891. URL <http://www.jstor.org/stable/24102916>.
- [11] J. Kanagaraj, T. Senthilvelan, R. C. Panda, and S. Kavitha. Eco-friendly waste management strategies for greener environment towards sustainable development in leather industry: a comprehensive review. *J. Cleaner Prod.*, 89:1–17, 2015. ISSN 0959-6526.
- [12] A. D. Covington. *Tanning chemistry: the science of leather*. RSC Publishing, 2009. URL <http://app.knovel.com/hotlink/toc/id:kpTCTSL002/tanning-chemistry-the>.
- [13] Z. Fang, Y-C. Yong, J. Zhang, G. Du, and J. Chen. Keratinolytic protease: a green biocatalyst for leather industry. *Appl. Microbiol. Biotechnol.*, 101(21):7771–7779, 2017. ISSN 0175-7598.
- [14] A. Ranjithkumar, J. Durga, R. Ramesh, C. Rose, and C. Muralidharan. Cleaner processing: a sulphide-free approach for depilation of skins. *Environ. Sci. Pollut. Res.*, 24(1):180–188, 2017. ISSN 0944-1344.
- [15] S. Saran, R. V. Mahajan, R. Kaushik, J. Isar, and R. K. Saxena. Enzyme mediated beam house operations of leather industry: a needed step towards greener technology. *J. Cleaner Prod.*, 54:315–322, 2013. ISSN 0959-6526. doi: <https://doi.org/10.1016/j.jclepro.2013.04.017>. URL <http://www.sciencedirect.com/science/article/pii/S0959652613002321>.
- [16] P. Sujitha, S. Kavitha, S. Shakilanishi, N. K. C. Babu, and C. Shanthi. Enzymatic dehairing: a comprehensive review on the mechanistic aspects with emphasis on enzyme specificity. *Int. J. Biol. Macromol.*, 118:168–179, 2018. ISSN 0141-8130.
- [17] R. B. Choudhary, A. K. Jana, and M. K. Jha. Enzyme technology applications in leather processing. *Indian J. Chem. Technol.*, 11:659–671, 2004. ISSN 0975-0991.
- [18] N. Kandasamy, P. Velmurugan, Sundarvel A., R. J. Raghava, C. Bangaru, and T. Palanisamy. Eco-benign enzymatic dehairing of goatskins utilizing a protease from a *Pseudomonas fluorescens* species isolated from fish visceral waste. *J. Cleaner Prod.*, 25:27–33, 2012. ISSN 0959-6526. doi: <https://doi.org/10.1016/j.jclepro.2011.12.007>. URL <http://www.sciencedirect.com/science/article/pii/S0959652611005324>.

- [19] M. Hutton and M. Shafahi. Water pollution caused by leather industry: a review. In *Proceedings of the ASME 2019 13th International Conference on Energy Sustainability collocated with the ASME 2019 Heat Transfer Summer Conference*, Bellevue, Washington, USA, July 14–17 2019. ASME 2019 13th International Conference on Energy Sustainability.

2 | Literature review

2.1 Skin

Skin, the largest organ of animals, is a complex structure. It provides a physical barrier against exogenous chemical and physical factors in the environment, participates in metabolic processes, regulates temperature, and is the first line of immunological defence against pathogenic microorganisms¹. Skin contains three general layers: the epidermis, dermis and hypodermis (Fig. 1).

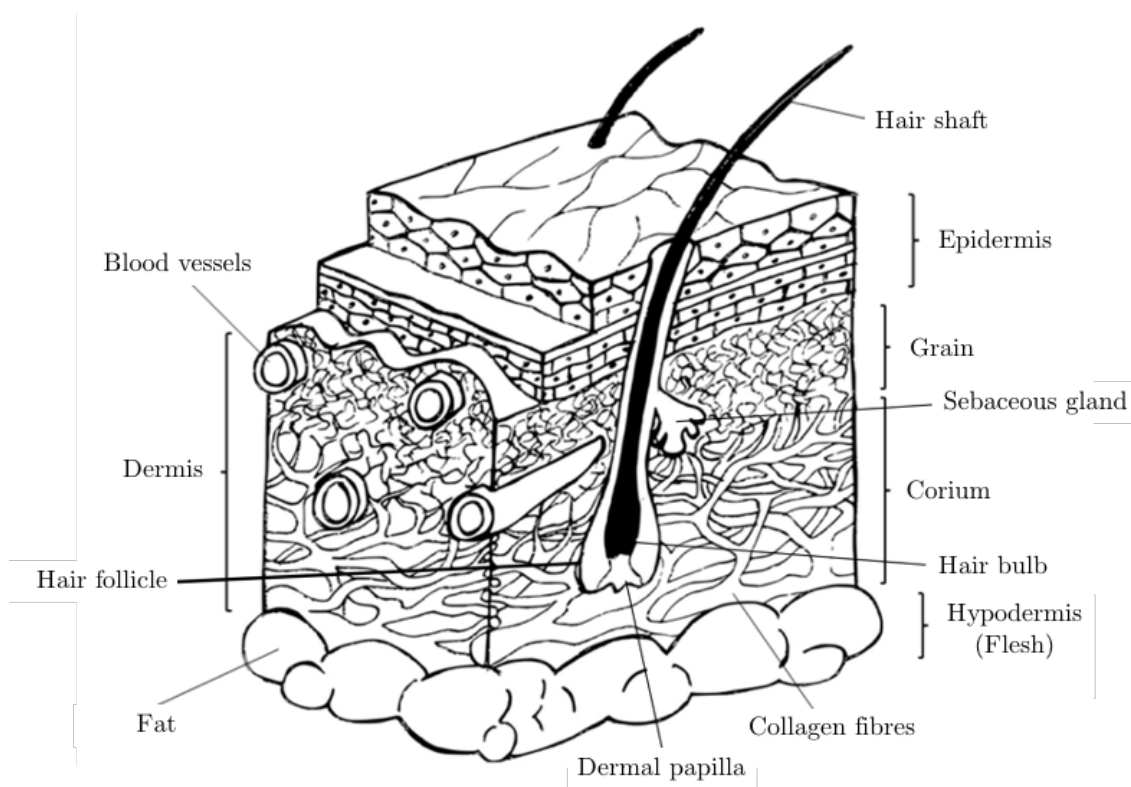


Figure 1: Diagram of the skin structure. Reprinted from Visser (2019) with permission from the author².

The epidermis (cuticle) is the outermost protective layer of the skin, is primarily composed of keratinocytes (95 %) and contains hair or wool, hair bulbs and hair shafts. Immediately below the epidermis is the dermis layer which makes up 90 % of the total skin weight, and is collectively termed the extracellular matrix (ECM)³. It is made up of collagen, elastin, laminin, and proteoglycans/glycosaminoglycans, as well as the fibroblasts that synthesise and secrete them and contains the hair bulbs and shafts, sebaceous and sweat glands and blood vessels. The dermis is often further divided into three layers when discussed from the leathersmakers' perspective: the grain, the grain-corium junction, and the corium. The grain, the uppermost layer of the dermis, is composed of interwoven fine and loose collagen fibres, mainly types I, III and VI, and the upper part of the hair follicle. Type I collagen is found to be

responsible for the structural stability of the grain layer, while the network of beaded filaments formed by collagen type VI is integral to its uppermost surface, also termed the enamel, and is responsible for the outward smooth appearance of the final leather product⁴. The grain-corium junction is the transitional zone between the very fine fibres of the grain and the larger fibres of the corium. It is composed of relatively small collagen fibres and carries other structural components of the skin, such as blood vessels, and only in sheep, lipocytes⁵. The corium layer contains thicker and more compact type I collagen fibres that form higher order structures or bundles which vary in size through the skin cross-section. The largest collagen bundles are approximately 0.1 mm in diameter, and subdivide, decreasing to around 0.01 mm in diameter as they approach the surface of the grain layer⁶. The hypodermis, also known as the flesh layer, is composed of mainly fat cells.

Sheepskin is composed of 53 % water, 27.5 % protein, 18.3 % lipids as well as trace minerals, salts, and nucleic acids⁷. The major protein scaffolds in skins are formed from fibrous collagen and elastin, both of which contribute to the strength and elasticity of the skin. The collagen and elastin are then 'glued' together by proteoglycans, that hydrate the skin⁸.

2.2 Collagen

2.2.1 The collagen family and structure

Collagen is the main structural protein found in the extracellular matrix of animal tissues, making approximately 30 % of the total body protein. More than half of the collagen in the body is found in fibrous tissues, such as skin, tendon, ligament, bone and teeth⁹. All members of the collagen family of proteins have three characteristic features: a) a repeating amino acid sequence $[\text{Gly-X-Y}]_n$, with or without interruptions; b) a high percentage of either the X or Y positions are proline or hydroxyproline; c) a right-handed triple helix made up from three left-handed α helices¹⁰. The amino acid tryptophan is not found in the collagen due to its bulky nature and the collagen amino acid sequence is characterised by three unusual post-translational modifications. First, proline can be hydroxylated by the enzyme prolyl-4-hydroxylase (procollagen-proline dioxygenase; E.C. 1.14.11.2) to form 4-hydroxyproline (Hyp). Secondly, lysine can be hydroxylated to form 3-hydroxylysine (Hyl) by lysyl hydroxylase (E.C. 1.14.11.4).

Roman numerals are used to number different types of collagens, in the order of

their discovery, and the Greek letter α followed by a number denotes the different α -chains of collagen. The trimeric nature of a collagen molecule allows for homo- and heterotopic arrangements of the α -chains allowing isoforms within an individual collagen type. For example, collagen type I generally exists as a heterotrimer of two $\alpha 1$ chains and one $\alpha 2$ chain, although, it can also be found as a homotrimer consisting of three $\alpha 1$ chains (Table 1). To date, 40 vertebrate collagen genes have been identified that form 29 distinct homo- or heterotrimeric collagen molecules. Table 1 summarises the functions, the tissues in which they are found, and the structures of the different collagen types. They can be classified into four main groups depending on their primary structure, the length of the helical domain, whether there are interruptions within the helical domain, the size and shape of the telopeptide regions (terminal domains), the molecular weight of the molecule, the charge profile along the helix, and differences in post-translational modifications. Table 2 shows the four main groups of collagens and the collagen types that fit into each group.

Fibrillar collagens are the largest group by far, with type I, II, and III collagens being the most abundant found in animals. Together they make up approximately 80 - 90 % of total mammalian collagen¹⁰. Type I collagen is found in skin, bone, tendon, cornea, lung, and vasculature; type II collagen is found mainly in cartilage, has been found in other tissues such as the vitreous humor of the eyeball, and the inner ear and in low abundance in skin^{2,11,12}; type III collagen is found in relatively elastic tissues, such as embryonic tissue, blood vessels, skin, and lung, and is the main component of reticular fibres. Type IV collagen, which is not fibrillar in structure, forms the secreted epithelium layer of the basement membrane, a specialised structure found at tissue boundaries. Type V collagen is found in hair, on cell surfaces, and in the placenta, as well as being a minor component of the skin where it associates with type I collagen. There are several other types of less common collagens that are categorised as fibrillar, including Type XI that is found in foetal cartilage, and associates with type II collagen.^{9,10,13,14}

Fibrillar collagen molecules are structurally defined as having an uninterrupted central coiled-coil triple helical domain flanked by two non-helical telopeptide domains at both the N- and C-termini. The tight packing of the three individual collagen α -chains in the helical domain can only occur because of the $[\text{Gly-X-Y}]_n$ repeat where every third amino acid is Gly, the only amino acid small enough to fit into the core of the triple helix. The repeat is commonly either Gly-Pro-X or Gly-X-Hyp with X being any other amino acid apart from Trp. The repeat sequence Gly-Pro-Hyp makes up 12 % of the former pattern. The super-helical trimer resembles a rope-like structure, has a molecular weight of approximately

Table 1: Collagen family characteristics and tissue distribution. Table adopted with modifications from KIELTY and GRANT (2002)¹⁵, SHOULDERS and RAINES (2009)¹⁴, and SORUSHANOVA *et al.* (2019)¹⁰.

Collagen type	Chains	Molecular assembly	Supramolecular structure	MWt (kDa)/ α -chain	Examples of tissue location
I (Heterotrimer)	$[\alpha 1(I)_2\alpha 2(I)]$	Monomers staggered by 67 nm	Large diameter, 67 nm banded fibrils	95	Skin, tendon, cornea, bone, ligament
I (Homotrimer)	$[\alpha 1(I)]_3$		67 nm banded fibrils		Tumours, dermis, bone
II	$[\alpha 1(II)]_3$	Monomers staggered by 67 nm	67 nm banded fibrils	95	Cartilage, vitreous (eye)
III	$[\alpha 1(III)]_3$	Monomers staggered by 67 nm	Small diameter, 67 nm banded fibrils	95	Dermis, aorta, uterus, tendon, blood vessels, intestine
IV	$[\alpha 1(IV)_2\alpha 2(IV)], \alpha 3(IV), \alpha 4(IV), \alpha 5(IV), \alpha 6(IV)$	Association of 4N- and 2C-termini	Non-fibrillar meshwork	170 - 180	Basement membrane
V	$[\alpha 1(V)]_2\alpha 2(V), [\alpha 1(V)]_3, [\alpha 1(V)\alpha 2(V)\alpha 3(V)]$	Monomers staggered by 67 nm	9 nm diameter banded fibrils	120 - 145	Placental tissue, bone, dermis, cornea
VI	$[\alpha 1(VI)\alpha 2(VI)\alpha 3(VI)]$	Association into tetramers that aggregate end to end	5 - 10-nm diameter beaded microfibrils, 100-nm periodicity	$\alpha 1/2$ (VI) 140	Uterus, dermis, cornea
VII	$[\alpha 1(VII)]_3$	Large aggregation of antiparallel dimers	Anchoring fibrils	$\alpha 3$ (VI) 340	cartilage, muscle
VIII	$[\alpha 1(VIII)]_2\alpha 2(VIII)$	Interrupted helical structure	Non-fibrillar, hexagonal lattice	170	Skin, amniotic membrane, cornea, mucosal epithelium
IX	$[\alpha 1(IX)\alpha 2(IX)\alpha 3(IX)]$	Covalently crosslinked to the surface of type II collagen fibrils	FACIT, non-fibrillar	61	Descemet's membrane, epithelial cells
X	$[\alpha 1(X)]_3$	Assemble a mat-like structure	Non-fibrillar, hexagonal lattice	68 - 115	Cartilage, vitreous, tendon
XI	$[\alpha 1(XI)\alpha 2(XI)\alpha 3(XI)]$	Monomers staggered by 67 nm	Fine fibrils similar to type V collagen	59	Calcifying cartilage (including parts of tendon)
XII	$[\alpha 1(XII)]_3$	Association with surface collagen fibrils	FACIT, non-fibrillar	110 - 145	Cartilage, intervertebral disc
XIII	$[\alpha 1(XIII)]_3$	150 nm rods with two flexible hinges	Transmembrane	220, 340	Dermis, tendon, cartilage
XIV	$[\alpha 1(XIV)]_3$	Disulfide-linked cross-shape	FACIT, non-fibrillar	62 - 67	Endothelial cells, epidermis

Table 1: Collagen family characteristics and tissue distribution (continued).

Collagen type	Chains	Molecular assembly	Supramolecular structure	MWt (kDa)/ α -chain	Examples of tissue location
XV	$[\alpha 1(\text{XV})]_3$	Figure 8 knot configuration	MULTIPLEXIN; non-fibrillar	125	Placenta, kidney, heart, ovary, testis
XVI	$[\alpha 1(\text{XVI})]_3$	Associates with dermal fibrillin, and banded collagen in cartilage	FACIT, non-fibrillar	150 - 160	Heart, kidney, smooth muscle
XVII	$[\alpha 1(\text{XVII})]_3$	Shed from cell surface into shorter soluble form	Membrane-intercalated	180	Hemidesmosomes of specialised epithelia (skin)
XVIII	$[\alpha 1(\text{XVIII})]_3$		MULTIPLEXIN; non-fibrillar	200	Kidney, liver, lung
XIX	$[\alpha 1(\text{XIX})]_3$	Sharply kinked and higher order complexes	FACIT; non-fibrillar	165	Fibroblast cell line, basement membrane, muscle cell, interneuron, hippocampal synapses
XX	$[\alpha 1(\text{XX})]_3$	Binds to collagen fibrils with amino termini away from fibril surface	FACIT	135, 170, 185	Corneal epithelium, embryonic skin, sternal cartilage, tendon
XXI	$[\alpha 1(\text{XXI})]_3$		FACIT		Blood vessel wall, secreted by smooth muscle cells
XXII	$[\alpha 1(\text{XXII})]_3$	Associates with cartilage microfibrils	FACIT	200	Tissue junction
XXIII	$[\alpha 1(\text{XXIII})]_3$		Transmembrane		Tumour (prostate)
XXIV	$[\alpha 1(\text{XXIV})]_3$	Associates with vertebrate fibrillar	Fibrillar, fibril associated		Regulation of type I collagen fibrillogenesis, osteoblast differentiation marker
XXV	$[\alpha 1(\text{XXV})]_3$	Binds to fibrillised A β	Transmembrane	50/100	Interacts with β amyloid plaques in Alzheimer's disease
XXVI	$[\alpha 1(\text{XXVI})]_3$		FACIT	~80	Ovary, testis
XXVII	$[\alpha 1(\text{XXVII})]_3$	10 nm network organisation	Thin non-striated fibrils		Hypertrophic cartilage
XXVIII	$[\alpha 1(\text{XXVIII})]_3$	Associates with non-myelinated regions	Beaded filament forming	~50	Basement membrane of Schwann cells, peripheral nervous system
XXIX	$[\alpha 1(\text{XXIX})]_3$		Non-fibrillar		Epidermis suprabasal cells, lung, small intestine, colon, testis

Table 2: Collagen groups based on general structural similarities.

Group	Collagen type	Description
1	I, II, III, V, XI, XXIV, XXVII	Fibril-forming collagens
2	IV, VII, XXVIII	Basement membrane collagens
3	VI, VIII, X	Short chain collagens
4	MULTIPLEXINs: XV, XVIII	Collagens with helical interruptions
	FACITs: IX, XII, XIV, XVI, XIX, XX, XXI, XXII, XXVI	MULTIPLEXINs: multiple triple helix domains with interruptions
	MACITs: XIII, XVII, XXIII, XXV	FACITs: fibril associated collagens with interrupted triple helices
		MACITs: membrane associated collagens with interrupted triple helices.

300,000 g/mol, is 300 nm in length, and has a diameter of 1.5 nm (Fig. 2). This structure is called tropocollagen, and is the basic structural unit of collagen. The triple helix is further stabilised by hydrogen bonds between Gly mainchain amides and mainchain carboxyl groups of the residue in the second position of the repeating sequence in an adjacent chain. They are further stabilised by another hydrogen bond between bridging water molecules and the hydroxyl groups of Hyl in adjacent chains. Because of their cyclic nature, Pro and Hyp help 'stiffen' the individual collagen chains, by preventing rotation around the C-N bonds. The post-translational modification of Lys to Hyl is also important for the stabilisation of the collagen molecule, as it is essential for the formation of covalent crosslinks both within the triple helix and between tropocollagen molecules within fibrils.^{10,16}

Fibrillar collagens form distinctive, long, unbranched, banded fibril structures that are made up from cross-linked tropocollagen molecules. Small angle x-ray diffraction studies (SAXS) and electron microscopy have shown they have a characteristic banding pattern or periodicity (D) of 67 nm¹⁷. The D-banding is characteristic of the parallel and quarter-staggered arrangement of the tropocollagen molecules (Fig. 2). The whole process of collagen fibril formation, fibrillogenesis, is directed by the distribution of hydrophobic and charged amino acid residues along the triple helix which maximises electrostatic and hydrophobic interactions between neighbouring molecules. Although the initial interaction between tropocollagens is driven by non-covalent interactions, the arrangement of molecules is cemented through the formation of stronger and permanent inter-polypeptide crosslinks.^{10,13,18}

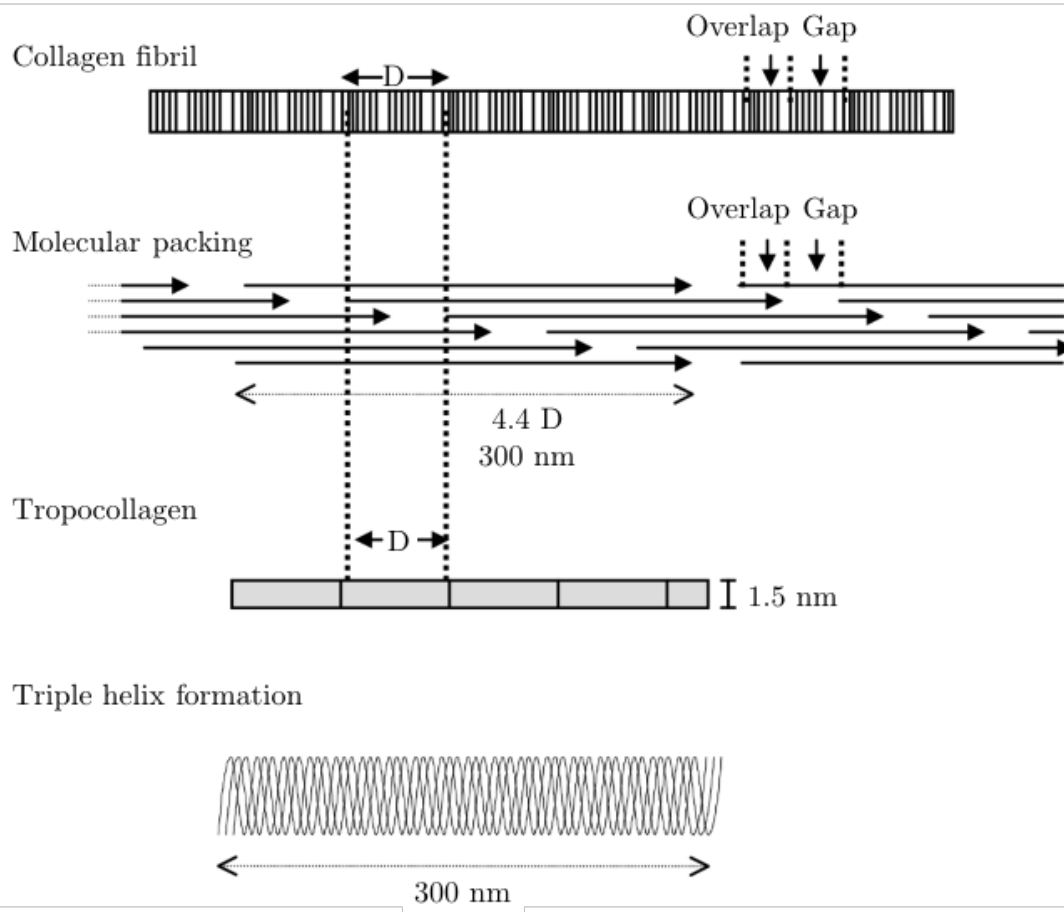


Figure 2: Schematic diagram of tropocollagen and an assembled collagen fibril. The right-handed tropocollagen superhelix is made up of three left-handed α -chains. The length of the tropocollagen is ~ 300 nm, (equivalent to $4.4 \times D$), and 1.5 nm in thickness. The staggered arrangement of tropocollagen molecules in the fibril gives rise to one overlap zone and one gap zone per D period. The characteristic periodicity of collagen is close to 67 nm. Reprinted from Kielty and Grant (2002)¹⁵ with permission from Wiley-Liss, Inc.

2.2.2 Methods used in this study for the analysis of collagen

Amino acid analysis was used to determine the protein concentration of the skins, more specifically the proportion of collagen in the treated skins. The concentration of collagen is typically estimated using Hyp, as it is an amino acid specific to collagen. Two techniques can be used: colorimetric assays with dyes specific to Hyp or high-pressure liquid chromatography (HPLC)^{19,20}. Though colorimetric assays are simpler and quicker, HPLC methods are more sensitive and accurate. An established amino acid analysis protocol by Cohen²¹ later optimised by Naffa (2017)¹⁹ for skin samples using 6-aminoquinolyl-N-hydroxysuccinimidyl carbamate (AQC) for the derivatisation of amino acids due to its rapid reaction with both primary and secondary amino acids that form stable fluorescent products was

used. The fluorescent derivatives were separated by high pressure liquid chromatography, detected by fluorescence and quantitated using a standard curve.

2.3 Collagen crosslinks

During collagen biosynthesis, collagen crosslinks are formed between α -chains of procollagens and also between tropocollagen molecules. Crosslinking of collagen molecules is important in stabilising the collagen fibrils and contributes to the mechanical strength of tissues, such as skin and tendon. Collagen crosslinks that are formed by enzyme catalysis are classified as collagen enzymatic crosslinks. A second type of crosslink, called glycation, doesn't involve enzyme catalysis, and is commonly associated with ageing. Such crosslinks are associated with a decrease in the mechanical strength of collagen fibres that occurs with ageing²². For more details, the reader is directed to an extensive review on collagen crosslinks by Gaar *et al.* (2020)²³.

2.3.1 Collagen non-enzymatic crosslinks

When collagen molecules are exposed to monosaccharides for a prolonged amount of time, at elevated temperatures such as body temperature, crosslinks can occur between spatially adjacent the free amino sidechains of Lys or Arg through a sugar molecule. The formation of the crosslink is mediated by the Maillard reaction, and subsequent Amadori rearrangement, in which in which a spontaneous bond forms between a reducing sugar and the amino group of Lys or Arg. The different products of this reaction are called advanced glycation end products (AGEs)²³. Collagen crosslinking by glycation is uncontrolled and can alter the structural and biological properties of collagen. Several studies have found that with non-enzymatic glycation crosslinking of collagen causes the tissue to become rigid and brittle as well as more resistant to proteases²⁴.

2.3.2 Collagen enzymatic crosslinks

During fibrillogenesis, collagen fibrils are mechanically stabilised by the formation of covalent crosslinks between neighbouring lysines and hydroxylysines due to the activity of the enzyme lysyl oxidase (LOX; E.C. 1.4.3.13). LOX enzymes are copper-dependent amine oxidases that require the presence of the cofactor lysine tyrosylquinone (LTQ)²⁵. Specific lysines and hydroxylysines in the helical and telopeptide regions of collagen are oxidatively deaminated by LOX to form their respective aldehydic forms, allysine (Lys^{ald}) and hydroxyallysine (Hyl^{ald}). These

aldehyde sidechains are highly reactive and spontaneously condense with the ϵ -amine of unmodified Lys or Hyl sidechains, or other aldehydes to form aldimine containing intramolecular or intermolecular crosslinks. These imine containing crosslinks are classified as immature (divalent) crosslinks, and can undergo further reactions with histidine residues to form mature trivalent or tetravalent crosslinks. The formation of such intermolecular crosslinks is highly specific, as the amino acid residues involved in the reactions are sequence limited, and have to be in close spatial proximity to allow the reaction to proceed²². Their formation therefore regulates the packing of tropocollagen into fibrils.

2.3.2.1 Immature collagen crosslinks

The formation of immature collagen crosslinks begins with the deamination of lysine (Lys) and hydroxylysine (Hyl) residues to form allysine (Lys^{ald}) and hydroxyallysine (Hyl^{ald}), respectively. The crosslinks form between a telopeptide allysine (t-Lys^{ald}) or hydroxyallysine (t-Hyl^{ald}) residue and a helical lysine (hel-Lys) or hydroxylysine (hel-Hyl) residue to produce an immature (divalent) crosslink such as: dehydro-lysino-norleucine (deH-LNL), dehydro-hydroxy-lysino-norleucine (deH-HLNL), and dehydro-dihydroxy-lysino-norleucine (deH-DHLNL). Fig. 3 shows the chemical pathway of crosslinking interactions initiated by the LOX enzyme.

The formation of the various types of immature crosslinks depends on the rate of Lys hydroxylation, the rate of deamination of Lys and Hyl at the telopeptide regions, and the availability of helical Lys and Hyl residues that are in close spatial proximity²⁶. When the rate of hydroxylation of Lys at the telopeptide regions is low, aldimine crosslinks are predominately formed. The aldimine crosslinks, deH-LNL and deH-HLNL, are commonly found in the collagens making up skin and rat tail tendon^{26,27,28}. It should be noted that, deH-HLNL is found in the collagen, whereas deH-LNL is associated with elastin²⁹. When the rate of Lys hydroxylation is high, ketoamine crosslinks, such as deH-DHLNL, are formed. Although deH-HLNL is initially classified as an aldimine crosslink, it undergoes a spontaneous Amadori rearrangement to form a ketoamine crosslink lysino-keto-norleucine (LKNL). In the same way, the ketoamine crosslink deH-DHLNL can be converted into another ketoamine crosslink hydroxy-lysino-keto-norleucine (HLKNL)³⁰. These ketoamine crosslinks are predominantly found in connective tissues that bear large mechanical loads, such as bone, collagen, cartilage, and tendon, and are not common in skin²⁷.

Due to the presence of a Schiff base double bond, all divalent crosslinks are acid and heat labile, and as a result, have to be reduced by sodium borohydride (NaBH_4) to be detected. The two aldimine crosslinks deH-LNL, deH-HLNL, and the ketoamine crosslink deH-DHLNL are reduced to their more stable forms lysino-norleucine (LNL), hydroxy-lysino-norleucine (HLNL), and dihydroxy-lysino-norleucine (DHLNL), respectively.

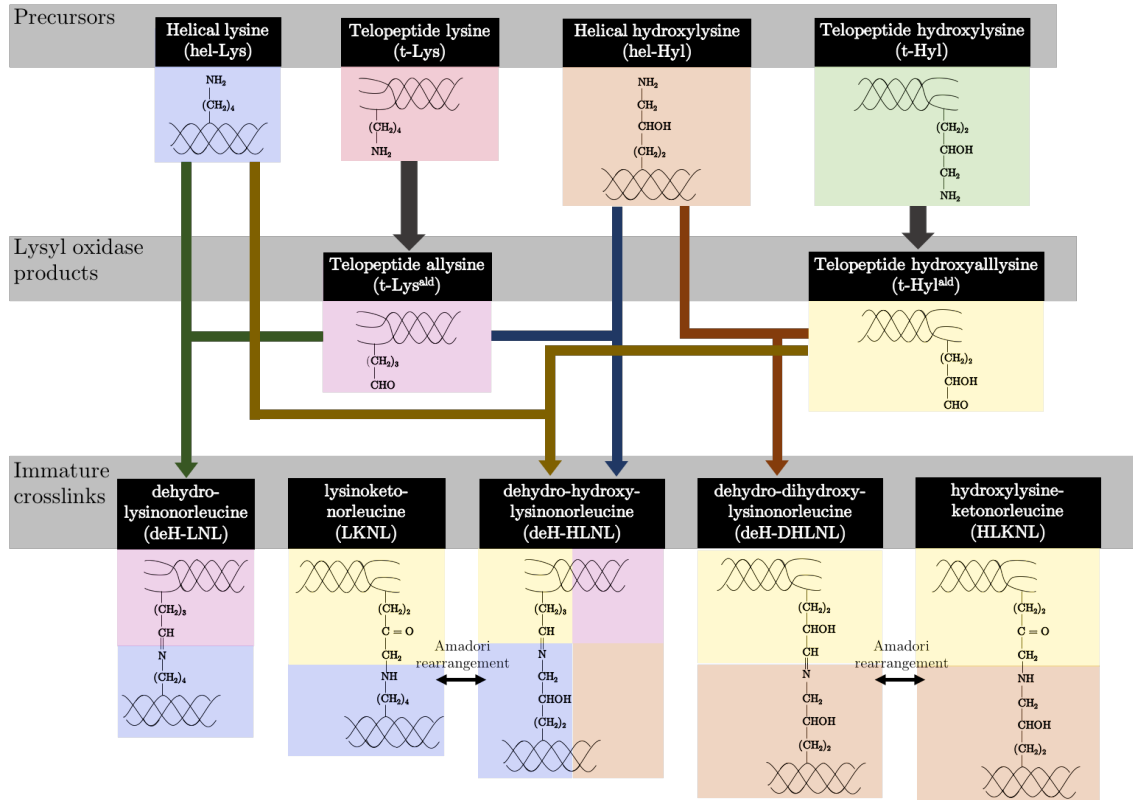


Figure 3: Collagen crosslink chemical pathway initiated by the LOX enzyme. The lysines of the triple-helix and telopeptide origin are tracked by the colour to the immature (divalent) crosslinks.

2.3.2.2 Mature collagen crosslinks found in skin

In most tissues, the concentration of immature crosslinks decreases as the tissues mature^{27,29}. The free aldehyde or aldol crosslink can further react with the ϵ -amine group of a Hyl or with the τ N of His to form a trivalent or tetravalent crosslink. These covalently bridge three or four collagen molecules together to stabilise the head to tail staggered arrangement of the collagen fibril^{31,32}. The fibrils then form bundles that can be aligned in various directions. Mature crosslinks are categorised as pyrrolic, pyridinium, or histidine-containing crosslinks.

2.3.2.2.1 Pyrrolic crosslinks

Pyrroles are trivalent maturation products of divalent ketoamine crosslinks that contain a pyrrole moiety. They were first detected when the peptides isolated from connective tissues formed a pink colour when reacted with Ehrlich's reagent (*p*-dimethylaminobenzaldehyde)³³. Pyrrole crosslinks are found mostly in the skeletal tissues, but due to their inherent acid and alkaline lability, quantitative analysis and characterisation has been limited. The biosynthesis of pyrrole crosslinks is thought to involve a condensation reaction between telopeptidyl Hyl^{ald}, telopeptidyl Lys^{ald}, and helical Hyl or Lys^{22,34,35}.

2.3.2.2.2 Pyridinium crosslinks

Pyridinolines are stable trivalent crosslinks that were first isolated and characterised by Fujimoto *et al.* (1977) due to their fluorescence³⁶. They are most commonly found in collagen in bones, cartilage, and tendon^{27,32,37}, are destroyed upon exposure to the UV, and cannot be reduced as they lack the Schiff base double bond^{38,39}. The two that have been most investigated are pyridinoline (Pyr) and deoxy-pyridinoline (d-Pyr), that were first identified by Fujimoto *et al.* (1977) and Ogawa *et al.* (1982), respectively^{36,40}. The formation of Pyr involves two residues of telopeptidyl Hyl^{ald} and one helical Hyl, whereas the formation of d-Pyr involves two telopeptidyl Hyl^{ald} with one helical Lys instead²². Although several mechanisms have been proposed for the biosynthesis of Pyr crosslinks^{36,41,42,43}, details have not yet been elucidated. Pyr is a maturational product of deH-DHLNL and links three collagen molecules together⁴⁴.

2.3.2.2.3 Histidine-containing crosslinks

There are two collagen crosslinks that contain a histidine residue as part of their structure: histidino-hydroxy-lysinonorleucine (HHL) and histidino-hydroxy-merodesmosine (HHMD). HHL is a trivalent crosslink found mainly in skin, and in tendon at much lower concentrations^{16,45,46,47}. It is formed between a telopeptidyl Lys^{ald}, and a helical Hyl^{ald} from an adjacent collagen molecule, to produce a divalent HLNL crosslink that then reacts with a helical His from another collagen molecule^{31,47}. Eyre *et al.* (2019) have recently reported that HHL is a laboratory artefact rather than a natural collagen crosslink^{42,48}. However, this finding was challenged by Yamauchi *et al.* (2019)⁴⁹ and Visser (2019)². Biosynthesis of HHL starts at birth, and after an initial rapid increase, a more gradual increase in production occurs as ageing proceeds⁴⁴. A decrease in the number of HLNL crosslinks with a concomitant increase in HHL crosslinks has been linked to the stiffness often characteristic of mature skin^{31,45,47,50}. HHMD is a tetravalent

crosslink produced from a His, Hyl, and an aldol condensation product, or by the reaction of HHL with DHLNL. The existence of HHMD *in vivo* is, however, debatable. Although it has been isolated and identified in several studies in different tissues, some researchers propose that it may be formed as an artefact of base-catalysed Michael addition during NaBH₄ reduction^{19,30,46,51,52,53,54,55,56,57}.

2.3.3 Methods used in this study to analyse collagen crosslinks

Cation exchange chromatography with UV detection and reversed phase chromatography coupled with mass spectrometry have been used previously for the detection and quantification of collagen crosslinks⁵⁰. Those methods, however, were unable to effectively separate and quantify all possible crosslinks in one run without pre- or post-derivatisation of the crosslinks^{58,59}. A method developed by Naffa *et al.* (2016)⁶⁰ was shown to be able to isolate and successfully separate seven non-derivatised crosslinks from skin using a silica hydride column with a short run time (10 minutes). This method was therefore used in this study for the identification and quantitation of the four main collagen crosslinks in the skin samples (Chapter 5).

2.4 Glycosaminoglycans and proteoglycans

The extracellular matrix (ECM) is composed primarily of collagen, elastin, and proteoglycans. Proteoglycans (PGs) are comprised of a core protein that is covalently modified by one or several glycosaminoglycans (GAGs). GAGs are long, linear, sulfated, and negatively charged polysaccharides ranging in molecular weight between 10 and 100 kDa. They take part in a wide range of intracellular activities, such as cell growth, migration, differentiation, metabolism, and adhesion⁶¹. GAGs also interact with ECM matrix molecules such as fibronectin, laminin, and most importantly collagen fibrils during fibrillogenesis⁶².

2.4.1 Proteoglycans

Proteoglycans (PGs) are proteins that are heavily glycosylated. Glycosylation is one of the most important post-translational modifications of proteins, where a mono- or oligosaccharide is covalently attached to the polypeptide chain in a reaction catalysed by glycosyl- or oligosaccharyl-transferases⁶³. The sugar-protein linkage can either be 1) through the sidechains of an Asn residue (N-glycosylation), or 2) through the sidechains of Ser, Thr, Tyr, Hyp, or Hyl

residues (O-glycosylation). The sugar moiety of the molecule is called a glycan. Proteoglycans are a special type of glycoprotein where the glycan consists of any type of GAG chain with the exception of HA. The molecular diversity and functions of PGs arise from the different types, lengths, and sulfation content of GAG chains attached to the core protein. PGs are classified into four main categories based on their cellular and sub-cellular locations, overall gene/protein homology, and the presence of specific protein modules within their respective protein cores⁶⁴. These are 1) Intracellular proteoglycans, 2) cell surface proteoglycans, 3) basement membrane proteoglycans, and 4) extracellular proteoglycans.⁶⁴ Basement membrane proteoglycans and extracellular proteoglycans are common proteoglycan components in the skin and will be discussed in the following paragraphs.

2.4.1.1 Basement membrane proteoglycans

The basement membrane is a thin layer of specialised ECM that sits between the epithelial and connective tissues. It is a fibrous matrix that consists of type IV XV, and XVIII collagens, laminin, the glycoproteins known as nidogens, and the heparan sulfate proteoglycans (HSPGs) perlecan and agrin. Perlecan is involved in many cellular activities, such as cell adhesion, lipid metabolism, and epidermal skin formation⁶⁵. Agrin is involved in the development of the neuromuscular junction during embryogenesis, renal filtration, and cell-matrix interactions^{66,67}. Type XVIII and XV collagens are members of the MULTIPLEXIN collagens (Table 2). They exhibit structural features of both collagens and proteoglycans, by having triple helical domains flanked by unique non-triple helical regions. Both collagens XVIII and XV contain a C-terminal non-collagenous domain that can be cleaved to form endostatin which inhibits tumour growth⁶⁸.

2.4.1.2 Extracellular proteoglycans

Extracellular proteoglycans are further categorised into three subgroups: 1) hyaluronan-and lectin-binding proteoglycans (hyalectans), 2) small leucine-rich proteoglycans (SLRPs), and 3) the testican/SPOCK family of proteoglycans.

2.4.1.2.1 Hyalectans

Hyalectans have three domains: An N-terminal domain that binds hyaluronan, a central domain that harbours CS or DS sidechains, and a C-terminal domain that binds lectins. There are four hyalectans, including aggrecan, versican, neurocan, and brevican. Aggrecan, as its name suggests, has the propensity to aggregate into

a large supramolecular structure that has a molecular weight larger than 2 MDa together with HA⁶⁴. The large aggregate generates a densely packed hydrated gel enmeshed with collagen fibrils and other PGs and glycoproteins. Aggrecan is the major PG of articular cartilage, although, it can also be found in the dermis^{69,70}. Versican is the predominant PG in the ECM of the skin, where it interacts with important ECM proteins such as HA, fibulin, fibronectin, and elastin⁷¹. It is also involved in the regulation of cell adhesion, migration and inflammation⁶⁴.

2.4.1.2.2 Small leucine-rich proteoglycans

Small leucine-rich proteoglycans (SLRPs) are the largest family of PGs. SLRPs are a class of PGs characterised by a relatively small protein core of 36 - 42 kDa and have multiple leucine-rich structural motif flanked by cysteines. SLRPs are grouped into five classes based on evolutionary conservation, homology at the protein and genomic level, and chromosomal organisation. The first three classes are canonical PGs, and the last two are PGs that do not carry GAG sidechains. However, as they are categorised as PGs is because they share close structural homology and functional properties with other PGs. Class I SLRPs includes biglycan, decorin, asporin, extracellular matrix 2 (ECM2) and the ECMX protein; class II includes fibromodulin, lumican, osteosteadherin, keratocan, and the proline/arginine-rich end leucine-rich repeat protein (PRELP); class III includes epiphycan (PG-Lb), osteoglycin (mimecan), and opticin (oculoglycan).

Class I SLRPs:

Decorin

Decorin is the most abundant SLRP in skin, accounting for approximately 80 % of the total PG content⁷². It is named for its ability to decorate collagen fibrils, including type I, II, III, VI, and XIV collagen⁷³. Decorins consist of three domains; an N-terminal domain with a single CS or DS GAG chain, a central domain (core protein) of 10 leucine-rich repeats, and a Cys-rich C-terminal domain. The core protein binds non-covalently to the intraperiod site on the surface of collagen fibrils about every D period (67 nm)⁷⁴. It has also been shown that the decorin protein core binds close to the C-terminus of the type I collagen $\alpha 1$ chain, which is also near an intermolecular crosslinking site⁷⁵. Furthermore, reports have shown that the N-terminal GAG chain of decorin plays a role in the early stages of collagen fibrillogenesis, reducing the collagen fibril diameter, and increasing the interfibrillar spacing to ultimately inhibit fibrillogenesis^{76,77,78,79}. Experiments using decorin-null mice showed the loss of this gene resulted in a skin fragility phenotype caused by thinning of the dermis and a concomitant reduction in tensile strength, which was

directly linked to an abnormal collagen network^{80,81}. It has also been shown that the presence of decorin facilitates fibrillar slippage in skin, improving the tensile strength of the collagen fibre network⁸².

Biglycan

Biglycan contains two Ser-Gly attachment sites in its N-terminal region, thus, its eponym meaning two GAG chains⁸³. Biglycan is highly homologous to decorin, sharing over 65 % sequence homology. It is characterised by a protein core of 47 kDa with an attachment of two CS or DS chains. Unlike decorin that is abundant in the dermis, biglycans are heavily expressed in the bone and other non-skeletal connective tissue such as the basement membrane and the tissue sheath around the hair follicle⁸⁴. Research has shown that biglycan knockout mice have a thin dermis and irregular collagen fibril formation, although, the skin phenotype is not as severe as that in the decorin knockout mice. In addition, biglycan knockout mice showed a clinically important phenotype of reduced bone mass and mineral content, similar to an osteoporosis phenotype^{85,86}.

Class II SLRPs:

Lumican and PRELP

Lumican is the major keratan sulfate proteoglycan (KSPG) that is found to co-localise with fibrillar collagen in cornea, skin, tendon, and muscle connective tissues. It plays an essential role in cornea clarity by maintaining the interfibrillar space of the corneal collagen architecture⁶⁴. Lumican knockout mice have shown phenotypes such as corneal opacities together with skin laxity and fragility^{87,88}. PRELP (proline/arginine-rich end leucine-rich repeat protein), also known as prolargin, got its name from its unique N-terminal domain enriched basic amino acid residues⁸⁹. The protein functions as a molecule that anchors the basement membrane to the underlying connective tissue. It has been shown to bind type I collagen to the basement membrane and type II collagen to cartilage^{90,91}.

Class III SLRPs:

Epiphycan, opticin, and osteoglycin

Epiphycan and opticin are not usually found in skin, so will not be discussed further. Osteoglycin, also known as mimecan, is known to be involved in collagen fibrillogenesis, cell proliferation and development⁹². It can be found in the cornea, skin, cartilage, and aorta⁹³. It has also been shown that extracellular osteoglycin binds directly to collagen fibrils and aids in collagen crosslinking⁹⁴.

2.4.2 Glycosaminoglycans

Glycosaminoglycans (GAGs) comprise of six different types of long, linear polysaccharide chains with specific disaccharide units, including chondroitin sulfate (CS), dermatan sulfate (DS), keratan sulfate (KS), heparan sulfate (HS), heparin (HP), and hyaluronic acid (HA) (Table 3). Other than HA, all other GAGs are generally highly glycosylated on their core proteins, whereas HA is synthesised as a single polysaccharide chain without a core protein partner. GAGs are made up of repeating disaccharides containing either a glucuronic acid (GlcA) or iduronic acid (IdoA) linked to *N*-acetylglucosamine, GlcNAc or *N*-acetylgalactosamine, GalNAc. The saccharide units are sulfated on either C₄, C₆, and/or on the non-acetylated nitrogen (Fig. 4) by a class of enzymes called sulfotransferase (SULTs). Due to the sulfation of the sugar moieties, GAGs are negatively charged, including HA whose negative charge is due to glucuronic acid. The biological activity of GAGs depends on several factors, such as molecular weight, monosaccharide constituents, and bonds between the disaccharide repeating units⁹⁵.

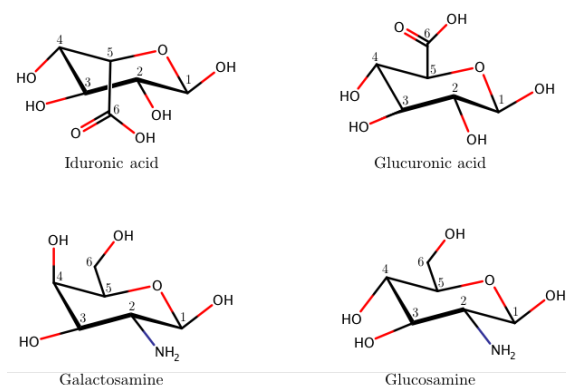


Figure 4: Structure of the saccharide moieties of GAGs.

2.4.2.1 Chondroitin sulfate

Chondroitin sulfate (CS) consists of repeating *N*-acetylgalactosamine (GalNAc)-glucuronic acid (GlcA) disaccharide units joined by β 1,4 and β 1,3 linkages, respectively. The *N*-acetylgalactosamine can have different degrees of sulfation on either the C₄ or C₆ OH groups of the sugar. When GalNAc is monosulfated on the C₄ the resulting GAG is called chondroitin-4-sulfate (CS-A), and when it's monosulfated on the C₆ it is called chondroitin-6-sulfate (CS-C). Glucuronic acid can also be monosulfated at C₂, and when it is linked to a monosulfated GalNAc, results in either a CS-B (4-sulfated GalNAc and 2-sulfated GlcA) or CS-D (6-sulfated GalNAc and 2-sulfated GlcA).⁹⁵

Table 3: Repeating disaccharide units of glycosaminoglycans.

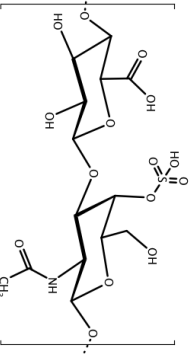
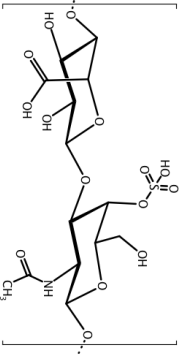
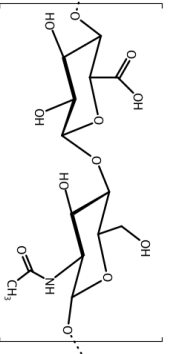
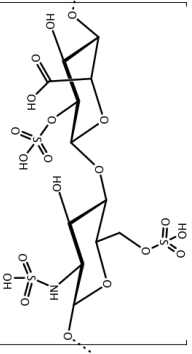
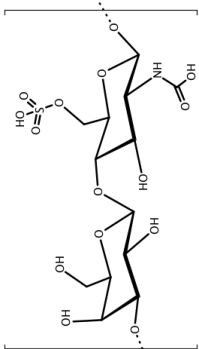
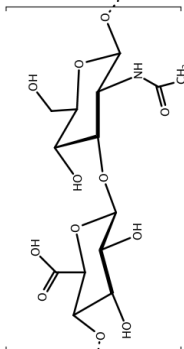
Glycosaminoglycan	Disaccharide unit	Molecular weight (kDa)	Location	Features
Chondroitin sulfate		5 - 50	Cartilage, tendon, ligament, aorta	Most abundant GAG in the body, binds to collagen to form PGs
Dermatan sulfate		15 - 40	Skin, heart valves, blood vessels	Key role in collagen fibrillogenesis, major GAG in skin
Heparin		10 - 12	Secretory granules of mast cells	Highest negative charge among all biomacromolecules
Heparan sulfate		10 - 70	Cell surfaces, ECM	Lower degree of modification compared to heparin

Table 3: Repeating disaccharide units of glycosaminoglycans (continued).

Glycosaminoglycan	Disaccharide unit	Molecular weight (kDa)	Location	Features
Keratan sulfate		4 - 19	KS I, cornea; KS II, cartilage KS III, brain	Most heterogeneous GAG, aggregates with CS
Hyaluronic acid		4 - 8000	ECM of connective tissue, synovial fluid, vitreous humour	Non-sulfated, non-covalently attached to proteins

Chondroitin sulfate is attached to core proteins, such as versican, and is one of the major components of the ECM. It is abundant in various biological tissues, including skin. Different sulfation patterns and lengths of chains attached to the core proteins result in different types of proteoglycans that have specific biological activities and functions⁷¹.

2.4.2.2 Dermatan sulfate

Dermatan sulfates (DSs) are stereoisomers of CSs, also known as chondroitin sulfate B (CS-B). They consist of repeating disaccharide units containing an IdoA and a GalNAc or GlcA joined by a β 1,3 linkage. DS is defined as a chondroitin sulfate by the presence of GalNAc; but, the presence of iduronic acid (IdoA) distinguishes it from CS-A and CS-C. Dermatan sulfates are the major GAGs found in skin as they are associated with decorin and biglycan. They bind to several types of collagens and elastic fibre components and are involved in collagen fibrillogenesis^{96,97,98}.

2.4.2.3 Heparin and heparan sulfate

Heparins (HPs) and heparan sulfates (HSs) are composed of repeating disaccharide units of GlcNAc-GlcA joined by α 1,4 and β 1,4 linkages, respectively. The sugars of the HP/HSs can be heavily modified, and thus, there are up to 24 different disaccharide units that can be formed from all the possible modifications of the monosaccharides⁹⁹. The modifications include *N*-deacetylation, *N*- and *O*-sulfation at different positions, resulting in glycan chains that are highly heterogeneous. They are not predominant in skin, so will not be discussed further.

2.4.2.4 Keratan sulfate

Keratan sulfates (KSs) are made up of repeating disaccharide units of galactose (Gal) and GlcNAc joined by a β 1,4 linkage¹⁰⁰. Depending on the linkages between the oligosaccharide and the core protein, keratan sulfates can be categorised into three types: 1) KS I, *N*-linked to Asn residues in the core protein; 2) KS II, *O*-linked to Ser or Thr residues in the core protein; 3) KS III, *O*-linked to Ser or Thr residues in the core protein *via* a mannose. KS polymers vary both in length and degree of sulfation on both sugar moieties. The sulfation on C₆ of the GlcNAc is found to be essential for the elongation of the KS chain, as sulfation and elongation occur concomitantly⁹⁵, and the C₆ on Gal can also be sulfated. Keratan sulfates are found in numerous epithelial tissues, and are responsible for cellular recognition, cell motility, among many other cellular functions¹⁰⁰. Lumican, a proteoglycan modified with KS, is essential for the regulation of collagen fibril assembly¹⁰¹.

2.4.2.5 Hyaluronic acid

Hyaluronic acid (HA) is composed of repeating disaccharide units of GlcA and GlcNAc joined by alternating β 1,3 and β 1,4 glycosidic bonds⁷¹. Unlike the other GAGs, HA is not sulfated and is a linear polyanion. The number of repeats can be as high as 20,000 and with a molecular weight of 8000 kDa. Due to its highly hydrophilic properties, HA can bind up to 1000-fold of its weight of H₂O molecules. This property is important for modulating tissue hydration and osmotic balance. Although HA is found primarily in the cartilage, synovial fluid, and the ECM of loose connective tissues, it has also been found intracellularly¹⁰², where it interacts with a number of receptors, resulting in the activation of signalling cascades that influence cell migration, proliferation, and gene expression¹⁰². In the ECM of the dermis, extracellular HA is either present as a free polymer or associates with PGs, such as versican, where it acts as a space filler and is responsible for absorbing shock⁷¹. It has been shown that when HA is crosslinked with other ECM proteins such as collagen a complex supramolecular structure forms that enhances the enzymatic resistance and the mechanical properties of collagen¹⁰³.

2.4.3 Methods used in this study for the analysis of GAGs

Many methods have been developed for the quantification of GAGs, including HPLC-based and dye-based spectrometric assays¹⁰⁴. In this study we have chosen a dye-based spectrometric assay using 1,9-dimethylmethylene blue (DMMB) that binds to sulfated GAGs and forms a precipitate. The precipitate is then dissolved and then dye released to produce a coloured solution whose absorbance can be measured spectroscopically.¹⁰⁵

2.5 Hair/wool

Mammalian hair and wool are both epidermal derivatives that are produced by the differentiation of germinative epidermal cells¹⁰⁶. Wool fibres are hairs, therefore for simplicity, the term hair is used. Hair has two separate structures: the hair follicle in the skin, and the hair shaft that is visible on the body surface. Hair shafts grow from hair follicles, epidermal structures that encloses the growing fibre and firmly anchor the hair in the dermis (Fig. 5).

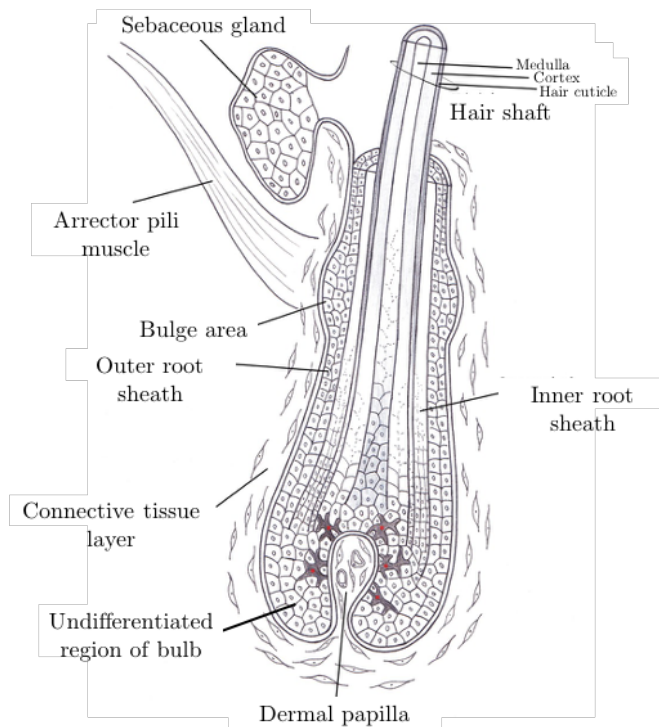


Figure 5: Diagram of the hair follicle structure. Reprinted from Buffoli (2014) with permission from the publisher¹⁰⁷.

2.5.1 Hair follicle

The layer of tissue that encloses a hair fibre is termed the hair follicle. Looking from the outside to the interior of the hair fibre, the structures are the connective tissue sheath (CTS), the basement membrane, the outer root sheath (ORS), the inner root sheath (IRS) and the hair bulb (Fig. 5). The connective tissue sheath surrounds the outside of the hair follicle and is connected with the dermis. It consists of collagen type I fibres and proteoglycans such as aggrecan, biglycan, and versican^{108,109}. Immediately adjacent the CTS is the basement membrane, which contains mostly proteoglycans, in particular, laminin, perlecan, and the glycoprotein nidogen, as well as collagen type IV¹¹⁰. The outer root sheath (ORS) is a region where multipotent stem cells, such as keratinocytes, are located. The inner root sheath (IRS) consists of three layers: Henle's layer, Huxley's layer, and the cuticle layer. The IRS cuticle layer adjoins the cuticle of the hair shaft, which anchors the hair shaft to the follicle. IRS cells produce keratins and trichohyalin that serve as an intracellular 'glue', giving strength to the IRS to support the growing hair shaft. An extensive review of the keratins found in different parts of the hair follicle was published by Moll *et al.* (2008)¹¹¹. The hair bulb at the base of the hair follicle, actively produces hair, and can be divided into two regions: a lower region containing

undifferentiated cells and an upper region where the cells are differentiated. The Auber's line, separates the two regions at the widest part of the papilla¹⁰⁷.

2.5.2 Hair shaft

The hair shaft consists of a cortex, cuticle cells, and in some cases, a medulla. The medulla is the central part of the hair, and is only present in the wool of only some New Zealand sheep breeds¹¹². The proportion of medullated fibres depends on a range of factors, including diet, season, and the age of the animal¹¹³. The cortex is composed of long keratinised cells and represents the majority of the hair fibre. Each cortical cell is made up of macrofibrils that are 0.05 to 0.2 μm in diameter and of variable length. The spaces between them are filled with degraded nuclei and other organelles. The macrofibrils are composed of microfibrillar rods made up from fibrous protein embedded in a matrix of amorphous protein and are approximately 7.5 nm in diameter¹⁰⁷. The cortex plays an important role in the physical and mechanical properties of hair. Scale-like cuticle cells made up from overlapping epidermal cells cover and protect the cortex from physical and chemical harm¹¹⁴.

2.6 Overview of the conventional leather making process

2.6.1 Preservation

Fresh skin is removed from the carcasses by hand flaying or mechanical pulling, before being washed with water to remove most of the dirt. Any remaining meat is then removed (fleshing) and if it cannot be processed immediately, the skin is dehydrated with 15 % (w/w) crystalline salt to minimise microbial putrefaction during storage.¹¹⁵

2.6.2 Depilation

Depilation is the process of removing hair from skin. Keratin and collagen are the two major protein components of wool and skin, respectively. Keratin is relatively resistant to acid but is rapidly attacked by sodium sulfide under strong alkaline conditions (pH 12 - 13); which breaks the disulfide bonds. Collagen on the other hand is susceptible to swelling in water that is weakly acidic or alkaline, and can be degraded by strong acid and base. In order to remove the wool, an alkaline solution containing sodium sulfide (Na_2S), sodium hydrosulfide (NaSH), sodium hydroxide (NaOH), and lime, (a mixture of calcium-containing inorganic material,

that includes calcium hydrosulfide ($\text{Ca}(\text{HS})_2$), and calcium hydroxide ($\text{Ca}(\text{OH})_2$), is painted on the flesh side of the pelt. The mixture soaks through the skin to reach the hair shaft where it acts to degrade the keratin at the pre-keratinised zone of the wool shaft. The high pH (12 - 13) of the solution is maintained by the NaOH and lime solution and results in the collagen fibres swelling and opening up to allow the sulfide to penetrate to the wool shaft detaching it from the skin. After soaking for two hours, the wool can be easily removed from the skin, either mechanically or by hand.¹¹⁵

2.6.3 Liming

The process known for liming is usually taken to completion during depilation. Its purpose is to swell the pelt to allow non-fibrous protein to be removed from the dermal layer. To achieve this, the skin that has been painted with the depilation solution is submerged in an alkaline solution, pH 12 to 13. The presence of alkali modifies the chemical properties of the collagen, hydrolysing amide groups on asparagine and glutamine to produce aspartic and glutamic acids, and the guanidine sidechain of arginine to produce ornithine¹¹⁵. These alkaline conditions will also hydrolyse peptide bonds, but because of its hierarchical fibrous structure, collagen hydrolysis proceeds much more slowly than that of globular proteins. Due to the difference in ionic concentration either side of the skin, it swells and as a result the collagen fibril bundles in the dermal layer split¹¹⁶. This causes the skin structure to open up, allowing the globular proteins and interfibrillary substances to be easily washed out. Unwanted fat components in the dermal layer are also saponified (*i.e.* converted into soap and glycerol) under the strong alkaline conditions used and removed during washing^{115,117}.

2.6.4 Deliming and bating

The process of deliming and bating are traditionally considered to be a single step, as the purpose of the former is to prepare the skin for the latter. Deliming is the process of lowering the pH of liming to one favouring bating. The most common and economical method is rinsing with water. Bating refers to the use of enzymes to remove any non-structural protein components in skin so that only collagen fibres remain¹¹⁶. As trypsin and chymotrypsin, are commonly used, the pH of the skin needs to be adjusted to between 8 and 9, for them to work efficiently. The hierarchical structure of collagen, together with its high proline concentration¹¹⁸, protects it from protease attack, and although there may be some cleavage of peptide bonds, the fibre structure remains intact^{115,119}.

2.6.5 Pickling

Pickling is a process that both preserves the skin and adjusts it to the conditions required for chrome tanning. The pH of the skin is lowered to between 2 and 3 through the addition of sulfuric acid (H_2SO_4) and sodium chloride (NaCl). The negatively charged carboxylate amino acid sidechains of collagen (Asp and Glu) become protonated enabling them to ligate chromium (III) during tanning. NaCl is added to prevent swelling because without it, differences in the ionic strength of the wet skin and the solutions used for pickling would result in the skin absorbing water and swelling. The presence of salt also aids in long-term preservation of skin, which is necessary, as pickled skins can sometimes be stored for up to a year before being further processed^{115,116,119}. As raw skins are also often salted before depilation to preserve them, the New Zealand leather industry is the largest consumer of salt in the country¹²⁰.

2.6.6 Degreasing

Sheepskins in New Zealand, Australia and the UK have a fat layer in the grain-corium junction, which has to be removed by a process called degreasing prior to tanning. If the fat content is not removed, it acts as a barrier to the penetration of tanning chemicals and may even cause odour when the fat turns rancid. Traditionally, pickled skins were treated with paraffin then rinsed with brine. However, this method has died out due to the use of organic solvent and detergents¹¹⁵.

2.6.7 Tanning

Tanning is a process in which the raw material of skin is permanently turned into a stable substance that resists heat, putrefaction by bacterial contamination and thermomechanical stress¹¹⁵. There are several ways in tanning pelts. The most common method is mineral tanning, particularly, chromium tanning, in which chromium (III) salts (commonly, chromium sulfate $\text{Cr}_2(\text{SO}_4)_3$) are incorporated into the collagen structure where they form inter- and intra-polypeptide crosslinks between the collagen molecules that make up the fibre structure. The pelt is incubated overnight in a solution containing the chromium salt at pH 3.7 - 3.9. After this process, the skin is called wet blue due to the colour of the protein carboxy-chromium complex.¹²¹

2.6.8 Neutralising, dyeing and fat liquoring

After tanning, the skin is neutralised by several rinses in a weak alkaline solution containing sodium formate (HCOONa) and sodium bicarbonate (NaHCO_3) to raise the pH to between 4.6 – 4.8¹¹⁵. It is then dyed to the desired colour. After dyeing, fat is added back into the skin by a process called fat liquoring to prevent the fibres sticking together during drying. As the leather dries, water is removed from the spaces between the collagen fibres, allowing undesirable interactions between the fibres. This is prevented by adding a thin coating of oil to the fibres to provide a lubricated surface allowing them to move freely relative to each other¹²².

2.6.9 Drying

During this step, water is removed from the system and therefore, the chemical condition is stabilised, and the final property of leather is determined.

2.7 Problems associated with conventional sulfide depilation

The conventional depilation process removes wool from the sheepskins by treating them with sodium sulfide solutions. This method is commonly being used as it is cost effective, reliable, and flexible. However, the leather industry is also a major contributor to world-wide environmental pollution due to the chemicals used in the pre-tanning processes. One third of this pollution is due to the sulfide and alkaline waste water from the depilation process¹²³. Under alkaline conditions, sulfides remain in solution. However, when the pH of the effluent (waste water) goes below 9.5, hydrogen sulfide (H_2S), a colourless, flammable gas that is poisonous when inhaled, is released. H_2S can cause irritation and inflammation of the eyes and damage to the respiratory system at low levels of exposure (10 - 20 ppm). At high concentrations (900 ppm), it can affect the nervous system and may lead to paralysis of the respiratory centre causing death^{124,125}. Furthermore, as a strong reducing agent, it interferes with the oxidation of organic wastes (*i.e.* hair/wool, proteins), and thus, contributes significantly to the chemical oxygen demand (COD) and biological oxygen demand (BOD) concentrations in waste water¹²⁶. In fact, H_2S is responsible for 50 - 70 % of the total load of COD and BOD in tannery waste water¹²⁷. Moreover, sulfide damages the quality of wool, by-product of depilation, significantly reducing its commercial value¹²⁸.

2.8 Other approaches to sulfide depilation

Although the sodium sulfide depilation method is the current standard for conventional sheepskin depilation, other chemical and physical depilation methods have also been reported in the literature and will be discussed in the following paragraphs.

2.8.1 Plucking, shearing, and scalding

Wool plucking involves the pulling of wool from the skin with no other pre-treatment. The major problem with this method is that although removing a stand of single hair is simple, a large force is required to remove all the wool from a pelt, which often results in severe damage to the skin¹²⁹. Currently, no technology exists for the commercial removal of wool through plucking. Shearing uses blades to remove any visible wool from sheepskins. However, the removal of wool is not complete as the remaining hair shaft is left in the hair follicle, and sulfide treatment is usually required to completely remove the wool from the hair follicle. Scalding involves heating of the skin to higher than 55 °C where the collagen fibre network undergoes thermal denaturation, and the wool root layers split apart resulting in the loosening of the wool. This procedure however damages the skin through thermal shrinkage and is thus no longer used in the leather industry.

2.8.2 Cryogenic depilation

Sheepskins are placed in liquid nitrogen at -195.8 °C where the wool becomes loose and can be removed with a comb or a brush¹³⁰. However, with extreme changes in temperature, the skin surface often cracks and the dermis becomes damaged. Though the mechanisms of this method have not been thoroughly investigated, the inventors believe that that extreme low temperature treatment of the skin opens the pores of the skin, exposing the wool shaft¹³⁰. However, because of the cost, this method would not be feasible on a commercial scale.

2.8.3 Chaotropic agents for depilation

Exposure of skins to chaotropic agents, substances that disrupt the hydrogen bonding network, have been used to depilate animal skins since the 1950's. In Australia, a method that uses acetic acid together with autolytic enzymes in the skins themselves, was commercially used to depilate sheepskins^{131,132}. The skins produced in this way unfortunately suffered damage to the grain layer. Schlosser *et*

al. (1986) developed a similar depilation method using a mixture of lactic acid and *Lactobacillus plantarum* culture and after five days of soaking, the wool could be easily removed¹³³. As both methods took an average of 3 -7 days to loosen the wool they were not further developed. It was postulated that the chaotropic agents acted by denaturing soluble substances in the epidermis and the hair root thereby loosening the hair in the hair follicle¹³⁴. It is also possible that the chaotropic agents had antimicrobial activity and controlled the growth of some of the environmental bacterial species at the beginning of the process, while allowing others to grow and secrete enzymes to bring about hair loosening⁷. As a result of these findings, chaotropes were shown to possibly be an effective addition to enzyme solutions for the depilation process.

2.8.4 Oxidative depilation

Oxidative depilation involves the use of strong oxidising agents such as hydrogen peroxide (H_2O_2), sodium percarbonate ($NaCO_3 \cdot 3H_2O_2$) or sodium chlorite ($NaClO_2$). The oxidant reacts with keratin to produce a soluble keratin sulfonic acid, which not damage the mature hair shaft as it only dissolves the soft pre-keratin. As a result, some short hairs remain after treatment¹³⁵. Oxidative depilation can be carried out in either acid or alkaline solutions, eliminating the use of sulfides^{135,136,137}. However, the presence of oxidising chemicals requires the whole process to be carefully managed and creates undesirable waste. Although options frequently appear in the literature, that claim to be safe and environmentally friendly, none has obtained industrial acceptance¹¹⁵.

2.8.5 Organic sulfur compound depilation

Organic compounds such as dithionite, thioglycolate and other "mercapto" type chemicals are commonly used in commercial removal of hair or wool. These compounds act as strong reducing agents, in the same way as sulfides. Although the risk of H_2S gas emission is reduced, the sulfur content in the effluent is not, and organo-sulphydryl by-products are produced. Furthermore, these organic compounds are much more expensive to compared to sodium sulfide¹³⁸.

2.8.6 Enzyme depilation

The use of enzymes to remove hair from animal skins is seen as a more environmentally friendly alternative compared to traditional methods. Some depilation enzymes identified in the laboratory do not require the use of sulfides,

thus avoiding H₂S release. Röme (1910) developed the first successful enzymatic depilation method termed the Arazym process in which pancreatic proteases were used under alkaline conditions¹³⁹. Since then, enzymes from a variety of origin (bacterial, fungal, and plant), have been tried and tested for their ability to depilate hides and pelts (Tables 4 and 5). The most common enzymes that have been incorporated into the processes are proteases that exhibit keratinase activity (Tables 4 and 5). Most enzymes depilate efficiently at alkaline pH over the course of 8 to 24 hours. The exception to this was the use of a *Lactobacillus* culture that depilated skin over 3 to 4 days at a pH value of 4.0¹³³. All of these enzymes were shown to cause little to no damage to the surface of the skin by microscopy (*e.g.* scanning electron microscopy). Skins that had been depilated were also subjected to physical tests (*e.g.* tensile strength, tear strength, and shrinkage temperature measurements) and most of them showed no significant differences to the skins depilated using the conventional sulfide method.

The use of enzymes, however, doesn't entirely exclude the use of the harsh chemical sodium sulfide. In some cases, adding sulfide to the enzyme mixture was necessary to improve depilation efficiency^{128,140,141,142,143}. Furthermore, current enzymatic depilation treatments require the purchase of recombinant enzymes, which cost more than the chemicals currently used. Although a handful of commercial depilation enzymes are currently available (Table 5), only limited research has been carried out on their depilation efficacy on an industrial scale. In fact, most enzymatic depilation trials have only been done on a laboratory scale^{144,145}. Reports on their use have also shown that not all wool or hair is completely removed, and the process requires the addition of substantial amounts of sulfide to achieve uniformity. Also, as enzymes are difficult to control, the skin can become damaged through the lack of precise control of temperature and the time of enzyme exposure. For these reasons the use of enzymes to depilate skins has not been adopted by the industry and a more affordable and controllable way remains to be discovered/developed.

Table 4: Enzymes used to depilate skin on a laboratory scale.

Enzyme	Microorganism	Treatment condition	Reference
Protease	<i>Aspergillus flavus</i> IMI 327634	20 hr, 32 °C, pH 9.0	146
Protease Amylase	<i>Aspergillus tamarii</i> MTCC 5152	18 hr, 30 °C, pH 9.0	147
Protease	<i>Bacillus altitudinis</i> GVC11	18 hr, 30 °C	148
Protease	<i>Bacillus cereus</i> MCM B-326	21 hr, 30 °C, pH 7.0	149
Protease	<i>Bacillus licheniformis</i> SBP-144	8 hr, 30 °C, pH 8.0	150
Protease	<i>Bacillus megaterium</i> DSM 319	16 hr, 30 °C, pH 8.0, *	143
Protease	<i>Bacillus pumilus</i> CBS	8 hr, 37 °C	151
Protease	<i>Bacillus sp.</i> SB12	12 hr, 37 °C, pH 9.0	152
Protease	<i>Bacillus subtilis</i> MTCC 6537	6 hr, pH 7.5, *	142
Protease	<i>Bacillus subtilis</i> S14	9 hr, 24 °C, pH 9.0	153
Protease	<i>Brevibacillus brevis</i> US575	10 hr, 37 °C	154
Protease	<i>Brevibacterium luteolum</i> MTCC 5982	8 hr, pH 9.0	155
Protease	<i>Bromeliaceae</i> species	24 hr, 25 °C	156
Protease	<i>Calotropis procera</i>	24 hr, 30 °C, *	141
Protease	<i>Conidiobolus brefeldianus</i> MTCC 5158	16 hr, 30 °C, pH 8.0	157
Protease	<i>Exiguobacterium sp.</i> DG1	24 hr, RT	158
Protease	<i>Idiomarina sp.</i> C9-1	10 hr, 40 °C, pH 9.0	159
Unknown substance	<i>Lactobacillus plantarum</i>	4 - 5 days, RT, pH 4.0	133
Protease	<i>Paenibacillus woosongensis</i> TKB2	14 hr, pH 8.0	160
Protease	<i>Pseudomonas aeruginosa</i> MCM B-327	16 hr, pH 8.0	161
Protease	<i>Pseudomonas fluorescens</i>	18 hr, pH 10.5, *	140
Protease	<i>Vibrio metschnikovii</i> MTCC 11401	16 hr, 25 °C, pH 8.0	162

* sulfide is needed in the enzymatic depilation treatment

Table 5: Examples of commercial depilation enzymes.

Name of commercial depilation enzyme	Type	Conditions	Reference
NovoLime [®]	Protease/lipase	—	163
Fibrozyme	Protease/amylase	12 hr, pH 8.5	164,165
Buzyme 7703	Protease		
Buzyme 2013	Lipase	12 hr, 28 °C, pH 12.0, *	145,166,167
Tanzyme CD 05	Protease		
Tanzyme DG	Lipase		
Riberzyme MPX	Protease	16 hr, 28 °C, *	144
Erhavis MC	Protease		

* sulfide is needed in the enzymatic depilation treatment.

2.9 'Omics' methods used in this study

The use of 'omic' techniques (*i.e.* proteomics, metabolomics, metagenomics, and transcriptomics) has gained attention in the past two decades to answer complex biological questions. Omics techniques provide a more comprehensive perspective on complex biological problems compared to traditional approaches. In this study, mass spectrometry-based bottom-up proteomics was used for the identification and relative quantitation of the proteins found in processed skin samples (Chapter 4). With the recent technological developments in mass spectrometry, such as improved sensitivity, speed and affordability, the identification of a wide range of low-abundance proteins in complex mixtures has become achievable. Two approaches are available for a proteomic-based quantitation study, labelled and label-free. In this study, a label-free approach was chosen for several reasons: (a) the simpler sample preparation workflow, (b) the cost of the labels, (c) flexibility in study design. Whilst the absolute abundances of chemically labelled proteins can be reliably measured, label-free quantitation measures spectral counts and therefore relative amounts of an analyte. In this method, the number of MSMS spectra originating from the same protein in each LC-MS/MS data set is compared. An increase in protein abundance usually results in an increase in the number of tryptic peptides produced from that protein which in turn results in an

increase in the total number of MSMS spectra for that protein. However the technique is heavily reliant on other parameters, such as normalisation of spectral counting datasets and statistical analysis. Normalisation is achieved through careful monitoring of sample concentration, the total ion chromatogram (TIC) of each sample prior to data acquisition, and manual normalisation based on the total spectral counts measured after data acquisition¹⁶⁸. Besides the identification and relative quantitation of proteins in the mixture, proteomics data can also provide information about the protein isoforms, and post-translational modifications¹⁶⁹.

Metabolomic fingerprinting was used in this study for the identification and relative quantitation of small molecules (generally smaller than 1000 Da) in the depilation solution that possess potential antimicrobial properties (Chapter 5). Several analytical platforms have been used for metabolomic applications, such as nuclear magnetic resonance (NMR), Fourier transform-infrared spectroscopy (FT-IR), and mass spectrometry. In our study, a mass spectrometry-based technique was chosen due to the complexity of the mixture (containing molecules from sheepskin, also microbial metabolites and a high concentration of lactose). To increase the signal to noise ratio and data quality (due to reduced background noise), samples are commonly fractionated using liquid chromatography prior to mass spectrometry analysis. The choice of column is of utmost importance for such studies, as metabolites can be both polar and non-polar. Therefore as well as the commonly used reversed phase chromatography (C₁₈), it is advisable to consider the use of other stationary phases that cater for more polar molecules such as hydrophilic interaction chromatography column (HILIC). Electrospray ionisation (ESI) mass spectrometry is usually combined with LC, and to obtain a broad coverage, ionisation should be performed in both positive and negative mode.¹⁷⁰

Culture-based techniques are traditionally used to isolate and identify microorganisms from either liquid media or solid surfaces. This involves growing the microorganisms in appropriate culture media, at an appropriate temperature and under aerobic or anaerobic conditions. Identification of microorganisms, especially at the species level, requires isolation of genomic DNA followed by the amplification of DNA sequences, usually ribosomal gene sequences, using specific primers. The 16S rRNA gene sequence is 1550 base pairs long and contains nine hypervariable (V1 - V9) regions that can provide species identification of bacteria (Fig. 6). Other regions of the sequence that can be used to identify fungi are nuclear ribosomal internal transcribed spacer (ITS) sequences¹⁷¹ (Fig. 6). Unfortunately, culture methods can only confirm the presence of microorganisms

that can grow on available media. It has been estimated that less than 1 % of the prokaryotes in most environments can be cultivated using such methods¹⁷². Therefore, culturing techniques may not be the most effective way to identify the presence of all microorganisms inhabiting a particular environment, especially unusual ones. The advances in next generation sequencing (NGS) has led to the establishment of the field of metagenomics. Metagenomics is the culture-independent genomic analysis of genetic material recovered directly from an 'environment' without prior need for culturing. Full shotgun metagenomics and marker gene amplification metagenomics are two methods used to analyse the microbiome. The first analyses the collective microbial genomes in the sample, and the latter uses the polymerase chain reaction (PCR) to amplify specific genes of interest. Difficulties arise however, when eukaryote and microbial DNA is present in the same sample, as some primers are not specific for prokaryote DNA¹⁷³. The choice of the 16S rRNA gene-encoding hypervariable regions or nuclear ribosomal ITS regions for amplification, and the primers that recognise them is therefore very important. Due to the variety of these sequences in each microorganism, primers do not have a similar affinity for all the possible DNA sequences of these regions, which introduces bias during PCR amplification¹⁷⁴. Using a more variable region enables the detection of different taxa within a community. Other sources of introduced bias include marker gene selection, amplicon size, and the number of PCR cycles^{175,176}.

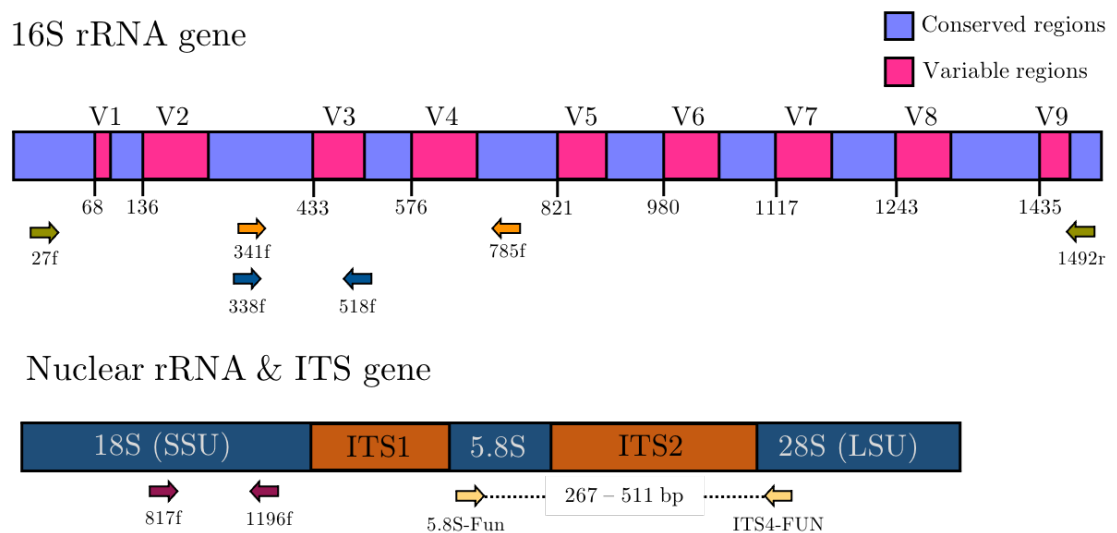


Figure 6: Map of ribosomal DNA indicating variable regions as well as the primers used in this study.

The QIIME2™ platform is commonly used for 16S rRNA and ITS amplicon sequence analysis¹⁷⁷. After the raw sequence data is imported, primer and adaptor sequences are removed and the sequences are denoised, using DADA2¹⁷⁸. The resulting output is a table of DNA sequences (representative sequences, rep-seqs) and counts of these DNA sequences per sample (feature-table). Taxonomic assignment is done first by training the SILVA¹⁷⁹ (16S rDNA) or UNITE¹⁸⁰ (ITS) database using a machine learning approach, (the naive Bayesian classifier¹⁸¹), to assign the representative sequences. However, due to the large number of unknown taxa, taxonomic resolution is poor and most sequences can only be assigned to the genus level¹⁷⁴. For species level identification, information on other house-keeping genes for DNA gyrase subunit B (*gyrB*), the TU elongation factor (*tuf*), and the 60 kDa chaperonin (*cpn60*) are often required¹⁸². The generated taxonomic data is a matrix that relates feature abundance to samples and can be subjected to alpha (species richness within individual samples) and beta (similarity between samples) diversity analysis for the investigation of the overall patterns in microbiome variation.

2.10 References

- [1] M. Venus, J. Waterman, and I. McNab. Basic physiology of the skin. *Surgery (Oxford)*, 29(10):471–474, 2011. ISSN 0263-9319. doi: <https://doi.org/10.1016/j.mpsur.2011.06.010>. URL <http://www.sciencedirect.com/science/article/pii/S0263931911001311>.
- [2] D. R. Visser. *Unravelling the molecular contributions to collagen higher order structure: a thesis presented in partial fulfilment of the requirements for the degree of Master of Science in Biochemistry at Massey University, Manawatu, New Zealand*. Thesis, Massey University, 2019.
- [3] C. Frantz, K. M. Stewart, and V. M. Weaver. The extracellular matrix at a glance. *J. Cell Sci.*, 123(24):4195, 2010. doi: 10.1242/jcs.023820. URL <http://jcs.biologists.org/content/123/24/4195.abstract>.
- [4] R. L. Edmonds, D. S. Choudhury, R. G. Haverkamp, M. Birtles, T. F. Allsop, and G. E. Norris. Using proteomics, immunohistology, and atomic force microscopy to characterize surface damage to lambskins observed after enzymatic dewooling. *J. Agric. Food. Chem.*, 56(17):7934–7941, 2008. ISSN 0021-8561. doi: 10.1021/jf800380y. URL <https://doi.org/10.1021/jf800380y>.
- [5] V. L. Addy, A. D. Covington, D. A. Langridge, and A. Watts. Microscopy methods to study fat cells. Part 1: Characterisation of ovine cutaneous lipids using microscopy. *J. Soc. Leath. Tech. Ch.*, 85(1):6–15, 2001. ISSN 0144-0322.

- [6] B. M. Haines and J. R. Barlow. The anatomy of leather. *J. Mater. Sci.*, 10(3):525–538, 1975. ISSN 1573-4803. doi: 10.1007/BF00543698. URL <https://doi.org/10.1007/BF00543698>.
- [7] R. L. Edmonds. *Proteolytic depilation of lambskins : a thesis presented in partial fulfilment of the requirements for the degree of Doctor of philosophy in Bioprocess Engineering at Massey University, Palmerston North, New Zealand*. Thesis, Massey University, 2008. URL <http://hdl.handle.net/10179/892>.
- [8] J. Uitto, D. R. Olsen, and M. J. Fazio. Extracellular matrix of the skin: 50 years of progress. *J. Invest. Dermatol.*, 92(4, Supplement):S61–S77, 1989. ISSN 0022-202X. doi: <https://doi.org/10.1038/jid.1989.34>. URL <http://www.sciencedirect.com/science/article/pii/S0022202X89907999>.
- [9] D. J. S. Hulmes. *Collagen diversity, synthesis and assembly*, pages 15–47. Springer US, Boston, MA, 2008. ISBN 978-0-387-73906-9. doi: 10.1007/978-0-387-73906-9_2. URL https://doi.org/10.1007/978-0-387-73906-9_2.
- [10] A. Soroushanova, L. M. Delgado, Z. Wu, N. Shologu, A. Kshirsagar, R. Raghunath, A. M. Mullen, Y. Bayon, A. Pandit, and M. Raghunath. The collagen suprafamily: from biosynthesis to advanced biomaterial development. *Adv. Mater.*, 31(1):1801651, 2019. ISSN 0935-9648.
- [11] C. A. Maidment, M. Ahn, R. Naffa, T. S. Loo, and G. E. Norris. Comparative analysis of the proteomic profile of cattle hides that produce loose and tight leather using in-gel tryptic digestion followed by LC-MS/MS. *J. Am. Leather Chem. Assoc.*, 115(11):399–408, 2020. ISSN 0002-9726.
- [12] L. M. Mikesch, L. R. Aramadhaka, C. Moskaluk, P. Zigrino, C. Mauch, and J. W. Fox. Proteomic anatomy of human skin. *J. Proteomics*, 84:190–200, 2013. ISSN 1874-3919. doi: 10.1016/j.jprot.2013.03.019.
- [13] D. E. Birk and P. Brückner. *Collagens, suprastructures, and collagen fibril assembly*, pages 77–115. Springer, 2011.
- [14] M. D. Shoulders and R. T. Raines. Collagen structure and stability. *Annu. Rev. Biochem.*, 78:929–58, 2009. ISSN 0066-4154. doi: 10.1146/annurev.biochem.77.032207.120833.
- [15] C. M. Kielty and M. E. Grant. *The collagen family: structure, assembly, and organization in the extracellular matrix*, pages 159–221. Wiley-Liss, Inc., 2002.
- [16] P. Fratzl. *Collagen: structure and mechanics, an introduction*, pages 1–13. Springer, 2008.

- [17] J. Gross and F. O. Schmitt. The structure of human skin collagen as studied with the electron microscope. *J. Exp. Med.*, 88(5):555–68, 1948. ISSN 0022-1007 (Print) 0022-1007. doi: 10.1084/jem.88.5.555.
- [18] A. Veis and K. Payne. *Collagen fibrillogenesis*, pages 113–138. CRC Press, 2018. ISBN 1351070797.
- [19] R. Naffa. *Understanding the molecular basis of the strength differences in skins used in leather manufacture : a dissertation presented in partial fulfillment of the requirements for the degree of Doctor of Philosophy at Massey University, Palmerston North, New Zealand*. Thesis, Massey University, 2017. URL <http://hdl.handle.net/10179/13154>.
- [20] R. E. Neuman and M. A. Logan. The determination of hydroxyproline. *J. Biol. Chem.*, 184(1):299–306, 1950. ISSN 0021-9258 (Print) 0021-9258.
- [21] S. A. Cohen and D. P. Michaud. Synthesis of a fluorescent derivatizing reagent, 6-aminoquinolyl-N-hydroxysuccinimidyl carbamate, and its application for the analysis of hydrolysate amino acids via high-performance liquid chromatography. *Anal. Biochem.*, 211(2):279–287, 1993. ISSN 0003-2697.
- [22] M. Yamauchi and M. Sricholpech. Lysine post-translational modifications of collagen. *Essays Biochem.*, 52:113–133, 2012. ISSN 1744-1358 0071-1365. doi: 10.1042/bse0520113. URL <https://pubmed.ncbi.nlm.nih.gov/22708567>.
- [23] J. Gaar, R. Naffa, and M. A. Brimble. Enzymatic and non-enzymatic crosslinks found in collagen and elastin and their chemical synthesis. *Org. Chem. Front.*, 2020.
- [24] N. C. Avery and A. J. Bailey. The effects of the Maillard reaction on the physical properties and cell interactions of collagen. *Pathol. Biol.*, 54(7):387–95, 2006. ISSN 0369-8114 (Print) 0369-8114. doi: 10.1016/j.patbio.2006.07.005.
- [25] L. I. Smith-Mungo and H. M. Kagan. Lysyl oxidase: properties, regulation and multiple functions in biology. *Matrix Biol.*, 16(7):387–398, 1998. ISSN 0945-053X. doi: [https://doi.org/10.1016/S0945-053X\(98\)90012-9](https://doi.org/10.1016/S0945-053X(98)90012-9). URL <http://www.sciencedirect.com/science/article/pii/S0945053X98900129>.
- [26] D. M. Hudson, M. A. Weis, and D. R. Eyre. *Collagen cross-linking and bone pathobiology*, pages 339–358. Elsevier, 2020.
- [27] D. R. Eyre, M. A. Paz, and P. M. Gallop. Cross-linking in collagen and elastin. *Annu. Rev. Biochem.*, 53(1):717–748, 1984. ISSN 0066-4154.
- [28] G. Mechanic, P. M. Gallop, and M. L. Tanzer. The nature of crosslinking in collagens from mineralized tissues. *Biochem. Biophys. Res. Commun.*, 45(3):644–653, 1971. ISSN 0006-291X.

- [29] A. J. Bailey and M. S. Shimokomaki. Age related changes in the reducible cross-links of collagen. *FEBS Lett.*, 16(2):86–88, 1971. ISSN 0014-5793. doi: [https://doi.org/10.1016/0014-5793\(71\)80338-1](https://doi.org/10.1016/0014-5793(71)80338-1). URL <http://www.sciencedirect.com/science/article/pii/0014579371803381>.
- [30] N. R. Davis. Stable crosslinks of collagen. *Biochem. Biophys. Res. Commun.*, 54(3):914–922, 1973. ISSN 0006-291X. doi: [https://doi.org/10.1016/0006-291X\(73\)90781-X](https://doi.org/10.1016/0006-291X(73)90781-X). URL <http://www.sciencedirect.com/science/article/pii/0006291X7390781X>.
- [31] A. J. Bailey, R. G. Paul, and L. Knott. Mechanisms of maturation and ageing of collagen. *Mech. Ageing Dev.*, 106(1-2):1–56, 1998. ISSN 0047-6374.
- [32] L. Knott and A. J. Bailey. Collagen cross-links in mineralizing tissues: a review of their chemistry, function, and clinical relevance. *Bone*, 22(3):181–187, 1998. ISSN 8756-3282.
- [33] J. E. Scott, E. W. Hughes, and A. Shuttleworth. A collagen-associated Ehrlich chromogen: a pyrrolic cross-link? *Biosci. Rep.*, 1(8):611–618, 1981. ISSN 0144-8463.
- [34] R. Kuypers, M. Tyler, L. B. Kurth, I. D. Jenkins, and D. J. Horgan. Identification of the loci of the collagen-associated Ehrlich chromogen in type I collagen confirms its role as a trivalent cross-link. *Biochem. J.*, 283(1):129–136, 1992. ISSN 0264-6021.
- [35] D. A. Hanson and D. R. Eyre. Molecular site specificity of pyridinoline and pyrrole cross-links in type I collagen of human bone. *J. Biol. Chem.*, 271(43):26508–26516, 1996. ISSN 0021-9258.
- [36] D. Fujimoto, K-Y. Akiba, and N. Nakamura. Isolation and characterization of a fluorescent material in bovine achilles tendon collagen. *Biochem. Biophys. Res. Commun.*, 76(4):1124–1129, 1977. ISSN 0006-291X.
- [37] D. F. Elsdon, N. D. Light, and A. J. Bailey. An investigation of pyridinoline, a putative collagen cross-link. *Biochem. J.*, 185(2):531–534, 1980. ISSN 0264-6021.
- [38] T. J. Koob, D. R. Eyre, and K. P. Van Ness. Defection and photolysis of hydroxypyridinium cross-links in cartilage collagen *in situ*. *Trans. Ortho. Res. Soc.*, 8:23–25, 1983.
- [39] S. Sakura and D. Fujimoto. Electrochemical behaviour of pyridinoline, a crosslinking amino acid of collagen. *J. Biochem.*, 89(5):1541–1546, 1981. ISSN 0021-924X.
- [40] T. Ogawa, T. Ono, M. Tsuda, and Y. Kawanishi. A novel fluor in insoluble collagen: a crosslinking moiety in collagen molecule. *Biochem. Biophys. Res. Commun.*, 107(4):1252–1257, 1982. ISSN 0006-291X.

- [41] D. R. Eyre and H. Oguchi. The hydroxypyridinium crosslinks of skeletal collagens: their measurement, properties and a proposed pathway of formation. *Biochem. Biophys. Res. Commun.*, 92(2):403–410, 1980. ISSN 0006-291X.
- [42] D. R. Eyre, M. A. Weis, and J. Rai. Analyses of lysine aldehyde cross-linking in collagen reveal that the mature cross-link histidinohydroxylysinonorleucine is an artifact. *J. Biol. Chem.*, 294(16):6578–6590, 2019. ISSN 0021-9258.
- [43] S. P. Robins and A. Duncan. Cross-linking of collagen. Location of pyridinoline in bovine articular cartilage at two sites of the molecule. *Biochem. J.*, 215(1):175–182, 1983. ISSN 0264-6021.
- [44] M. Yamauchi, D. T. Woodley, and G. L. Mechanic. Aging and cross-linking of skin collagen. *Biochem. Biophys. Res. Commun.*, 152(2):898–903, 1988. ISSN 0006-291X (Print) 0006-291x. doi: 10.1016/s0006-291x(88)80124-4.
- [45] E. C. Naylor, R. E. B. Watson, and M. J. Sherratt. Molecular aspects of skin ageing. *Maturitas*, 69(3):249–256, 2011. ISSN 0378-5122.
- [46] M. L. Tanzer, T. Housley, L. Berube, R. Fairweather, C. Franzblau, and P. M. Gallop. Structure of two histidine-containing cross-links from collagen. *J. Biol. Chem.*, 248(2):393–402, 1973. ISSN 0021-9258.
- [47] M. Yamauchi, R. E. London, C. Guenat, F. Hashimoto, and G. L. Mechanic. Structure and formation of a stable histidine-based trifunctional cross-link in skin collagen. *J. Biol. Chem.*, 262(24):11428–11434, 1987. ISSN 0021-9258. URL <http://europepmc.org/abstract/MED/3624221>.
- [48] D. R. Eyre, M. A. Weis, and J. Rai. Reply to Yamauchi *et al.*: Analyses of lysine aldehyde cross-linking in collagen reveal that the mature cross-link histidinohydroxylysinonorleucine is an artifact. *J. Biol. Chem.*, 294(38):14164–14164, 2019. ISSN 0021-9258.
- [49] M. Yamauchi, Y. Taga, and M. Terajima. Analyses of lysine aldehyde cross-linking in collagen reveal that the mature cross-link histidinohydroxylysinonorleucine is an artifact. *J. Biol. Chem.*, 294(38):14163–14163, 2019. ISSN 0021-9258.
- [50] D. R. Eyre, M. A. Weis, and J-J. Wu. Advances in collagen cross-link analysis. *Methods*, 45(1):65–74, 2008. ISSN 1046-2023.
- [51] P. H. Bernstein and G. L. Mechanic. A natural histidine-based imminium cross-link in collagen and its location. *J. Biol. Chem.*, 255(21):10414–10422, 1980. ISSN 0021-9258.
- [52] E. Hunt and H. R. Morris. Collagen cross-links. A mass-spectrometric and ^1H - and ^{13}C -nuclear-magnetic-resonance study. *Biochem. J.*, 135(4):833–843, 1973. ISSN 0264-6021.

- [53] K. M. Reiser, S. M. Hennessy, and J. A. Last. Analysis of age-associated changes in collagen crosslinking in the skin and lung in monkeys and rats. *Biochim. Biophys. Acta, Gen. Subjects*, 926(3):339–348, 1987. ISSN 0304-4165.
- [54] S. P. Robins and A. J. Bailey. The chemistry of the collagen cross-links. the characterization of fraction C, a possible artifact produced during the reduction of collagen fibres with borohydride. *Biochem. J.*, 135(4):657–665, 1973. ISSN 0264-6021.
- [55] M. Rojkind, O. O. Blumenfeld, and P. M. Gallop. Localization and partial characterization of an aldehydic component in tropocollagen. *J. Biol. Chem.*, 241(7):1530–1536, 1966. ISSN 0021-9258.
- [56] M. Stammers, I. M. Ivanova, I. S. Niewczas, A. Segonds-Pichon, M. Streeter, D. A. Spiegel, and J. Clark. Age-related changes in the physical properties, cross-linking, and glycation of collagen from mouse tail tendon. *J. Biol. Chem.*, 295(31):10562–10571, 2020. ISSN 0021-9258. doi: 10.1074/jbc.RA119.011031.
- [57] M. L. Tanzer, R. Fairweather, and P. M. Gallop. Isolation of the crosslink, hydroxymerodesmosine, from borohydride-reduced collagen. *Biochim. Biophys. Acta, Protein Struct.*, 310(1):130–136, 1973. ISSN 0005-2795.
- [58] E. Gineyts, O. Borel, R. Chapurlat, and P. Garnero. Quantification of immature and mature collagen crosslinks by liquid chromatography-electrospray ionization mass spectrometry in connective tissues. *J. Chromatogr. B. Analyt. Technol. Biomed. Life Sci.*, 878(19):1449–54, 2010. ISSN 1570-0232. doi: 10.1016/j.jchromb.2010.03.039.
- [59] T. J. Sims and A. J. Bailey. Quantitative analysis of collagen and elastin cross-links using a single-column system. *J. Chromatogr.*, 582(1-2):49–55, 1992. doi: 10.1016/0378-4347(92)80301-6.
- [60] R. Naffa, G. Holmes, M. Ahn, D. Harding, and G. E. Norris. Liquid chromatography-electrospray ionization mass spectrometry for the simultaneous quantitation of collagen and elastin crosslinks. *J. Chromatogr. A*, 1478:60–67, 2016. ISSN 0021-9673. doi: 10.1016/j.chroma.2016.11.060.
- [61] R. L. Jackson, S. J. Busch, and A. D. Cardin. Glycosaminoglycans: molecular properties, protein interactions, and role in physiological processes. *Physiol. Rev.*, 71(2):481–539, 1991. ISSN 0031-9333 (Print) 0031-9333. doi: 10.1152/physrev.1991.71.2.481.
- [62] J. D. S. Antonio and R. V. Lozzo. *Glycosaminoglycans: structure and biological functions*. eLS, 2001. doi: 10.1038/npg.els.0000704. URL <https://onlinelibrary.wiley.com/doi/abs/10.1038/npg.els.0000704>.

- [63] D. P. Gamblin, E. M. Scanlan, and B. G. Davis. Glycoprotein synthesis: an update. *Chem. Rev.*, 109(1):131–163, 2009. ISSN 0009-2665. doi: 10.1021/cr078291i. URL <https://doi.org/10.1021/cr078291i>.
- [64] R. V. Iozzo and L. Schaefer. Proteoglycan form and function: a comprehensive nomenclature of proteoglycans. *Matrix Biol.*, 42:11–55, 2015. ISSN 0945-053X. doi: <https://doi.org/10.1016/j.matbio.2015.02.003>. URL <http://www.sciencedirect.com/science/article/pii/S0945053X15000402>.
- [65] I. Sher, S. Zisman-Rozen, L. Eliahu, J. M. Whitelock, N. Maas-Szabowski, Y. Yamada, D. Breitkreutz, N. E. Fusenig, E. Arikawa-Hirasawa, and R. V. Iozzo. Targeting perlecan in human keratinocytes reveals novel roles for perlecan in epidermal formation. *J. Biol. Chem.*, 281(8):5178–5187, 2006. ISSN 0021-9258.
- [66] M. P. Daniels. The role of agrin in synaptic development, plasticity and signaling in the central nervous system. *Neurochem. Int.*, 61(6):848–53, 2012. ISSN 0197-0186 (Print) 0197-0186. doi: 10.1016/j.neuint.2012.02.028.
- [67] A. J. Groffen, M. A. Ruegg, H. Dijkman, T. J. van de Velden, C. A. Buskens, J. van den Born, K. J. Assmann, L. A. Monnens, J. H. Veerkamp, and L. P. van den Heuvel. Agrin is a major heparan sulfate proteoglycan in the human glomerular basement membrane. *J. Histochem. Cytochem.*, 46(1):19–27, 1998. ISSN 0022-1554 (Print) 0022-1554. doi: 10.1177/002215549804600104.
- [68] M. S. O’Reilly, T. Boehm, Y. Shing, N. Fukai, G. Vasios, W. S. Lane, E. Flynn, J. R. Birkhead, B. R. Olsen, and J. Folkman. Endostatin: an endogenous inhibitor of angiogenesis and tumor growth. *Cell*, 88(2):277–85, 1997. ISSN 0092-8674 (Print) 0092-8674. doi: 10.1016/s0092-8674(00)81848-6.
- [69] C. Kiani, L. Chen, Y. J. Wu, A. J. Yee, and B. B. Yang. Structure and function of aggrecan. *Cell Res.*, 12(1):19–32, 2002. ISSN 1748-7838. doi: 10.1038/sj.cr.7290106. URL <https://doi.org/10.1038/sj.cr.7290106>.
- [70] G. E. Westgate, A. G. Messenger, L. P. Watson, and W. T. Gibson. Distribution of proteoglycans during the hair growth cycle in human skin. *J. Invest. Dermatol.*, 96(2):191–195, 1991. ISSN 0022-202X. doi: 10.1111/1523-1747.ep12461019. URL <http://europepmc.org/abstract/MED/1704038>.
- [71] D. H. Lee, J-H. Oh, and J. H. Chung. Glycosaminoglycan and proteoglycan in skin aging. *J. Dermatol. Sci.*, 83(3):174–181, 2016. ISSN 0923-1811.
- [72] C. T. Thorpe, H. L. Birch, P. D. Clegg, and H. R. Screen. The role of the non-collagenous matrix in tendon function. *Int. J. Exp. Pathol.*, 94(4):248–59, 2013. ISSN 0959-9673 (Print) 0959-9673. doi: 10.1111/iep.12027.

- [73] E. Ruoslahti. Structure and biology of proteoglycans. *Annu. Rev. Cell. Biol.*, 4:229–55, 1988. ISSN 0743-4634 (Print) 0743-4634. doi: 10.1146/annurev.cb.04.110188.001305.
- [74] J. E. Scott. Proteoglycan-fibrillar collagen interactions. *Biochem. J.*, 252(2):313–323, 1988. ISSN 0264-6021 1470-8728. doi: 10.1042/bj2520313. URL <https://pubmed.ncbi.nlm.nih.gov/3046606>.
- [75] D. R. Keene, J. D. San Antonio, R. Mayne, D. J. McQuillan, G. Sarris, S. A. Santoro, and R. V. Iozzo. Decorin binds near the C terminus of type I collagen. *J. Biol. Chem.*, 275(29):21801–4, 2000. ISSN 0021-9258 (Print) 0021-9258. doi: 10.1074/jbc.C000278200.
- [76] A. A. Dunkman, M. R. Buckley, M. J. Mienaltowski, S. M. Adams, S. J. Thomas, L. Satchell, A. Kumar, L. Pathmanathan, D. P. Beason, R. V. Iozzo, D. E. Birk, and L. J. Soslowsky. Decorin expression is important for age-related changes in tendon structure and mechanical properties. *Matrix Biol.*, 32(1):3–13, 2013. ISSN 0945-053X. doi: <https://doi.org/10.1016/j.matbio.2012.11.005>. URL <http://www.sciencedirect.com/science/article/pii/S0945053X12001254>.
- [77] M. Raspanti, M. Viola, A. Forlino, R. Tenni, C. Gruppi, and M. E. Tira. Glycosaminoglycans show a specific periodic interaction with type I collagen fibrils. *J. Struct. Biol.*, 164(1):134–9, 2008. ISSN 1047-8477. doi: 10.1016/j.jsb.2008.07.001.
- [78] C. Rühland, E. Schönherr, H. Robenek, U. Hansen, R. V. Iozzo, P. Bruckner, and D. G. Seidler. The glycosaminoglycan chain of decorin plays an important role in collagen fibril formation at the early stages of fibrillogenesis. *FEBS J.*, 274(16):4246–55, 2007. ISSN 1742-464X (Print) 1742-464x. doi: 10.1111/j.1742-4658.2007.05951.x.
- [79] D. R. Stamov, A. Müller, Y. Wegrowski, S. Brezillon, and C. M. Franz. Quantitative analysis of type I collagen fibril regulation by lumican and decorin using AFM. *J. Struct. Biol.*, 183(3):394–403, 2013. ISSN 1047-8477. doi: <https://doi.org/10.1016/j.jsb.2013.05.022>. URL <http://www.sciencedirect.com/science/article/pii/S1047847713001548>.
- [80] P. H. Byers and M. L. Murray. Ehlers-Danlos syndrome: a showcase of conditions that lead to understanding matrix biology. *Matrix Biol.*, 33:10–15, 2014. ISSN 0945-053X. doi: <https://doi.org/10.1016/j.matbio.2013.07.005>. URL <http://www.sciencedirect.com/science/article/pii/S0945053X1300098X>.
- [81] C. C. Reed and R. V. Iozzo. The role of decorin in collagen fibrillogenesis and skin homeostasis. *Glycoconjugate J.*, 19(4):249–255, 2002. ISSN 1573-4986. doi: 10.1023/A:1025383913444. URL <https://doi.org/10.1023/A:1025383913444>.
- [82] G. D. Pins, D. L. Christiansen, R. Patel, and F. H. Silver. Self-assembly of collagen fibers. Influence of fibrillar alignment and decorin on mechanical properties.

Biophys. J., 73(4):2164–2172, 1997. ISSN 0006-3495. doi: [https://doi.org/10.1016/S0006-3495\(97\)78247-X](https://doi.org/10.1016/S0006-3495(97)78247-X). URL <http://www.sciencedirect.com/science/article/pii/S000634959778247X>.

- [83] L. W. Fisher, J. D. Termine, and M. F. Young. Deduced protein sequence of bone small proteoglycan I (biglycan) shows homology with proteoglycan II (decorin) and several nonconnective tissue proteins in a variety of species. *J. Biol. Chem.*, 264(8): 4571–6, 1989. ISSN 0021-9258 (Print) 0021-9258.
- [84] P. Sujitha, S. Kavitha, S. Shakilanishi, N. K. C. Babu, and C. Shanthi. Enzymatic dehairing: a comprehensive review on the mechanistic aspects with emphasis on enzyme specificity. *Int. J. Biol. Macromol.*, 118:168–179, 2018. ISSN 0141-8130.
- [85] A. Corsi, T. Xu, X. D. Chen, A. Boyde, J. Liang, M. Mankani, B. Sommer, R. V. Iozzo, I. Eichstetter, P. G. Robey, P. Bianco, and M. F. Young. Phenotypic effects of biglycan deficiency are linked to collagen fibril abnormalities, are synergized by decorin deficiency, and mimic Ehlers-Danlos-like changes in bone and other connective tissues. *J. Bone Miner. Res.*, 17(7):1180–9, 2002. ISSN 0884-0431 (Print) 0884-0431. doi: 10.1359/jbmr.2002.17.7.1180.
- [86] T. Xu, P. Bianco, L. W. Fisher, G. Longenecker, E. Smith, S. Goldstein, J. Bonadio, Adele Boskey, A-M. Heegaard, B. Sommer, K. Satomura, P. Dominguez, C. Zhao, A. B. Kulkarni, P. G. Robey, and M. F. Young. Targeted disruption of the biglycan gene leads to an osteoporosis-like phenotype in mice. *Nat. Genet.*, 20(1):78–82, 1998. ISSN 1546-1718. doi: 10.1038/1746. URL <https://doi.org/10.1038/1746>.
- [87] S. Chakravarti, R. L. Stallings, N. SundarRaj, P. K. Cornuet, and J. R. Hassell. Primary structure of human lumican (keratan sulfate proteoglycan) and localization of the gene (LUM) to chromosome 12q21.3-q22. *Genomics*, 27(3):481–8, 1995. ISSN 0888-7543 (Print) 0888-7543. doi: 10.1006/geno.1995.1080.
- [88] S. Chakravarti, T. Magnuson, J. H. Lass, K. J. Jepsen, C. LaMantia, and H. Carroll. Lumican regulates collagen fibril assembly: skin fragility and corneal opacity in the absence of lumican. *J. Cell Biol.*, 141(5):1277–1286, 1998. ISSN 0021-9525 1540-8140. doi: 10.1083/jcb.141.5.1277. URL <https://pubmed.ncbi.nlm.nih.gov/9606218>.
- [89] E. Bengtsson, P. J. Neame, D. Heinegård, and Y. Sommarin. The primary structure of a basic leucine-rich repeat protein, PRELP, found in connective tissues. *J. Biol. Chem.*, 270(43):25639–25644, 1995. ISSN 0021-9258.
- [90] E. Bengtsson, T. Mörgelin, M. and Sasaki, R. Timpl, D. Heinegård, and A. Aspberg. The leucine-rich repeat protein PRELP binds perlecan and collagens and may function as a basement membrane anchor. *J. Biol. Chem.*, 277(17):15061–15068, 2002. ISSN 0021-9258.

- [91] M. Lewis. PRELP, collagen, and a theory of Hutchinson-Gilford progeria. *Ageing Res. Rev.*, 2(1):95–105, 2003. ISSN 1568-1637. doi: [https://doi.org/10.1016/S1568-1637\(02\)00044-2](https://doi.org/10.1016/S1568-1637(02)00044-2). URL <http://www.sciencedirect.com/science/article/pii/S1568163702000442>.
- [92] S. Deckx, S. Heymans, and A-P. Papageorgiou. The diverse functions of osteoglycin: a deceitful dwarf, or a master regulator of disease? *FASEB J.*, 30(8):2651–2661, 2016. ISSN 0892-6638.
- [93] J. L. Funderburgh, L. M. Corpuz, M. R. Roth, M. L. Funderburgh, E. S. Tasheva, and G. W. Conrad. Mimecan, the 25-kDa corneal keratan sulfate proteoglycan, is a product of the gene producing osteoglycin. *J. Biol. Chem.*, 272(44):28089–28095, 1997. ISSN 0021-9258.
- [94] Y. Zhang, A. H. Conrad, and G. W. Conrad. Effects of ultraviolet-A and riboflavin on the interaction of collagen and proteoglycans during corneal cross-linking. *J. Biol. Chem.*, 286(15):13011–13022, 2011. ISSN 0021-9258.
- [95] D. S. da Costa, R. L. Reis, and I. Pashkuleva. Sulfation of glycosaminoglycans and its implications in human health and disorders. *Annu. Rev. Biomed. Eng.*, 19(1):1–26, 2017. doi: 10.1146/annurev-bioeng-071516-044610. URL <https://www.annualreviews.org/doi/abs/10.1146/annurev-bioeng-071516-044610>.
- [96] K. G. Danielson, H. Baribault, D. F. Holmes, H. Graham, K. E. Kadler, and R. V. Iozzo. Targeted disruption of decorin leads to abnormal collagen fibril morphology and skin fragility. *J. Cell Biol.*, 136(3):729–743, 1997. ISSN 0021-9525 1540-8140. doi: 10.1083/jcb.136.3.729. URL <https://pubmed.ncbi.nlm.nih.gov/9024701>.
- [97] C. L. Jin, J. H. Oh, M. Han, M. K. Shin, C. Yao, C. H. Park, Z. H. Jin, and J. H. Chung. UV irradiation-induced production of monoglycosylated biglycan through downregulation of xylosyltransferase 1 in cultured human dermal fibroblasts. *J. Dermatol. Sci.*, 79(1):20–9, 2015. ISSN 0923-1811. doi: 10.1016/j.jdermsci.2015.03.018.
- [98] B. ÖBrink. The influence of glycosaminoglycans on the formation of fibers from monomeric tropocollagen in vitro. *Eur. J. Biochem.*, 34(1):129–137, 1973. ISSN 0014-2956. doi: 10.1111/j.1432-1033.1973.tb02739.x. URL <https://doi.org/10.1111/j.1432-1033.1973.tb02739.x>.
- [99] D. L. Rabenstein. Heparin and heparan sulfate: structure and function. *Nat. Prod. Rep.*, 19(3):312–331, 2002. ISSN 0265-0568. doi: 10.1039/B100916H. URL <http://dx.doi.org/10.1039/B100916H>.
- [100] J. L. Funderburgh. Keratan sulfate: structure, biosynthesis, and function. *Glycobiology*, 10(10):951–958, 2000. ISSN 0959-6658. doi: 10.1093/glycob/10.10.951. URL <https://doi.org/10.1093/glycob/10.10.951>.

- [101] B. Caterson and J. Melrose. Keratan sulfate, a complex glycosaminoglycan with unique functional capability. *Glycobiology*, 28(4):182–206, 2018. ISSN 1460-2423. doi: 10.1093/glycob/cwy003. URL <https://doi.org/10.1093/glycob/cwy003>.
- [102] J. Necas, L. Bartosikova, P. Brauner, and J. Kolar. Hyaluronic acid (hyaluronan): a review. *Vet. Med.*, 53(8):397–411, 2008.
- [103] S. P. Evanko, M. I. Tammi, R. H. Tammi, and T. N. Wight. Hyaluronan-dependent pericellular matrix. *Adv. Drug Deliv. Rev.*, 59(13):1351–65, 2007. ISSN 0169-409X (Print) 0169-409x. doi: 10.1016/j.addr.2007.08.008.
- [104] S. B. Frazier, K. A. Roodhouse, D. E. Hourcade, and L. Zhang. The quantification of glycosaminoglycans: a comparison of HPLC, carbazole, and alcian blue methods. *Open Glycoscience*, 1:31–39, 2008. ISSN 1875-3981. doi: 10.2174/1875398100801010031. URL <https://pubmed.ncbi.nlm.nih.gov/20640171>.
- [105] I. Barbosa, S. Garcia, V. Barbier-Chassefière, J. P. Caruelle, I. Martelly, and D. Papy-García. Improved and simple micro assay for sulfated glycosaminoglycans quantification in biological extracts and its use in skin and muscle tissue studies. *Glycobiology*, 13(9):647–53, 2003. ISSN 0959-6658 (Print) 0959-6658. doi: 10.1093/glycob/cwg082.
- [106] A. J. Reynolds and C. A. Jahoda. Hair matrix germinative epidermal cells confer follicle-inducing capabilities on dermal sheath and high passage papilla cells. *Development*, 122(10):3085–3094, 1996. ISSN 0950-1991.
- [107] B. Buffoli, F. Rinaldi, M. Labanca, E. Sorbellini, A. Trink, E. Guanziroli, R. Rezzani, and L. F. Rodella. The human hair: from anatomy to physiology. *Int. J. Dermatol.*, 53(3):331–341, 2014. ISSN 0011-9059. doi: 10.1111/ijd.12362. URL <https://doi.org/10.1111/ijd.12362>.
- [108] A. J. G. McDonagh, L. Cawood, and A. G. Messenger. Expression of extracellular matrix in hair follicle mesenchyme in alopecia areata. *Br. J. Dermatol.*, 123(6):717–724, 1990. ISSN 0007-0963. doi: <https://doi.org/10.1111/j.1365-2133.1990.tb04188.x>. URL <https://doi.org/10.1111/j.1365-2133.1990.tb04188.x>.
- [109] J. Wadstein, E. Thom, and A. Gadzhigroeva. Integral roles of specific proteoglycans in hair growth and hair loss: mechanisms behind the bioactivity of proteoglycan replacement therapy with Nourkrin[®] with Marilex[®] in pattern hair loss and telogen effluvium. *Dermatol. Res. Pract.*, 2020:8125081, 2020. ISSN 1687-6105. doi: 10.1155/2020/8125081. URL <https://doi.org/10.1155/2020/8125081>.
- [110] D. Breikreutz, I. Koxholt, K. Thiemann, and R. Nischt. Skin basement membrane: the foundation of epidermal integrity-BM functions and diverse roles of bridging molecules nidogen and perlecan. *BioMed Res. Int.*, 2013:179784–179784, 2013. ISSN

- 2314-6141 2314-6133. doi: 10.1155/2013/179784. URL <https://pubmed.ncbi.nlm.nih.gov/23586018>.
- [111] R. Moll, M. Divo, and L. Langbein. The human keratins: biology and pathology. *Histochem. Cell Biol.*, 129(6):705–733, 2008. ISSN 0948-6143 1432-119X. doi: 10.1007/s00418-008-0435-6. URL <https://pubmed.ncbi.nlm.nih.gov/18461349>.
- [112] I. G. Maddocks and N. Jackson. *Structural studies of sheep, cattle & goat skin*. CSIRO Australia, 1988.
- [113] D. R. Scobie, A. R. Bray, and N. C. Merrick. Medullation and average fibre diameter vary independently in the wool of Romney sheep. *N. Z. J. Agric. Res.*, 41(1):101–110, 1998. ISSN 0028-8233. doi: 10.1080/00288233.1998.9513292. URL <https://doi.org/10.1080/00288233.1998.9513292>.
- [114] R. E. Chapman. *Hair, wool, quill, nail, claw, hoof, and horn*, pages 293–317. Springer Berlin Heidelberg, Berlin, Heidelberg, 1986. ISBN 978-3-662-00989-5. doi: 10.1007/978-3-662-00989-5_17. URL https://doi.org/10.1007/978-3-662-00989-5_17.
- [115] A. D. Covington. *Tanning chemistry: the science of leather*. RSC Publishing, 2009. URL <http://app.knovel.com/hotlink/toc/id:kpTCTSL002/tanning-chemistry-the>.
- [116] T. Ramasami and B. G. S. Prasad. Environmental aspects of leather processing. *Proceedings of the LEXPO–XV, Calcutta, India*, page 43, 1991.
- [117] T. Ramasami, J. Rao, N. K. Chandra Babu, K. Parthasarathi, P. Rao, P. Saravanan, R. Gayathri, and K. J. Sreeram. Beamhouse and tanning operations: process chemistry revisited. *J. Soc. Leather Technol. Chem.*, 83:39–45, 1999.
- [118] J. Rauterberg and K. Kühn. Acid soluble calf skin collagen. *Eur. J. Biochem.*, 19(3):398–407, 1971. ISSN 0014-2956. doi: 10.1111/j.1432-1033.1971.tb01329.x. URL <https://febs.onlinelibrary.wiley.com/doi/abs/10.1111/j.1432-1033.1971.tb01329.x>.
- [119] P. Thanikaivelan, J. R. Rao, B. U. Nair, and T. Ramasami. Progress and recent trends in biotechnological methods for leather processing. *Trends Biotechnol.*, 22(4):181–188, 2004. ISSN 0167-7799. doi: <https://doi.org/10.1016/j.tibtech.2004.02.008>. URL <http://www.sciencedirect.com/science/article/pii/S0167779904000551>.
- [120] A. D. Miller. *The salt recovery process: chemical processes in New Zealand*. New Zealand Institute of Chemistry Inc., Auckland, New Zealand, 1998.
- [121] A. D. Covington. Modern tanning chemistry. *Chem. Soc. Rev.*, 26(2):111–126, 1997. ISSN 0306-0012. doi: 10.1039/CS9972600111. URL <http://dx.doi.org/10.1039/CS9972600111>.

- [122] Y. Zhang and L. Wang. Recent research progress on leather fatliquoring agents. *Polym. Plast. Technol. Eng.*, 48(3):285–291, 2009. ISSN 0360-2559. doi: 10.1080/03602550802675611. URL <https://doi.org/10.1080/03602550802675611>.
- [123] N. R. Kamini, C. Hemachander, J. G. S. Mala, and R. Puvanakrishnan. Microbial enzyme technology as an alternative to conventional chemicals in leather industry. *Curr. Sci. India*, 77(1):80–86, 1999. ISSN 00113891. URL <http://www.jstor.org/stable/24102916>.
- [124] R. O. Jr. Beauchamp, J. S. Bus, J. A. Popp, C. J. Boreiko, and D. A. Andjelkovich. A critical review of the literature on hydrogen sulfide toxicity. *Crit. Rev. Toxicol.*, 13(1):25–97, 1984. ISSN 1040-8444 (Print) 1040-8444. doi: 10.3109/10408448409029321.
- [125] J. Buljan, J. Hannak, and G. Jayaraj. How to deal with hydrogen sulphide gas in tanneries and effluent treatment plants. Report, United Nations Industrial Development Organisation, 2015. URL <https://leatherpanel.org/content/how-deal-hydrogen-sulphide-gas-tanneries-and-etps>.
- [126] W. Steven. The treatment of beamhouse and fellmongering waste waters. *J. Am. Leather Chem. Assoc.*, 67:127–131, 1983.
- [127] P. Thanikaivelan, J. R. Rao, B. U. Nair, and T. Ramasami. Approach towards zero discharge tanning: role of concentration on the development of eco-friendly liming-reliming processes. *J. Cleaner Prod.*, 11(1):79–90, 2003. ISSN 0959-6526. doi: [https://doi.org/10.1016/S0959-6526\(01\)00058-0](https://doi.org/10.1016/S0959-6526(01)00058-0). URL <http://www.sciencedirect.com/science/article/pii/S0959652601000580>.
- [128] P. Thanikaivelan, J. R. Rao, B. U. Nair, and T. Ramasami. Recent trends in leather making: processes, problems, and pathways. *Crit. Rev. Env. Sci. Tec.*, 35(1):37–79, 2005. ISSN 1064-3389. doi: 10.1080/10643380590521436. URL <https://doi.org/10.1080/10643380590521436>.
- [129] A. J. Gordon. The measurement of, and factors affecting, the strength of attachment of wool to the skin of sheep. *Aust. J. Exp. Agric.*, 20(102):40–49, 1980. ISSN 1446-5574.
- [130] J. C. Tana and E. C. Tana. Procedure for removing the layer of hairy elements from a complete animal skin, September 13 1988. US Patent 4,770,010.
- [131] S. C. Hawkins and J. Wassenberg. Endogenous enzyme fellmongering. Skin structure and properties. *IULTCS XXIV Congress*, September 11-14 1997.
- [132] C. A. Money. Unhairing and dewooling - requirements for quality and the environment. *J. Soc. Leather Technol. Chem.*, 80:175–186, 1996.

- [133] L. Schlosser, A. Hein, W. Keller, and E. Heidemann. Utilisation of a *Lactobacillus* culture in the beamhouse. *J. Soc. Leather Technol. Chem.*, 70:163–8, 1986. ISSN 0144-0322.
- [134] D. Burton. The methods and mechanisms of unhairing. *J. Soc. Leather Technol. Chem.*, 42:403–414, 1958.
- [135] S. Bronco, D. Castiello, G. d Elia, M. Salvadori, M. Seggiani, and S. Vitolo. Oxidative unhairing with hydrogen peroxide: development of an industrial scale process for high-quality upper leather. *J. Am. Leather Chem. Assoc.*, 100:45–53, 2005.
- [136] W. N. Marmer and R. L. Dudley. The use of oxidative chemicals for the removal of hair from cattle hides in the beamhouse. *J. Am. Leather Chem. Assoc.*, 99(9): 386–392, 2004. ISSN 0002-9726.
- [137] B. Shi, X. Lu, and D. Sun. Further investigations of oxidative unhairing using hydrogen peroxide. *J. Am. Leather Chem. Assoc.*, 98(5):185–192, 2003. ISSN 0002-9726.
- [138] W. Frendrup. Hair-save unhairing methods in leather processing. Technical report, United Nations Industrial Development Organisation, 2000.
- [139] O. Röhm. Verfahren zum beizen von häuten. German Patent DE 200, 519, July 21 1910.
- [140] N. Kandasamy, P. Velmurugan, Sundarvel A., R. J. Raghava, C. Bangaru, and T. Palanisamy. Eco-benign enzymatic dehairing of goatskins utilizing a protease from a *Pseudomonas fluorescens* species isolated from fish visceral waste. *J. Cleaner Prod.*, 25:27–33, 2012. ISSN 0959-6526. doi: <https://doi.org/10.1016/j.jclepro.2011.12.007>. URL <http://www.sciencedirect.com/science/article/pii/S0959652611005324>.
- [141] L. M. I. López, C. A. Viana, M. E. Errasti, M. L. Garro, J. E. Martegani, G. A. Mazzilli, C. D. T. Freitas, Í. M. S. Araújo, R. O. da Silva, and M. V. Ramos. Latex peptidases of *Calotropis procera* for dehairing of leather as an alternative to environmentally toxic sodium sulfide treatment. *Bioproc. Biosyst. Eng.*, 40(9): 1391–1398, 2017. ISSN 1615-7605. doi: 10.1007/s00449-017-1796-9. URL <https://doi.org/10.1007/s00449-017-1796-9>.
- [142] S. Sivasubramanian, B. Murali Manohar, A. Rajaram, and R. Puvanakrishnan. Ecofriendly lime and sulfide free enzymatic dehairing of skins and hides using a bacterial alkaline protease. *Chemosphere*, 70(6):1015–1024, 2008. ISSN 0045-6535. doi: <https://doi.org/10.1016/j.chemosphere.2007.09.036>. URL <http://www.sciencedirect.com/science/article/pii/S0045653507011605>.

- [143] B. Wahyuntari and H. Hendrawati. Properties of an extracellular protease of *Bacillus megaterium* DSM 319 as depilating aid of hides. *Microbiology Indonesia*, 6(2):4–4, 2012. ISSN 2087-8575.
- [144] A. Crispim and M. Mota. Unhairing with enzymes. *J. Soc. Leather Technol. Chem.*, 87(5):198–202, 2003. ISSN 0144-0322.
- [145] M. Sousa. Advances in understanding of enzymatic unhairing of bovine hides. *J. Am. Leather Chem. Assoc.*, 109:268–277, 2014.
- [146] S. Malathi and R. Chakraborty. Production of alkaline protease by a new *Aspergillus flavus* isolate under solid-substrate fermentation conditions for use as a depilation agent. *Appl. Environ. Microbiol.*, 57(3):712–716, 1991. URL <https://aem.asm.org/content/aem/57/3/712.full.pdf>.
- [147] M. Shanmugavel, A. Premalatha, A. Dayanandan, R. Ramesh, A. Gnanamani, L. Sounderraj, N. K. Chandrababau, A. Jayaprakash, A. Mandal, and G. S. Rajakumar. Enzyme consortium of *Aspergillus tamarii* MTCC5152 for greener beam house processing of hides. *31st IULTCS Congress*, 2011.
- [148] E. Vijay Kumar, M. Srijana, K. Kiran Kumar, N. Harikrishna, and G. Reddy. A novel serine alkaline protease from *Bacillus altitudinis* GVC11 and its application as a dehairing agent. *Bioprocess. Biosyst. Eng.*, 34(4):403–409, 2011. ISSN 1615-7605. doi: 10.1007/s00449-010-0483-x. URL <https://doi.org/10.1007/s00449-010-0483-x>.
- [149] S. S. Nilegaonkar, V. P. Zambare, P. P. Kanekar, P. K. Dhakephalkar, and S. S. Sarnaik. Production and partial characterization of dehairing protease from *Bacillus cereus* MCM B-326. *Bioresour. Technol.*, 98(6):1238–45, 2007. ISSN 0960-8524 (Print) 0960-8524. doi: 10.1016/j.biortech.2006.05.003.
- [150] S. Saran, R. V. Mahajan, R. Kaushik, J. Isar, and R. K. Saxena. Enzyme mediated beam house operations of leather industry: a needed step towards greener technology. *J. Cleaner Prod.*, 54:315–322, 2013. ISSN 0959-6526. doi: <https://doi.org/10.1016/j.jclepro.2013.04.017>. URL <http://www.sciencedirect.com/science/article/pii/S0959652613002321>.
- [151] N. Z. Jaouadi, B. Jaouadi, Hilma B. H., H. Rekik, M. Belhoul, M. Hmidi, H. S. B. Aicha, C. G. Hila, A. Toumi, N. Aghajari, and S. Bejar. Probing the crucial role of Leu31 and Thr33 of the *Bacillus pumilus* CBS alkaline protease in substrate recognition and enzymatic depilation of animal hide. *PLoS One*, 9(9):e108367, 2014. doi: 10.1371/journal.pone.0108367. URL <https://doi.org/10.1371/journal.pone.0108367>.
- [152] S. Briki, O. Hamdi, and A. Landoulsi. Enzymatic dehairing of goat skins using alkaline protease from *Bacillus sp.* SB12. *Protein Expr. Purif.*, 121:9–16, 2016. ISSN 1046-5928. doi: 10.1016/j.pep.2015.12.021.

- [153] A. J. Macedo, W. O. B. da Silva, R. Gava, D. Driemeier, J. A. P. Henriques, and C. Termignoni. Novel keratinase from *Bacillus subtilis* S14 exhibiting remarkable dehairing capabilities. *Appl. Biochem. Biotechnol.*, 71(1):594–596, 2005. ISSN 0099-2240 1098-5336. doi: 10.1128/AEM.71.1.594-596.2005. URL <https://pubmed.ncbi.nlm.nih.gov/15640244>.
- [154] N. Z. Jaouadi, H. Rekik, A. Badis, S. Trabelsi, M. Belhoul, C. G. Hila, A. Irmani, H. Khemir, A. Toumi, S. Bejar, and B. Jaouadi. The promising keratin-biodegradation and hide-dehairing activities of the keratinase KERUS from *Brevibacillus brevis* strain US575. In Amjad Kallel, Mohamed Ksibi, Hamed Ben Dhia, and Nabil Khélifi, editors, *Recent Advances in Environmental Science from the Euro-Mediterranean and Surrounding Regions*, pages 133–135. Springer International Publishing, 2017. ISBN 978-3-319-70548-4.
- [155] R. R. Rao, M. Vimudha, N. R. Kamini, M. K. Gowthaman, B. Chandrasekran, and P. Saravanan. Alkaline protease production from *Brevibacterium luteolum* (MTCC 5982) under solid-state fermentation and its application for sulfide-free unhairing of cowhides. *Appl. Biochem. Biotechnol.*, 182(2):511–528, 2017. ISSN 1559-0291. doi: 10.1007/s12010-016-2341-z. URL <https://doi.org/10.1007/s12010-016-2341-z>.
- [156] M. E. Errasti, N. O. Caffini, and L. M. I. López. Proteolytic extracts of three *Bromeliaceae* species as eco-compatible tools for leather industry. *Environ. Sci. Pollut. Res.*, 25(22):21459–21466, 2018. ISSN 1614-7499. doi: 10.1007/s11356-017-1096-6. URL <https://doi.org/10.1007/s11356-017-1096-6>.
- [157] H. B. Khandelwal, S. V. More, K. M. Kalal, and R. S. Laxman. Eco-friendly enzymatic dehairing of skins and hides by *C. brefeldianus* protease. *Clean Technol. Environ. Policy*, 17(2):393–405, 2015. ISSN 1618-9558. doi: 10.1007/s10098-014-0791-y. URL <https://doi.org/10.1007/s10098-014-0791-y>.
- [158] J. Gumilar, S. Triatmojo, M. Lies, L. M. Yusiati, and A. Pertiwinigrum. Isolation, identification and dehairing activity of Indonesian native keratinolytic bacteria *Exiguobacterium* sp. DG1. *Pakistan J. Biotechnol.*, 12:41–48, 2015.
- [159] C. Zhou, H. Qin, X. Chen, Y. Zhang, Y. Xue, and Y. Ma. A novel alkaline protease from alkaliphilic *Idiomarina* sp. C9-1 with potential application for eco-friendly enzymatic dehairing in the leather industry. *Sci. Rep.*, 8(1):16467, 2018. ISSN 2045-2322. doi: 10.1038/s41598-018-34416-5. URL <https://doi.org/10.1038/s41598-018-34416-5>.
- [160] T. Paul, A. Das, A. Mandal, A. Jana, C. Maity, A. Adak, S. K. Halder, P. K. DasMohapatra, B. R. Pati, and K. C. Mondal. Effective dehairing properties of keratinase from *Paenibacillus woosongensis* TKb2 obtained under solid state fermentation. *Waste Biomass Valorization*, 5(1):97–107, 2014. ISSN 1877-265X. doi: 10.1007/s12649-013-9217-z. URL <https://doi.org/10.1007/s12649-013-9217-z>.

- [161] E. V. P. Pandeeti, G. K. Pitchika, J. Jotshi, S. S. Nilegaonkar, P. P. Kanekar, and D. Siddavattam. Enzymatic depilation of animal hide: identification of elastase (LasB) from *Pseudomonas aeruginosa* MCM B-327 as a depilating protease. *PLoS One*, 6(2):e16742, 2011. doi: 10.1371/journal.pone.0016742. URL <https://doi.org/10.1371/journal.pone.0016742>.
- [162] N. George, P. S. Chauhan, V. Kumar, N. Puri, and N. Gupta. Approach to ecofriendly leather: characterization and application of an alkaline protease for chemical free dehairing of skins and hides at pilot scale. *J. Cleaner Prod.*, 79:249–257, 2014. ISSN 0959-6526. doi: <https://doi.org/10.1016/j.jclepro.2014.05.046>. URL <http://www.sciencedirect.com/science/article/pii/S0959652614005150>.
- [163] P. Chandra, Enespa, R. Singh, and P. K. Arora. Microbial lipases and their industrial applications: a comprehensive review. *Microb. Cell Fact.*, 19(1):169, 2020. ISSN 1475-2859. doi: 10.1186/s12934-020-01428-8. URL <https://doi.org/10.1186/s12934-020-01428-8>.
- [164] J. G. Christopher, S. Ganesh, S. Palanivel, M. Ranganathan, and R. R. Jonnalagadda. Cohesive system for enzymatic unhairing and fibre opening: an architecture towards eco-benign pretanning operation. *J. Cleaner Prod.*, 83:428–436, 2014. ISSN 0959-6526. doi: <https://doi.org/10.1016/j.jclepro.2014.07.039>. URL <http://www.sciencedirect.com/science/article/pii/S0959652614007471>.
- [165] G. Jayakumar, M. Sathish, R. Aravindhana, and J. Raghava-Rao. Studies on the use of bi-functional enzyme for leather making. *J. Am. Leather Chem. Assoc.*, 111(12):455–460, 2016. ISSN 0002-9726.
- [166] A. Dettmer, M. A. Z. Ayub, and M. Gutterres. Hide unhairing and characterization of commercial enzymes used in leather manufacture. *Braz. J. Chem. Eng.*, 28:373–380, 2011. ISSN 0104-6632. URL <https://www.scielo.br/j/bjce/a/3J997xnFZdv7M99cjyWQnk/?lang=en>.
- [167] F. R. de Souza and M. Gutterres. Application of enzymes in leather processing: a comparison between chemical and coenzymatic processes. *Braz. J. Chem. Eng.*, 29:473–482, 2012. ISSN 0104-6632. URL http://www.scielo.br/scielo.php?script=sci_arttext&pid=S0104-66322012000300004&nrm=iso.
- [168] J. W. H. Wong and G. Cagney. *An overview of label-free quantitation methods in proteomics by mass spectrometry*, pages 273–283. Humana Press, Totowa, NJ, 2010. ISBN 978-1-60761-444-9. doi: 10.1007/978-1-60761-444-9_18. URL https://doi.org/10.1007/978-1-60761-444-9_18.
- [169] C. M. Huang, C. A. Elmetts, K. R. van Kampen, T. S. Desilva, S. Barnes, H. Kim, and D. C. Tang. Prospective highlights of functional skin proteomics. *Mass Spectrom. Rev.*, 24(5):647–60, 2005. ISSN 0277-7037 (Print) 0277-7037. doi: 10.1002/mas.20037.

- [170] K. Dettmer, P. A. Aronov, and B. D. Hammock. Mass spectrometry-based metabolomics. *Mass Spectrom. Rev.*, 26(1):51–78, 2007. ISSN 0277-7037. doi: <https://doi.org/10.1002/mas.20108>. URL <https://doi.org/10.1002/mas.20108>.
- [171] K. A. Seifert. Progress towards DNA barcoding of fungi. *Mol. Ecol. Resour.*, 9(s1):83–89, 2009. ISSN 1755-098X. doi: <https://doi.org/10.1111/j.1755-0998.2009.02635.x>. URL <https://doi.org/10.1111/j.1755-0998.2009.02635.x>.
- [172] R. I. Amann, B. J. Binder, R. J. Olson, S. W. Chisholm, R. Devereux, and D. A. Stahl. Combination of 16S rRNA-targeted oligonucleotide probes with flow cytometry for analyzing mixed microbial populations. *Appl. Environ. Microbiol.*, 56(6):1919–25, 1990. ISSN 0099-2240 (Print) 0099-2240. doi: 10.1128/aem.56.6.1919-1925.1990.
- [173] Y-X. Liu, Y. Qin, T. Chen, M. Lu, X. Qian, X. Guo, and Y. Bai. A practical guide to amplicon and metagenomic analysis of microbiome data. *Protein Cell*, 12:315–330, 2021. ISSN 1674-800X.
- [174] R. Knight, A. Vrbanac, B. C. Taylor, A. Aksenov, C. Callewaert, J. Debelius, A. Gonzalez, T. Kosciolk, L-I. McCall, D. McDonald, A. V. Melnik, J. T. Morton, J. Navas, R. A. Quinn, J. G. Sanders, A. D. Swafford, L. R. Thompson, A. Tripathi, Z. Z. Xu, J. R. Zaneveld, Q. Zhu, J. G. Caporaso, and P. C. C. Dorrestein. Best practices for analysing microbiomes. *Nat. Rev. Microbiol.*, 16(7):410–422, 2018. ISSN 1740-1534. doi: 10.1038/s41579-018-0029-9. URL <https://doi.org/10.1038/s41579-018-0029-9>.
- [175] A. W. Walker, J. C. Martin, P. Scott, J. Parkhill, H. J. Flint, and K. P. Scott. 16s rRNA gene-based profiling of the human infant gut microbiota is strongly influenced by sample processing and PCR primer choice. *Microbiome*, 3(1):26, 2015. ISSN 2049-2618. doi: 10.1186/s40168-015-0087-4. URL <https://doi.org/10.1186/s40168-015-0087-4>.
- [176] R. Bonnet, A. Suaui, J. Doré, G. R. Gibson, and M. D. Collins. Differences in rDNA libraries of faecal bacteria derived from 10- and 25-cycle PCRs. *Int. J. Syst. Evol. Microbiol.*, 52(Pt 3):757–763, 2002. ISSN 1466-5026 (Print) 1466-5026. doi: 10.1099/00207713-52-3-757.
- [177] E. Bolyen, J. R. Rideout, M. R. Dillon, N. A. Bokulich, C. C. Abnet, G. A. Al-Ghalith, H. Alexander, E. J. Alm, M. Arumugam, F. Asnicar, Y. Bai, J. E. Bisanz, K. Bittinger, A. Brejnrod, C. J. Brislawn, C. T. Brown, B. J. Callahan, A. M. Caraballo-Rodríguez, J. Chase, E. K. Cope, R. Da Silva, C. Diener, P. C. Dorrestein, G. M. Douglas, D. M. Durall, C. Duvallet, C. F. Edwardson, M. Ernst, M. Estaki, J. Fouquier, J. M. Gauglitz, S. M. Gibbons, D. L. Gibson, A. Gonzalez, K. Gorlick, J. Guo, B. Hillmann, S. Holmes, H. Holste, C. Huttenhower, G. A. Huttley, S. Janssen, A. K. Jarmusch, L. Jiang, B. D. Kaehler, K. B. Kang, C. R.

- Keefe, P. Keim, S. T. Kelley, D. Knights, I. Koester, T. Kosciulek, J. Kreps, M. G. I. Langille, J. Lee, R. Ley, Y-X. Liu, E. Loftfield, C. Lozupone, M. Maher, C. Marotz, B. D. Martin, D. McDonald, L. J. McIver, A. V. Melnik, J. L. Metcalf, S. C. Morgan, J. T. Morton, A. T. Naimey, J. A. Navas-Molina, L. F. Nothias, S. B. Orchanian, T. Pearson, S. L. Peoples, D. Petras, M. L. Preuss, E. Pruesse, L. B. Rasmussen, A. Rivers, M. S. Robeson, P. Rosenthal, N. Segata, M. Shaffer, A. Shiffer, R. Sinha, S. J. Song, J. R. Spear, A. D. Swafford, L. R. Thompson, P. J. Torres, P. Trinh, A. Tripathi, P. J. Turnbaugh, S. Ul-Hasan, J. J. J. van der Hooft, F. Vargas, Y. Vázquez-Baeza, E. Vogtmann, M. von Hippel, W. Walters, et al. Reproducible, interactive, scalable and extensible microbiome data science using QIIME 2. *Nat. Biotechnol.*, 37(8):852–857, 2019. ISSN 1546-1696. doi: 10.1038/s41587-019-0209-9. URL <https://doi.org/10.1038/s41587-019-0209-9>.
- [178] B. J. Callahan, P. J. McMurdie, M. J. Rosen, A. W. Han, A. J. Johnson, and S. P. Holmes. DADA2: high-resolution sample inference from Illumina amplicon data. *Nat. Methods*, 13(7):581–3, 2016. ISSN 1548-7091 (Print) 1548-7091. doi: 10.1038/nmeth.3869.
- [179] C. Quast, E. Pruesse, P. Yilmaz, J. Gerken, T. Schweer, P. Yarza, J. Peplies, and F. O. Glöckner. The SILVA ribosomal RNA gene database project: improved data processing and web-based tools. *Nucleic Acids Res.*, 41(D1):D590–D596, 2013. ISSN 0305-1048. doi: 10.1093/nar/gks1219. URL <https://doi.org/10.1093/nar/gks1219>.
- [180] K. Abarenkov, A. Zirk, T. Piirmann, R. Pöhönen, F. Ivanov, R. H. Nilsson, and U. Kõljalg. UNITE QIIME release for Fungi, 2020. URL <https://plutof.ut.ee/#/doi/10.15156/BIO/786385>.
- [181] N. A. Bokulich, B. D. Kaehler, J. R. Rideout, M. Dillon, E. Bolyen, R. Knight, G. A. Huttley, and Gregory C. J. Optimizing taxonomic classification of marker-gene amplicon sequences with QIIME 2’s q2-feature-classifier plugin. *Microbiome*, 6(1):90, 2018. ISSN 2049-2618. doi: 10.1186/s40168-018-0470-z. URL <https://doi.org/10.1186/s40168-018-0470-z>.
- [182] J-C. Ogier, S. Pagès, M. Galan, M. Barret, and S. Gaudriault. *rpoB*, a promising marker for analyzing the diversity of bacterial communities by amplicon sequencing. *BMC Microbiol.*, 19(1):171, 2019. ISSN 1471-2180. doi: 10.1186/s12866-019-1546-z. URL <https://doi.org/10.1186/s12866-019-1546-z>.

3 | Physical analysis of sheepskin

The use of natural products in the leather industry: Depilation without damage

Yi-Hsuan Tu¹, Meekyung Ahn², Jasna Rakonjac¹, Geoff Holmes², and Gillian E. Norris¹

¹School of Fundamental Sciences, Palmerston North, Massey University, New Zealand

²New Zealand Leather and Shoe Research Association, Palmerston North, New Zealand

Address correspondence to:

Gillian E. Norris, G.Norris@massey.ac.nz

Publication status: manuscript in preparation to be submitted to the Journal of Cleaner Production

Abstract

In this work, we chart the discovery of the use of a milk product to both preserve unwashed sheepskins and depilate them, removing the need for salt, sulfide and lime and reducing the copious amounts of water used by the leather industry. This method can completely replace the first five steps of the traditional beamhouse process and the depilated skins can be taken straight to degreasing and tanning. In order to evaluate the products of this process, the depilated skin surface was evaluated not only by eye, but with both scanning electron microscopy (SEM) and transmission electron microscopy (TEM) which showed there was no apparent damage to the grain or fraying of the collagen bundles. The depilated skin was also processed to leather which was subjected to tear, tensile and shrinkage temperature measurements that were almost identical to those of leather made using the traditional process. To try and understand the process, microbial culturing was carried out on the milk product at the conclusion of depilation. Two bacterial species (*Lactococcus lactis* and *Lactobacillus plantarum*) and two fungal species (*Geotrichum candidum* and *Yarrowia lipolytica*), were routinely identified. We predict that the secretion of antimicrobial substances and extracellular enzymes from these microorganisms are responsible for the preservation and depilation of sheepskin. This process shows excellent potential to be further developed and could replace the current chemical processes used by the leather industry.

3.1 Introduction

Leather products are manufactured from animal skins that have been subjected to various chemical procedures to form a product with high tensile and tear strengths and is both insulating and water resistant. Because of these properties, leather has been used to make clothing, shelters, tools and other objects since 5,000 BCE, and it has been estimated that by 2027, the global leather industry will be worth \$306.1 billion to the world economy¹. However, the industry is facing the negative impact of environmental pollution caused by the chemicals used, and the solid and liquid wastes produced during the manufacturing process. Sheepskins make up 15 % of the raw material used by the world leather industry². They are a by-product of the meat industry that must be disposed of if not used, incurring a significant cost to farmers. If processed, the environmental pollution caused by the current beamhouse processes poses a problem that will, because of changes in legislation that have been introduced to control environmental pollution, incur significant costs to the industry. Furthermore, the current process uses copious volumes of water, a precious resource in these times of climate change. Therefore, it is imperative that leather technologists and scientists worldwide find environmentally friendly alternatives for skin/hide preservation and leather production.

Animal skin is made up of three main layers: the epidermis, dermis, and hypodermis. The epidermis is the outer-most protective layer of skin and consists of keratinocytes (keratin-producing cells) and parts of the hair shaft (fibre). Beneath the epidermis lies the epidermis-dermis junction, that contains the coarse basement membrane, a special structure made up from types IV and VII collagens, as well as proteoglycans (heavily glycosylated proteins)³. The dermis of sheepskin contains water (53 %), protein (27.5 %), fat (18.3 %) as well as trace minerals. The major structural components of dermis are collagen types I and III, which make up approximately 60 - 70 % of the dry weight of skin⁴. The uppermost layer of the dermis, also termed the enamel, is responsible for the outward appearance of the final leather product which is thought to be due to the presence of the beaded microfilament network formed by collagen VI⁵. The bottom layer of skin, the hypodermis, is made up muscle and fat. Both the epidermis and hypodermis are removed during leather making.

Once the skin has been removed from the animal, it needs to be preserved, especially in warm weather, or when stacks of skins are plastic wrapped for transport to the tannery. The conventional method is the application of salt (30 - 40 %, w/w), which then has to be removed and the skins rehydrated, which uses large volumes of water⁶. The first step of leather processing, known as depilation, is the removal

of hair or wool from the hides or skins by painting a thick strong alkaline sulfide-lime solution (Na_2S , NaSH , NaOH , $\text{Ca}(\text{SH})_2$, $\text{Ca}(\text{OH})_2$) on the flesh side of the pelt and allowing it to soak through to the dermis⁶. The alkaline conditions open up the major protein network formed by the collagen fibres, allowing the chemicals to reach the hair shaft where they act to degrade the keratins in the hair follicle, and the hair to be removed either mechanically or by hand. Na_2S is, however, a strong reducing agent, that interferes with the oxidation of organic wastes (*i.e.* hair/wool and proteins), and as a result, contributes to the high chemical oxygen demand (COD) and biological oxygen demand (BOD) of the effluent. In fact, 50 – 70 % of the total COD and BOD load from leather making is due to Na_2S . Even worse, when the pH of the effluent drops below 9.5, H_2S , a colourless, flammable gas that is poisonous when inhaled, is released. The depilation process is estimated to contribute to one-third of the pollution produced throughout the whole leather making process⁷.

After depilation, the skin is washed several times in water before being incubated with enzymes such as trypsin or chymotrypsin that degrade the non-collagenous proteins in the skins in a process called bating. The skins are then immersed in a solution of sulfuric acid and salt at pH 2 - 3 that both preserves and prepares them for tanning, a process called pickling. Due to their high fat content, sheepskins in New Zealand undergo a process called degreasing right after pickling to remove the fat layer in the skin before it is tanned⁶. The purpose of this is to allow the uniform penetration of tanning reagents into the skin matrix and through the pelt cross section during tanning. After degreasing, the skins are then tanned and the raw skin is permanently turned into a stable substance.

Much effort has gone into the search for 'greener' depilation agents. Interest has largely been focused on the use of proteolytic enzymes as depilation agents because they are safer to handle and biodegradable. Many enzymes of bacterial origin have been trialled on a laboratory scale and have been shown to successfully remove hair from skins^{8,9}. However, most have also damaged the skin surface, and in many cases, sulfide has had to be added to the enzyme mixture to increase depilation efficiency^{10,11,12,13,14}. Furthermore, the use of enzymes requires stringent control of both pH and temperature to produce consistent depilation. Although recombinant protein technology has seen a decrease in the purchase price of enzymes, they are still expensive in comparison to the traditional chemical methods, thus, although significant advances have been made, the use of enzymes to depilate skins has not been widely adopted by the leather industry¹⁵.

We report here the development of a process that removes wool from sheepskins using whey or whey permeate, both by-products of the cheese-making industry. This process is environmentally friendly as it not only omits the use of sulfide and alkali for depilation, but also prevents microbial degradation of skins for up to a week at ambient temperature. Sheepskins immersed directly in whey or permeate without washing could be both preserved and depilated during transport to the tannery. Furthermore, skins depilated using whey or permeate can be taken straight to degreasing, skipping the lime, delime, bate and pickle pre-tanning steps. Our research into understanding the mechanism of both preservation and depilation of sheepskin is discussed, and the quality of skins processed using permeate compared to those processed using the traditional sulfide method using scanning electron microscopy, transmission electron microscopy, tear strength, tensile strength, and shrinkage temperature

3.2 Materials and methods

3.2.1 Materials

All sheepskins were collected from a local freezing works (Ovation Ltd., Fielding, New Zealand). The unwashed skins were transported to New Zealand Leather and Shoe Research Association (LASRA) where the flesh was removed using a flesher (Rizzi, Italy). Depilation trials with milk products and by-products were carried out on approximately 15×8 cm pieces of defleshed sheepskin cut from the official sampling position (OSP). Milk products, including homogenised milk, UHT milk and milk powder (Anchor, Auckland, New Zealand), were commercially sourced from the supermarket. Fresh liquid whey was obtained from the Cartwheel Creamery, Pohangina, New Zealand. Fresh liquid whey was sterilised at 121°C for 15 minutes. The resulting precipitate was centrifuged at $10,000 \times g$ for 20 minutes, leaving a straw coloured liquid. Whey protein powder (Red8, Auckland, New Zealand) and milk powder were made up to 6.25 % (w/v), and 12.5 % (w/v) with H_2O , respectively. For simplicity, artificial whey permeate solution (4.5 % (w/v) lactose, 0.0035 % (w/v) CaCl_2 , 0.0045 % (w/v) NaCl , 0.14 % (w/v) KCl , and 0.05 % lactic acid (v/v), autoclaved at 121°C for 15 minutes. This will be referred to as permeate solution in this paper. The following is a list of tanning chemicals and their manufacturers: Lime (Websters, New Zealand), Solvitose[®] (Avebe, Veendam, Netherlands), Pancreol NB (Clariant, Munich, Germany), Unislip (Union Specialties Inc., Newburyport, MA, USA), fungicide TCMTB (Lamirsa, Barcelona, Spain), Zoldine ZE (ANGUS Chemical Company, Buffalo Grove, IL, USA), Tetrapol LTN (Shamrock, Auckland, New Zealand), Felierm DP

and Tanicor PW (Stahl Europe BV, Amsterdam, Netherlands), Chromosal[®] B and Tannigan PAK-N (Lanxess, Cologne, Germany), Mimosa (Tanac, Montenegro, Brazil), Sulphirool EG60 (Smit & Zoon, Weesp, Netherlands), and formic acid (Clark Products, Napier, New Zealand). All water used was from Barnstead[™] Nanopure[™] (Thermo Fisher Scientific, MA, USA) that produces water largely free of bacteria, particles and dissolved solute contaminants.

3.2.2 Depilation trials using milk products and permeate solution

Ten pieces of unwashed sheepskin (15 × 8 cm) were cut from the skin of a single animal, placed in sterilised glass containers then submerged in enough liquid (milk, UHT milk, milk powder, whey, sterilised whey, whey powder and permeate solution) to ensure the wool was completely covered. All the following procedures were carried out in a biohazard hood. The process of depilation was followed by monitoring the pH of the liquid, and its smell until the wool could be easily removed from the skin using gentle thumb pressure. Controls of H₂O, acetic acid and lactic acid solution with an initial pH of 4.5 were included to ensure that the antimicrobial and depilation effects were not due to pH alone, or to lactic acid which is the acid produced by many microorganisms cultured in milk¹⁶. After the samples were depilated, they were subjected to TEM and SEM, and samples of the depilation liquid at completion of the process were taken for microbiological analysis. In order to test for reproducibility, the experiment was repeated using a second animal.

3.2.3 Scaled up trials using permeate

Three pieces of sheepskin, each from a different animal (9 in total) were used in this study. Each was cut in half, and one half depilated using the conventional sulfide method, while the other was treated with permeate. Due to the different sizes of each piece of sheepskin, the volume of permeate solution used varied. Each piece of skin was placed in a sterile plastic container large enough to let it lie flat, then submerged in enough sterile permeate solution to completely cover all the wool. After the liquid was added, a lid was used to seal the container, which was then left at room temperature until depilation was complete. To check progress, the lids were removed every 12 hours and the skins visually inspected and tested for ease of depilation using gentle thumb pressure. A sample of the liquid was also taken and its pH measured using a pH strip. After three to four days, depending on the ambient temperature, when depilation was complete, the skins were removed from the permeate solution and depilated. Part of the skin was taken for tear and tensile

Table 1: Standard LASRA protocol for tanning sheepskins.

Process	Chemical	Amount (pelt weight %)	Procedure
Depilate/ lime paint	H ₂ O	500 mL/skin	Painted on the flesh side of skin, left for 2 hrs, then remove wool and weigh the pelt.
	Na ₂ S	200 g/L	
	NaOH	45 g/L	
	Lime	50 g/L	
	Solvitose	25 g/L	
Delime	H ₂ O	80	20 °C, O/N
	H ₂ O	200	20 °C, 1 hr, × 4
Bate	H ₂ O	100	35 °C, 2 mins
	NH ₄ Cl	2	
	Commercial enzyme (Pancreol NB)	0.12	35 °C, 75 mins
	H ₂ O ₂	0.2	
Pickle	H ₂ O	100	20 °C, 20 mins, × 3
	H ₂ O	90	20 °C, 10 mins
	NaCl	20	
	Unislip	0.1	
	Fungicide TCMTB	0.06	20 °C, 90 mins
	H ₂ SO ₄	2	
Degrease	H ₂ O	50	35 °C, 10 mins
	NaCl	5	
	Tetrapol LTN	4	35 °C, 20 mins
	Zoldine ZE	2	
	HCOONa	1	
	NaHCO ₃	1	35 °C, 20 mins, × 3
	Check pH 7.0 – 8.0		
	H ₂ O	100	42 °C, 60 mins
	H ₂ O	150	42 °C, 30 mins
	Tetrapol LTN	1	
H ₂ O	150	42 °C, 20 mins, × 4	
Tan	H ₂ O	100	25 °C, 20 mins
	Unislip	0.1	
	Disodium phthalate	1	
	33 % Chrome powder	4.5	
Neutralise	H ₂ O	100	35 °C, 60 mins
	Tannigan PAK-N	1	
	HCOONa	1	
	NaHCO ₃	0.15	
Retannage	H ₂ O	200	35 °C, 15 mins
	H ₂ O	100	
	Tanicor PW	2	
Fatliquor	Mimosa	3	50 °C, 45 mins
	Sulphirol EG60	1.5	
Fix	Polyol AK	3.5	30 mins
	85 % Formic acid	0.5	
Wash	H ₂ O	300	20 °C, 15 mins

Final product dried on horse.

strength analysis (pre-tanning samples), and the rest processed to leather using the LASRA standard protocol from the degreasing stage (Table 1). The other half of the pelt was both depilated and processed using the standard LASRA protocol (Table 1).

3.2.4 Scanning electron microscopy (SEM) evaluation of permeate-depilated sheepskin

SEM samples were prepared by Manawatu Microscopy Imaging Centre (MMIC, Massey University, Palmerston North, New Zealand) using the following protocol: Freshly depilated sheepskin samples were cut into 10 mm x 10 mm pieces and placed in modified Karnovsky's fixative, made up from 3 % glutaraldehyde and 2 % formaldehyde in 0.1 M phosphate buffer (pH 7.2). The samples were fixed for 8 hours at room temperature and then rinsed three times with 0.1 M phosphate buffer (pH 7.2). The samples were then sequentially dehydrated with 25 %, 50 %, 75 %, 95 %, and absolute ethanol for 15 minutes each, with a final absolute ethanol wash for 1 hour. Samples were dried to critical point using liquid CO₂ as the critical point fluid and absolute ethanol as the intermediary with the Polaron E3000 series II (Quorum Technologies, UK) critical point drying apparatus. Samples were then mounted onto aluminium stubs using double sided tape and sputter coated with approximately 100 nm of gold with a Baltec SCD 050 sputter coater (Capovani Brothers Inc., USA), and examined using the FEI Quanta 200 Environmental Scanning Electron Microscope (Thermo Fisher Scientific, USA) at an accelerating voltage of 20 kV.

3.2.5 Transmission electron microscopy (TEM) evaluation of the permeate-depilated sheepskin

Permeate-depilated skin samples were cut into 1 mm thin slices using a sterile scalpel blade and fixed overnight using a fixative containing 2.5 % (v/v) glutaraldehyde and 0.06 % (w/v) cuproinic blue in 50 mM acetate buffer (pH 5.6) supplemented with 0.3 M MgCl₂. After fixing, the samples were rinsed three times with the same fixative solution omitting cuproinic blue. Samples were treated for an hour with 0.5 % sodium tungstate in 50 mM acetate buffer (pH 5.6), and then overnight with 0.5 % sodium tungstate in 30 % ethanol. The following steps were carried out by MMIC. Samples were dehydrated sequentially with 25 %, 50 %, 75 %, 95 %, and 100 % acetone twice, then treated with a 1:1 mixture of acetone and Procure 812 resin (ProSciTech, Australia), and left to polymerise overnight. The samples were trimmed and cut into 1 μ m sections with a Leica EM UC7 ultra-microtome (Leica

Biosystems, Wetzlar, Germany), and fixed onto a glass slide. Sample blocks were further cut to 100 nm with a diamond knife (Diatome, Switzerland). The cuts were stretched with chloroform vapour, mounted on grids using a Quick Coat G pen (Daido Sangyo, Japan), and stained with uranyl acetate in 50 % ethanol for one hour. They were then washed with 50 % ethanol, and further stained with lead citrate for four minutes to visualise the collagen fibrils. Samples were examined with a Technai G2 Spirit BioTWIN Transmission Electron Microscope (FEI, Czech Republic).

3.2.6 Identification of the viable microorganisms in the milk media at the completion of depilation.

Five culture media (TSB, LB, MRS, malt and Wilson's media¹⁷) were used to culture viable microorganisms from the milk, UHT milk, milk powder, whey, sterilised whey, and permeate solutions at the completion of depilation. TSB and LB are general high-nutrient culture media for bacteria; MRS is a media specifically designed to culture lactobacilli; malt and Wilson's media are general media with high and low-nutrient contents respectively, that are optimised for fungi. Sterile agar plates (1.5 %) were made for each sample replicate using the five different media to comprise a set of plates for each depilation solution. One hundred (100) μL of the liquid from each completed depilation was pipetted onto each set of sterile nutrient plates, then spread over the surface using a sterilised glass spreader. The TSB, LB, and MRS plates were incubated overnight at 37 °C, while the malt and Wilson's media plates were incubated at 30 °C. Morphologically distinctive colonies were picked at random and re-streaked onto new sterile plates. Microbial genomic DNA (gDNA) was extracted from cells using the standard procedure of Gussow and Clackson¹⁸. The crude gDNA was used as a template to amplify the 16S- and 18S rRNA gene-encoding regions with primers 27f/1492r, Eub338/Eub518, and nu-SSU-0817-5'/nu-SSU-1196-3' (Table 2) and PCR conditions described in Table S1. The resulting amplicons were purified by ethanol precipitation¹⁹ and sent to Massey Genome Service (MGS, Massey University, Palmerston North) to be sequenced (Capillary ABI3730 DNA analyzer, Thermo Fisher Scientific, USA). Sequences were analysed using the blastn algorithm against NCBI²⁰ nucleotide collection (nr/nt) database. Species identified were those that had at least 97.5 % sequence identity. The process was repeated a second time with the solutions obtained using a different animal.

Table 2: PCR primer sets for bacteria 16S and fungal 18S ribosomal ribonucleic acid (rRNA) encoding gene amplification.

Primer name	Sequence (5' → 3')	Target gene	Amplicon length (bp)	Reference
27f	AGAGTTTGATCCTGGCTCAG	Full length 16S rRNA	1400	21
1492r	GGTTACCTTGTTACGACTT			
Eub338	ACTCCTACGGGAGGCAGGAG	V3 region of 16S rRNA	200	22,23
Eub518	ATTACCGCGGCTGCTGCTGG			
nu-SSU-0817-5'	TTAGCATGGAATAATRRRAATAGGA	Nuclear small subunit of 18S rRNA	420	24
nu-SSU-1196-3'	TCTGGACCTGGTGAGTTTCC			

3.2.7 Tear strength analysis of depilated skins and the final leather product

Tear strength measurements were carried out using the TA.XT Plus Texture Analyser (Stable Micro Systems, Surrey, UK) according to the international standard ISO 3377-2:2016²⁵. Fresh permeate-depilated skin samples taken from 3 different sheepskins were cut into four rectangular shaped pieces (50 mm × 27 mm) parallel to the backbone. A slit was cut in the centre of the rectangular sample and the thickness of the leather at either end of this slit was measured using a Baty C1 thickness gauge (Bowers Group, UK) to provide an average thickness for the test sample. At the same time samples from the same animals that had been processed using the LASRA process (*i.e.* sulfide depilation, lime, delime, bate, pickle) were prepared in the same way. At a later stage samples were taken from matched leather samples processed using either permeate or the traditional LASRA process (24 samples in total). The leather samples were conditioned at a constant temperature and humidity (20 °C and 65 % relative humidity) for 24 hours before testing.

The slit was placed over the two hooks of the instrument and the skin stretched at a constant rate of 1 mm/sec with the long axis of the slit perpendicular to the direction of the pull (Fig. 1). The samples were pulled until rupture and the force (N) required to reach this point was recorded. The tear strength was calculated as tear force divided by the thickness of the tested sample (N/mm). The final tear strength for the skin of each animal was calculated from the average of the four technical replicates, with the exception of OSP2 with three technical replicates. To compare the effects of the different processes on the skins, the values obtained for each of the three biological replicates were averaged.

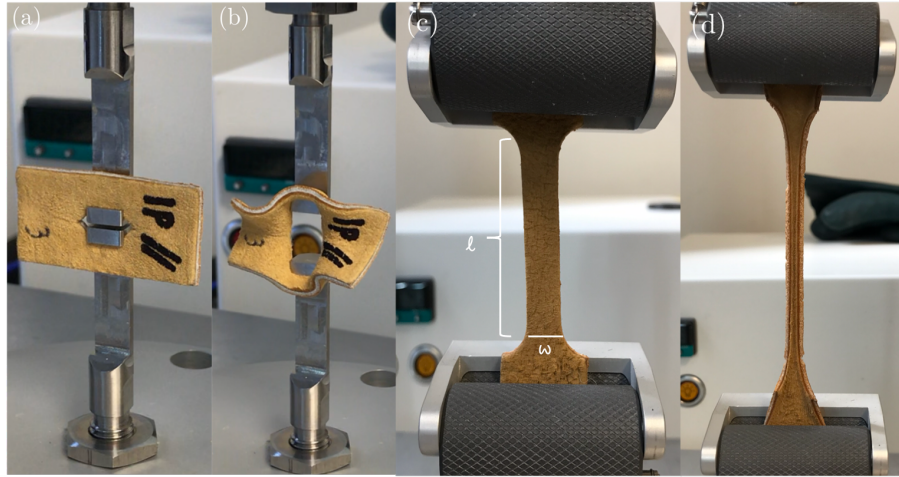


Figure 1: Image showing the instrument setup for the measurement of the tear and tensile strength of skin and leather samples. (a) and (b), tear strength measurements. (c) and (d), tensile strength measurements. Each showing leather samples at the start (a), (c), and part way through (b), (d) the tests.

3.2.8 Tensile strength analysis of depilated skins and final leather product

Tensile strength measurements were carried out using the TA.XT Plus Texture Analyzer (Stable Micro Systems, Surrey, UK) at room temperature. Test samples were prepared at the same time as the tear strength samples except they were cut into a 'dog bone' shape of 100 mm x 20 mm pieces parallel to the backbone. Uniaxial tensile tests were conducted using a load cell of 7500 N. Each end of the sample was securely clamped into specifically designed grips (Fig. 1). Exponent software (Stable Micro Systems, Surrey, UK) was used to stretch the samples at a constant rate of 0.1 mm/sec. The effective sample length (l) of approximately 50.0 mm was measured as the distance from the ends of the two clamps; the width (w) was 10.0 mm, and was measured at the thinner part of the 'dog bone'; the thickness, also called the height (h), was the average thickness of the thinner part of the 'dog bone'. For each test, the force (N) was plotted against the distance (mm) stretched until rupture. The sample cross-sectional area was calculated from thickness/height (mm) x width (mm). Stress (N/mm^2) was then calculated by dividing the force (N) by the cross-sectional area (mm^2). Strain (mm/mm) was calculated from the distance of the stretch (mm) divided by sample effective length (mm). Tensile strength curves were generated by plotting strain (mm/mm) against stress (N/mm^2) using GraphPad Prism software (v. 9.1.1 for macOS, San Diego, CA, USA).

3.2.9 Leather shrinkage temperature measurements

The thermal stability of leather was measured by its shrinkage temperature ($^{\circ}\text{C}$). The shrinkage temperatures of chrome-tanned leather made from both permeate- and chemically-depilated sheepskins were measured according to the ISO 3380:2015 standard protocol²⁶. The leather samples from the OSP were cut into $1.5\text{ cm} \times 5\text{ cm}$ pieces and submerged in water at $40\text{ }^{\circ}\text{C}$ for at least an hour before measurement. Two small holes were punched in the two ends of each leather piece allowing it to be hooked onto the Theis leather shrinkage meter²⁷. It was then submerged in a solution of 100 % glycerol and heated with continuous stirring until the indicator moved, indicating the collagen fibres had shrunk, and the shrinkage temperature recorded.

3.3 Results and discussion

3.3.1 Sheepskin depilation using milk products and by-products.

An experiment carried out by Schlosser *et al.*²⁸ in 1986 using an undisclosed *Lactobacillus* culture to preserve hides was based on the fact that many lactic acid bacteria were being used in the food industry for the preservation of food. They incubated hides in a *Lactobacillus* culture, to find that not only were the hides preserved, but they were also depilated. However, no further research was carried out to understand the mechanisms of either preservation or depilation. This experiment was therefore repeated using commercially sourced yoghurt and found it prevented putrefaction and depilated unwashed sheepskins after three to four days of incubation (unpublished result). As yoghurt is a fermented milk product, further trials were carried out using other milk products, such as, milk, UHT milk, milk reconstituted from milk powder, whey, sterilised whey, and whey protein solutions. Controls of H_2O , and water acidified to pH 4.5 with both acetic and lactic acids were included in the experiment and the course of the depilation was monitored through pH, and smell (Table 3).

Although all media tested eventually depilated skins, including the H_2O and acid controls, two major differences were observed. Sheepskin that was depilated with milk products except for whey protein solution, smelled like fermented milk, whereas, the others (H_2O , acid controls and the solution made from powdered whey protein) had the unpleasant smell of putrefaction. The other difference was the change in pH during depilation. All media that smelled like fermented milk at

the end of the depilation trial had an initial pH around 6.5 – 6.8, that dropped to approximately 4.5 as the incubation continued. At this stage, wool could easily be removed from the skin samples, and the skin appeared to be pink, plump, and shiny. In contrast, in the other group of samples the pH increased over the course of depilation, eventually plateauing between 7.5 and 8.0. Surface damage was obvious, the skin was grey and smelt rotten. Interestingly, all the milk products trialled were able to depilate sheepskin without any obvious damage, with the exception of whey protein powder. Whey powder is manufactured by ultrafiltration of liquid whey, which retains the proteins but removes lactose and other minerals, suggesting that it was not an antimicrobial milk peptide or protein that was responsible for the preservation of the skins. Because it was impossible to source commercially prepared permeate, an artificial permeate solution containing only lactose and traces of metal ions was made, and when this was used to incubate the skins, they were preserved and depilated with the same efficiency seen for milk and whey.

Table 3: Depilation trials with milk products and by-products.

	Initial pH of solution	Final pH	Days to depilate	Smell	Depilated skin condition
Milk	6.8	4.5	3		
UHT milk	6.7	4.5	3		
12.5 % (w/v) milk powder solution	6.8	4.5	3	Fermented /sour milk	Pink, shiny, plump and very smooth
Whey	6.2	4.5	3		
Sterilised whey	6.0	4.5	3		
Sterilised permeate	6.0	4.5	3		
6.25 % (w/v) whey protein solution	6.5	6.0	5		Grey, easily broken into pieces, and rigid
H ₂ O	7.0	7.5	5	Putrefied and rotten	
H ₂ O with acetic acid	4.5	7.5	3		
H ₂ O with lactic acid	4.5	8.0	3		

3.3.2 Physical appearance of the permeate-depilated sheepskins.

After incubating the sheepskins in permeate for three to four days, the wool was easily removed by scraping with the thumb. Fig. 2a shows that despite leaving the unwashed piece of skin in permeate at room temperature for three to four days, the skin did not go rotten, and the surface showed no visible damage. To test whether this process was effective on a larger scale, one-quarter of the sheepskin was processed using permeate while the other was processed using traditional beamhouse methods. The wool was easily removed after three days and both pieces were then degreased and chrome tanned using the standard LASRA process (Table 1, Fig. 2b and c). Although not tested in any way, the wool consistently had a silky feel and did not appear to be damaged during removal. To visualise any damage that was less obvious to the eyes, SEM images of the surface of the depilated skin were taken. The grain appeared to be smoother than that of the conventional sulfide depilated bated and pickled skins (Fig. 3a and b), and the wool was cleanly removed from the follicle without damage to the skin (Fig. 3c and d). Interestingly, bacteria could be seen on the surface of the skin and in the hair follicle (Fig. 3e), which was not unexpected due to the fact that various bacteria, especially lactococci and lactobacilli, could be cultured from the permeate that depilated sheepskin (Section 3.3.3). TEM was used to visualise the arrangement of collagen fibrils in permeate-depilated sheepskin and showed that individual collagen fibrils were densely packed and nicely aligned (Fig. 4).

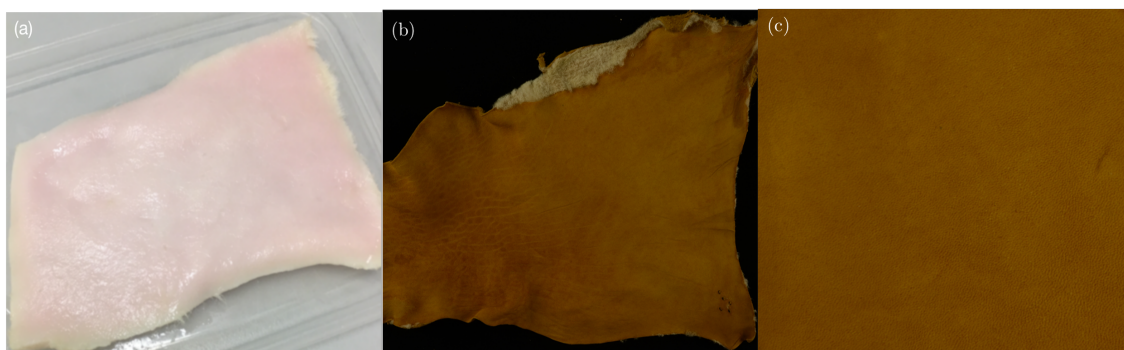


Figure 2: Images of the sheepskin depilated with permeate and the final leather product. (a) Overview of the OSP region depilated with permeate. (b) One quarter of a sheepskin depilated using permeate and made into leather. (c) Closer look of the grain of the leather.

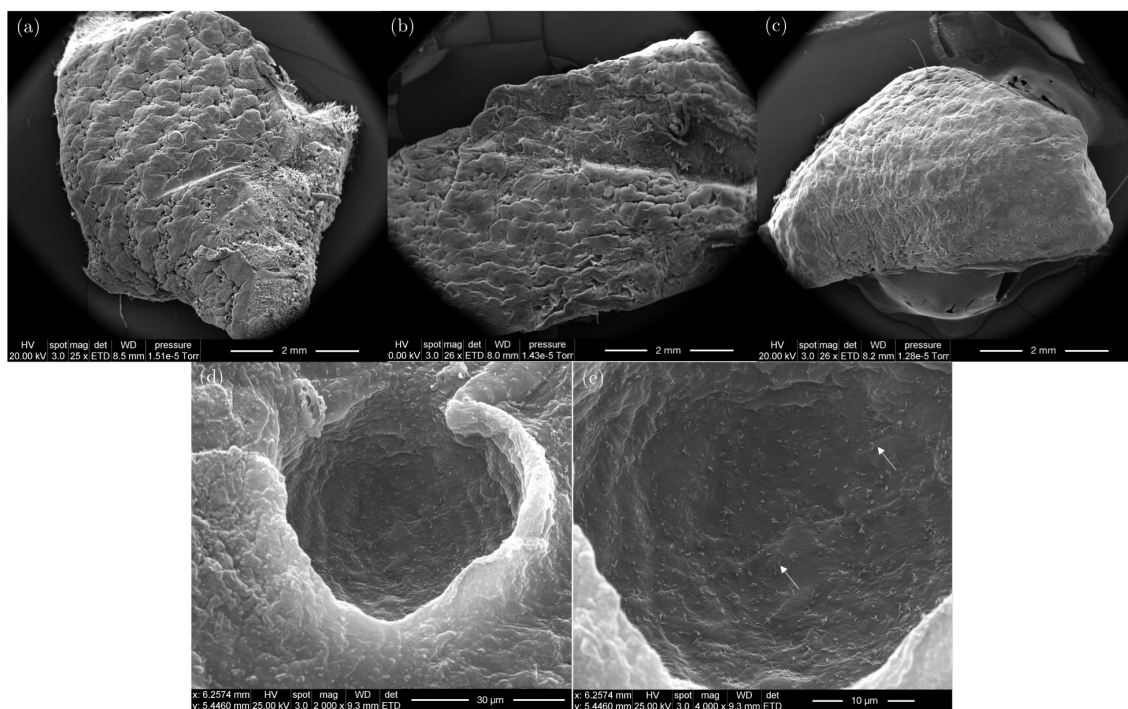


Figure 3: SEM images of the sheepskin depilated with permeate and conventional sulfide method. Sheepskin depilated using (a) the conventional sulfide method, (b) the conventional sulfide method then processed to bate, (c) permeate, (d) higher magnification showing the empty wool follicle of permeate-depilated skin, and (e) empty wool follicle, showing microorganisms residing on the wall.

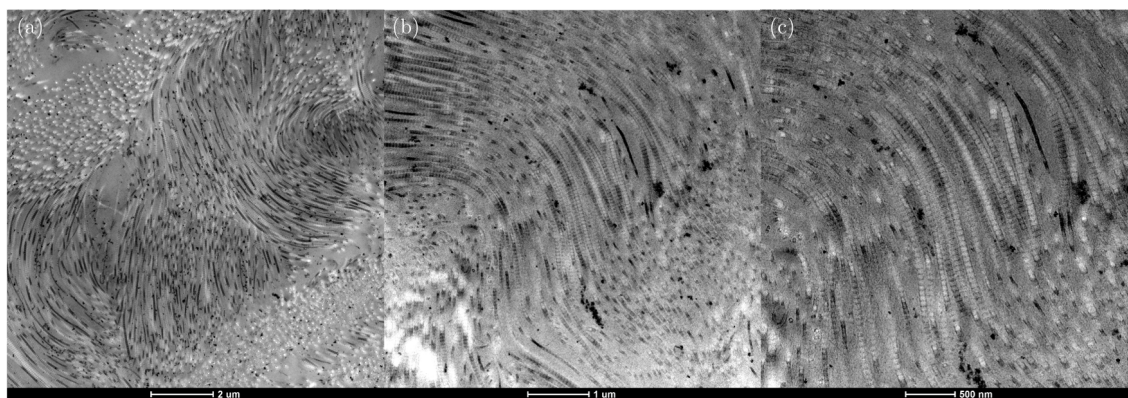


Figure 4: TEM images of a section of the corium of permeate-depilated sheepskins. The collagen fibrils are stained with lead citrate. (a), (b), and (c) are at different magnifications as shown by the bar at the base of each image. The characteristic D-banding of collagen fibrils can clearly be seen in (b) and (c).

3.3.3 Identification of microorganisms isolated from depilation trials with various milk products.

Conventional microbial culturing methods were used to isolate and identify the microorganisms present in the depilation solutions (*i.e.*, sheepskin immersed in a specific milk product) at the end of each depilation trial. Three biological replicates were tested for each milk product. Differences in the colony morphologies of the microorganisms grown on nutrient agar plates were observed (Fig. S1), and a total of 75 colonies were randomly selected for colony PCR and their full length or partial 16S- and 18S rRNA genes amplified and sequenced. Out of these, 21 bacterial and six fungal species were identified (Tables 4 and 5). Bacteria was classified into three phyla (Bacteriodetes, Firmicutes and Proteobacteria), four classes, six orders, 12 families, 17 genera, and 22 species (Table 4). The most frequently identified genera were: *Lactococcus*, *Lactobacillus* (now known as *Latiplantibacillus*/*Levilactobacillus*/*Latilactobacillus* and 22 other genera²⁹), and *Hafnia*. Fungi were classified into two phyla (Ascomycota and Basidiomycota), three classes (Microbotryomycetes, Saccharomycetes and Tremellomycetes), three orders, four families, five genera (*Galactomyces candidum* is the teleomorph of *Geotrichum candidum*) and five species (Table 5). *Geotrichum candidum* (*Galactomyces candidum*) and *Yarrowia lipolytica* were the two most frequently isolated and identified fungi.

Two of the most frequently isolated and identified bacterial genera, *Lactococcus* and *Lactobacillus*, are lactic acid bacteria (LAB). LABs are known to produce antimicrobial metabolites (*e.g.* lactic acid and acetic acid) and bacteriocins (proteinaceous or peptidic toxins), and are widely used in the food industry for preservation purposes³⁰. LABs are able to use lactose in their energy production pathway, unlike other bacteria, and produce lactic acid as a major metabolite. *Lactobacillus plantarum*, *Geotrichum candidum*, and *Yarrowia lipolytica* have all been reported to secrete extracellular enzymes (proteases, lipases, and glycosidases) as they are commonly used in the cheese-making process^{31,32,33}. We therefore speculate that enzymes secreted by these microorganisms specifically degrade the structural components at hair root, facilitating the loosening of wool from the hair follicles and allowing it to be easily removed.

Table 4: Bacteria species identified in the sheepskin depilation trials using various milk products and by-products.

NCBI BLAST identification	NCBI Accession	Primers used	% identity	Culturing media	Depilation media
<i>Bacteroides xylanolyticus</i>	MT192666.1	27f/1492r	98.6	Malt	Sterilised permeate
	MT459291.1	Eub338/Eub518	100.0		
<i>Citrobacter europaeus</i>	NR_156052.1	Eub338/Eub518	98.8	Malt	Whey
<i>Enterobacter sp.</i>	MH477686.1	Eub338/Eub518	99.4	Wilson's media	Sterilised permeate
<i>Enterococcus faecalis</i>	MT158867.1	Eub338/Eub518	100.0	Wilson's media	Whey
<i>Empedobacter felsenii</i>	MN198120.1	Eub338/Eub518	98.7	MRS	Sterilised permeate
<i>Escherichia fergusonii</i>	NR_074902.1	27f/1492r	99.1	LB	Whey
	MT645516.1		100.0	MRS	Sterilised permeate
<i>Escherichia coli</i>	CP066366.1	27f/1492r	100.0	LB	Whey
	MW846276.1	Eub338/Eub518	100.0	MRS	Sterilised permeate
<i>Hafnia alvei</i>	LR699008.1	27f/1492r	98.9	TSB	Whey
	KC210872.1		99.1	Wilson's media	Sterilised permeate
	KX674363.1		99.4	Milk	
<i>Hafnia paralvei</i>	MT470952.1	27f/1492r	99.2	TSB	Whey
	NR_116898.1		99.7	MRS	Sterilised permeate
	NR_025334.1		98.8	Wilson's media	Milk
	MT470952.1	99.2	Milk powder		
	MN868256.1	Eub338/Eub518	99.4	Milk	
<i>Klebsiella aerogenes</i>	MW784626.1	Eub338/Eub518	99.3	Malt	Sterilised permeate
<i>Kurthia gibsonii</i>	MN966854.1	27f/1492r	99.5	Wilson's media	Sterilised permeate
	MK898830.1	Eub338/Eub518	100.0		
<i>Lactobacillus brevis</i>	NR_116238.1	27f/1492r	99.5	MRS	Whey
	MG722900.1	Eub338/Eub518	99.4		
				100.0	Malt
<i>Lactobacillus curvatus</i>	MT645312.1	Eub338/Eub518	99.4	MRS	Sterilised permeate
<i>Lactobacillus graminis</i>	MN640858.1	Eub338/Eub518	99.3	MRS	Milk
<i>Lactobacillus plantarum</i>	MF623219.1	27f/1492r	97.9	MRS	Milk
	MK652787.1		100.0		
	KT626385.1	Eub338/Eub518	100.0		Sterilised permeate
			99.4	Malt	Sterilised whey
<i>Lactococcus lactis</i> subsp. <i>cremoris</i>	NR_040954.1	27f/1492r	99.3	Wilson's media	Milk powder
<i>Lactococcus lactis</i> subsp. <i>lactis</i>	MF108188.1	27f/1492r	99.7	Malt	Sterilised permeate

Table 4: Bacteria species identified in the sheepskin depilation trials using various milk products and by-products (continued).

NCBI BLAST identification	NCBI Accession	Primers used	% identity	Culturing media	Depilation media	
<i>Lactococcus lactis</i>	NR_113960.1	27f/1492r	100.0	TSB	Whey	
			99.2	Malt	Milk	
	98.5		MRS		Sterilised whey	
	98.2			permeate		
	MT545096.1		99.5	Wilson's media	Sterilised whey	
	MT597705.1		99.9		permeate	
	MH666046.1		Eub338/Eub518	98.6	Wilson's media	Sterilised whey
				99.3		permeate
<i>Leuconostoc holzapfelii</i>	NR_042620.1	Eub338/Eub518	98.8	Malt	Milk	
<i>Lysinibacillus macroides</i>	NR_114920.1	27f/1492r	97.9	MRS	UHT milk	
<i>Pseudomonas sp.</i>	KJ496054.1	27f/1492r	100.0	Malt	Sterilised whey	
	MW844014.1	Eub338/Eub518	100.0		permeate	
<i>Proteus vulgaris</i>	KX867797.1	27f/1492r	98.1	MRS	Sterilised whey	

Table 5: Fungal species identified in the sheepskin depilation trials using various milk products and by-products.

NCBI BLAST identification	NCBI Accession	% identity	Culturing media	Depilation media
<i>Galactomyces candidum</i>	KY457577.1	99.7	Wilson's media	Milk
		99.5		UHT milk
		99.7	TSB/LB/MRS/Malt/Wilson's media	Fresh whey
<i>Geotrichum candidum</i>	KY977411.1	99.7	MRS/Malt	Sterilised permeate
		99.7	Malt	Sterilised whey
<i>Pichia insulana</i>	NG_063091.1	99.5	Malt	Sterilised whey
<i>Rhodotorula spp.</i>	MT569975.1	99.5	Malt	UHT milk
<i>Trichosporon lactis</i>	NG_070852.1	99.7	Wilson's media	Milk powder
<i>Yarrowia lipolytica</i>	MH545931.1	99.2	Wilson's media	Sterilised permeate
		99.1	Malt	Sterilised whey
	NG_013120.1	99.7		Milk

3.3.4 Tear and tensile strength analysis of permeate-depilated sheepskins

To confirm that processing sheepskins with permeate resulted in a product as least as good as that produced using traditional methods, two sets of tear and tensile strength measurements were made for skins from the same animal that had been processed using both methods: (a) skin depilated using permeate against pickled skin that had been sulfide depilated, (b) the final leather product made from permeate-depilated skin *vs.* skin depilated with sulfide. Although tear and tensile strengths are related, they are not identical measurements. Both, however, are indicative of the strength of a material. The tear strength of leather reflects the 'toughness' of the material and its ability to resist rupture. As a result, it is commonly used as the industry standard for strength as it relates closely to physical performance. Tensile strength on the other hand, measures the mechanical properties of leather more precisely, as it is related to the strength of the collagen fibres in the skin³⁴. Both tear and tensile strengths were measured on three pieces of sheepskin from three different animals taken parallel to the backbone, then normalised to the thickness of the skins. There were no significant differences in the tear strengths of the final leather products produced from skins depilated using the two different methods, despite permeate-depilated skin having a slightly higher tear strength compared to that of pickled skin (Fig. 5a, one-way ANOVA, p -value = 0.001). Although pickled skin had a slightly higher stress value at rupture compared to permeate-depilated skins (Fig. 5c, p -value = 0.001), it did not appear to affect the tensile strength of the tanned leather products which had similar tensile strengths regardless of the process (Figs. 5b, c and d). Table 6 shows the force, stress and strain at rupture for tanned-leather and pre-tanned skin.

A stress-strain curve for skin can be drawn from the tensile strength results, and typically shows three parts, the toe, heel, and the linear regions. In the toe region, at low strain, the skin behaves elastically, reflecting the removal of macroscopic crimps in the collagen fibres as force is applied. As the force is increased, the heel region of the curve is seen at medium strain, where the kinks in the collagen molecules are straightened out. Under high force the curve becomes linear as the collagen molecules are stretched out and glide against each other, uniformly aligning. Eventually, the skin ruptures and curls back.³⁵ All leather and skin samples showed typical stress-strain curves in these three regions (Fig. 6).

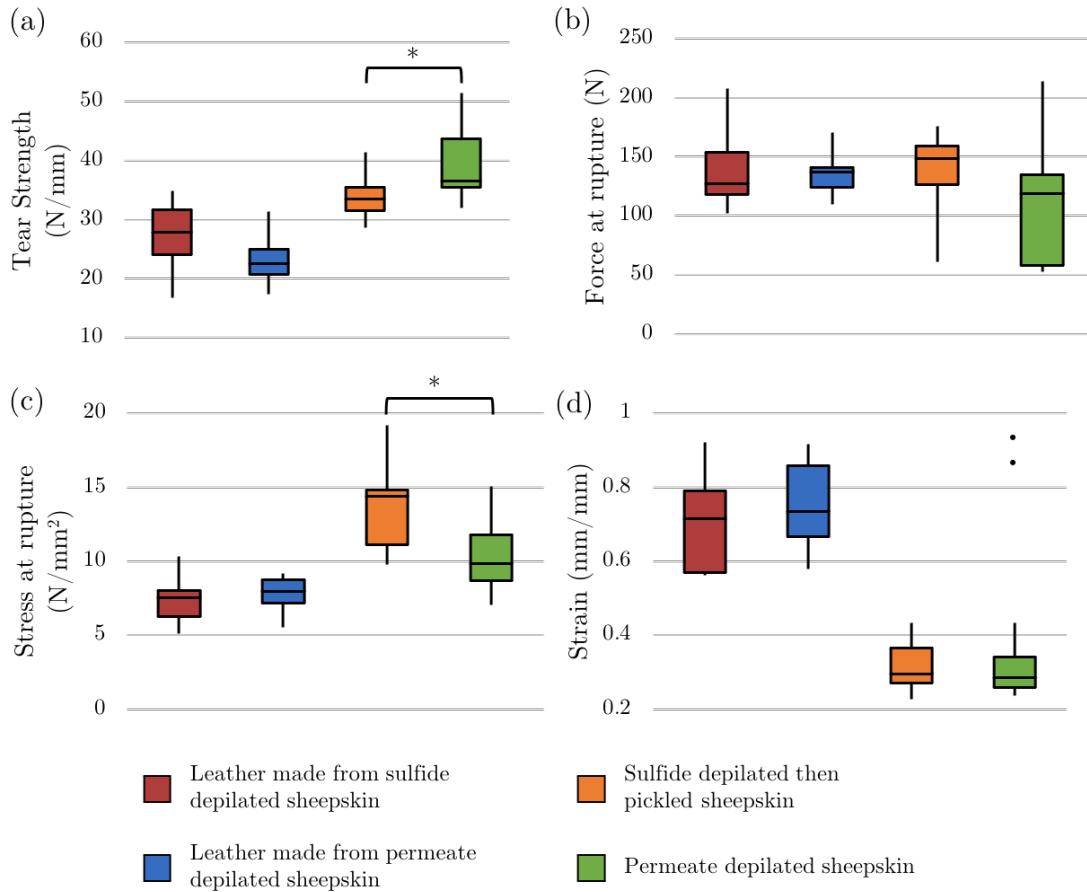


Figure 5: Comparison of tear and tensile strength of tanned leather and pre-tanned skins. (a) Tear strength, (b), (c), and (d) Tensile strength measurements. *, p -value < 0.01 . (d) dots represent outliers.

Table 6: Comparison of tensile strength of tanned leather and pre-tanned skins. Each measurement was done on three different sheepskins, with four technical repeats on each skin. The values in the table represent the average of each measurement.

Sample type		Thickness (mm)	Force at rupture (N)	Stress at rupture (N/mm ²)	Strain at rupture (mm/mm)
Leather made from	Sulfide depilated skin	1.9	140.5	7.3	0.7
	Permeate depilated skin	1.7	134.3	7.7	0.8
Pre-tanned skin	Pickled	1.0	138.3	14.1	0.3
	Permeate depilated	1.0	116.7	10.4	0.3

To visualise the linear and non-linear ranges in the stress-strain curve, the first derivative (the slope) of the stress-strain curve was calculated and shown in Fig. 6. Typically, a linear region has a constant slope, therefore, its first derivative would be a relatively flat line with a constant value (*i.e.* the slope is unchanged). In a non-linear region, the slope constantly changes, generating a curved line in the first derivative plot. There were no significant differences in the first derivatives of the final leather products made from the two processes. They were both flat with similar slopes (between strain 0.1 and 0.5, slope of permeate-depilated skin leather product 25.2 *cf.* slope of pickled skin leather product 21.6) strongly indicating there is no difference in the tensile strengths of these leathers (Figs. 6a and b). Furthermore, no significant difference was observed between the pre-tanned skins (*i.e.* pickled skins and permeate-depilated skins, Figs 6c and d). There are, however, obvious differences in the ranges of both the linear and non-linear regions of the curves for leather and pre-tanned skin. Pre-tanned skin samples in general, had a steeper slope in the linear region compared to leather samples, which is characteristic of brittle substance³⁶. This suggests that after tanning, the leather samples are more ductile, as shown by their ability to stretch. In other words, both pre-tanned skin samples were more brittle (or stiff), as evident from the low strain (0.37 *cf.* 0.8 for leather) and the steeper slope of the first derivative plot (Fig. 6) for the pre-tanned skin samples. Even although the pre-tanned skin samples (pickled and permeate-depilated skins) were more brittle, they were able to withstand a higher stress than their matched leather samples before rupture (Figs. 6c and d).

3.3.5 Leather shrinkage temperature

The hydrothermal stability of skin, whether in its natural state, or chemically modified, is routinely measured by leather technologists as shrinkage temperature. The shrinkage temperature is defined as the effect of wet heat on the integrity of the material, and it can vary greatly depending on the tanning efficiency and structure of the collagen fibre network of the material⁶. The shrinkage temperature of skin, including leather, is reported to be correlated to the thermal transition of the collagen tropocollagen helical structure to random coil upon heat denaturation^{6,37}. In the case of native collagen, the shrinkage temperature is 65 - 70 °C, while chromium (III) sulfate tanned leather is typically around 105 - 115 °C⁶.

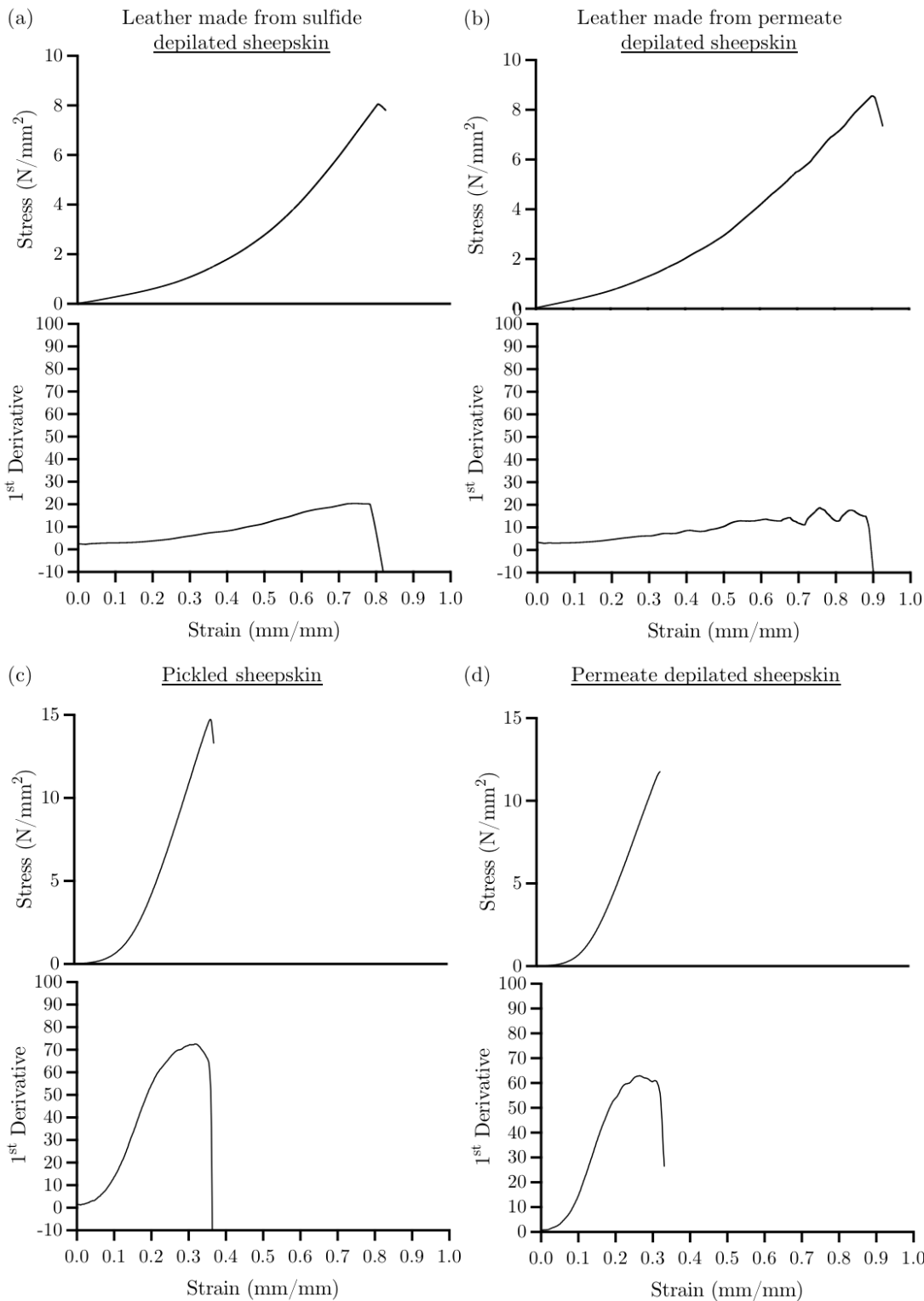


Figure 6: Representative stress-strain curves of sheepskin depilated using permeate and sulfide, and their respective final leather products, and their first derivative (slope) curves.

The shrinkage temperatures of the leather depilated with permeate compared to conventional sodium sulfide is shown in Fig. 7. No significant difference was found

between the shrinkage temperatures of leather depilated using the two different methods. The leather made from chemically depilated sheepskins underwent three extra steps, delime, bate and pickle, to remove all non-collagenous proteins before the skin was degreased and the collagen network was crosslinked with chromium (III) at tanning. In contrast, permeate-depilated leather samples went straight from depilation to degreasing then tanning, and on the basis of biochemical analyses retained more non-collagenous proteins (as found in the amino acid and proteomic analyses of sheepskin, Chapter 4). It has been long thought by leather chemists and technologists that the removal of non-collagenous proteins is essential for the efficient crosslinks to form between chromium (III) and adjacent aspartic and glutamic acid sidechains in collagen microfibrils⁶. On the basis of the observed shrinkage temperatures, the presence of these extra proteoglycans has clearly not attenuated the number of chrome crosslinks being formed. In fact the whisker plot suggests that the structure of the permeate processed leather is much more consistent than the leather produced by the beamhouse process. Whether the complete removal of non-collagenous proteins, such as proteoglycans from the skin matrix is necessary and beneficial for chrome crosslinks is therefore challenged and requires further research.

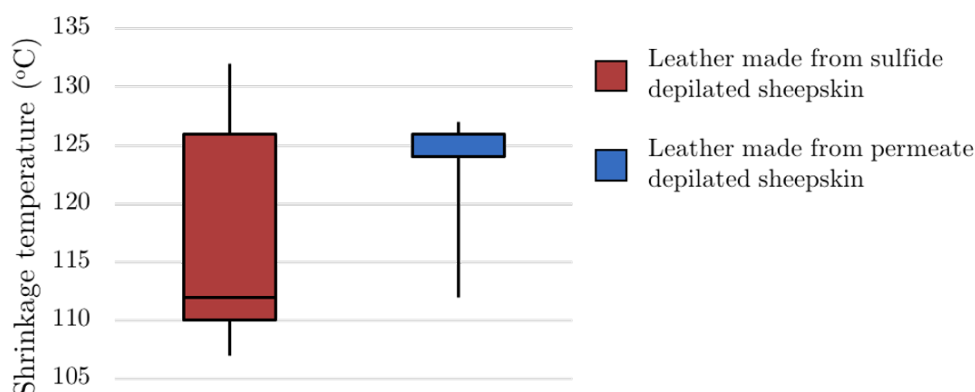


Figure 7: Shrinkage temperature of leather made from sheepskin depilated using sulfide and permeate. p -value = 0.08

3.4 Conclusion

In this work, we have shown on a laboratory scale that a novel and environmentally friendly process for depilating and tanning sheepskin produces leather that is indistinguishable from that produced using the traditional beamhouse methods. The process eliminates the need for NaCl, Na₂S, NaSH, NaOH, Ca(SH)₂, and Ca(OH)₂, and uses far less water than is currently used in the pre-tanning steps of current processes. Furthermore, waste products are

comprised mainly of water protein and microorganisms that are already prevalent in the environment. Using this method to process a large number of randomly selected skins showed they were consistently depilated without damage using whey or whey permeate, both by-products of the dairy industry. It does not require careful temperature or pH control, and as long as the skin is left in permeate we showed it could be preserved up to a week without putrefaction. We also showed that the skin depilated using permeate is equivalent to pickled sheepskin, and can be degreased and tanned, eliminating four pre-tanning steps. It also raised the question of whether it is necessary to completely remove all non-collagenous proteins from the skin matrix to produce good leather from sheepskin.

Our experiments have allowed us to propose a mechanism for the observed preservation and depilation mechanism. It became obvious that the prevention of putrefaction was due to the high concentrations of lactose at the initial stages of the process. We speculate that both restricting the carbon source at the early stages of depilation combined with the gradual reduction in the pH of the depilation liquid, most likely due to the production of lactic acid, initially controlled the growth of the bacteria on the unwashed skin and wool. *Lactobacillus* and *Lactococcus* species are also known to produce many antimicrobial substances. As depilation proceeded and protein and other macromolecules were released from the skin, such substances were able to control the number of microorganisms now able to grow especially those associated with putrefaction. *Lactococcus lactis*, in particular, is known for its production of nisin, a wide spectrum bacteriocin that is often used as a preservative by the food industry. However when fresh sheepskin was incubated in PBS supplemented with nisin, putrefaction still occurred (results not shown) indicating the process of preservation is complex, and not due to a single compound.

Bacteria and fungi are also known to secrete proteases and glycosidases, and those found to be present in this environment are known to secrete enzymes that could preferentially attack the structure around the hair follicle, loosening it to allow easy removal, but without disrupting the collagen structure of the skin. These claims require further research that was carried out as part of this project and will be reported elsewhere (Chapter 5). The use of whey or permeate, both by-products and in some cases waste products of the dairy industry to incubate sheepskins appears to be a technically simple and cost-effective process for removing wool and pretanning, and has the potential to provide the leather industry with a cost-effective option to reduce its waste load on the environment. While a comprehensive study of its

environmental COD and BOD loads was not carried out, this should be done to strengthen the claim that it is, for sheepskin at least, a 'green' process for the leather industry. Lastly, the observations about the quality of the wool removed using whey or permeate depilation warrants further investigation. It is possible that it has gained some desirable properties that could be exploited by an industry that is trying to find new high-value products.

Acknowledgements

The authors thank LASRA (Palmerston North, New Zealand) for the supply of sheepskins, Mr. and Mrs. Walcroft from Cartwheel creamery for the whey, Mr. Steve Glasgow for the assistance with the texture analyser, and Manawatu Microscopy Imaging Centre (MMIC, Manawatu, New Zealand) for the microscopy technical support.

Author contributions

MA initiated the research idea and with GEN designed the research. GEN edited the manuscript. GEN and JR monitored the culturing experiments and provided advice. GH tanned the sheepskins and provided tanning technical advice throughout the research. Y-HT wrote the manuscript and carried out the research.

3.5 References

- [1] Global Industry Analysts. Global leather goods industry. Report, April 2021.
- [2] United Nations Industrial Development Organisation. Future trends in the world leather and leather products industry and trade, 2010.
- [3] D. Breitzkreutz, I. Koxholt, K. Thiemann, and R. Nischt. Skin basement membrane: the foundation of epidermal integrity-BM functions and diverse roles of bridging molecules nidogen and perlecan. *BioMed Res. Int.*, 2013:179784–179784, 2013. ISSN 2314-6141 2314-6133. doi: 10.1155/2013/179784. URL <https://pubmed.ncbi.nlm.nih.gov/23586018>.
- [4] C. Frantz, K. M. Stewart, and V. M. Weaver. The extracellular matrix at a glance. *J. Cell Sci.*, 123(24):4195, 2010. doi: 10.1242/jcs.023820. URL <http://jcs.biologists.org/content/123/24/4195.abstract>.
- [5] R. L. Edmonds, D. S. Choudhury, R. G. Haverkamp, M. Birtles, T. F. Allsop, and G. E. Norris. Using proteomics, immunohistology, and atomic force microscopy to

- characterize surface damage to lambskins observed after enzymatic dewooling. *J. Agric. Food. Chem.*, 56(17):7934–7941, 2008. ISSN 0021-8561. doi: 10.1021/jf800380y. URL <https://doi.org/10.1021/jf800380y>.
- [6] A. D. Covington. *Tanning chemistry: the science of leather*. RSC Publishing, 2009. URL <http://app.knovel.com/hotlink/toc/id:kpTCTSL002/tanning-chemistry-the>.
- [7] N. R. Kamini, C. Hemachander, J. G. S. Mala, and R. Puvanakrishnan. Microbial enzyme technology as an alternative to conventional chemicals in leather industry. *Curr. Sci. India*, 77(1):80–86, 1999. ISSN 00113891. URL <http://www.jstor.org/stable/24102916>.
- [8] A. Dettmer, É. Cavalli, M. A. Z. Ayub, and M. Gutterres. Environmentally friendly hide unhairing: enzymatic hide processing for the replacement of sodium sulfide and deliming. *J. Cleaner Prod.*, 47:11–18, 2013. ISSN 0959-6526. doi: <https://doi.org/10.1016/j.jclepro.2012.04.024>. URL <https://www.sciencedirect.com/science/article/pii/S0959652612002119>.
- [9] M. Sousa. Advances in understanding of enzymatic unhairing of bovine hides. *J. Am. Leather Chem. Assoc.*, 109:268–277, 2014.
- [10] N. Kandasamy, P. Velmurugan, Sundarvel A., R. J. Raghava, C. Bangaru, and T. Palanisamy. Eco-benign enzymatic dehairing of goatskins utilizing a protease from a *Pseudomonas fluorescens* species isolated from fish visceral waste. *J. Cleaner Prod.*, 25:27–33, 2012. ISSN 0959-6526. doi: <https://doi.org/10.1016/j.jclepro.2011.12.007>. URL <http://www.sciencedirect.com/science/article/pii/S0959652611005324>.
- [11] L. M. I. Lopéz, C. A. Viana, M. E. Errasti, M. L. Garro, J. E. Martegani, G. A. Mazzilli, C. D. T. Freitas, Í. M. S. Araújo, R. O. da Silva, and M. V. Ramos. Latex peptidases of *Calotropis procera* for dehairing of leather as an alternative to environmentally toxic sodium sulfide treatment. *Bioproc. Biosyst. Eng.*, 40(9): 1391–1398, 2017. ISSN 1615-7605. doi: 10.1007/s00449-017-1796-9. URL <https://doi.org/10.1007/s00449-017-1796-9>.
- [12] S. Sivasubramanian, B. Murali Manohar, A. Rajaram, and R. Puvanakrishnan. Ecofriendly lime and sulfide free enzymatic dehairing of skins and hides using a bacterial alkaline protease. *Chemosphere*, 70(6):1015–1024, 2008. ISSN 0045-6535. doi: <https://doi.org/10.1016/j.chemosphere.2007.09.036>. URL <http://www.sciencedirect.com/science/article/pii/S0045653507011605>.
- [13] P. Thanikaivelan, J. R. Rao, B. U. Nair, and T. Ramasami. Recent trends in leather making: processes, problems, and pathways. *Crit. Rev. Env. Sci. Tec.*, 35(1):37–79, 2005. ISSN 1064-3389. doi: 10.1080/10643380590521436. URL <https://doi.org/10.1080/10643380590521436>.

- [14] B. Wahyuntari and H. Hendrawati. Properties of an extracellular protease of *Bacillus megaterium* DSM 319 as depilating aid of hides. *Microbiology Indonesia*, 6(2):4–4, 2012. ISSN 2087-8575.
- [15] P. Sujitha, S. Kavitha, S. Shakilanishi, N. K. C. Babu, and C. Shanthi. Enzymatic dehairing: a comprehensive review on the mechanistic aspects with emphasis on enzyme specificity. *Int. J. Biol. Macromol.*, 118:168–179, 2018. ISSN 0141-8130.
- [16] G. Oikonomou, M. F. Addis, C. Chassard, M. E. F. Nader-Macias, I. Grant, C. Delbès, C. I. Bogni, Y. Le Loir, and S. Even. Milk microbiota: what are we exactly talking about? *Front. Microbiol.*, 11(60), 2020. ISSN 1664-302X. doi: 10.3389/fmicb.2020.00060. URL <https://www.frontiersin.org/article/10.3389/fmicb.2020.00060>.
- [17] K. Wilson, A. A. Padhye, and J. W. Carmichael. Antifungal activity of *Wallemia ichthyophaga* (= *Hemispora stellata* Vuill. = *Torula epizoa* Corda). *Antonie van Leeuwenhoek*, 35(1):529–532, 1969. ISSN 1572-9699. doi: 10.1007/BF02219170. URL <https://doi.org/10.1007/BF02219170>.
- [18] D. Gussow and T. Clackson. Direct clone characterization from plaques and colonies by the polymerase chain reaction. *Nucleic Acids Res.*, 17(10):4000, 1989. ISSN 0305-1048 (Print) 0305-1048.
- [19] J. Sambrook, E. F. Fritsch, and T. Maniatis. *Molecular cloning: a laboratory manual*. Cold Spring Harbor Laboratory Press, 1989. ISBN 0879693096.
- [20] S. F. Altschul, W. Gish, W. Miller, E. W. Myers, and D. J. Lipman. Basic local alignment search tool. *J. Mol. Biol.*, 215(3):403–10, 1990. ISSN 0022-2836 (Print) 0022-2836. doi: 10.1016/s0022-2836(05)80360-2.
- [21] W. G. Weisburg, S. M. Barns, D. A. Pelletier, and D. J. Lane. 16S ribosomal DNA amplification for phylogenetic study. *J. Bacteriol.*, 173(2):697–703, 1991. ISSN 0021-9193 (Print) 0021-9193.
- [22] DJ Lane. *16S/23S rRNA sequencing*. John Wiley Sons, West Sussex, United Kingdom, 1991.
- [23] G. Muyzer, E. C. de Waal, and A. G. Uitterlinden. Profiling of complex microbial populations by denaturing gradient gel electrophoresis analysis of polymerase chain reaction-amplified genes coding for 16S rRNA. *Appl. Environ. Microbiol.*, 59(3):695–700, 1993. ISSN 0099-2240 1098-5336. doi: 10.1128/AEM.59.3.695-700.1993. URL <https://pubmed.ncbi.nlm.nih.gov/7683183>.
- [24] J. Borneman and R. J. Hartin. PCR primers that amplify fungal rRNA genes from environmental samples. *Appl. Environ. Microbiol.*, 66(10):4356–4360, 2000. ISSN 0099-2240 1098-5336. URL <http://www.ncbi.nlm.nih.gov/pmc/articles/PMC92308/>.

- [25] J. M. V. Williams. IULTCS (IUP) test methods: measurement of tear load-double edge tear. *J. Soc. Leather Technol. Chem.*, 84:327–329, 2000.
- [26] I. U. L. T. C. S. ISO 3380:2015-11 Leather - Physical and mechanical tests - Determination of shrinkage temperature up to 100 °c. Online, 2015.
- [27] G. D. McLaughlin and E. R. Thesis. *The chemistry of leather manufacture*. Number p. 133. Reinhold Publishing Corp., New York, USA, 1945.
- [28] L. Schlosser, A. Hein, W. Keller, and E. Heidemann. Utilisation of a *Lactobacillus* culture in the beamhouse. *J. Soc. Leather Technol. Chem.*, 70:163–8, 1986. ISSN 0144-0322.
- [29] J. Zheng, S. Wittouck, E. Salvetti, C. M. A. P. Franz, H. M. B. Harris, P. Mattarelli, P. W. O’Toole, B. Pot, P. Vandamme, J. Walter, K. Watanabe, S. Wuyts, G. E. Felis, M. G. Gänzle, and S. Lebeer. A taxonomic note on the genus *Lactobacillus*: Description of 23 novel genera, emended description of the genus *Lactobacillus Beijerinck* 1901, and union of *Lactobacillaceae* and *Leuconostocaceae*. *Int. J. Syst. Evol. Microbiol.*, 70(4):2782–2858, 2020. ISSN 1466-5034. doi: <https://doi.org/10.1099/ijsem.0.004107>. URL <https://www.microbiologyresearch.org/content/journal/ijsem/10.1099/ijsem.0.004107>.
- [30] B. Collins, P. D. Cotter, C. Hill, and P. Ross. *Applications of lactic acid bacteria-produced bacteriocins*, pages 89–109. Blackwell Publishing, 2010. doi: <https://doi.org/10.1002/9780813820866.ch5>. URL <https://onlinelibrary.wiley.com/doi/abs/10.1002/9780813820866.ch5>.
- [31] C. Duan, S. Li, Z. Zhao, C. Wang, Y. Zhao, G. E. Yang, C. Niu, L. Gao, X. Liu, and L. Zhao. Proteolytic activity of *Lactobacillus plantarum* strains in cheddar cheese as adjunct cultures. *J. Food Prot.*, 82(12):2108–2118, 2019. ISSN 0362-028x. doi: 10.4315/0362-028x.Jfp-19-276.
- [32] R. Boutrou, L. Kerriou, and J-Y. Gassi. Contribution of *Geotrichum candidum* to the proteolysis of soft cheese. *Int. Dairy J.*, 16(7):775–783, 2006. ISSN 0958-6946. doi: <https://doi.org/10.1016/j.idairyj.2005.07.007>. URL <http://www.sciencedirect.com/science/article/pii/S0958694605001470>.
- [33] C. I. Gonzalez-Lopez, R. Szabo, S. Blanchin-Roland, and C. Gaillardin. Genetic control of extracellular protease synthesis in the yeast *Yarrowia lipolytica*. *Genetics*, 160(2):417–27, 2002. ISSN 0016-6731 (Print) 0016-6731.
- [34] K. H. Sizeland, M. M. Basil-Jones, R. L. Edmonds, S. M. Cooper, N. Kirby, A. Hawley, and R. G. Haverkamp. Collagen orientation and leather strength for selected mammals. *J. Agric. Food. Chem.*, 61(4):887–892, 2013. ISSN 0021-8561. doi: 10.1021/jf3043067. URL <https://doi.org/10.1021/jf3043067>.

- [35] W. Yang, V. R. Sherman, B. Gludovatz, E. Schaible, P. Stewart, R. O. Ritchie, and M. A. Meyers. On the tear resistance of skin. *Nat. Commun.*, 6(1):6649, 2015. ISSN 2041-1723. doi: 10.1038/ncomms7649. URL <https://doi.org/10.1038/ncomms7649>.
- [36] J. Diamant, A. Keller, E. Baer, M. Litt, R. G. C. Arridge, and F. C. Frank. Collagen; ultrastructure and its relation to mechanical properties as a function of ageing. *Proc. R. Soc. London, Ser. B. Biological Sciences*, 180(1060):293–315, 1972. doi: 10.1098/rspb.1972.0019. URL <https://doi.org/10.1098/rspb.1972.0019>.
- [37] A. W. Thomas. The chemistry of tanning processes. *J. Chem. Educ.*, 33(12):650, 1956. ISSN 0021-9584. doi: 10.1021/ed033p650.2. URL <https://doi.org/10.1021/ed033p650.2>.

3.6 Supplementary information

Table S1: PCR conditions.

PCR using <i>Taq</i> DNA polymerase		
Steps	Temperature (°C)	Duration (sec)
Initial denaturation	95	30
Amplification: (30 cycles)		
Denaturation	95	10
Annealing		
27f/1492r	50	30
Eub338/Eub518	55	
nu-SSU-0817-5'/nu-SSU-1196-3	55	
Elongation	72	30 sec/kb
Final elongation	72	300

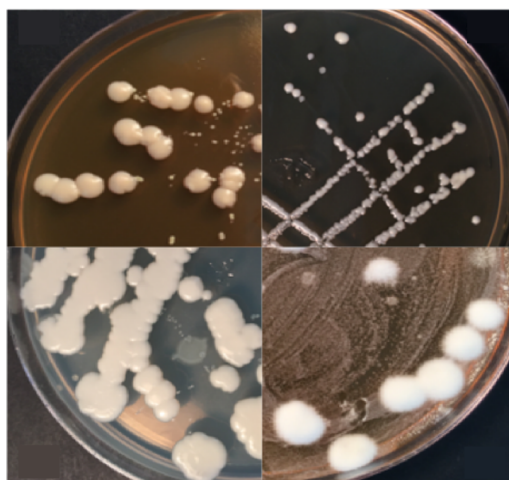


Figure S1: Examples of the different morphologies of microorganisms cultured from spent depilation liquid.

4 |

Using biochemical analyses to compare the molecular structures of sulfide and permeate depilated sheepskins

Using biochemical analyses to compare the molecular structures of sulfide and permeate-depilated sheepskins

Yi-Hsuan Tu¹, Trevor S. Loo¹, Dragana Gagic^{1,2}, Mark L. Patchett¹, and Gillian E. Norris¹

¹School of Fundamental Sciences, Palmerston North, Massey University, New Zealand

²School of Veterinary Sciences, Palmerston North, Massey University, New Zealand

Address correspondence to:

Gillian E. Norris, G.Norris@massey.ac.nz

Publication status: manuscript in preparation to be submitted to the Journal of Agricultural and Food Chemistry

Abstract

An environmentally friendly method for depilating sheepskins has been reported in which the authors found no differences in the physical properties of sheepskin depilated with whey or permeate compared to those of its pre-tan equivalent produced using traditional sulfide (pickled sheepskin). However, the appearance of the whey/whey product depilated skin seemed smoother and it was clear that the wool had been completely and cleanly removed from the hair follicle. In this work, we examined sheepskins depilated using whey/permeate at the molecular level to investigate the potential changes responsible for this observation. Quantitative biochemical analyses of sheepskins depilated with permeate were compared to the results of similar analyses of raw and pickled sheepskins obtained from either this study and/or previous studies reported in the literature. They included: amino acid analysis to obtain the total collagen concentration, collagen crosslink analysis, glycosaminoglycan (GAG) analysis, and a proteomic analysis that provided the abundance of the proteins in permeate depilated sheepskin relative to that in matched chemically depilated (pickled) sheepskin. Results showed no significant differences in collagen, and collagen crosslink concentrations in contrast to the 10-fold increase in GAG concentration. Proteomic analysis showed a higher retention of proteins in the basement membrane of the skin, supporting the observation that permeate depilated skins were smoother than their sulfide depilated counterparts and produced leather with a superior surface.

4.1 Introduction

Sheepskin, a by-product of the meat industry, is used to manufacture a light supple leather that is in demand for luxury high-end fashion garments and accessories, as well as soft wool-lined clothing, gloves, and hats. Unfortunately, the market is in decline, necessitating the waste/disposal of sheepskin not used by the leather industry. Sheepskin is comprised of water (53 %), protein (27.5 %), lipids (18.3 %), and trace minerals. Like all animal skins, it is composed of three general layers: the epidermis, dermis and hypodermis (Fig. 1). The epidermis, the outer-most protective layer of the skin, contains mainly keratinocytes (keratin-producing cells) and parts of the hair shaft (hair fibre) and is usually destroyed by chemical depilation¹. At the junction of epidermis and dermis, there is a coarse basement membrane that, after removal of the epidermis, becomes the surface of the leather. This layer contains collagens type IV, VII, XV and XVIII, laminin, nidogen, and perlecan (a basement membrane-specific heparan-sulfate proteoglycan core protein)². The dermis (true skin) makes up 90 % of the total skin weight and is rich in collagen fibres (collagens type I and III) that give it its strength. Dermal fibroblasts synthesise and secrete the major protein components of skin; collagen, elastin, laminin, and proteoglycans (PGs), that are collectively termed the extracellular matrix (ECM)³.

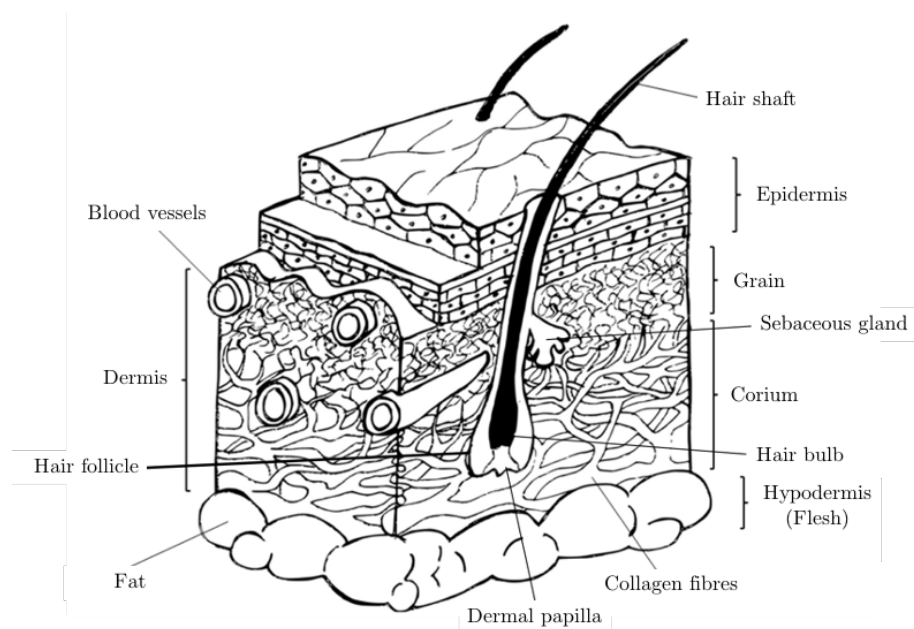


Figure 1: Diagram of the skin structure. Reprinted from Visser (2019) with permission from the author⁴.

Collagen, approximately 60 – 70 % of the dry weight of skin, is largely made up of a repeat sequence containing three amino acids Gly-X-Y, where X and Y are commonly proline (Pro) and 4-hydroxyproline (Hyp), respectively. Although Hyp was once thought to be unique to collagen, it is also found in elastin and two other intracellular proteins, hypoxia-inducible factor (HIF) and argonaute 2 (Ago2)⁵. Nevertheless, Hyp continues to be used as an indicator to determine the collagen content of skin. In collagen, Hyp is involved in both the formation of collagen microfibrils and their structural and thermal stability⁶. Non-covalent interactions between these microfibrils direct the assembly and interactions of collagen fibres, 'gluing' them together to form fibre bundles⁷. Crosslinks that are spontaneously formed between neighbouring lysine (Lys) or deaminated hydroxylysine (Hyl) residues and other lysine or hydroxylysine sidechains further stabilise the fibrils⁸. Finally, the proteoglycans and their sugar components, glycosaminoglycans act as cement to hold the fibres and fibre bundles in place. From the leathermakers' perspective, the dermis is often further divided into three layers: the grain, the grain-corium junction, and the corium (Fig. 1). The grain layer, the uppermost layer of the dermis, is composed of fine interwoven collagen fibres (mainly types I, III and VI), the entire length of the hair follicle, small blood vessels and capillaries^{9,10,11}. The uppermost surface of the grain layer, also termed the enamel, is responsible for the outward appearance of the final leather product which is thought to be due to the presence of the beaded microfilament network formed by collagen VI¹². The grain-corium junction is the transitional zone between the very fine fibres of the grain and the larger fibres of the corium layer. This layer is composed of relatively small collagen fibres (I, III, V, VI, XII, XIV, XVI) and carries the other structural components of the skin, such as blood vessels and for sheep, lipocytes¹³. The corium layer contains thicker and more compact types I and III collagen fibres that form higher order structures varying in diameter. As these bundles form the major part of the leather, their relative orientations are responsible for its strength^{14,15}. The bottom layer of skin, the hypodermis, is also known as the flesh layer, is composed of mainly fat cells and is commonly removed prior to depilation¹⁶.

Five steps, together known as the beamhouse process, are required to prepare the sheepskins for tanning: depilation, liming, deliming/bating, pickling and degreasing. If the skins have been salted, they are rehydrated and washed to remove the salt. To depilate the skins, a thick alkaline sulfide depilatory solution (Na_2S , NaSH , NaOH , $\text{Ca}(\text{SH})_2$, $\text{Ca}(\text{OH})_2$) is painted on the flesh side of the pelt and left penetrate through the skin. When it reaches the hair shaft, it acts to degrade the keratin and loosens the wool or hair. Next, the skins are limed,

although this usually happens simultaneously with depilation. During this procedure the skin is subjected to a high pH (12 - 13) that swells and opens up the collagenous fibre network, allowing alkali-soluble proteins and interfibrillar substances to be removed. During the process, the epidermal keratins are destroyed, and most of the proteoglycans removed from the skin during this process¹⁷. The effluent from the alkaline sulfide step must be treated before being discharged into the environment to prevent the release of hydrogen sulfide which is both toxic and flammable. Research has shown that one-third of the pollution produced from the leather industry is due to the depilation/liming process¹⁸. To combat the problem, much effort has gone into the search for 'greener' depilation agents. Although many enzymes have been trialled as depilation agents on a laboratory scale^{19,20}, most were shown to damage the skin, and many required the addition of sulfide to the enzyme mixture to increase depilation efficiency^{21,22,23,24,25}. Most of all, they are not cost effective in comparison to the traditional chemical methods. Hence, at present, although significant advances have been made, the use of enzymes for skin depilation has not been adopted by the industry. After depilation and liming, the skins are washed (delimed) several times and then treated with a commercially available protease mix (bated) at pH 8 - 9 and 35 °C to ensure the removal of most of the non-collagenous proteins from the skin matrix. Then, they are immersed in a pickling solution consisting of salt and sulfuric acid at pH 2 - 3 which stabilises the skin structure and prevents spoilage. Due to the high fat content of sheepskin, sheepskins in New Zealand undergo a process called degreasing right after pickling to remove the fat layer in the skin before it can be tanned²⁶. The purpose of this is to allow uniform reactions through the cross sections of the pelt during tanning.

Preliminary experiments in our laboratory showed that incubation of fresh, unwashed sheepskins in whey, a by-product of cheese manufacture, prevented putrefaction, and preserved the skin for up to a week at room temperature (18 - 25 °C). Moreover, after three to four days, the wool could be removed from the skin using gentle thumb pressure. Not only did this procedure remove the wool from sheepskin without any damage to the skin surface, it also bypassed four pre-tanning steps (lime, delime, bate, pickle), as the resulting skin could be degreased and tanned directly after depilation (Chapter 3). Investigations into the mechanism of depilation using whey led to trials with sterilised whey in which most of the protein was precipitated and removed, which in turn led to trials using an artificial whey permeate solution. At this stage the skins showed no signs of damage, the wool was cleanly and completely removed, and a number of physical tests showed that both skins and the leather produced from them showed no

differences to those produced using traditional methods (Chapter 3). In order to delve further into possible changes in their molecular structures, matched pieces of skin from the same area of a single animal were depilated with permeate or taken to pickle using sulfide depilation, then subjected to quantitative proteomic analyses in order to compare the relative abundances of proteins present in the skin after each treatment. In addition quantitative biochemical analyses of skins depilated using permeate were used to measure the changes in amino acid and collagen crosslink composition and concentration, as well as the glycosaminoglycan concentration, compared to the levels in raw skin and levels reported by others in pickled skin. The purpose of this study was to correlate any changes seen in the molecular building blocks of skin with the physical properties of leather made using both permeate and traditional beamhouse methods. The results provide the foundation for the development of a 'green' leather industry that is cost effective.

4.2 Materials and Methods

4.2.1 Chemicals and materials

Chemicals were purchased from Sigma-Aldrich (St. Louis, MO, USA) except for the following items. Zirconium/silica beads was purchased from dnature diagnostics research Ltd (NZ). Mass spectrometry grade water, acetonitrile (MeCN), formic acid, and trifluoroacetic acid (TFA) were purchased from Fisher Scientific (Fair Lawn, NJ, USA). 6-aminoquinolyl-N-hydroxysuccinimidyl carbamate (AQC) was purchased from SYNCHEM (Altenburg, Germany). CF11 cellulose was purchased from Merck (Kenilworth, NJ, USA). Dihydroxylysino-leucine (DHLNL) was purchased from Santa Cruz Biotechnology (Delaware Ave, CA, USA). Hydroxylysino-leucine (HLNL), histidino-hydroxylysino-leucine (HHL) and histidino-hydroxymerodesmosine (HHMD) were isolated and purified in our laboratory by Dr. R. Naffa. Papain was purchased from BDH Lab supplies (Poole, UK). Sulfuric acid 98 % was purchased from Ajax Finechem (NSW, Australia). Chondroitin sulfate A was purchased from Biocolor Ltd (Carrickfergus, UK). Mini-PROTEAN[®] TGX[™] 4 - 15 % gradient SDS gels were purchased from Bio-Rad (Hercules, CA, USA). cOmplete[™] protease inhibitor cocktail tablets were purchased from Roche Diagnostics GmbH (Mannheim, Germany).

4.2.2 Preparation of skin samples and the permeate solution

All sheepskins analysed were collected from a local freezing works (Ovation Ltd, Feilding, NZ). The skins were transported to New Zealand Leather Shoe Research Association (LASRA) and the flesh removed. The skins were then taken back to the laboratory to be sampled. Two pieces of sheepskin approximately 15×8 cm were cut from two sides of backbone from the official sampling position (OSP) of three different animal skins. One side was processed with permeate as described in Chapter 3 and the other side kept as control. For simplicity, the artificial permeate solution (4.5 % (w/v) lactose, 0.0035 % (w/v) CaCl_2 , 0.0045 % (w/v) NaCl, 0.14 % (w/v) KCl, and 0.05 % lactic acid (v/v)) will be referred to as permeate solution from now on. For proteomic analysis, two pieces of skin (15×8 cm) were cut from the OSP region on either side of the backbone. One of these was processed by permeate, and the other taken to pickle using the LASRA process (Chapter 3, Table 1). At the completion of the process, each was cut into five separate pieces (3×3 cm) for proteomic analysis.

4.2.3 Amino acid analysis of sheepskins

In order to estimate the amount of collagen in depilated skins, amino acid analyses of raw and permeate-depilated skins were carried out as described by Naffa *et al.* (2019)²⁷. A detailed description can be found in the supplementary information (SI).

4.2.4 Collagen crosslink analysis of sheepskins

Three raw shaved (using a standard electric hair clipper) and three permeate-depilated sheepskins were randomly cut into three 3×3 cm squares which were finely chopped using a clean scalpel blade on a clean glass plate, then lyophilised. Samples were then reduced using NaBH_4 and the crosslinks from each sample separated by CF-11 chromatography as described by Naffa *et al.* (2016)²⁸. Crosslinks in the resulting 18 samples were fractionated by HPLC using a silica hydride column then quantified using mass spectrometry with additional ion fragmentation (Tables S2 and S3). Parallel reaction monitoring (PRM) using tandem MS acquisition (Table S4) with an inclusion list of ions was used to detect and quantitate the relevant ions for each crosslink (Table S5). Fragment ion spectra produced *via* high-energy collision-induced dissociation (HCD) were acquired with a resolution setting of 35,000. Data was processed using Xcalibur™ Software v.4.1.31.9 (Thermo Scientific™, USA) then exported and the data

quantified using Excel. FreeStyle™ Software v.1.3.115.19 (Thermo Scientific™, USA) was used for data visualisation. A detailed description is given in the SI methods.

4.2.5 Glycosaminoglycan analysis of the sheepskins

GAG extraction

GAGs were extracted from three raw and three permeate depilated sheepskins using the method of Farndale *et al.* (1982)²⁹ as optimised by Naffa (2017)³⁰. Briefly, wool was removed from raw sheepskin using an electric hair shaver. 3×3 cm squares were randomly cut from each of the three skin samples and finely chopped using a clean scalpel blade to produce nine samples that were then lyophilised. One (1) mL of papain extraction solution (200 mM $\text{NaH}_2\text{PO}_4 \cdot 2\text{H}_2\text{O}$, pH 6.4, containing 100 mM sodium acetate, 50 mM EDTA disodium salt, 5 mM cysteine HCl, papain:skin 1:20 w/w ratio) was mixed with 100 mg of each lyophilised skin sample and incubated for 24 hours at 65 °C. After incubation, the insoluble material was removed by centrifugation at $13,000 \times g$ for 30 minutes at room temperature. The supernatant was then transferred to a clean tube and the precipitate re-extracted using the same protocol as above. The two supernatants were combined for analysis.

GAG quantitation

The concentration of GAGs was determined as described by Farndale *et al.*²⁹ with minor modifications. Fifty (50) μL of the supernatant collected from the papain extraction was made up to 100 μL with H_2O , then mixed with 1 mL of 1,9-dimethylmethylene blue (DMMB) solution (1.85 mM DMMB, 200 mM guanidine hydrochloride, 0.2 % formic acid and 0.5 % sodium formate). The mixture was vortexed for 30 minutes at room temperature, and the pellet isolated by centrifugation at $16,500 \times g$ for 30 minutes. The coloured supernatant was carefully removed with a pipette and the dark purple-coloured pellet was dissolved in 250 μL GAG-precipitating solution (4 M guanidine hydrochloride, 50 mM sodium acetate, 10 % propan-1-ol). The mixture was then vortexed and left mixing by rotation for 30 minutes at room temperature. The absorbance was measured at 656 nm using a PowerWave XS microplate spectrophotometer (BioTech Instruments, Inc., Vermont, USA). Chondroitin sulfate A was used to make up standards at concentrations of 0, 10, 20, 30, 40, and 50 $\mu\text{g}/\text{mL}$. A lactose solution of 2 mM and a 2 mg/mL BSA solution were used as negative controls.

4.2.6 Proteomic analysis of sheepskins

As the purpose of this experiment was to examine the effect of two different depilation treatments on the sheepskin proteome, only one biological sample was used as it was thought that the variation between skins would be greater than those due to the treatments used. Therefore, one sheepskin from the OSP region was used and divided into two parts. One was depilated and taken through to pickle using the conventional process while the other was treated with permeate. Five separate 3×3 cm squares were randomly cut from each processed skin piece and finely chopped using a new scalpel blade and a clean glass plate before being lyophilised. Proteins were sequentially extracted from these five separate samples using three different methods. A schematic diagram of the sample preparation workflow is shown in Fig. S2.

First, each lyophilised skin sample was immersed in a 1 M NaCl solution at room temperature for 12 hours with gentle agitation (Table 1). Insoluble material was pelleted by centrifugation ($13,000 \times g$ for 20 minutes at 4°C), then extracted in a urea solution for 12 hours with gentle agitation at room temperature, and the remaining insoluble material was treated with cyanogen bromide (CNBr) (Table 1). A detailed description of the extraction protocol is provided in the SI. The extracted proteins were precipitated using the standard TCA/acetone method for the removal of metabolites and resolubilised with 10 % SDS. The protein concentration of the samples was determined using the standard Bradford assay and normalised to approximately 1 mg/mL before being separated on 4 – 15 % gradient SDS gels. In-gel tryptic digestion was carried out as described in Shevchenko *et al.* (2006)³¹ with modifications (SI methods).

Mass spectrometry analysis

The in-gel digested peptide samples were desalted using an on-line reversed-phase peptide trap before being separated by reversed-phase nano-LC (Thermo Scientific™) using a 50 cm PepMap™ 300 C₁₈ LC column (Thermo Scientific™). Eluted peptides were analysed by mass spectrometry (Q Exactive™ Plus Hybrid Quadrupole-Orbitrap™, with a Nano Flex ion source, Thermo Fisher Scientific, Bremen, Germany) using a data-dependent tandem MS acquisition. Details for the chromatographic and mass spectrometry settings are provided in the supplementary information. Sample concentrations were normalised on the basis of total ion current (TIC) for each MS1 spectrum before data collection. Raw data files were processed using Proteome Discoverer™ v. 2.4 and searched against the *Ovis aries* (sheep) database. Detailed search parameters are listed in Table S9.

The reverse database search option was used as a filter to satisfy a false discovery rate (FDR) of 1 %. Abundance and abundance count data for proteins identified with high confidence by Proteome Discoverer™ were then exported into Excel and renormalised for the calculation of relative abundances. A two-tailed student's t-test was done to obtain the p -values.

Table 1: Components and concentrations of the protein extraction buffers.

Salt extraction buffer	Final concentration
NaCl	1 M
DTT	65 mM
Ammonium bicarbonate	100 mM
EDTA, pH 8.0	1 mM
cOmplete® protease inhibitor†	1 ×
Urea extraction buffer	
Urea	7 M
Thiourea	2 M
DTT	65 mM
Ammonium bicarbonate	100 mM
CHAPS	4 %
EDTA, pH 8.0	1 mM
cOmplete® protease inhibitor†	1 ×
CNBr extraction buffer	
Formic acid	70 %
DTT	65 mM
EDTA, pH 8.0	1 mM
CNBr§	0.05 mg/mL
cOmplete® protease inhibitor†	1 ×

†Made according to the manufacturer's manual.

§1 mg/mL dissolved in 50 % MeCN.

4.3 Results and Discussion

4.3.1 Amino acid composition of raw and permeate-depilated sheepskins

This analysis was carried out to determine whether there was any detrimental effect to the collagen content of the skin as a result of the permeate depilation process. It is critical that the collagen content is not compromised as it is the major component of leather and responsible for its organoleptic properties. Because hydroxyproline (Hyp) in skin is found only in collagen and the relatively low abundance in elastin, the collagen content in tissues can be estimated from the assumption that Hyp makes up ~ 13.5 % (w/w) of collagen in mammals^{32,33}.

Results showed that although there was no significant change in the relative overall protein content, permeate-depilated sheepskin had a much higher Hyp (collagen) content than that found in raw sheepskin, due to the removal of other non-collagenous proteins in the skin (Table 2, Fig. 2). A similar result was also seen in chemically depilated sheepskins processed to pickled skins where the collagen concentration in the processed skin increased to approximately 70 % *cf.* 36 % in raw skin³⁰. Because collagen makes up approximately 60 - 70 % of the dry weight of skin this makes perfect sense and reflects the loss of other proteins and the retention of collagen during processing. Our proteomic analysis supports this result as it showed a significant reduction in the abundance of the major proteoglycan, decorin, in permeate-depilated sheepskin (Table S10), which will result in the opening up of the collagen fibre network promoting the removal of non-collagenous proteins from the skins.

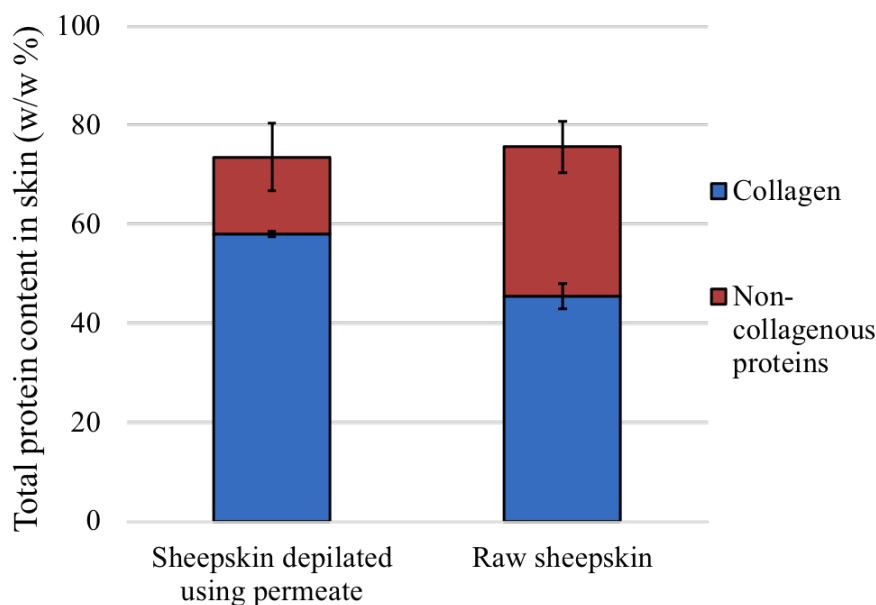


Figure 2: Total protein content in dried sheepskins before and after permeate depilation. the collagen content was based on the concentration of Hyp in each sample. Error bars represent standard deviation of three biological replicates and 12 technical replicates.

As expected, glycine was the dominant amino acid, in permeate-depilated sheepskin, comprising approximately 28 % of the total amino acids (Table 2). Because collagen type I $\alpha 1$ is the dominant protein in skin, its theoretical amino acid composition was determined from the translated helical region (aa 118 - 1238, the helical region, telopeptide region excluded) of the collagen type I $\alpha 1$ chain (COL1A1; W5P481) gene sequence for *Ovis aries* from the UniProtKB database (www.uniprot.org), and

is shown in Table 2. Proline was the second most represented amino acid after glycine, with a mole percentage of approximately 17 %. Previous studies on collagen structure have suggested that the ratio of Pro:Hyp in collagen is approximately 1.2 - 1.5:1^{34,35}. Raw sheepskin had a Pro:Hyp ratio of 3:1, and skin samples depilated with permeate, a ratio of 2:1, both of which are much higher than previously reported values^{34,35}. As whole skin samples were hydrolysed, and proteins other than collagen that also contain proline were present, this is not surprising. Amino acid analysis of pickled sheepskins gave a Pro:Hyp ratio of 1.4:1³⁰, suggesting that depilation with permeate is less harsh resulting in the retention of more non-collagenous proteins compared to the traditional sulfide treatment. However, this did not appear to detract from the quality of the leather produced from these skins as reported in Chapter 3.

Hydroxylation of lysine in collagen influences collagen fibrillogenesis and crosslinking, and thus serves an important role in the stabilisation of collagen fibrils³⁶. The theoretical mole percentage of post-translationally modified hydroxylysine 1 (Hyl1) and hydroxylysine 2 (Hyl2) cannot, however, be predicted on the basis of DNA sequence. Therefore, the theoretical mole percentage of lysine (Lys) was compared to the sum of the experimentally determined mole percentages of Lys, Hyl1 and Hyl2. Samples taken from raw sheepskin and permeate-depilated sheepskin had combined Lys + Hyl1 + Hyl2 mole percentages of approximately 3.6 %, which is not significantly different to the value obtained by Naffa³⁰ (3.8 %) and with the value reported for pickled sheepskin (3.6 %³⁰). The remainder of the amino acid mole percentages are not significantly different to those reported for raw skins (Table 2), indicating there should be no detrimental effects from this process. Interestingly, Cys was detected in permeate-depilated sheepskins, but not in pickled sheepskin³⁰, another indication that conventional processing of sheepskin is much harsher than depilation with permeate.

4.3.2 Collagen crosslink analysis of sheepskins

Intermolecular collagen crosslinks are essential for the integrity of the skin structure contributing to the strength, stability, and quaternary structure of the collagen fibrils⁸. To quantify the different collagen crosslinks in matching raw and permeate-depilated sheepskin samples, three biological replicates were used with each biological replicate being tested for extraction efficiency using three technical replicates. Though present in various ratios, all skin samples were shown to contain hydroxylysinonorleucine (HLNL), dihydroxylysinonorleucine (DHLNL), histidinohydroxylysinonorleucine (HHL), and histidinohydroxymerodesmosine (HHMD) crosslinks (Fig. 3).

Table 2: Comparison of amino acid profile in ovine skin or collagen as reported by other research groups with those obtained in this study and the theoretical value of the amino acid profile of *Ovis aries* collagen type I α I chain. All values are presented as mole percentages of each amino acid.

	Sheepskin depilated with permeate		Raw sheepskin CV (%)		Previous studies		<i>Ovis aries</i> COL1A1
					Raw sheepskin (Naffa, 2017)	Collagen extracted from sheepskin (Becker <i>et al.</i> 1976)	
Gly	27.71	5.72	23.03	5.86	24.27	32.73	31.0
Pro	17.06	5.50	18.77	6.28	9.85	12.84	22.8
Ala	9.70	3.13	8.54	3.81	9.51	11.51	11.7
Glx	7.91	4.71	9.11	5.83	10.70	7.42	7.2
Hyp	7.89	5.01	5.97	8.64	5.74	9.71	**
Asx	5.02	3.79	5.40	3.56	5.58	4.19	4.7
Arg	4.66	2.33	4.86	2.95	7.07	5.04	5.3
Ser	3.24	12.58	4.15	12.46	4.27	3.90	4.0
Leu	3.09	6.16	4.07	6.09	4.89	2.19	2.5
Lys	2.67	3.34	2.96	3.61	3.67	3.24	3.5
Val	2.57	4.14	3.15	5.24	4.05	1.43	1.9
Thr	2.18	9.57	2.72	8.27	1.80	2.00	1.8
Ile	1.52	6.04	1.93	5.90	2.29	0.86	0.9
Phe	1.48	12.45	1.68	4.98	2.01	1.14	1.2
Met	0.71	11.55	0.77	5.28	0.95	0.67	0.7
Tyr	0.67	19.26	1.18	13.96	1.50	0.38	0.4
His	0.64	6.10	0.76	10.15	0.83	0.29	0.5
Hyl2	0.59	16.07	0.42	14.28	0.03		
Hyl1	0.36	93.74	0.20	44.61	0.13	0.48*	-
Cys	0.32	94.34	0.34	125	0.88	0.0	0.0

*, Hyl1 and Hyl2 combined. **, Hyp estimated as part of Pro.

Glx represents glutamic acid and glutamine. Asx represents aspartic acid and asparagine.

Overall, the permeate-depilated skin lost approximately 60 % its HLNL (immature) crosslinks compared to the concentration found in raw sheepskin (Fig. 3d). The results, as expected, varied considerably between biological replicates, as shown by the box and whisker plots. Interestingly, permeate depilation did not seem to affect the concentration of DHLNL, an immature crosslink, but instead, removed the mature crosslink HHMD almost completely (Figs. 3c and f). This was unexpected as all crosslinks, apart from HHL, are acid labile^{37,38}, and will be broken under acid conditions implying some permeate-specific degradation of HHMD occurred. Although permeate at pH 4.5 is only mildly acidic and would not normally be expected to completely hydrolyse the acid labile crosslinks, the length of exposure of

the skins to permeate at room temperature could have resulted in its slow hydrolysis, leaving the DHLNL crosslinks intact (Fig. 3e).

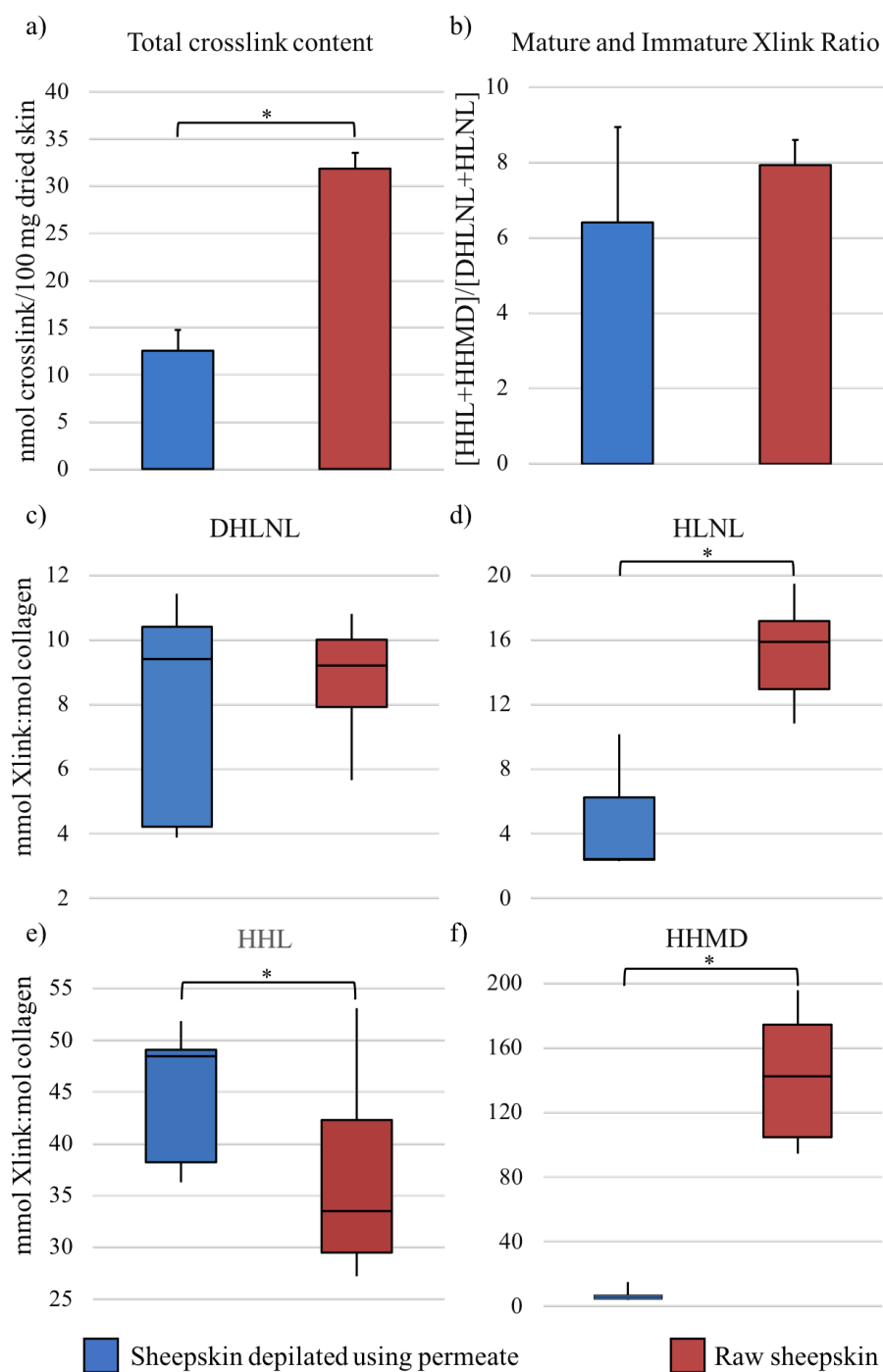


Figure 3: Collagen crosslinks in raw sheepskins and sheepskins depilated using permeate. All values were normalised to the collagen content based on hydroxyproline concentration in skins. Each result presented was the average of three biological replicates and their respective three extraction technical replicates. A one-way ANOVA test was done to obtain the p -values. *, p -value < 0.05.

The significantly higher concentration of HHL in the permeate-depilated skin compared to that in raw skin is harder to explain. There are three possibilities that could explain it. The first is a consistent error in sample preparation. This seems unlikely as the concentration of HHL in raw skin was almost identical to that found by Naffa (2017)³⁰ and Visser (2019)⁴. The second, but more unlikely is the presence of an amine oxidase in the permeate liquid derived from the microbial population allowing spontaneous formation of new HHL crosslinks, although the complex order of events required for the formation of a trivalent crosslink (Chapter 2, Fig. 3) makes this possibility extremely unlikely. Nevertheless, fungi are known to produce amine oxidases³⁹, and *Pichia*, a fungi was identified in the depilation liquid that produces this enzyme (Chapter 3). A more rational explanation is that because the collagen network of processed skins is opened up compared to that in raw skins, the hydrolysis efficiency and hence crosslink extraction may have been more efficient. However, if this was the case, the concentrations of the other three crosslinks should also have increased rather than decreased. A similar result was reported by Zhang *et al.* (2019)⁴⁰, where reduced pickled sheepskin had a higher HHL concentration compared to that found in reduced raw sheepskin, adding credence to this possibility, but interestingly, no explanation was provided by the authors for the observation. There was, however, no significant difference between the ratios of total mature (HHL + HHMD) to total immature (DHLNL + HLNL) crosslinks for the two treatments (Fig. 3b).

Research showing a direct correlation between collagen crosslinks and skin strength is lacking. Naffa *et al.* (2019)²⁷ reported that the total concentration of collagen crosslinks is positively correlated to skin strength, *i.e.* the higher the crosslink concentration, the stronger the skin. Although the collagen crosslink concentrations of pickled sheepskins were not measured in this study, another study found that pickled sheepskins had approximately 50 % less total collagen crosslinks compared to value in raw skin⁴⁰, which is similar to the decrease seen for the permeate-depilated skins (~ 55 %) in this study. Based on these findings, permeate-depilated sheepskins and pickled sheepskins should have similar tear strengths, a fact that was confirmed by the measurement of their tear and tensile strengths (Chapter 3, Fig. 5). Therefore, it is clear that there is no detrimental effect to the resultant leather made using this alternative process.

4.3.3 Glycosaminoglycan analysis of sheepskins

While total carbohydrate concentration could not be measured in permeate processed skin because of the high concentration of lactose in the depilation liquid, it was possible to measure the GAG concentration. The extraction of GAGs from skin samples was optimised by Naffa (2017)³⁰ who found that two sequential overnight papain digestions were required to release 99 % of the GAGs. That study showed that raw sheepskin contained approximately 0.9 % (w/w) GAGs, which reduced to < 0.05 % (w/w) in pickled sheepskins. While this study found similar levels of GAGs in raw sheepskins, those depilated with permeate retained at least 40 % (0.4 %, w/w) of the GAGs found in raw sheepskins (Fig. 4).

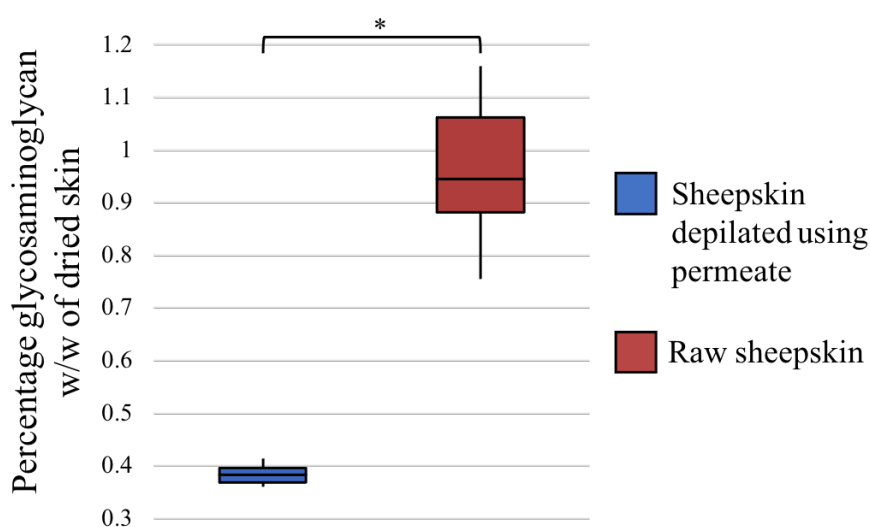


Figure 4: Percentages of glycosaminoglycans in raw sheepskins and sheepskins depilated using permeate. Three biological replicates were included. For each biological replicate 6 extraction technical replicates were done for sheepskins depilated using permeate and 9 extraction technical replicates were done for raw sheepskins. A one-way ANOVA test was done to obtain the p -value. *, p -value < 0.001.

A widely accepted opinion held by leather technologists is that the removal of PGs and their associated GAGs from the skin is closely related to the opening up of collagen fibres during processing¹, improving leather properties such as softness. A reduction in dermatan sulfate, the most common GAG found in skins, to 0.2 - 0.3 % (w/w) was found to be optimal to achieve the desired physical properties in the finished leather product¹. Research aimed at increasing hair removal efficiency introduced proteases and glycosidases at the depilation stage, and as a result, proteoglycans in skins were almost completely removed^{41,42}. In this study, the increase in GAGs could be related to detection of the core proteins linked to them. Therefore although the GAG concentration was higher than the ideal, there was a

decrease compared to raw skins. Skin proteomics analysis showed that the proteoglycans decorin and lumican, which are modified with sulfated GAG chains were less abundant in permeate-depilated sheepskins than in pickled skins while those in the basement membrane were more abundant in the permeate-depilated skins (Table 5). Jayakumar *et al.* (2016)⁴¹ speculated that the use of proteases and glycosidases to achieve depilation destroyed glyco-protein conjugates in the hair root sheath, the hair papillae and the basement membrane holding the hair root. However, it was shown that this treatment also damaged the collagen structure of the skin, especially around the wool follicle. Using permeate, no such damage is seen (Chapter 3, Fig. 3). Thus the removal of proteoglycans from the dermis (decorin and lumican), paired with retention of proteoglycans in the basement membrane (versican, perlecan and biglycan) seems to be favourable to leather quality. We therefore speculate that the microbial community that develops in the permeate during incubation secretes enzymes that specifically but gently open the collagen network at the same time as loosening the wool from its follicle, allowing depilation to occur without damaging the collagen fibril network.

4.3.4 Proteomic analysis of sheepskins

Various methods have been reported for the extraction of proteins from different mammalian tissues, including skin. To examine the differences in the protein composition of pickled sheepskins and sheepskins depilated using permeate, we extracted proteins from the skins using a combination of mechanical and chemical methods and subjected the extracted proteins to gel-LC-MS/MS analysis (Fig. S3). This method was chosen because of the superior results obtained using gel pre-fractionation of skins in previous studies, despite its acknowledged limitations⁴³. After strict criteria filtering, a total of 189 proteins were identified of high confidence from both of the skin samples (Table S10). This suggests that subjecting the skin to the pre-tanning treatments and the permeate treatment both removed a substantial number of proteins. Fig. 5 shows the volcano plot of permeate-depilated skin versus pickled skin for the 189 proteins found in this analysis. Sheepskin depilated with permeate generally had a higher relative abundance of proteins (permeate-depilated : pickled sheepskin, 52:29), confirming the AAA findings that the depilation treatment was not as harsh. The 50 most abundant proteins based on relative peptide spectrum matches, (PSMs) were identified and grouped according to their type and biological function (Table 3).

Table 3: Top 50 abundant proteins identified in sheepskin depilated using permeate and pickled sheepskin. Each group of proteins listed according to peptide spectrum matches (PSMs). Fold difference is the apparent relative abundance of permeate-depilated skin to pickled skin. *, proteins that are significantly abundant with at least 2-fold difference between treatments.

Proteins	Accession number	PSM	Fold difference	<i>p</i> -value
Collagens				
Collagen 1 α 1 chain	XP_027830506.1	18252	1.00	0.78
Collagen 1 α 2 chain	XP_004007775.1	17367	0.92	0.64
Collagen III α 1 chain	XP_004004563.1	4872	0.99	0.85
Collagen VI α III chain	XP_027823071.1	1594	1.70	0.01
Collagen II α I chain	XP_027823200.1	657	0.52	0.12
Collagen VI α 2 chain	XP_027817063.1	416	1.49	0.08
Collagen VI α 1 chain	XP_027817050.1	263	0.97	0.60
Collagen XII α 1 chain*	XP_014952772.2	190	2.43	0.04
Keratins				
Keratin, type II cytoskeletal 5	XP_027823079.1	11807	1.08	0.69
Keratin, type II cytoskeletal 75	XP_027823083.1	8076	2.14	0.15
Keratin, type II cytoskeletal 6A	XP_012029607.2	7277	1.35	0.27
Keratin, type I cytoskeletal 14	XP_014954266.2	5731	1.60	0.18
Keratin, type II cytoskeletal 5-like	XP_012029610.1	5278	1.39	0.12
Keratin, type II cytoskeletal 7*	XP_004006382.2	4969	2.76	0.005
Keratin, type II cytoskeletal 4	XP_027823076.1	4683	8.12	0.09
Keratin, type II cytoskeletal 79	XP_027823077.1	4263	2.38	0.07
Keratin, type I cytoskeletal 42*	XP_027830327.1	4253	4.18	0.03
Keratin, type II cytoskeletal 80	XP_027823090.1	4210	1.45	0.28
Keratin, type I 17	AGW21585.1	3462	1.30	0.26
Keratin, type I cytoskeletal 10	XP_027830375.1	3044	0.89	0.41
Keratin, type II cytoskeletal 1	XP_014950133.2	2697	1.05	0.17
Keratin, type II cytoskeletal 8	XP_012029598.2	2401	1.54	0.06
Keratin, type I cytoskeletal 24*	XP_004012920.2	2261	0.48	0.02
Keratin, type I cytoskeletal 16	XP_004023219.4	1925	1.42	0.25
Hair type II keratin intermediate filament protein	CAA44368.1	1886	0.63	0.14
Keratin, type II cytoskeletal 71*	NP_001267645.1	1439	0.60	0.05
Keratin, type II 83	NP_001185998.1	1136	1.22	0.98
Keratin, type II cytoskeletal 77	XP_027823078.1	1025	0.66	0.10
Keratin, type II cytoskeletal 72*	XP_004006372.2	959	0.42	0.01
Keratin, type I microfibrillar, component 8C-1 (K31)	P02534.2	905	0.75	0.38
Keratin, type II microfibrillar, component 5 (K85)	P25691.1	805	3.09	0.11
Keratin, type I microfibrillar, low-sulfur keratin (K33a)*	P25690.2	662	72.2	0.04
Keratin, type I cytoskeletal 27*	NP_001108235.1	460	0.23	0.02
Keratin, type I cytoskeletal 25	NP_001009739.1	345	1.35	0.17

Table 3 continued from previous page

Proteins	Accession number	PSM	Fold difference	<i>p</i> -value
Other extracellular matrix proteins				
Lumican	XP_012029466.1	332	0.55	0.03
Cellular proteins				
Desmoplakin	XP_027814264.1	1233	1.31	0.38
Annexin A2*	A2SW69.1	791	2.91	0.002
Junction plakoglobin	XP_027830318.1	733	0.97	0.84
Cytoplasmic 1 beta actin	P60713.1	542	0.65	0.05
Vimentin	ABP48145.1	374	0.88	0.54
Myosin-11*	XP_027817220.1	287	3.89	0.002
Elongation factor 1 α 1	XP_004008202.2	253	1.36	0.12
Desmoglein-1*	XP_004020502.2	205	0.26	0.003
Histone H2B type 1	XP_004019124.2	195	1.37	0.06
Serum proteins				
Albumin precursor	NP_001009376.1	4282	1.49	0.05
Immunoglobulin γ 1*	CAA49451.1	835	6.78	0.0004
Immunoglobulin λ chain C region*		361	6.28	0.001
Complement C3*	XP_027825575.1	350	3.89	0.002
Immunoglobulin λ 1 light chain-like	XP_027812629.1	323	3.86	0.0003
β globulin chain*	ABC86524.1	238	0.49	0.016
Uncharacterised protein				
Uncharacterised protein LOC101108868*	XP_014958051.2	300	0.46	0.002

Collagens

Of all the proteins identified, there were 14 different collagen chains representing nine types of collagen (I, II, III, IV, V, VI, VII, XII, XIV) (Table 4). Collagen types I (α 1 and α 2), and III (α 1) are the main fibril-forming collagens of the skin, and are resistant to pre-tanning procedures such as liming, bating and pickling^{44,45}. It was, therefore, no surprise that these were the most abundant collagens identified in skin. The fact that they had similar relative abundances in both permeate-depilated and sulfide-pickled skins showed that despite the extended time the permeate-depilated skins spent in solution which would normally result in swelling and loss of collagen, the abundances of these important structural proteins remained essentially the same implying that the resultant leather structure should be similar for both treatments.

Although collagen type II is mainly associated with cartilage, it has been identified at low abundance but with high confidence in other proteomic studies of skin^{4,47,48}. The results of this study showed that the levels of collagen type II did not significantly change between the two treatments, but it is mentioned because it confirms other results which show the presence of this collagen in sheepskin^{4,47,48}.

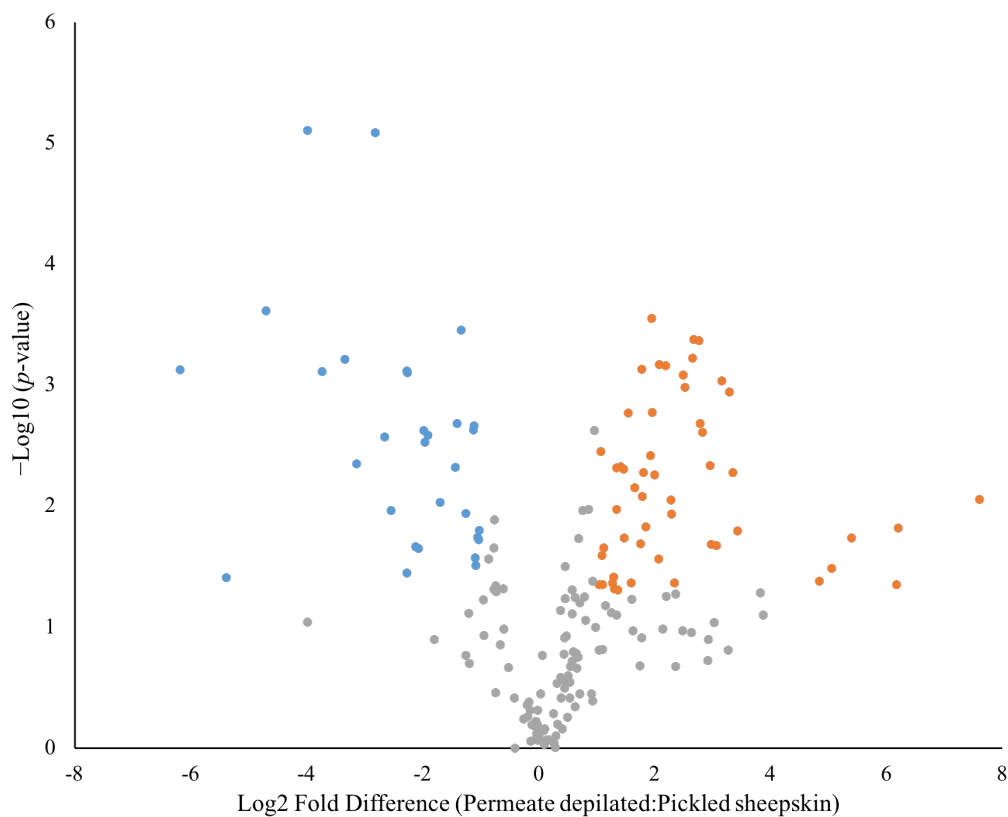


Figure 5: Volcano plot of the differentially abundant proteins found in sheepskins depilated using permeate and pickled sheepskins. The $-\text{Log}_{10} p$ -value is plotted against the Log_2 (fold change of permeate depilated sheepskin/pickled sheepskin). Orange dots, proteins that are at least 2-fold more abundant in permeate depilated sheepskins; Blue dots, proteins that are at least 2-fold more abundant in pickled sheepskins; Grey dots, proteins that are not significantly different in the two skin samples.

Collagen type IV, found mainly in the basement membrane, is part of a highly specialised ECM interface between the epidermis and the dermis, where it interacts with collagen types V, VI, and VII, laminin, nidogen and the basement membrane-specific heparan sulfate proteoglycan core protein, also named perlecan^{2,49,50,51} (Fig. 6). Among the six different α IV chains known, the most predominant heterotrimer is formed from two $\alpha 1$ and one $\alpha 2$ chains, which then associate to form lattice like networks that interact with collagen VI⁵². In light of this we cannot explain why only the $\alpha 2$ isoform is present in significantly higher relative abundance in the permeate-depilated skins. It is possible that this isoform is interacting with other molecules retained in the basement membrane such as nidogen, biglycan, perlecan, and collagen VI (in the dermis), which are all also more abundant in permeate processed skin. Nevertheless, the results support the fact that the grain of the leather produced by the permeate process appears to be smoother than that of pickled skin (Chapter 3, Fig. 3).

Table 4: Types of collagen identified in sheepskin depilated with permeate and pickled sheepskin and their literature tissue distribution⁴⁶. Collagen types highlighted blue were found to have significant differences in the apparent relative abundance between the two types of treatments.

Collagen type	Accession number	PSM	Fold difference (permeate:pickled)	<i>p</i> -value	Tissue distribution
Collagen I α 1 chain	XP_027830506.1	18252	1.00	0.78	Skin
Collagen I α 2 chain	XP_004007775.1	17367	0.92	0.64	
Collagen II α 1 chain	XP_027823200.1	657	0.52	0.12	Cartilage, tendon
Collagen III α 1 chain	XP_004004563.1	4872	0.99	0.85	Dermis
Collagen IV α 1 chain	XP_027829587.1	18	0.98	0.67	Basement membrane
Collagen IV α 2 chain	XP_027829588.1	51	3.43	0.0007	
Collagen V α 1 chain	XP_027821918.1	59	0.83	0.57	Dermis
Collagen V α 2 chain	XP_004004562.1	135	0.91	0.86	
Collagen VI α 1 chain	XP_027817050.1	263	0.97	0.60	Dermis
Collagen VI α 2 chain	XP_027817063.1	416	1.49	0.08	
Collagen VI α 3 chain	XP_027823071.1	1594	1.70	0.01	
Collagen VII α 1 chain	XP_027813474.1	26	3.61	0.01	Skin
Collagen XII α 1 chain	XP_014952772.2	190	2.43	0.04	Dermis, tendon, cartilage
Collagen XIV α 1 chain	XP_027829073.1	105	4.87	0.01	Dermis, tendon, cartilage

Collagen type VI (isoforms α 1, α 2, α 3), is the third most abundant collagen identified and isoform 3 is almost twice as abundant in the permeate-depilated skins, similar to the α 2 isoform of collagen IV which 3 times more abundant. Although isoforms 1 and 2 show no significant change in relative abundance, isoform 2 is found at slightly higher abundance. Because isoform 3 controls the formation of the triple helix of collagen VI⁵³, the results suggest that the collagen VI matrix may be protected during permeate depilation in contrast to sulfide depilation where the skins are exposed to low pH at the pickle stage. In contrast to other collagens, the collagen VI triple helix forms disulfide-bonded tetramers that associate end to end to form an extensive network of beaded micro-filaments that are distributed throughout the dermal matrix and interspersed between the major collagen fibres (Fig. 6). It is particularly abundant just below the basement membrane at the epidermal-dermal junction^{54,55}, the region of the skin that forms the grain layer in leather. Early proteomic studies identified collagen VI in sheepskins that produced high quality leather⁵⁶. The smooth, even appearance of the leather produced in the two-step tanning process incorporating permeate depilation (Chapter 3, Fig. 3) could therefore be related to the retention of collagen VI, and its interaction with collagen IV and the proteoglycans laminin, perlecan, and lumican⁵² to keep the basement membrane intact.

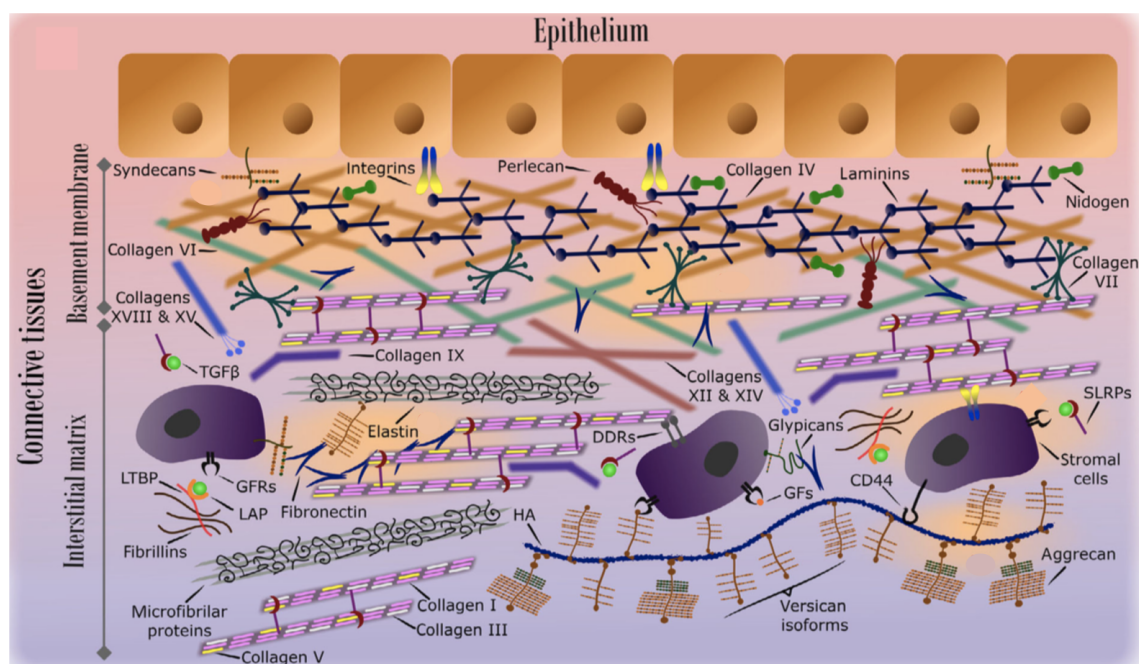


Figure 6: Schematic organisation of the collagens and proteoglycans in the ECM of skin. Reprinted from Theocharis *et al.*, (2019)⁵¹ with permission from FEBS Press.

Collagen VII is most abundant in the basement membrane, where it forms antiparallel collagen fibril dimers with each fibril composed of three identical α chains. The dimers 'loop' down from the basement membrane and 'hook' onto collagen fibrils of the upper dermis interacting with principal components of the basement membrane such as laminin and collagen type IV⁵⁵, conferring tensile strength to the tissue (Fig. 6). In this study it was significantly retained in the permeate-depilated skin compared to pickled skin. The fact that collagens IV, VI and VII are more abundant in permeate-depilated skin, all of which are involved in stabilising the interaction of the basement membrane with the interstitial collagen fibres in the dermis, suggests that permeate depilation keeps the skin structure more intact at the surface, which is supported by the appearance of the depilated skins when examined by SEM (Chapter 3, Fig. 3).

Two of the fibril-associated collagens with interrupted helices, collagen types XII, and XIV (known as FACIT collagens), that associate with the major structural collagen (type I) in skin⁵⁷ (Fig. 6), were also found in significantly higher relative abundances in permeate-depilated skin. Collagen XII, a homotrimer, is thought to modify the interactions between collagen I fibrils and the surrounding matrix and is commonly found in the dermis around hair follicles⁵⁸. It is present at 3-fold higher relative abundance in permeate-depilated skin compared to pickled skin. Because incubation of raw sheepskin in permeate resulted in complete removal of

the wool fibre without damage to the hair follicle, it is perhaps not surprising that more collagen type XII was extracted from these skins. Of all the collagens showing differential abundances in skins processed using the two different methods, collagen type XIV showed the largest difference, being nearly 5-fold more abundant in permeate-depilated skin. Collagen XIV is an important component of the fibre network in skin as it regulates fibrillogenesis and is responsible for the biomechanical function of skin. Both collagens XII and XIV are involved in the maintenance of skin integrity^{59,60}. The fact that a higher proportion of these is retained in permeate-depilated skins strongly suggests that the original collagen matrix of the skin is more preserved using this novel method of depilation, which includes pre-tanning and may be related to the improved appearance shown for leather produced from this novel two-step process.

Keratins and trichohyalin

Keratins are important structural proteins found primarily in the epidermis, the hair follicle, and the ECM (Fig. 7). Most of the keratins identified in the 50 most abundant proteins were epithelial keratins, *i.e.* cytoskeletal keratins expressed in the epidermal cells (Table 3). However, a wool keratin, K33a, was found to be 72-fold more abundant in permeate-depilated sheepskins. This particular type of keratin is the structural component of the wool fibre⁶⁶. As the depilation process involved soaking whole sheepskin (*i.e.* with wool attached) in permeate for three to four days it is not surprising that the wool structure itself was affected. The fact that it had a silky texture compared to wool removed using the sulfide method suggests some modification to its structure occurred during the process that could have released some type I microfibrillar low sulfur keratin into the solution, which was then trapped on the skins. The process also possibly dissolved keratins 25 - 28 and 71 - 75 that are specifically found in the root sheaths of the hair follicle⁶³, as more than half of them were found to have a lower abundance in permeate-depilated skin compared to pickled skin (K25, K27, K71, K72, K75) (Table 3). In particular, keratins 27, 71 and 72 were found to be approximately 1.5 to 4-fold less abundant in samples depilated with permeate compared to those depilated with sulfide and pickled (p -value < 0.05; Table 3). Some keratins are specifically expressed in the inner root sheath (IRS), a channel formed to protect the growing hair fibre (Fig. 7). The lower abundance of these keratins found in the permeate-depilated skin could potentially explain its relatively easy depilation, with these keratins being removed by microbial enzymes (most likely a mix of proteases and glycosidases) secreted into the permeate solution loosening the wool fibre. Trichohyalin (THH) is highly expressed in the IRS of the hair follicle, where it serves a biomechanical role by forming crosslinks with keratin intermediate filaments (KIFs) and other THHs, to

form the rigid structure of the IRS^{67,68}. Though present in low abundance, THH was approximately 2-fold less abundant in the sheepskin depilated with permeate compared to that in pickled skin (p -value < 0.05; Table S10), suggesting a greater breakdown of the sheath structure.

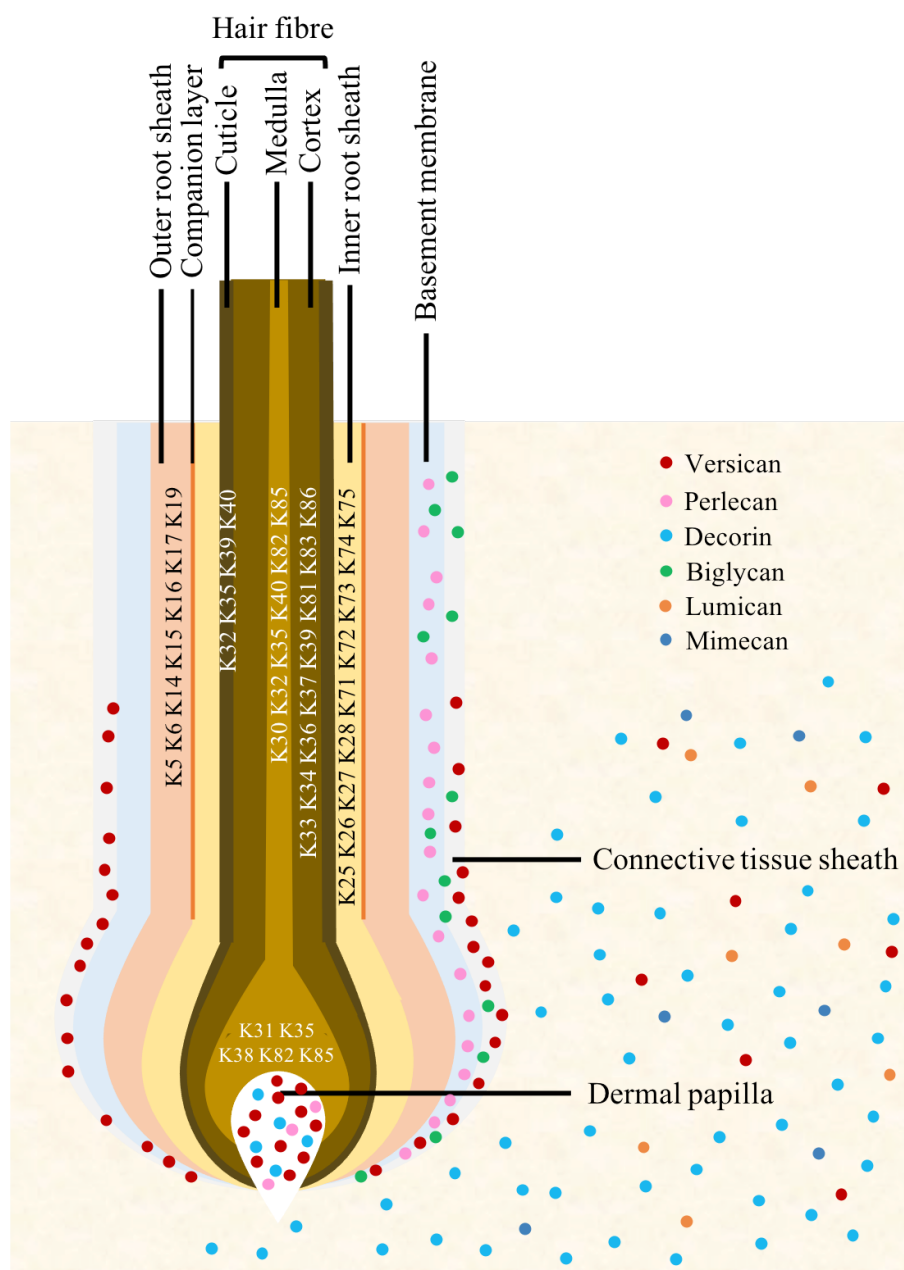


Figure 7: Schematic longitudinal view of the mammalian hair with key keratins (K) and proteoglycans.^{61,62,63,64,65}

ECM proteins

Proteoglycans are glycoprotein conjugates comprised of a core protein with glycosaminoglycan moieties, such as chondroitin sulfate, dermatan sulfate, and heparin sulfate. They are important collagen interfibrillary proteins distributed throughout the skin and the hair follicle and are known to contribute to the skin and hair structure by interacting with collagen fibrils and other ECM proteins (Figs. 6 and 7). The major collagen-interacting PGs in skin, such as versican, basement membrane-specific heparan sulfate proteoglycan core protein (perlecan), and also some small leucine-rich proteoglycans (SLRPs), including decorin, biglycan, lumican, mimecan, and asporin were identified in this study and those present in significantly different abundances to those in pickled skin are highlighted in blue in Table 5. Decorin and lumican, identified as proteoglycans interacting with collagens IV, VI and VII, in the basement membrane appear to be present in lower abundances in permeate-depilated skin compared to pickled skin, a result hard to correlate with the increase in the relative abundances of those same collagens in this study. Decorin, which was named for its decoration of collagen fibrils, is the most abundant PG found in the skin ECM and mediates collagen fibrillogenesis⁶⁹. As it can also interact with collagen types I and III^{70,71}, the major collagens in the dermis or corium, it is possible that the main losses of decorin are coming from this region of skin rather than the basement membrane. It has been shown that the collagen fibre 'opening-up process' is related to the loss of decorin interactions with collagen fibrils, although the mechanism is not fully elucidated, and that the pre-tanning processes reduce the abundance of decorin in skins⁷². Previous research has shown that the presence of residual amounts of decorin has a detrimental effect on the grain quality of the final leather product *i.e.* higher decorin content results in inflexible leather⁴⁵. Thus the reduction in decorin in the permeate-depilated skins could result in a better leather product, although that remains to be seen. Lumican, a keratan sulfate PG, co-localises with fibrillar collagens and decorin in the ECM and like decorin is involved in collagen fibrillogenesis⁷³. Similarly, its relative concentration in permeate-depilated skin was approximately half that found in pickled sheepskins. These findings indicate that the treatment with permeate potentially opens up the collagen fibre network of the dermis by removing the major 'glue' proteoglycans decorin and lumican.

Asporin, biglycan versican, mimecan and the basement membrane-specific heparan sulfate proteoglycan (perlecan) are, in contrast, more abundant in permeate-depilated skins. Biglycan is highly expressed in the basement membrane and the connective tissue sheath along the hair follicle⁶⁴. While the removal of biglycan may promote hair/wool root loosening⁶², its retention is in line with the

Table 5: ECM proteins identified in sheepskin depilated with permeate and pickled sheepskin. Proteins highlighted in blue show significant differences in the apparent relative abundances between the two treatments.

ECM proteins	Accession number	# of PSM	Fold difference (permeate:pickled)	<i>p</i> -value
Dermatopontin	XP_004013720.1	12	9.80	0.001
<i>Glycoproteins</i>				
Fibronectin isoform X4	XP_004004955.2	29	10.76	0.02
Microfibril-associated glycoprotein 4	XP_027830620.1	36	3.81	0.004
<i>Proteoglycans & Small leucine-rich repeat proteins (SLRPs)</i>				
Decorin	AAF00585.1	188	0.60	0.05
Lumican	XP_012029466.1	332	0.55	0.03
Mimecan	XP_004004124.1	183	2.55	0.01
Asporin	XP_004004126.1	5	3.36	0.21
Biglycan precursor	AAB87988.1	26	1.41	0.55
Versican core protein	XP_004009116.2	15	73.94	0.02
Basement membrane-specific heparan sulfate proteoglycan core protein (perlecan)	XP_027821348.1	25	2.06	0.04

observed increase in the relative abundance of basement membrane collagens supporting the probability that permeate depilation does not damage this membrane and hence the integrity of the grain structure. Mimecan, also called osteoglycan, regulates fibrillogenesis of collagen in the ECM by binding directly to collagens, and is responsible for the elasticity and tensile strength of skin⁷⁴. The relative abundance of mimecan was increased 2.5-fold in permeate-depilated sheepskin but the significance of this result is difficult to explain, as mimecan interacts with the collagen fibrils in the dermis and would therefore be expected to follow the same trend as decorin and lumican. Versican, a large proteoglycan belonging to the hyalectan family, is abundant at the dermal papilla and proximal part of the connective tissue sheath (*i.e.* around the hair follicles)⁶². It co-localises with elastic fibres (*e.g.* elastin and fibrillin) in the dermis, and interacts with hyaluronan in the ECM^{64,75}. Perlecan is specifically expressed in the basement membrane and interacts with collagen IV and laminin to stabilise the basement membrane and dermal papilla⁶⁴. Both versican and perlecan are found around the hair follicle, and thus their higher concentration (74-fold and 2-fold, respectively) in permeate-depilated sheepskin indicates the structure around the hair/wool follicle may suffer less damage after permeate depilation than in treatment with sulfide. As a result, the skin structure, and especially that of the basement membrane should be better preserved.

Other proteins found in higher relative abundance in permeate-depilated skin include dermatopontin, fibronectin and microfibril-associated glycoprotein 4 (Table 5). Dermatopontin, a structural ECM protein, is almost 10-fold more abundant in the sheepskin depilated with permeate. It interacts with decorin and accelerates collagen fibril formation, influencing the arrangement of the collagen fibrils within the ECM⁷⁶. Fibronectin, a high molecular weight glycoprotein in the ECM, binds to collagens and heparan sulfate proteoglycans, and is essential in the organisation and stability of ECM matrix⁷⁷. Microfibril-associated glycoprotein 4 also interacts with ECM fibres such as elastin and collagen. Although present in relatively low relative abundance, these proteins are all involved in the formation and maintenance of the collagen architecture of skin in its natural state. As raw sheepskin is inherently strong, the presence of these proteins should be beneficial to the product resulting from the process. *i.e.*, the natural structure of the skin should be maintained to a greater extent in leather made using this novel two-step process than it is in the traditional beamhouse process. As reported in an earlier paper (Chapter 3), this was indeed the case.

Overall, these results show that on a macro level, there is little difference in the protein building blocks of skins processed using either permeate or sulfide/lime/delime/bate/pickle. There are however differences in the detail that appear to be an advantage to the permeate depilation method. The most important of these appears to be the increased integrity of the basement membrane in the permeate processed skin that may have implications for the appearance of leather made using this process. The higher relative abundance of collagens IV and VII in the permeate-depilated skin, responsible for the structural integrity of the basement membrane; collagen VI that forms a structural network of beaded micro-filaments at the junction of the basement membrane and dermis; and perlecan and versican proteoglycans found at the basement membrane and connective tissue sheath, indicate that the treatment of permeate is milder than sulfide, and preserves these structural proteins. The lower abundance of decorin and lumican, however, shows the removal of these 'glue' proteins in the dermis, results in the 'opening-up' of the collagen fibre network, and the loss of interfibrillar proteins resulting in the lower number of proteins identified in this proteomic study. Finally, the lower relative abundance of keratins 27, 71 and 72 in the inner root sheath, probably reflects the reason the hair fibre is loosened in the hair follicle, allowing it to be easily removed.

Acknowledgement

The authors would like to thank Dr. Rafea Naffa for the isolation of collagen crosslink standards and the advice given for the analysis of collagen crosslink and amino acid analysis, and LASRA for supplying the sheepskins.

Funding Sources

Massey University Agricultural and Life Sciences Trust (Project number RM3000028979) and New Zealand Leather and Shoe Research Association (LASRA) through the Ministry of Business, Innovation and Employment (MBIE) grant number LSRX1801.

Author contributions

GEN designed the research, monitored the research and edited the manuscript. MLP monitored the experiments and edited the manuscript. DG monitored the experiments. Y-HT conducted all the experimental work, analysed the results, carried out the proteomic analysis and wrote the manuscript. TSL collected mass spectrometry data.

4.4 References

- [1] K. T. W. Alexander, B. M. Haines, and M. P. Walker. Influence of proteoglycan removal on opening-up in the beamhouse. *J. Am. Leather Chem. Assoc.*, 81:85–102, 1986.
- [2] D. Breitkreutz, I. Koxholt, K. Thiemann, and R. Nischt. Skin basement membrane: the foundation of epidermal integrity-BM functions and diverse roles of bridging molecules nidogen and perlecan. *BioMed Res. Int.*, 2013:179784–179784, 2013. ISSN 2314-6141 2314-6133. doi: 10.1155/2013/179784. URL <https://pubmed.ncbi.nlm.nih.gov/23586018>.
- [3] C. Frantz, K. M. Stewart, and V. M. Weaver. The extracellular matrix at a glance. *J. Cell Sci.*, 123(24):4195, 2010. doi: 10.1242/jcs.023820. URL <http://jcs.biologists.org/content/123/24/4195.abstract>.
- [4] D. R. Visser. *Unravelling the molecular contributions to collagen higher order structure: a thesis presented in partial fulfilment of the requirements for the degree of Master of Science in Biochemistry at Massey University, Manawatu, New Zealand*. Thesis, Massey University, 2019.

- [5] W. G. Kaelin Jr. Proline hydroxylation and gene expression. *Annu. Rev. Biochem.*, 74:115–128, 2005. ISSN 0066-4154.
- [6] M. D. Shoulders and R. T. Raines. Collagen structure and stability. *Annu. Rev. Biochem.*, 78:929–58, 2009. ISSN 0066-4154. doi: 10.1146/annurev.biochem.77.032207.120833.
- [7] L. C. Junqueira and G. S. Montes. Biology of collagen-proteoglycan interaction. *Arch. Histol. Jpn.*, 46(5):589–629, 1983. ISSN 0004-0681 (Print) 0004-0681. doi: 10.1679/aohc.46.589.
- [8] J. Gaar, R. Naffa, and M. A. Brimble. Enzymatic and non-enzymatic crosslinks found in collagen and elastin and their chemical synthesis. *Org. Chem. Front.*, 2020.
- [9] D. G. Bailey. *Encyclopedia of Polymer Science and Technology*, volume 15, journal article Leather. John Wiley Sons Inc., 4th ed. edition, 2002.
- [10] K. Kabashima, T. Honda, F. Ginhoux, and G. Egawa. The immunological anatomy of the skin. *Nat. Rev. Immuno.*, 19(1):19–30, 2019. ISSN 1474-1741.
- [11] C. A. Maidment. *Investigating the molecular building blocks of loose and tight cattle hide : a thesis presented in partial fulfilment of the requirements for the degree of Master of Science in Biochemistry at Massey University, Manawatu, New Zealand*. Thesis, Massey University, 2019. URL <http://hdl.handle.net/10179/15632>.
- [12] R. L. Edmonds, D. S. Choudhury, R. G. Haverkamp, M. Birtles, T. F. Allsop, and G. E. Norris. Using proteomics, immunohistology, and atomic force microscopy to characterize surface damage to lambskins observed after enzymatic dewooling. *J. Agric. Food. Chem.*, 56(17):7934–7941, 2008. ISSN 0021-8561. doi: 10.1021/jf800380y. URL <https://doi.org/10.1021/jf800380y>.
- [13] V. L. Addy, A. D. Covington, D. A. Langridge, and A. Watts. Microscopy methods to study fat cells. Part 1: Characterisation of ovine cutaneous lipids using microscopy. *J. Soc. Leath. Tech. Ch.*, 85(1):6–15, 2001. ISSN 0144-0322.
- [14] B. M. Haines and J. R. Barlow. The anatomy of leather. *J. Mater. Sci.*, 10(3):525–538, 1975. ISSN 1573-4803. doi: 10.1007/BF00543698. URL <https://doi.org/10.1007/BF00543698>.
- [15] K. H. Sizeland, M. M. Basil-Jones, R. L. Edmonds, S. M. Cooper, N. Kirby, A. Hawley, and R. G. Haverkamp. Collagen orientation and leather strength for selected mammals. *J. Agric. Food. Chem.*, 61(4):887–892, 2013. ISSN 0021-8561. doi: 10.1021/jf3043067. URL <https://doi.org/10.1021/jf3043067>.
- [16] D. W. Nazer, R. M. Al-Sa’ed, and M.A. Siebel. Reducing the environmental impact of the unhairing-liming process in the leather tanning industry. *J.*

- Cleaner Prod.*, 14(1):65–74, 2006. ISSN 0959-6526. doi: <https://doi.org/10.1016/j.jclepro.2005.04.002>. URL <https://www.sciencedirect.com/science/article/pii/S0959652605000934>.
- [17] B. Madhan, J. R. Rao, and B. U. Nair. Studies on the removal of inter-fibrillary materials part 1: removal of protein, proteoglycan, glycosaminoglycans from conventional beamhouse process. *J. Am. Leather Chem. Assoc.*, 105(05):145–149, 2010. ISSN 0002-9726.
- [18] N. R. Kamini, C. Hemachander, J. G. S. Mala, and R. Puvanakrishnan. Microbial enzyme technology as an alternative to conventional chemicals in leather industry. *Curr. Sci. India*, 77(1):80–86, 1999. ISSN 00113891. URL <http://www.jstor.org/stable/24102916>.
- [19] A. Dettmer, M. A. Z. Ayub, and M. Gutterres. Hide unhairing and characterization of commercial enzymes used in leather manufacture. *Braz. J. Chem. Eng.*, 28:373–380, 2011. ISSN 0104-6632. URL <https://www.scielo.br/j/bjce/a/3J997xnFZdvV7M99cjyWQNk/?lang=en>.
- [20] M. Sousa. Advances in understanding of enzymatic unhairing of bovine hides. *J. Am. Leather Chem. Assoc.*, 109:268–277, 2014.
- [21] N. Kandasamy, P. Velmurugan, Sundarvel A., R. J. Raghava, C. Bangaru, and T. Palanisamy. Eco-benign enzymatic dehairing of goatskins utilizing a protease from a *Pseudomonas fluorescens* species isolated from fish visceral waste. *J. Cleaner Prod.*, 25:27–33, 2012. ISSN 0959-6526. doi: <https://doi.org/10.1016/j.jclepro.2011.12.007>. URL <http://www.sciencedirect.com/science/article/pii/S0959652611005324>.
- [22] L. M. I. López, C. A. Viana, M. E. Errasti, M. L. Garro, J. E. Martegani, G. A. Mazzilli, C. D. T. Freitas, Í. M. S. Araújo, R. O. da Silva, and M. V. Ramos. Latex peptidases of *Calotropis procera* for dehairing of leather as an alternative to environmentally toxic sodium sulfide treatment. *Bioproc. Biosyst. Eng.*, 40(9): 1391–1398, 2017. ISSN 1615-7605. doi: 10.1007/s00449-017-1796-9. URL <https://doi.org/10.1007/s00449-017-1796-9>.
- [23] S. Sivasubramanian, B. Murali Manohar, A. Rajaram, and R. Puvanakrishnan. Ecofriendly lime and sulfide free enzymatic dehairing of skins and hides using a bacterial alkaline protease. *Chemosphere*, 70(6):1015–1024, 2008. ISSN 0045-6535. doi: <https://doi.org/10.1016/j.chemosphere.2007.09.036>. URL <http://www.sciencedirect.com/science/article/pii/S0045653507011605>.
- [24] P. Thanikaivelan, J. R. Rao, B. U. Nair, and T. Ramasami. Recent trends in leather making: processes, problems, and pathways. *Crit. Rev. Env. Sci. Tec.*, 35(1):37–79, 2005. ISSN 1064-3389. doi: 10.1080/10643380590521436. URL <https://doi.org/10.1080/10643380590521436>.

- [25] B. Wahyuntari and H. Hendrawati. Properties of an extracellular protease of *Bacillus megaterium* DSM 319 as depilating aid of hides. *Microbiology Indonesia*, 6(2):4–4, 2012. ISSN 2087-8575.
- [26] A. D. Covington. *Tanning chemistry: the science of leather*. RSC Publishing, 2009. URL <http://app.knovel.com/hotlink/toc/id:kpTCTSL002/tanning-chemistry-the>.
- [27] R. Naffa, C. A. Maidment, G. Holmes, and G. E. Norris. Insights into the molecular composition of the skins and hides used in leather manufacture. *J. Am. Leather Chem. Assoc.*, 114(1), 2019. ISSN 0002-9726.
- [28] R. Naffa, G. Holmes, M. Ahn, D. Harding, and G. E. Norris. Liquid chromatography-electrospray ionization mass spectrometry for the simultaneous quantitation of collagen and elastin crosslinks. *J. Chromatogr. A*, 1478:60–67, 2016. ISSN 0021-9673. doi: 10.1016/j.chroma.2016.11.060.
- [29] R. W. Farndale, C. A. Sayers, and A. J. Barrett. A direct spectrophotometric microassay for sulfated glycosaminoglycans in cartilage cultures. *Connect. Tissue Res.*, 9(4):247–8, 1982. ISSN 0300-8207 (Print) 0300-8207. doi: 10.3109/03008208209160269.
- [30] R. Naffa. *Understanding the molecular basis of the strength differences in skins used in leather manufacture : a dissertation presented in partial fulfillment of the requirements for the degree of Doctor of Philosophy at Massey University, Palmerston North, New Zealand*. Thesis, Massey University, 2017. URL <http://hdl.handle.net/10179/13154>.
- [31] A. Shevchenko, H. Tomas, J. Havli, J. V. Olsen, and M. Mann. In-gel digestion for mass spectrometric characterization of proteins and proteomes. *Nat. Protoc.*, 1(6):2856–2860, 2006. ISSN 1750-2799. doi: 10.1038/nprot.2006.468. URL <https://doi.org/10.1038/nprot.2006.468>.
- [32] R. E. Neuman and M. A. Logan. The determination of hydroxyproline. *J. Biol. Chem.*, 184(1):299–306, 1950. ISSN 0021-9258 (Print) 0021-9258.
- [33] R. E. Neuman and M. A. Logan. The determination of collagen and elastin in tissues. *J. Biol. Chem.*, 186(2):549–56, 1950. ISSN 0021-9258 (Print) 0021-9258.
- [34] N. Y. Ignat’eva, N. A. Danilov, S. V. Averkiev, M. V. Obrezkova, V. V. Lunin, and E. N. Sobol’. Determination of hydroxyproline in tissues and the evaluation of the collagen content of the tissues. *J. Anal. Chem.*, 62(1):51–57, 2007. ISSN 1608-3199. doi: 10.1134/S106193480701011X. URL <https://doi.org/10.1134/S106193480701011X>.

- [35] A. Meister, N. Stone, and J. M. Manning. *Conversion of proline to hydroxyproline in collagen synthesis*, volume 44 of *Advances in Chemistry*, book section 5, pages 67–81. American Chemical Society, 1964. ISBN 9780841200456. doi: doi:10.1021/ba-1964-0044.ch00510.1021/ba-1964-0044.ch005. URL <https://doi.org/10.1021/ba-1964-0044.ch005>.
- [36] I. Scott, M. Yamauchi, and M. Sricholpech. Lysine post-translational modifications of collagen. *Essays Biochem.*, 52:113–133, 2012. ISSN 0071-1365.
- [37] A. J. Bailey and M. S. Shimokomaki. Age related changes in the reducible cross-links of collagen. *FEBS Lett.*, 16(2):86–88, 1971. ISSN 0014-5793. doi: [https://doi.org/10.1016/0014-5793\(71\)80338-1](https://doi.org/10.1016/0014-5793(71)80338-1). URL <http://www.sciencedirect.com/science/article/pii/0014579371803381>.
- [38] M. Yamauchi, D. T. Woodley, and G. L. Mechanic. Aging and cross-linking of skin collagen. *Biochem. Biophys. Res. Commun.*, 152(2):898–903, 1988. ISSN 0006-291X (Print) 0006-291x. doi: 10.1016/s0006-291x(88)80124-4.
- [39] A. P. Duff, A. E. Cohen, P. J. Ellis, J. A. Kuchar, D. B. Langley, E. M. Shepard, D. M. Dooley, H. C. Freeman, and J. M. Guss. The crystal structure of *Pichia pastoris* lysyl oxidase. *Biochemistry*, 42(51):15148–57, 2003. ISSN 0006-2960 (Print) 0006-2960. doi: 10.1021/bi035338v.
- [40] Y. Zhang, R. Naffa, C. J. Garvey, C. A. Maidment, and S. Prabakar. Quantitative and structural analysis of isotopically labelled natural crosslinks in type I skin collagen using LC-HRMS and SANS. *J. Leather Sci. Eng.*, 1(1):10, 2019. ISSN 2524-7859. doi: 10.1186/s42825-019-0012-x. URL <https://doi.org/10.1186/s42825-019-0012-x>.
- [41] G. Jayakumar, M. Sathish, R. Aravindhan, and J. Raghava-Rao. Studies on the use of bi-functional enzyme for leather making. *J. Am. Leather Chem. Assoc.*, 111(12):455–460, 2016. ISSN 0002-9726.
- [42] F. R. de Souza and M. Gutterres. Application of enzymes in leather processing: a comparison between chemical and coenzymatic processes. *Braz. J. Chem. Eng.*, 29:473–482, 2012. ISSN 0104-6632. URL http://www.scielo.br/scielo.php?script=sci_arttext&pid=S0104-66322012000300004&nrm=iso.
- [43] M. Dzieciatkowska, R. Hill, and K. C. Hansen. GeLC-MS/MS analysis of complex protein mixtures. *Methods Mol. Biol.*, 1156:53–66, 2014. ISSN 1940-6029 1064-3745. doi: 10.1007/978-1-4939-0685-7_4. URL <https://pubmed.ncbi.nlm.nih.gov/2479198>.
- [44] P. L. Kronick and S. Iandola. Persistence of minority macromolecules of hide through the beamhouse. II. Removal of collagen type XIV. *J. Am. Leather Chem. Assoc.*, 1997. ISSN 0002-9726.

- [45] P. L. Kronick and S. K. Iandola. Persistence of minority macromolecules of hide through the beamhouse. III. Persistence of decorin. *J. Am. Leather Chem. Assoc.*, 1998. ISSN 0002-9726.
- [46] A. Sorushanova, L. M. Delgado, Z. Wu, N. Shologu, A. Kshirsagar, R. Raghunath, A. M. Mullen, Y. Bayon, A. Pandit, and M. Raghunath. The collagen suprafamily: from biosynthesis to advanced biomaterial development. *Adv. Mater.*, 31(1):1801651, 2019. ISSN 0935-9648.
- [47] C. A. Maidment, M. Ahn, R. Naffa, T. S. Loo, and G. E. Norris. Comparative analysis of the proteomic profile of cattle hides that produce loose and tight leather using in-gel tryptic digestion followed by LC-MS/MS. *J. Am. Leather Chem. Assoc.*, 115(11): 399–408, 2020. ISSN 0002-9726.
- [48] L. M. Mikesh, L. R. Aramadhaka, C. Moskaluk, P. Zigrino, C. Mauch, and J. W. Fox. Proteomic anatomy of human skin. *J. Proteomics*, 84:190–200, 2013. ISSN 1874-3919. doi: 10.1016/j.jprot.2013.03.019.
- [49] R. E. Burgeson, G. P. Lunstrum, B. Rokosova, C. S. Rimberg, L. M. Rosenbaum, and D. R. Keene. The structure and function of type VII collagen. *Ann. N. Y. Acad. Sci.*, 580:32–43, 1990. ISSN 0077-8923 (Print) 0077-8923. doi: 10.1111/j.1749-6632.1990.tb17915.x.
- [50] H. Chanut-Delalande, C. Bonod-Bidaud, S. Cogne, M. Malbouyres, F. Ramirez, A. Fichard, and F. Ruggiero. Development of a functional skin matrix requires deposition of collagen V heterotrimers. *Mol. Cell Biol.*, 24(13):6049–6057, 2004. ISSN 0270-7306 1098-5549. doi: 10.1128/MCB.24.13.6049-6057.2004. URL <https://pubmed.ncbi.nlm.nih.gov/15199158>.
- [51] A. D. Theocharis, D. Manou, and N. K. Karamanos. The extracellular matrix as a multitasking player in disease. *FEBS J.*, 286(15):2830–2869, 2019. ISSN 1742-464X. doi: <https://doi.org/10.1111/febs.14818>. URL <https://doi.org/10.1111/febs.14818>.
- [52] M. Cescon, F. Gattazzo, P. Chen, and P. Bonaldo. Collagen VI at a glance. *J. Cell Sci.*, 128(19):3525–31, 2015. ISSN 0021-9533. doi: 10.1242/jcs.169748.
- [53] S. R. Lamandé, E. Sigalas, T-C. Pan, M-L. Chu, M. Dziadek, R. Timpl, and J. F. Bateman. The role of the $\alpha 3(\text{VI})$ chain in collagen VI assembly: expression of an $\alpha 3(\text{VI})$ chain lacking N-terminal modules N10-N7 restores collagen VI assembly, secretion, and matrix deposition in an $\alpha 3(\text{VI})$ -deficient cell line. *J. Biol. Chem.*, 273(13):7423–7430, 1998. ISSN 0021-9258. doi: <https://doi.org/10.1074/jbc.273.13.7423>. URL <https://www.sciencedirect.com/science/article/pii/S0021925818617120>.

- [54] C. M. Kielty and C. A. Shuttleworth. Microfibrillar elements of the dermal matrix. *Microsc. Res. Techniq.*, 38(4):413–427, 1997. ISSN 1059-910X. doi: [https://doi.org/10.1002/\(SICI\)1097-0029\(19970815\)38:4<413::AID-JEMT9>3.0.CO;2-J](https://doi.org/10.1002/(SICI)1097-0029(19970815)38:4<413::AID-JEMT9>3.0.CO;2-J).
- [55] G. Theocharidis and J. T. Connelly. Minor collagens of the skin with not so minor functions. *J. Anat.*, 235(2):418–429, 2019. ISSN 0021-8782. doi: <https://doi.org/10.1111/joa.12584>. URL <https://doi.org/10.1111/joa.12584>.
- [56] S. D. Choudhury, T. Allsop, A. Passman, and G. E. Norris. Use of a proteomics approach to identify favourable conditions for production of good quality lambskin leather. *Anal. Bioanal. Chem.*, 384(3):723–735, 2006. ISSN 1618-2642.
- [57] P. Agarwal, D. Zwolanek, D. R. Keene, J-N. Schulz, K. Blumbach, D. Heinegård, F. Zaucke, M. Paulsson, T. Krieg, M. Koch, and B. Eckes. Collagen XII and XIV, new partners of cartilage oligomeric matrix protein in the skin extracellular matrix suprastructure. *J. Biol. Chem.*, 287(27):22549–22559, 2012. ISSN 0021-9258. doi: <https://doi.org/10.1074/jbc.M111.335935>. URL <https://www.sciencedirect.com/science/article/pii/S002192582043426X>.
- [58] F. Berthod, L. Germain, R. Guignard, C. Lethias, R. Garrone, O. Damour, M. van der Rest, and F. A. Auger. Differential expression of collagens XII and XIV in human skin and in reconstructed skin. *J. Invest. Dermatol.*, 108(5):737–742, 1997. ISSN 0022-202X. doi: <https://doi.org/10.1111/1523-1747.ep12292122>. URL <https://www.sciencedirect.com/science/article/pii/S0022202X15428891>.
- [59] E. Reichenberger, S. Baur, C. Sukotjo, B. R. Olsen, N. Y. Karimbux, and I. Nishimura. Collagen XII mutation disrupts matrix structure of periodontal ligament and skin. *J. Dent. Res.*, 79(12):1962–8, 2000. ISSN 0022-0345 (Print) 0022-0345. doi: [10.1177/00220345000790120701](https://doi.org/10.1177/00220345000790120701).
- [60] H. L. Ansorge, X. Meng, G. Zhang, G. Veit, M. Sun, J. F. Klement, D. P. Beason, L. J. Soslowsky, M. Koch, and D. E. Birk. Type XIV collagen regulates fibrillogenesis: Premature collagen fibril growth and tissue dysfunction in null mice. *J. Biol. Chem.*, 284(13):8427–38, 2009. ISSN 0021-9258 (Print) 0021-9258. doi: [10.1074/jbc.M805582200](https://doi.org/10.1074/jbc.M805582200).
- [61] M. R. Harkey. Anatomy and physiology of hair. *Forensic Sci. Int.*, 63(1-3):9–18, 1993. ISSN 0379-0738.
- [62] F. Luo, X. Zhong, M. Gao, B. Peng, and Z. Long. Progress and mechanism of breaking glycoconjugates by glycosidases in skin for promoting unhairing and fiber opening-up in leather manufacture. A review. *J. Leather Sci. Eng.*, 2:1–16, 2020.
- [63] R. Moll, M. Divo, and L. Langbein. The human keratins: biology and pathology. *Histochem. Cell Biol.*, 129(6):705–733, 2008. ISSN 0948-6143 1432-119X. doi: [10.1007/s00418-008-0435-6](https://doi.org/10.1007/s00418-008-0435-6). URL <https://pubmed.ncbi.nlm.nih.gov/18461349>.

- [64] P. Sujitha, S. Kavitha, S. Shakilanishi, N. K. C. Babu, and C. Shanthi. Enzymatic dehairing: a comprehensive review on the mechanistic aspects with emphasis on enzyme specificity. *Int. J. Biol. Macromol.*, 118:168–179, 2018. ISSN 0141-8130.
- [65] J. Wadstein, E. Thom, and A. Gadzhigoroeva. Integral roles of specific proteoglycans in hair growth and hair loss: mechanisms behind the bioactivity of proteoglycan replacement therapy with Nourkrin[®] with Marilex[®] in pattern hair loss and telogen effluvium. *Dermatol. Res. Pract.*, 2020:8125081, 2020. ISSN 1687-6105. doi: 10.1155/2020/8125081. URL <https://doi.org/10.1155/2020/8125081>.
- [66] B. W. Wilson, K. J. Edwards, M. J. Sleigh, C. R. Byrne, and K. A. Ward. Complete sequence of a type-I microfibrillar wool keratin gene. *Gene*, 73(1):21–31, 1988. ISSN 0378-1119 (Print) 0378-1119. doi: 10.1016/0378-1119(88)90309-5.
- [67] J. A. Rothnagel and G. E. Rogers. Trichohyalin, an intermediate filament-associated protein of the hair follicle. *J. Biol. Chem.*, 102(4):1419–1429, 1986. ISSN 0021-9525 1540-8140. doi: 10.1083/jcb.102.4.1419. URL <https://pubmed.ncbi.nlm.nih.gov/3958055>.
- [68] P. M. Steinert, D. A. D. Parry, and L. N. Marekov. Trichohyalin mechanically strengthens the hair follicle: multiple cross-bridging roles in the inner root sheath. *J. Biol. Chem.*, 278(42):41409–41419, 2003. ISSN 0021-9258. doi: <https://doi.org/10.1074/jbc.M302037200>. URL <https://www.sciencedirect.com/science/article/pii/S0021925820829445>.
- [69] C. C. Reed and R. V. Iozzo. The role of decorin in collagen fibrillogenesis and skin homeostasis. *Glycoconjugate J.*, 19(4):249–255, 2002. ISSN 1573-4986. doi: 10.1023/A:1025383913444. URL <https://doi.org/10.1023/A:1025383913444>.
- [70] M. Raspanti, M. Viola, A. Forlino, R. Tenni, C. Gruppi, and M. E. Tira. Glycosaminoglycans show a specific periodic interaction with type I collagen fibrils. *J. Struct. Biol.*, 164(1):134–9, 2008. ISSN 1047-8477. doi: 10.1016/j.jsb.2008.07.001.
- [71] C. Rühland, E. Schönherr, H. Robenek, U. Hansen, R. V. Iozzo, P. Bruckner, and D. G. Seidler. The glycosaminoglycan chain of decorin plays an important role in collagen fibril formation at the early stages of fibrillogenesis. *FEBS J.*, 274(16):4246–55, 2007. ISSN 1742-464X (Print) 1742-464x. doi: 10.1111/j.1742-4658.2007.05951.x.
- [72] S. Shakilanishi and C. Shanthi. Specificity studies on proteases for dehairing in leather processing using decorin as model conjugated protein. *Int. J. Biol. Macromol.*, 103:1069–1076, 2017. ISSN 0141-8130. doi: <https://doi.org/10.1016/j.ijbiomac.2017.05.134>. URL <https://www.sciencedirect.com/science/article/pii/S0141813017309807>.
- [73] S. Chakravarti, T. Magnuson, J. H. Lass, K. J. Jepsen, C. LaMantia, and H. Carroll. Lumican regulates collagen fibril assembly: skin fragility and corneal opacity in the

absence of lumican. *J. Cell Biol.*, 141(5):1277–1286, 1998. ISSN 0021-9525 1540-8140. doi: 10.1083/jcb.141.5.1277. URL <https://pubmed.ncbi.nlm.nih.gov/9606218>.

- [74] A. Kampmann, B. Fernández, E. Deindl, T. Kubin, F. Pipp, I. Eitenmüller, I. E. Hofer, W. Schaper, and R. Zimmermann. The proteoglycan osteoglycin/mimecan is correlated with arteriogenesis. *Mol. Cell. Biochem.*, 322(1):15–23, 2009. ISSN 1573-4919. doi: 10.1007/s11010-008-9935-x. URL <https://doi.org/10.1007/s11010-008-9935-x>.
- [75] Y. J. Wu, D. P. L. A. Pierre, J. Wu, A. J. Yee, and B. B. Yang. The interaction of versican with its binding partners. *Cell Res.*, 15(7):483–494, 2005. ISSN 1748-7838. doi: 10.1038/sj.cr.7290318. URL <https://doi.org/10.1038/sj.cr.7290318>.
- [76] U. Takeda, A. Utani, J. Wu, E. Adachi, H. Koseki, M. Taniguchi, T. Matsumoto, T. Ohashi, M. Sato, and H. Shinkai. Targeted disruption of dermatopontin causes abnormal collagen fibrillogenesis. *J. Invest. Dermatol.*, 119(3):678–83, 2002. ISSN 0022-202X (Print) 0022-202x. doi: 10.1046/j.1523-1747.2002.01863.x.
- [77] L. E. Tracy, R. A. Minasian, and E. J. Caterson. Extracellular matrix and dermal fibroblast function in the healing wound. *Adv. Wound Care*, 5(3):119–136, 2016. ISSN 2162-1918 2162-1934. doi: 10.1089/wound.2014.0561. URL <https://pubmed.ncbi.nlm.nih.gov/26989578>.
- [78] G. R. Guy, R. Philip, and Y. H. Tan. Analysis of cellular phosphoproteins by two-dimensional gel electrophoresis: applications for cell signaling in normal and cancer cells. *Electrophoresis*, 15(1):417–440, 1994. ISSN 0173-0835. doi: 10.1002/elps.1150150160. URL <https://onlinelibrary.wiley.com/doi/abs/10.1002/elps.1150150160>.
- [79] Richard J Simpson. *Proteins and Proteomics: A Laboratory Manual Cold Spring*. Cold Spring Harbor Laboratory Press, New York, 2003.

4.5 Supplementary information - Methods

4.5.1 Amino acid analysis of sheepskin

Amino acid standard preparation

Individual amino acid stock solutions were prepared as stock solutions of 100 pmol/ μ L. A commercial amino acid standard (Sigma amino acid standard for collagen hydrolysates, discontinued) containing all the standard amino acids plus hydroxyproline and hydroxylysine was diluted to 100 pmol/ μ L, (exceptions cysteine at 50 pmol/ μ L, proline and hydroxyproline at 500 pmol/ μ L), and 10 μ L of the diluted standard solution was derivatised.

Amino acid extraction from skins

Skin samples were lyophilised and cut into 3 mm \times 3 mm cubes. To hydrolyse the skin, 100 mg of lyophilised skin was placed in an acid-washed 15 mL Pyrex[®] screw cap (PTFE) borosilicate glass tube (Thermo Fisher Scientific, USA). Five (5) mL of 6 M HCl containing 3 % phenol was added to the glass tube, and hydrolysed at 110 °C for 24 hours. After this time, any undissolved material was removed by filtration through glass-wool plugged plastic syringes. The resultant hydrolysate was kept in an acid washed glass scintillation vial (Thermo Fisher Scientific, USA), covered with Parafilm[®], and lyophilised. The lyophilised sample was then dissolved in 1 mL H₂O and 900 μ L was used for collagen crosslink analysis (Section 4.5.2), and the remaining 100 μ L was diluted 100 times for derivatisation.

Amino acid derivatisation

To derivatise samples, 6-aminoquinolyl-N-hydroxysuccinimidyl carbamate (AQC) was first dissolved in MeCN with vigorous vortexing to a 15 nmol/ μ L concentration. Ten μ L of 100 pmol/ μ L norleucine was added to 10 μ L of amino acid standard. The sample was then mixed with 70 μ L of 0.2 M borate buffer (pH adjusted to 9.0), and 20 μ L of AQC-MeCN solution and incubated at 55 °C for 10 minutes, taking care to exclude light. After centrifugation at 13,000 \times g for 1 minute, the AQC-derivatised sample was then added to 900 μ L of H₂O and centrifuged again at 13,000 \times g for 10 minutes prior to HPLC analysis.

Separation of AQC-derivatised amino acids by RP-HPLC

Derivatised amino acids were separated and analysed using a Dionex[™] UltiMate[™] 3000 UHPLC system equipped with a RS pump and a RS auto-sample injector (Thermo Fisher Scientific, USA). The sample was injected onto a guard column attached to the Gemini[®] 5 μ m C₁₈ column (150 \times 4.6 mm, 5 μ m particle size,

110 Å pore size)(Phenomenex[®], USA). The column was pre-equilibrated at 35 °C in solvent A: 50 mM ammonium acetate adjusted to pH 5.03 with glacial acetic acid. Solvent B was 60 % MeCN in H₂O. For the separation of derivatised amino acids, a linear gradient of 0 to 60 % MeCN was applied over 20 minutes (Table S1). Eluted peaks were monitored using a Dionex[™] UltiMate[™] 3000 fluorescence detector (Thermo Fisher Scientific, USA) with excitation and emission wavelengths of 245 nm and 395 nm, respectively (Fig. S1). At the end of each run, the column was washed with 5 column volumes of solvent B followed by re-equilibration in 5 column volumes of solvent A. A H₂O blank was run between each sample using the same programme.

Table S1: HPLC separation gradient for amino acid analysis

Time (min)	Flow (mL/min)	% B
0	1	0
20	1	70
21	1	100
25	1	100
26	1	0
30	1	0

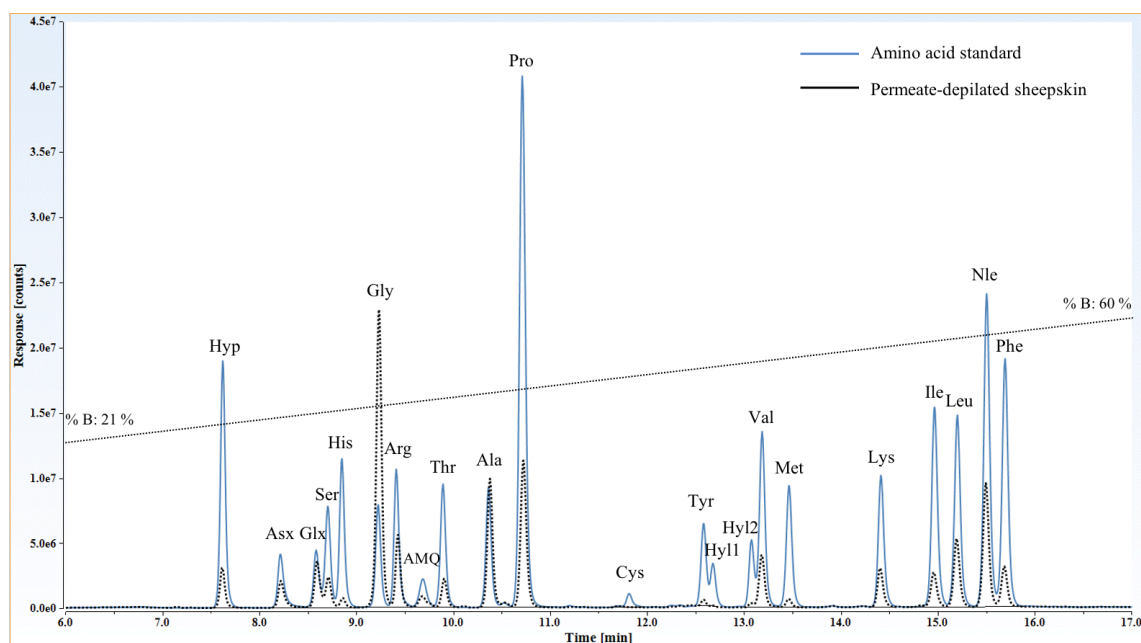


Figure S1: HPLC chromatogram of the separation of amino acid standards and permeate-depilated sheepskin derivatised with AQC dissolved in MeCN. Buffer A, 5 mM ammonium acetate, pH 5.05. Buffer B, 60 % MeCN.

Amino acid data analysis

Calibration standard curves were produced by injecting various volumes of 1.0 to 13.0 μL of the amino acid standard solution (supplemented with norleucine). For each amino acid, a response factor was calculated by dividing the area under the peak by the amount injected (pmol). For the analysis of sheepskins, three biological replicates of raw and permeate-depilated sheepskins were prepared, and 12 technical replicates were used for quantitation. Amino acid concentrations were determined from calibration curves calculated using Thermo Scientific™ Dionex™ Chromeleon™ chromatography data system software version 6.60 SR13 build 3967. The collagen content was calculated based on the amount of hydroxyproline in each sample as previously described by Neuman *et al.* (1950)³³.

4.5.2 Collagen crosslink analysis of sheepskin

Reduction of skin samples

100 mg of lyophilised skin samples were each suspended in 1 mL of phosphate buffered saline. Three mg of sodium borohydride was dissolved in 1 mL of 1 mM cold sodium hydroxide (4 °C) to give a 1:30 ratio of sodium borohydride to dry skin, then added to the skin samples. The sample mixture was incubated for 2 hours at 37 °C then stopped by adding glacial acetic acid until the pH dropped to 3.0. Samples were centrifuged at $5000 \times g$ for 15 minutes and the supernatant was discarded. The pellets were washed three times with H_2O to remove excess acetic acid and salt before being lyophilised and acid hydrolysed.

Collagen crosslink enrichment

Amino acids from the skin hydrolysate were removed from the solution by using the CF11 cellulose (Merck; USA) column chromatography. A 5 % CF11 slurry (w/v) was suspended in a butanol-water-acetic acid solution (4:1:1, v/v/v). Column were prepared using a 10 mL plastic syringe (0.5 cm \times 10 cm). The columns were plugged with glass-wool, which took up to 1 mL of the volume, then washed with 10 mL of H_2O before being filled with a 5 % CF11 slurry. They were then washed at least three column volumes of the butanol-water-acetic acid solution before 900 μL of the skin amino acid hydrolysate was carefully loaded onto the surface of the CF11 column so as not to disturb it. The initial flow through was discarded and the CF11 column was washed with 50 mL of the butanol-water-acetic acid solution to remove most of the free amino acids. The collagen crosslinks were eluted in 50 mL of H_2O , then lyophilised, rehydrated in 1 mL of H_2O , and stored at -80 °C until further analysis.

Quantitation of collagen crosslinks

Collagen crosslinks were separated by liquid chromatography using a LC system with a 15 cm Cogent Diamond Hydride™ HPLC column (PM Separations, Capalaba, Queensland, Australia). The liquid chromatography system was coupled to an Q Exactive™ Focus mass spectrometer equipped with a high-energy collision-induced dissociation (HCD) collision cell, an Orbitrap mass analyser and a HESI-II ion source (Thermo Fisher Scientific, USA). Details for the chromatographic and mass spectrometry settings are listed in Tables S2, S4, S3 and S5.

Table S2: Instrument configuration for collagen crosslink analysis

LC system	Dionex UltiMate™ LPG-3400RS Rapid Separation Quaternary Pump (Thermo Fisher Scientific, USA)
Mass spectrometer	Q Exactive™ Focus (Thermo Fisher Scientific, Bremen, Germany)
Ionisation source	HESI-II (Thermo Fisher Scientific, USA)
Analytical column	Cogent Diamond Hydride™ HPLC column, 2.2 µm particle size, 2.1 mm inner diameter, 150 mm length, 100 Å pore size (Thermo Fisher Scientific, USA)
Flow rate	Analytical column: 0.4 mL/min
Column oven temperature	25 °C
Gradient	80 - 10 % B for 11 mins, 1min hold at 10 % B, 0 - 80 % B for 3 mins, 5 min equilibration at 80 % B
Buffers	A: 0.1 % Formic acid/H ₂ O B: 0.1 % Formic acid/ 80 % MeCN/H ₂ O

Table S3: Mass spectrometer source settings for collagen crosslink analysis

Capillary temperature (°C)	350
S-Lens RF level (%)	50
Polarity	Positive
Source voltage (kV)	4.0
Sheath gas flow rate (L/min)	35
Aux gas flow rate (L/min)	6
Aux gas heater temperature (°C)	300

Table S4: Mass spectrometry settings for the detection of collagen crosslinks

Resolution	35,000
Isolation window	3.0 m/z
Normalised collision energy	20
Default charge	1
AGC target	2×10^4
Maximum injection time	Auto
Number of micro-scans	1
Spectrum data type	Centroid

Table S5: Inclusion list for PRM analysis

Mass (m/z)	CS [z]	Polarity	Start (min)	End (min)	CE	Peptide ID
308.1816	1	Positive	5.7	6.3	24	DHLNL
292.1867	1	Positive	5.85	6.4	24	HLNL
445.2426	1	Positive	6.6	7.4	20	HHL
287.6635	1	Positive	8.15	9.1	12	HHMD

4.5.3 Proteomic analysis of sheepskin

Protein extraction

For the salt extraction, 100 mg of diced skin pieces were transferred into a cryotube containing 0.1 g of zirconium/silica beads and 1 mL of the salt extraction buffer. Samples were homogenised at 4 °C in a Hybaid Ribolyzer (Thermo Fisher Scientific, USA) using 6 rounds of 20 second beating at 5.5 magnitude, with a 30 second cooling period between each run. The tubes were then transferred to a rotating inverter and left mixing by rotation overnight at 4 °C. After incubation, the tubes were centrifuged for 20 minutes at $16,000 \times g$ at 4 °C. The supernatants were transferred to new LoBind tubes (Eppendorf[®], USA) by carefully submerging the pipette tip into the sample between the fat layer and the cellular debris pellet. 400 μ L of the salt extraction buffer was used to resuspend the pellet by vortexing. Samples were again subjected to centrifugation at $16,000 \times g$ for 20 minutes at 4 °C, and the supernatant removed as before, combined with the first, and stored at -80 °C until required. The pellets were retained for extraction with urea. For the urea extraction, 1 mL of the urea extraction buffer was added to the cryotubes containing the pellets and zirconium/silica beads (dnature diagnostics research Ltd., New Zealand). Samples were re-homogenised using the same procedure as before then again mixed by rotation overnight at 4 °C. After centrifugation at $16,000 \times g$ for 20 minutes at 4 °C, the supernatants were transferred into new LoBind tubes. The remaining pellets were washed by vortexing with 500 μ L of the urea extraction buffer, and any insoluble material removed by centrifugation. The supernatants

were pooled, labelled, and stored at $-80\text{ }^{\circ}\text{C}$ until further processing. One (1) mL of CNBr extraction buffer was then added to the cryotubes containing zirconium/silica beads and remaining skin pellets, purged with N_2 for 5 minutes and then left mixing by rotation for 24 hours at ambient temperature in the dark. The tubes were then centrifuged at $16,000 \times g$ for 20 minutes at $4\text{ }^{\circ}\text{C}$, and the supernatant transferred to LoBind tubes in $2 \times 500\text{ }\mu\text{L}$ lots chilled on ice, labelled and stored at $-80\text{ }^{\circ}\text{C}$ until required. A schematic diagram of the sample preparation workflow is shown in Fig. S2.

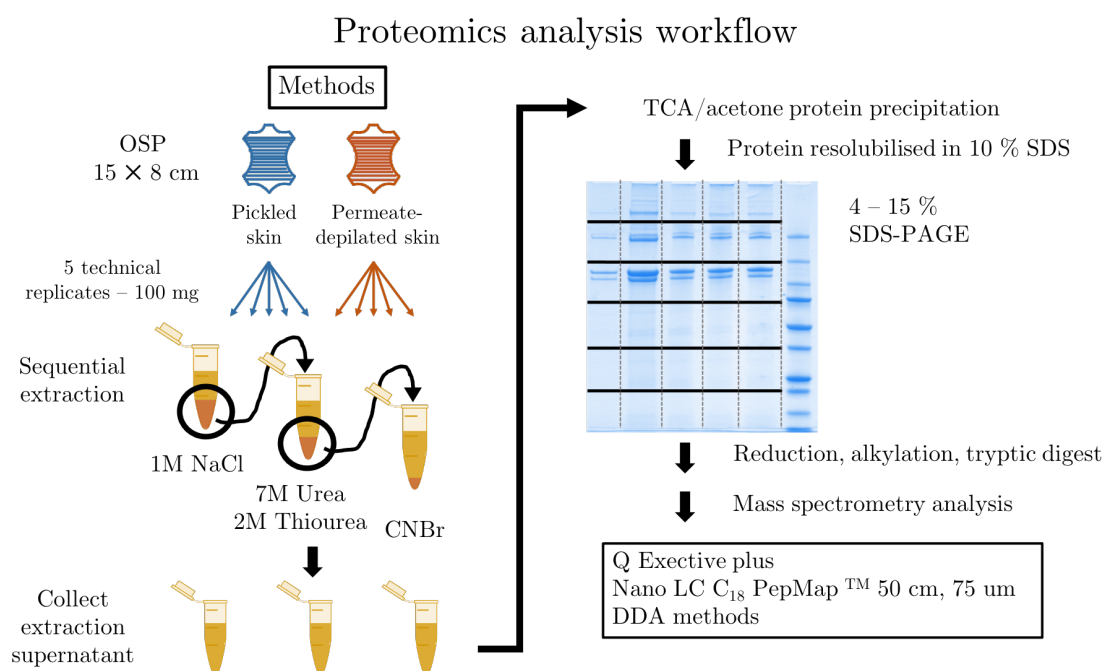


Figure S2: Diagram of the proteomic analysis workflow.

Removal of metabolites and protein resolubilisation

Metabolites were removed from the extracted proteins using the standard TCA-acetone method⁷⁸. To make the TCA (trichloroacetic acid)-acetone solution, 8 volumes of acetone was mixed with 1 volume of TCA. DTT was added to the mixture to a final concentration of 20 mM just prior to use. Nine (9) parts of TCA-acetone solution was added to 1 part of extract, mixed by inversion and incubated at $-20\text{ }^{\circ}\text{C}$ overnight. After centrifugation at $16,000 \times g$ for 20 minutes at $4\text{ }^{\circ}\text{C}$, the supernatant was immediately removed, discarded and the pellets resuspended in 1 mL of $-20\text{ }^{\circ}\text{C}$ chilled acetone solution (containing 20 mM DTT) by pipetting and vortexing. The pellets were washed three times, centrifuged as before and the acetone solution discarded. After the final wash, the pellets were air

dried at room temperature in a fume hood for 5 minutes then stored at -80 °C until needed. TCA-precipitated protein pellets were solubilised by the addition of 20 μ L of 10 % SDS and pipetting the mixture up and down. The samples were stored at -80 °C until fractionated on 4-15 % gradient SDS gels. Gels were stained with Colloidal Coomassie G-250 stain⁷⁹ in 20 % methanol overnight at room temperature with gentle agitation.

In-gel tryptic digestion

In-gel tryptic digestion was carried out as described in Shevchenko *et al.* (2006)³¹ with modifications. Briefly, each lane of the 4 - 15 % gels was cut into 6 approximately equal pieces on a clean glass plate using a clean scalpel blade as shown in Fig. S2. Each block was then transferred into a LoBind tube and processed as follows.

Destain

The bands were destained with 50 % methanol (MeOH) in 50 mM ammonium bicarbonate (AmBic) at 45 °C until the gel slices became colourless. They were then dehydrated by the addition of 300 μ L of 80 % MeCN. When the pieces became shrunken and opaque white (after approximately 1 minute), the supernatant was removed and the gel pieces were dried in their tubes using a vacuum centrifugal evaporator, SpeedVac[™] (Savant, Thermo Fisher Scientific, USA), for 10 minutes.

Reduction, alkylation and tryptic digestion

Dried gel pieces were reduced using 200 μ L of fresh reducing solution (Table S6) for 1 hour at 37 °C with periodic shaking. The supernatant was removed and the gel pieces washed again with 200 μ L of 50 mM AmBic for 5 minutes. The liquid was removed and the gel pieces were dehydrated with 200 μ L 80 % MeCN for 1 minute. After the supernatant was removed, and the gel pieces were dried for 10 minutes using the SpeedVac[™]. To alkylate the proteins, 200 μ L of freshly prepared alkylation solution (Table S6) was added to the gel pieces and incubated for 30 minutes in the dark at room temperature. The supernatant was removed and the gel pieces washed with 200 μ L of 50 mM AmBic before being dehydrated with 200 μ L of 80 % MeCN. The gel pieces were rehydrated and washed again with AmBic and dehydrated as described above. The liquid was removed from the tubes and the gel pieces were dried completely in the SpeedVac[™] for 10 minutes. The dried gel pieces were then placed in 100 μ L of digestion solution (Table S6) on ice for 10 minutes to allow the gel pieces to fully swell, then incubated overnight at 37 °C.

Table S6: Solutions used for reduction, alkylation and proteolytic digestion

Component	Concentration
Reducing solution	
DTT	10 mM
AmBic	50 mM
Alkylating solution	
Iodoacetamide	20 mM
AmBic	50 mM
Digestion solution	
Trypsin	20 ng/ μ L
AmBic	50 mM

Protein extraction

After overnight tryptic digestion, the tubes were centrifuged briefly ($16,000 \times g$, 30 seconds) and sonicated in an ultrasonic bath for 2 minutes. The supernatants were carefully removed and placed in new LoBind tubes and pooled together with supernatants from the following washes: first, 100 μ L of 5 % formic acid in 50 % MeCN; second, 100 μ L of 0.1% formic acid in 80 % MeCN. In both cases the gel pellets were sonicated for 2 minutes before centrifugation, and the transfer of the supernatants to the LoBind tubes. The volumes of the samples were reduced to approximately 30 μ L by vacuum centrifugation, then stored at $-80\text{ }^{\circ}\text{C}$ until further analysis. For mass spectrometry analysis, the samples were first centrifuged at $16,000 \times g$ for 20 minutes, the 20 μ L of the top of the supernatant carefully transferred into clean MS glass sample vials.

Proteomic mass spectrometry analysis

The in-gel digested peptide samples were desalted using an on-line reversed-phase peptide trap before being separated by reversed-phase nano-LC (Thermo ScientificTM) using a 50 cm PepMapTM 300 C₁₈ LC column (Thermo ScientificTM). Eluted peptides were analysed by mass spectrometry (Q ExactiveTM Plus Hybrid Quadrupole-OrbitrapTM, with a Nano Flex ion source (Thermo Fisher Scientific, Bremen, Germany) using data-dependent tandem MS acquisition. Details for the chromatographic and mass spectrometry settings are listed in below Tables S7 and S8. Full MS1 scans were acquired over a mass range of 375 - 1,600 m/z at a resolution of 70,000. Fragment ion spectra produced *via* higher-energy collisional dissociation (HCD) were acquired with a resolution setting of 17,500 and the top ten most intense ions were selected for fragmentation in each full scan cycle. MS/MS fragment ion spectra were detected at a peak width of 1.4 m/z and exclusion conditions were optimised according to the observed total ion current (TIC) chromatogram peak widths.

Table S7: Mass spectrometer configuration used for proteomics analysis

nanoLC system	Dionex UltiMate™ 3000 Binary RSLCnano system (Thermo Fisher Scientific, USA)
Mass spectrometer	Q Exactive™ Plus (Thermo Fisher Scientific, Bremen, Germany)
Ionisation source	Nanospray Flex™ (Thermo Fisher Scientific, USA)
Trapping column	Acclaim™ PepMap™ 100 C ₁₈ , 3 µm particle size, 75 µm inner diameter, 1 cm length (Thermo Fisher Scientific, USA)
Analytical column	Acclaim™ PepMap™ C ₁₈ , 2 µm particle size, 75 µm inner diameter, 50 cm length (Thermo Fisher Scientific, USA)
Flow rates	Trap column: 15 µL/min Analytical column: 300 nL/min
Column oven temperature	50 °C
Gradient	3 - 30 % MeCN in 0.1 % formic acid over 60 minutes
Buffers	Trap loading: 0.1 % TFA/ 2 % MeCN/H ₂ O Analytical A: 0.1 % Formic acid/ 2 % MeCN/H ₂ O Analytical B: 0.1 % Formic acid/ 98 % MeCN/H ₂ O

Table S8: Parameter used for proteomic analysis

Capillary temperature (°C)	250
S-Lens RF level (%)	50
Polarity	Positive
Source voltage (kV)	1.5
AGC target	Full MS 3×10^6 , MS2 (HCD) 1×10^5
Maximum injection times (ms)	Full MS 100 ms, MS2 (HCD) 110 ms
Full MS mass range	375 - 1600 m/z
Resolution settings	Full MS 70,000, MS2 (HCD) 17,500
Number of micro-scans	1
Isolation width	1.4 m/z
Loop count (TopN)	10
MSX count	1
Collision energies	25, 30, 35
Charge exclusion	Unassigned, 1, > 7
Peptide match	Preferred
Exclude isotopes	On
Dynamic exclusion	12 seconds
Spectrum data type	Centroid

Proteomic data analysis

The raw data files were processed using Proteome Discoverer™ version 2.4. The search parameters applied in the database searches are listed in Table S9. The NCBI *Ovis aries* protein database was used and the reverse database search option was used as a filter to satisfy a false discovery rate (FDR) of 1 %.

Table S9: Parameters used for proteomic data analysis

Search engine	Proteome Discoverer™ v. 2.4
Databases	Non-redundant NCBI compiled on 8 th of January, 2020 + Contaminant
Taxonomy	<i>Ovis aries</i>
Enzyme	Trypsin
Maximum number of missed cleavages	2
Minimum peptide length	6
Precursor mass tolerance	10 ppm
Fragment mass tolerance	0.02 Da
Peptide charge	2 - 7
Protein mass	Unrestricted
Decoy database search	Enabled (default)
Significance threshold	0.01 %
Static modifications	Carbamidomethyl, + 57.021 (C)
Variable modifications	Oxidation, + 15.995 Da (K, M, P) Acetylation, + 42.011 Da (N-Terminus) Galactosyl, + 178.048 Da (K) Glucosylgalactosyl, + 340.101 Da (K) Hex, + 162.053 Da (N, S, T) HexNAc, + 203.079 Da (N, S, T)
False discovery rate	≤ 1 %

4.6 Supplementary information - Results

Table S10: Proteins identified in the proteomic analysis of sheepskin.

Description	Accession number	PSMs	Fold difference	<i>p</i> -value
collagen α 1 (I) chain	XP_027830506.1	18252	1.00	0.78
collagen α 2 (I) chain	XP_004007775.1	17367	0.92	0.64
keratin, type II cytoskeletal 5	XP_027823079.1	11807	1.08	0.69
keratin, type II cytoskeletal 75	XP_027823083.1	8076	2.14	0.15
keratin, type II cytoskeletal 6A	XP_012029607.2	7277	1.35	0.27
keratin, type I cytoskeletal 14	XP_014954266.2	5731	1.60	0.18
keratin, type II cytoskeletal 5-like	XP_012029610.1	5278	1.39	0.12
keratin, type II cytoskeletal 7	XP_004006382.2	4969	2.76	0.005
collagen α 1 (III) chain	XP_004004563.1	4872	0.99	0.85
keratin, type II cytoskeletal 4	XP_027823076.1	4683	8.12	0.09
albumin precursor	NP_001009376.1	4282	1.49	0.05
keratin, type II cytoskeletal 79	XP_027823077.1	4263	2.38	0.07
keratin, type I cytoskeletal 42	XP_027830327.1	4253	4.18	0.03
keratin, type II cytoskeletal 80	XP_027823090.1	4210	1.45	0.28
keratin 17	AGW21585.1	3462	1.30	0.26
keratin, type I cytoskeletal 10	XP_027830375.1	3044	0.89	0.41
keratin, type II cytoskeletal 1	XP_014950133.2	2697	1.05	0.17
keratin, type II cytoskeletal 8	XP_012029598.2	2401	1.54	0.06
keratin, type I cytoskeletal 24	XP_004012920.2	2261	0.48	0.02
keratin, type I cytoskeletal 16	XP_004023219.4	1925	1.42	0.25
hair type II keratin intermediate filament protein	CAA44368.1	1886	0.63	0.14
collagen α 3 (VI) chain	XP_027823071.1	1594	1.70	0.01
keratin, type II cytoskeletal 71	NP_001267645.1	1439	0.60	0.05
desmoplakin isoform X1	XP_027814264.1	1233	1.31	0.38
keratin 83	NP_001185998.1	1136	1.22	0.98
keratin, type II cytoskeletal 1b	XP_027823078.1	1025	0.66	0.10
keratin, type II cytoskeletal 72	XP_004006372.2	959	0.42	0.01
keratin, type I microfibrillar 48 kDa, component 8C-1	P02534.2	905	0.75	0.38
immunoglobulin γ 1 chain	CAA49451.1	835	6.78	0.0004
keratin, type II microfibrillar, component 5	P25691.1	806	3.09	0.11
Annexin A2	A2SW69.1	791	2.91	0.002
junction plakoglobin	XP_027830318.1	733	0.97	0.84
keratin, type I microfibrillar, 47.6 kDa	P25690.2	662	72.21	0.04
collagen α 1 (II) chain	XP_027823200.1	657	0.52	0.12
actin, cytoplasmic 1 β -actin	P60713.1	542	0.65	0.05
keratin, type I cytoskeletal 27	NP_001108235.1	460	0.23	0.02
collagen α 2 (VI) chain	XP_027817063.1	416	1.49	0.08
vimentin	ABP48145.1	374	0.88	0.54

Table S10 continued from previous page

Description	Accession number	PSMs	Fold difference	<i>p</i> -value
B30554 Ig λ chain C		361	6.28	0.0006
complement C3	XP_027825575.1	350	3.89	0.002
keratin, type I cytoskeletal 25	NP_001009739.1	345	1.35	0.17
lumican	XP_012029466.1	332	0.55	0.03
immunoglobulin λ 1 light chain-like	XP_027812629.1	323	3.86	0.0003
uncharacterized protein LOC101108868	XP_014958051.2	300	0.46	0.002
myosin-11 isoform X1	XP_027817220.1	287	1.36	0.12
collagen α 1 (VI) chain	XP_027817050.1	263	0.97	0.60
elongation factor 1- α 1	XP_004008202.2	253	0.26	0.003
β globin chain	ABC86524.1	238	0.49	0.02
desmoglein-1	XP_004020502.2	205	1.37	0.06
histone H2B type 1	XP_004019124.2	195	0.21	0.0008
collagen α 1 (XII) chain	XP_014952772.2	190	2.43	0.04
decorin	AAF00585.1	188	0.60	0.05
mimectan	XP_004004124.1	183	2.55	0.01
keratin, type II cytoskeletal 78	XP_012029600.2	161	1.07	0.93
histone H2A	XP_004002479.1	154	0.14	0.00001
keratin, type I cuticular 35	B0LKP1.1	151	1.25	0.63
hemoglobin subunit α -1/2	P68240.2	148	0.47	0.03
tubulin α 1D chain	XP_004004997.1	144	0.39	0.0003
S25705 Ig μ chain	CAA42611.1	143	8.91	0.0009
serpin A3-1	XP_027813161.1	138	1.14	0.85
filamin-A isoform X1	XP_027819076.1	135	1.73	0.06
collagen α 2 (V) chain	XP_004004562.1	135	0.91	0.86
pyruvate kinase PKM	XP_004010328.1	132	0.98	0.76
annexin A1	XP_004004354.1	129	2.46	0.05
myosin-9	XP_027823550.1	128	0.37	0.005
alpha-2-macroglobulin	XP_012030833.2	122	1.37	0.03
serpin A3-5	XP_027813163.1	117	2.66	0.005
epiplakin	XP_027829279.1	110	0.04	0.0002
collagen α 1 (XIV) chain	XP_027829073.1	105	4.87	0.01
ubiquitin-40S ribosomal protein S27a	XP_027829423.1	100	0.59	0.01
serpin A3-8	XP_011954394.2	90	7.05	0.002
tropomyosin β chain	XP_004004325.1	87	1.63	0.06
peroxiredoxin-2 isoform X1	XP_027824977.1	79	0.90	0.48
annexin A5	XP_012034784.2	75	4.58	0.06
gelsolin isoform X1	XP_027819674.1	70	0.46	0.002
tubulin alpha 4a	ACR56697.1	67	0.49	0.02
desmin	XP_004005001.1	67	0.70	0.21
α -actinin-1	XP_027827748.1	67	1.06	0.71
trichohyalin	XP_027832307.1	63	0.25	0.002

Table S10 continued from previous page

Description	Accession number	PSMs	Fold difference	<i>p</i> -value
nucleolin isoform X1	XP_027821112.1	57	0.07	0.0008
heat shock protein β 1	XP_027817273.1	57	0.27	0.003
transthyretin	CAA33600.1	53	7.76	0.005
collagen α 2 (IV) chain	XP_027829588.1	51	3.43	0.0007
tropomyosin α 1 chain	XP_012035972.1	49	3.04	0.06
collagen α 1 (V) chain	XP_027821918.1	49	0.83	0.57
glutathione S-transferase μ 1	XP_027828552.1	47	0.99	0.64
serotransferrin	XP_027816111.1	45	1.20	0.91
ATP synthase subunit α	XP_004020569.1	43	0.58	0.02
cofilin-1	AAT77679.1	42	0.06	0.09
aldehyde dehydrogenase	XP_004017458.1	42	2.10	0.004
tropomyosin α 3 chain	XP_004002592.2	42	1.56	0.16
peptidyl-prolyl cis-trans isomerase A	NP_001295507.1	40	0.10	0.0006
serpin A3-7-like	XP_011963749.2	39	1.97	0.10
methanethiol oxidase	XP_004002539.2	38	1.51	0.16
lamin	XP_027832136.1	37	0.47	0.03
microfibril-associated glycoprotein 4	XP_027830620.1	36	3.81	0.004
ATP synthase subunit β	XP_004006621.1	35	0.60	0.35
voltage-dependent anion-selective channel protein 1	NP_001119824.1	33	6.88	0.002
protein S100-A10	XP_014947734.1	33	2.18	0.02
annexin A6	XP_004009036.1	30	4.00	0.01
fibronectin	XP_004004955.2	29	10.76	0.02
serpin B12	XP_027816619.1	27	1.61	0.02
collagen α 1 (VII) chain	XP_027813474.1	26	3.61	0.01
biglycan precursor	AAB87988.1	26	1.41	0.55
protein AHNAK2	XP_027813087.1	25	0.01	0.0007
perlecan	XP_027821348.1	25	2.06	0.04
heat shock protein α	ABI99473.1	25	0.24	0.02
annexin A4	XP_004005861.1	24	3.02	0.04
endoplasmic reticulum chaperone BiP	XP_004005686.1	24	1.00	0.80
liver carboxylesterase-like	XP_004015041.2	23	10.17	0.01
cathepsin D	Q9MZS8.1	23	4.90	0.01
protein disulfide isomerase family A member 3	ACS34987.1	23	2.58	0.05
elongation factor 2	XP_012033467.1	23	0.43	0.08
voltage-dependent anion-selective channel protein 2	XP_004021550.1	22	33.12	0.03
keratin, type II cuticular Hb5-like	XP_027823084.1	21	14.16	0.05
nucleophosmin isoform X1	XP_027835783.1	21	5.04	0.04
phospholipase B-like 1	XP_004006888.1	21	1.75	0.09

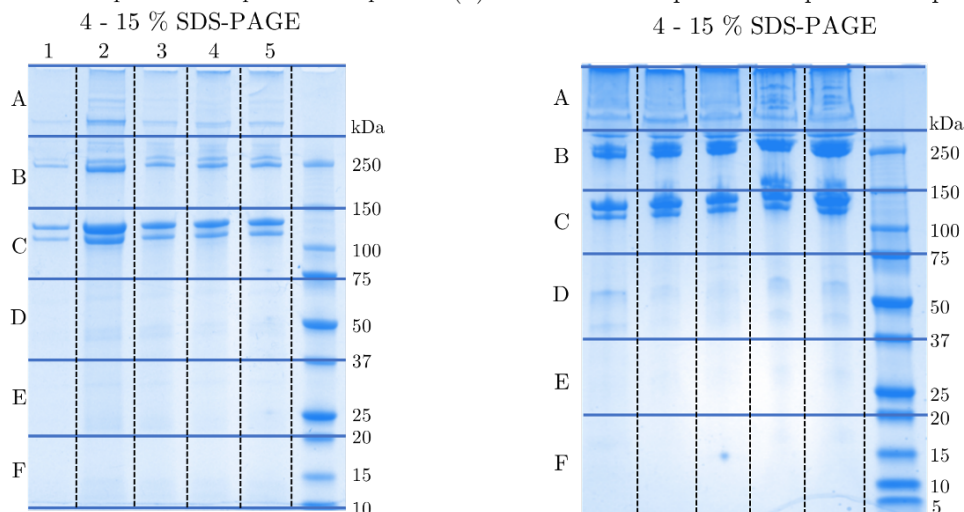
Table S10 continued from previous page

Description	Accession number	PSMs	Fold difference	<i>p</i> -value
profilin-1	XP_027830885.1	20	0.17	0.01
short palate, lung and nasal epithelium carcinoma-associated protein 2A-like	XP_027832882.1	20	3.16	0.01
galectin-3	XP_004010713.2	20	0.58	0.05
neuroblast differentiation-associated protein AHNAK	XP_027815717.1	19	0.11	0.004
barrier-to-autointegration factor	XP_027815615.1	18	4.56	0.0007
60S ribosomal protein L6	XP_004004943.2	18	0.06	0.00001
serpin H1 isoform X1	XP_027834780.1	18	9.61	0.15
calmodulin 2	AAL02363.1	18	1.24	0.29
peroxiredoxin-1	XP_011982042.2	18	0.87	0.43
collagen α 1 (IV) chain	XP_027829587.1	18	0.98	0.67
proteasome subunit α type-7	XP_027832783.1	16	3.50	0.01
adiponectin	AJG42209.1	16	2.44	0.04
C-reactive protein	XP_004002700.1	16	2.22	0.07
versican core protein	XP_004009116.2	15	73.94	0.02
thioredoxin	CAA81083.1	15	6.37	0.0004
fructose-bisphosphate aldolase A	XP_011959751.1	15	1.32	0.69
heat shock protein 70	AEX55801.1	13	0.21	0.0008
proteasome subunit α type-2	XP_004008046.1	13	7.60	0.13
alpha-aminoadipic semialdehyde dehydrogenase	XP_004008714.2	13	1.82	0.01
filamin-C	XP_027824589.1	13	1.90	0.04
S33161 Ig κ chain	CAA38046.1	13	28.66	0.04
alpha-1-acid glycoprotein	XP_004004031.1	13	1.87	0.35
catalase isoform X1	XP_004016445.1	12	5.73	0.001
dermatopontin	XP_004013720.1	12	9.80	0.001
placenta-expressed transcript 1 protein	XP_004016076.2	12	193.45	0.01
periostin isoform X1	XP_004012160.2	12	0.52	0.06
filamin-B isoform X1	XP_027814047.1	12	3.42	0.12
cytosol aminopeptidase	XP_012035088.2	12	1.09	0.85
inter-alpha-trypsin inhibitor heavy chain H1	XP_004018442.2	11	3.44	0.01
alpha-1-antitrypsin transcript variant 1	AFI71068.1	11	3.37	0.02
proteasome subunit β type-3	XP_004012874.1	11	1.36	0.32
protein POF1B	XP_004022280.2	11	1.90	0.40
complement C5	XP_004004015.2	11	1.58	0.22
60 kDa heat shock protein	XP_027820862.1	10	5.61	0.0008
transgelin-2	XP_004002705.1	9	0.31	0.01
vinculin isoform X1	XP_027818088.1	9	1.30	0.07
fatty acid binding protein 5	ABB46354.1	9	8.34	0.02

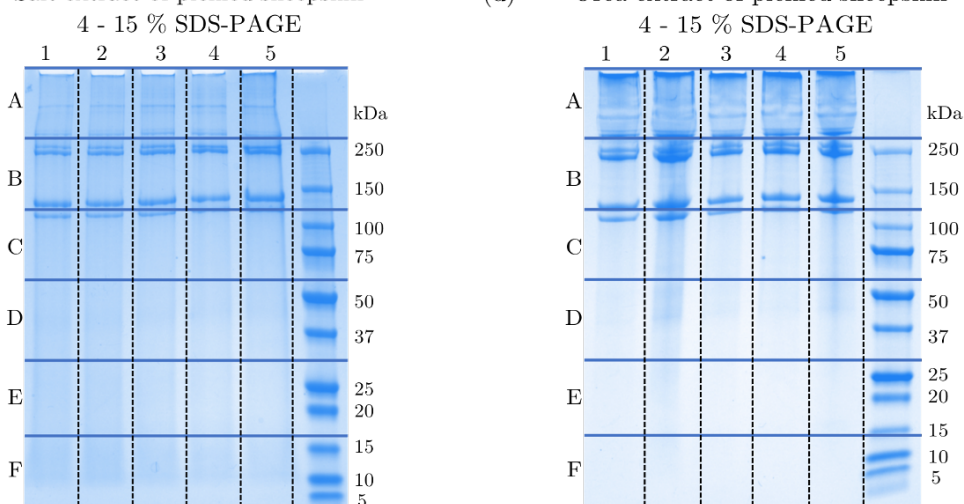
Table S10 continued from previous page

Description	Accession number	PSMs	Fold difference	<i>p</i> -value
ADP-ribosylation factor 4	ACR55755.1	9	0.42	0.17
peroxiredoxin-4 isoform X1	XP_027818838.1	8	4.40	0.10
fatty acid-binding protein 9	XP_004011812.1	8	0.16	0.003
prohibitin	XP_004012839.1	8	1.63	0.35
xaa-Pro dipeptidase	XP_004015193.1	7	2.78	0.02
glutathione S-transferase ω 1-like	XP_027816072.1	7	14.60	0.08
aminopeptidase N	XP_014957374.2	7	2.54	0.005
antithrombin-III	P32262.1	7	2.15	0.04
dipeptidyl peptidase 1	XP_004019812.3	7	5.12	0.05
adenosylhomocysteinase	XP_004014555.1	7	0.29	0.12
protein disulfide-isomerase	XP_027830078.1	7	0.75	0.99
nucleoside diphosphate kinase A1	XP_012041249.1	7	0.99	0.48
eukaryotic translation initiation factor 6 isoform X1	XP_012043461.1	6	5.59	0.11
serpin A3-6-like	XP_027813164.1	6	6.19	0.11
adipocyte fatty acid-binding protein 4	ABY25854.1	6	2.13	0.03
plasma serine protease inhibitor	XP_004018025.1	6	1.54	0.45
creatine kinase M-type	XP_012045938.1	6	1.02	0.35
asporin	XP_004004126.1	5	3.36	0.21
proteasome subunit α type-3	XP_004010730.1	5	1.49	0.19
plectin	XP_027829099.1	5	0.44	0.20
ribosomal protein S25	ABB46364.1	4	0.02	0.04
proteasome subunit α type 6	ACI46679.1	4	4.23	0.0007
desmocollin-3	XP_027816513.1	4	7.90	0.02
glycogen phosphorylase, muscle form	NP_001009192.1	4	5.14	0.21
phosphoglycerate kinase 1	ACJ53934.1	4	1.45	0.38
malate dehydrogenase, mitochondrial	XP_004021309.2	3	0.38	0.002
sushi repeat-containing protein SRPX	XP_027818715.1	3	1.94	0.002
apolipoprotein A-I	XP_011950887.2	3	0.21	0.04
glutathione S-transferase P	XP_027815273.1	3	2.54	0.08
protein disulfide-isomerase A6	XP_014949707.1	3	2.06	0.15
thrombospondin-1	XP_027827466.1	3	1.46	0.21
4F2 cell-surface antigen heavy chain	XP_004019669.2	2	41.96	0.02
myoglobin isoform X1	XP_012015345.1	2	7.55	0.19
endoplasmin	XP_012030315.1	2	1.22	0.78
insulin-degrading enzyme	XP_014958813.2	2	1.19	0.51

(a) Salt extract of permeate depilated sheepskin (b) Urea extract of permeate depilated sheepskin



(c) Salt extract of pickled sheepskin (d) Urea extract of pickled sheepskin



(e) CNBr extract
Permeate depilated sheepskin Pickled sheepskin

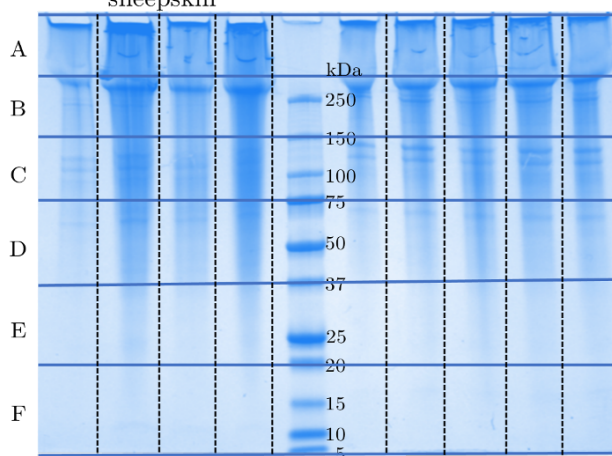


Figure S3: 4 - 15 % SDS-PAGE gels for sheepskin proteomic analysis. (a), (b) permeate-depilated sheepskin salt and urea extracted samples, respectively. (c), (d) pickled sheepskin salt and urea extracted samples, respectively. (e) CNBr extracted permeate-depilated and pickled sheepskin samples.

5 | Microbial analysis of the depilation process

Using OMICs to probe the mechanism of permeate depilation of sheepskins: sulfide *vs.* permeate

Yi-Hsuan Tu¹, Trevor S. Loo¹, Mark L. Patchett¹, Gillian E. Norris¹, and Dragana Gagic^{1,2}

¹School of Fundamental Sciences, Massey University, Palmerston North, New Zealand

²School of Veterinary Sciences, Palmerston North, Massey University, New Zealand

Address correspondence to:

Dragana Gagic, D.Gagic@massey.ac.nz

Publication status: manuscript in preparation to be submitted to Applied and Environmental Microbiology.

Abstract

Both milk and its by-products have been reported to both preserve and depilate sheepskins, potentially replacing the environmentally unfriendly salt and sulfide processes that are currently used. An initial investigation used traditional culturing methods to isolate and identify microorganisms present in the depilation solution after the wool had been removed to determine possible mechanisms for the effects observed. As culturing was done at the end of the depilation process, a metagenomic study of the changes in the microbial community over the time course of the depilation process has been undertaken using universal phylogenetic markers, bacterial 16S rRNA and fungal ITS regions, for amplicon sequencing. Results showed a concomitant increase in the relative abundance of *Lactococcus lactis* that matched the decrease in *Acinetobacter sp.* by the end of the depilation treatment. Proteomic and metabolomic analysis of the depilation liquid also identified bacteriocins and antimicrobial metabolites that could potentially contribute to the preservation of skins during depilation. This metagenomics study complements the results of the previous report and provides a better understanding of the preservation and depilation processes.

5.1 Introduction

Sheepskin, a common skin type used to manufacture leather for luxury garments, is also a by-product of the meat industry, that requires disposal if not used by the leather industry. Five steps are required to prepare sheepskins for tanning: depilation, liming, deliming/bating, pickling and degreasing. Depilation, the first step in this process, removes the hair or wool from the skins, by applying a thick alkaline sulfide solution (Na_2S , NaSH , NaOH , $\text{Ca}(\text{SH})_2$, $\text{Ca}(\text{OH})_2$) on the flesh side of the pelt. The chemicals soak through the skin and reach the hair shaft where they act to degrade the keratin in the wool follicle thus loosening the wool so it can be removed by scraping. This method has been used for centuries as it is effective, cheap, and has proven to be robust. However, the pollution, caused by the process, affects the environment and in recent years an increased awareness of the potential problems caused by such chemicals on land and in waterways, has raised concern about the people working and living near tanneries¹. Large quantities of both solid and liquid waste are produced by these pre-tanning processes, with the sulfide and alkaline water waste from the depilation process accounting for one-third of the global pollution generated from the leather industry^{2,3}.

To address problem of this pollution, much effort has been invested in the search for alternative environmentally friendly depilation methods that retain the properties of the skin. Various enzymes, such as keratinases, proteases, and lipases have been shown to successfully remove hair from skins. However, most of these also cause unacceptable damage to the skin. Furthermore, in many cases, the addition of sulfide to the enzyme mixture remains necessary for depilation efficiency^{4,5,6,7,8}. Although significant advances have been made in the use of enzymes for depilation, the process has proven to be costly at an industrial scale. In 1986, as a result of searching for a way to preserve sheepskins during transport to the tanneries, Schlosser *et al.*⁹ reported that a certain undisclosed *Lactobacillus* culture could cause depilation of sheepskin. Their idea was based on the fact that many lactic acid bacteria were being used in the food industry for the preservation of meat, vegetables, cheese and other fermented foods^{10,11}. Findings from the study showed that the raw skins could be kept for a week or longer without signs of putrefaction when incubated with the *Lactobacillus* culture, and that the depilation occurred during the incubation. The mechanisms of preservation and depilation, however, were not elucidated, and no further research was carried out to explain this phenomenon.

Without the knowledge of the strains of *Lactobacillus* used, commercially sourced yoghurt was initially trialled to test its efficacy to depilate and preserve unwashed fresh sheepskins. After four days of incubation at room temperature (20 - 25 °C), wool could be easily removed by gentle thumb pressure, and there were no signs of damage to the skins. Further testing of other dairy products, including commercially available milk and whey, showed they had the same depilatory and preservation activity (Chapter 3), which led to the development of an artificial permeate solution (for simplicity, referred to permeate hereafter) that has the same function.

The question therefore arises, what components are in these milk products that prevented the skins from putrefying and at the same time depilated the skins. Approximately 10^5 - 10^6 microorganisms colonise 1 gram of skin¹². Due to the nutritious (protein, fat and carbohydrate) and physical nature of skin (*i.e.*, high moisture and temperature), it is a favourable medium for the growth of a large number of different microorganisms¹³. Commensal bacteria on sheepskins and hides include *Acinetobacter*, *Aerococcus*, *Aeromonas*, *Bacillus*, *Corynebacterium*, *Enterococcus*, *Escherichia*, *Lactobacillus*, *Micrococcus*, *Moraxella*, *Neisseria*, *Pseudomonas*, *Staphylococcus*, and *Streptococcus*^{14,15,16}. When skin putrefying microorganisms dominate, the skins give off an offensive odour and show hair slippage¹⁷. Bacteria reported to be involved in hide and skin putrefaction include *Bacillus cereus/megaterium/subtilis*, *Corynebacterium bovis/xerosis*, *Enterococcus faecalis*, *Escherichia coli*, *Hafnia alvei*, *Lactobacillus jensenii*, *Micrococcus agilis/luteus/lylae/variants*, *Proteus vulgaris*, *Pseudomonas fluorescens/putida*, *Shewanella putrefaciens*, *Staphylococcus cohnii/epidermidis/hyicus/sciuri/simulans/xylosus*^{12,15,17}.

The oldest depilation method recorded was called sweating, which made use of putrefying bacteria already on the skins and present in the environment to cause mild breakdown of the skin structure thus loosening the hair. This process died out around the 1880s as the type and quantity of bacteria could not be controlled resulting in damage to the skin surface^{3,18}. Simple experiments in which skins are left at room temperature or in water at room temperature show that they putrefy quickly (within four days) even at low temperatures, *e.g.*, when stored at 10 °C¹³. Interestingly, when fresh unwashed sheepskins were immersed in milk, whey or permeate, they lasted for up to a week at room temperature without any signs of putrefaction. However, it is well known that milk products deteriorate more quickly than this when exposed to air at room temperature. Therefore, we hypothesised there were compounds and/or microorganisms in the media (milk

products) that created an environment which suppressed the growth of putrefying microorganisms while encouraging the growth of others that produce the molecules responsible for depilation as well as antimicrobial substances that controlled the microbial community abundance and/or diversity.

As sterilised whey was just as effective as other milk products, we trialled an artificial permeate solution that proved to be just as effective. To understand the changes in microbial diversity and relative abundance at the point of depilation and throughout the whole process, both traditional culture and culture-independent methods were used. Microorganisms present in the depilation solution were cultured, isolated and their phylogenetically informative markers, 16S rRNA and internal transcribed spacer (ITS) encoding genes were sequenced, resulting in a handful of species being consistently identified (Chapter 3).

To investigate the unculturable microbiome, a metabarcoding (amplicon) sequencing analysis was used to monitor the change in the depilation liquid during the depilation process, and a proteomic approach was used to identify peptides and proteins of microbial origin in the spent permeate solution. Results showed a concomitant decrease of *Acinetobacter* and increase of *Lactococcus* during the course of depilation. A proteomic analysis of the depilation liquid at the end of the process identified peptides and proteins produced by the bacteria and fungi identified using both traditional culturing methods and culture-independent analysis. Lastly, results of a preliminary metabolomic study identified increases in specific metabolites known to have antimicrobial properties, especially against gram-negative bacteria. This paper describes the first steps made to understand the changes in the microbial community that potentially contribute to the preservation and depilatory phenomena of this novel depilation process. Results of this analysis have identified the organisms most likely to be responsible for depilation, and suggest a mechanism for both preservation and depilation that could lead the leather industry towards an environmentally friendly process.

5.2 Materials and Methods

5.2.1 Chemicals, materials, and kits

All sheepskins used were collected from a local freezing works (Ovation Ltd, Feilding, NZ). The unwashed skins were transported to the New Zealand Leather & Shoe Research Association (LASRA) and the flesh removed using the fleshing machine (Rizzi, PI, Italy). Three pieces of sheepskin approximately 15×8 cm were cut from the official sampling position (OSP) of three different animals and processed. For simplicity, the artificial whey permeate solution (4.5 % (w/v) lactose, 0.0035 % (w/v) CaCl_2 , 0.0045 % (w/v) NaCl, 0.14 % (w/v) KCl, and 0.05 % lactic acid (v/v)), will be referred to as permeate solution in this paper.

Chemicals were purchased from Sigma-Aldrich (St. Louis, MO, USA) except for the followings: tryptone soya broth (TSB), M17 broth, and malt extract broth were purchased from Oxoid™ (Hampshire, United Kingdom). Wilson’s media was made up according to Wilson *et al.* (1969)¹⁹. Luria broth (LB) and the Qubit dsDNA HS assay kit were purchased from Invitrogen. *Lactobacilli* MRS broth was purchased from Neogen® (Lansing, MI, USA). Phusion® DNA polymerase and buffers were purchased from New England BioLabs (Ipswich, MA, USA). The DNeasy® PowerSoil® kit was purchased from Qiagen (Hilden, Germany). Mass spectrometry grade water, acetonitrile (MeCN), formic acid, and trifluoroacetic acid (TFA) were purchased from Fisher Scientific (Fair Lawn, NJ, USA). Oligonucleotide primers were purchased from Integrated DNA Technologies (Singapore) and are listed in Table 1.

Table 1: Oligonucleotide primers used in this paper.

Primer name	Sequence (5' - 3')	Target gene	Amplicon length (bp)	Literature reference
Illumina-index-f	TCGTCGGCAGCGTCAGATGTGTATAAGAGACAG			20
Illumina-index-r	GTCTCGTGGGCTCGGAGATGTGTATAAGAGACAG			
S-D-Bact-0341-b-S-17	CCTACGGGNGGCWGCAG	V3-V4 region	465	21
S-D-Bact-0785-a-A-21	GACTACHVGGGTATCTAATCC	of 16S rDNA		
5.8S-FUN	AACTTTYRRCAAYGGATCWCT	ITS2 region	267 - 511	22
ITS4-FUN	AGCCTCCGCTTATTGATATGCTTAART	of rDNA		

5.2.2 Metagenomic analysis of the microbial community throughout the permeate depilation of sheepskin.

5.2.2.1 Amplicon sequencing sample preparation

Three pieces of unwashed fresh sheepskin from the OSP region from three separate animals were used in this experiment. Each piece of skin was cut into two equal parts and subjected to a different treatment: one was incubated in $1 \times$ sterilised phosphate buffered saline (PBS, 137 mM NaCl, 2.7 mM KCl, 8 mM Na₂HPO₄, and 2 mM KH₂PO₄) overnight to sample the sheepskin microbiome, at time zero, while the other was incubated in sterilised permeate for the duration of the depilation treatment. All six samples were incubated at room temperature (20 – 25 °C) in sterilised glass containers. Five (5) mL of liquid from the samples incubated with permeate were collected in a biohazard hood at 8, 16, 24, 32, 40, 48, 56, 64, and 72 hours when the wool could be easily removed with gentle thumb pressure. The samples in PBS were disposed of after \sim 15 hours. A negative environmental control (sterile water at time zero) was included in the analysis to test for possible environmental contamination. Microbial gDNA extraction was carried out using the DNeasy[®] PowerSoil[®] Kit (Qiagen) according to the manufacturer’s instructions. Partial 16S rRNA and ITS gene-encoding sequences were amplified using sets of oligonucleotides, S-D-Bact-0341-b-S-17/S-D-Bact-0785-a-A-21 and 5.8S-FUN/ITS4-FUN, flanked by Illumina adapter overhang sequences (Illumina-index-f/Illumina-index-r) (Table 1). The PCR conditions are listed in Table S1. The amplified DNA was quantified using a Qubit dsDNA HS assay kit (Invitrogen). Index PCR and sequencing was outsourced to the Massey Genome Service (MGS) and prepared according to the 16S rRNA metagenomic sequencing library preparation protocol (part no. 15044223 Rev. B; Illumina)²⁰. Sequencing was carried out in one lane on the Illumina MiSeq platform and generated 250 bp paired-end sequence reads.

5.2.2.2 Bioinformatics and statistical analysis

The 16S rRNA and ITS gene-encoding sequences obtained were analysed using the Quantitative Insights Into Microbial Ecology bioinformatics pipeline, QIIME2 (version 2020.8; <https://view.qiime2.org/>)²³. The adaptor and primer sequences were removed using the cutadapt²⁴ plugin, and the resulting reads were denoised using the DADA2 pipeline which also removed PhiX contamination, trimmed the reads, removed chimeras, and dereplicated identical sequences²⁵. Representative sequences (rep-seqs) and their abundances were extracted using the feature-table²⁶ plugin, then filtered using the *feature-table filter-features* method, which removed

rep-seqs that appeared in less than two samples, as well as those with a total frequency abundance less than 50 across all samples. The resulting rep-seqs and feature table files were then merged for downstream analysis within QIIME2. Biological replicates (*i.e.* OSP1, OSP2, and OSP3) from the same timepoint were grouped using the *feature-table group* function using the 'sum' mode to combine the frequencies across all bio-reps. Bacterial taxonomic classification was assigned using a trained SILVA²⁷ database (version 138.1 SSU; clustered at 99 % similarity) which is specific for the V3/V4 16S rRNA region. Fungal taxonomic classification was assigned using the UNITE²⁸ database (QIIME release version 8.2, full reference sequence, including global and 97 % singletons). All taxonomic classifications were implemented within QIIME2 and assigned using the naïve Bayesian algorithm, developed for the QIIME2 plugin *sklearn classifier*. For phylogenetic diversity analysis, sequences were aligned using the MAFFT²⁹ plugin. The 16S rDNA feature table was rarefied to a sampling depth of 23,274, which retained 28.23 % (2,225,728) of sequences and all 27 samples. The ITS rDNA feature table was rarefied to a sampling depth of 33,802 which retained 16.97 % (845,050) of sequences and 25 out of 27 samples. The sampling depth was selected based on the maximum depth that retained most samples for analysis. Alpha diversity (Shannon's index, observed amplicon sequence variants (ASVs), Pielou's evenness) and beta diversity (Bray-Curtis distance) matrices were calculated using the QIIME2 *q2*-diversity plugin, and principle coordinate analysis (PCoA) plots were generated using Emperor³⁰. Group significance of alpha diversity indexes was calculated using a one-way ANOVA followed by a post hoc Tukey-Kramer test. Group significance of beta diversity indexes was calculated using QIIME2 permutational multivariate analysis of variance (PERMANOVA). Differential abundance between timepoint groups at the genus and species level was tested using Analysis of Composition of Microbes (ANCOM)³¹ with manual NCBI blastn annotation. ANCOM performs group-wise comparisons of the relative abundance of a taxon by applying statistical tests on data transformed by Aitchison's log-ratio of abundance for each taxon relative to the abundance of all remaining taxa one at a time. The W-value generated by ANCOM shows the count of the number of sub-hypotheses (Aitchison's log-ratio) of a chosen taxon that are significantly different across all taxa, and the F-statistic (centred log ratio, clr) measures the significance of that difference for the chosen taxon between the study groups.

5.2.3 Proteomic analysis of the permeate used to depilate sheepskin

After depilation of the three sheepskin samples was complete, 15 mL samples of permeate were taken from each and used for proteomic analysis. After $4,700 \times g$ at $4\text{ }^{\circ}\text{C}$ for 20 minutes, two (2) mL of the supernatant was passed through a 2 kDa centrifugal spin filter and desalted by passing through 8 mL of H_2O . The retentate was lyophilised and the resulting powder solubilised in 200 μL of digestion buffer (50 mM Tris-HCl, 10 mM CaCl_2 , 40 % MeCN, pH 8.0), then sonicated for 10 minutes. Twenty-five (25) μL of the reconstituted sample was taken for *in-situ* tryptic digestion. Briefly, the sample was diluted with an equal volume of digestion buffer (without MeCN) and mixed with 20 mM dithiothreitol (DTT) and incubated at $50\text{ }^{\circ}\text{C}$ for an hour then alkylated with 20 mM iodoacetamide for another hour at room temperature in the dark. The samples were digested at $37\text{ }^{\circ}\text{C}$ for 16 hours with 1 μg SOLu-Trypsin (Sigma-Aldrich) and the reaction stopped by the addition of formic acid (to a final concentration of 0.2 % (v/v)). The samples were concentrated using vacuum centrifugation to $\sim 30\text{ }\mu\text{L}$ then centrifuged at $17,000 \times g$ for 20 minutes at $4\text{ }^{\circ}\text{C}$, and 20 μL transferred from the surface into a clean MS sample vial and kept at $4\text{ }^{\circ}\text{C}$ until use.

MS samples were separated by reversed-phase nano-LC (Thermo ScientificTM) using a 50 cm PepMapTM 300 C_{18} LC column (Thermo ScientificTM). Eluted peptides were analysed by mass spectrometry (Q ExactiveTM Plus Hybrid Quadrupole-OrbitrapTM, with a Nano Flex ion source, Thermo Fisher Scientific, Bremen, Germany) using data-dependent tandem MS acquisition. Details of the chromatographic and mass spectrometry settings are listed in Tables S2 and S3. The raw data files were processed using Proteome DiscovererTM version 2.5. The search parameters applied in the database searches and the databases used are listed in Tables S4 and S5. The reverse database search option was used as a filter to satisfy a false discovery rate (FDR) of 1 %.

5.2.4 Metabolomic analysis of the permeate used to depilate sheepskin

After the sheepskin was depilated, one (1) mL of the final permeate solution from each skin sample was collected and used for metabolomic analysis. One (1) mL of permeate was centrifuged at $13,000 \times g$ at $4\text{ }^{\circ}\text{C}$ for 20 minutes. Four hundred (400) μL of ice-cold methanol was added to 600 μL of the centrifuged supernatant and vigorously vortexed for 30 seconds then incubated at $-20\text{ }^{\circ}\text{C}$ overnight. The

precipitated material was removed by centrifugation at $13,000 \times g$ at $4\text{ }^{\circ}\text{C}$ for 20 minutes, and the supernatant immediately transferred to LoBind tubes. Samples were concentrated approximately four times using vacuum centrifugation and $40\text{ }\mu\text{L}$ transferred into a clean MS vial.

The compounds were separated by two types of chromatography, reversed-phase, and hydrophilic interaction liquid chromatography (HILIC) in both positive and negative ionisation modes. Details of the liquid chromatography configuration are listed in Table S6. Eluted compounds were analysed by mass spectrometry (Q ExactiveTM Focus with a HESI-II ion source, Thermo Fisher Scientific, Bremen, Germany) using data-dependent tandem MS acquisition. Details for the mass spectrometry settings are listed in Table S7. The raw data files were processed using Compound DiscovererTM version 2.1 SP1 (Thermo Fisher Scientific, USA).

5.3 Results and discussion

Depilation of sheepskin using permeate is a process that has the potential to provide an environmentally friendly alternative to conventional sodium sulfide depilation. Culturing experiments using samples of permeate incubated with sheepskin, identified 22 bacterial and six fungal species by the time the wool could be easily removed (Chapter 3, Tables 4 and 5). However, to monitor the changes in microbial diversity throughout depilation, and to identify any low abundance or unculturable microorganisms, amplicon sequencing analysis was carried out. Illumina sequencing of the 16S rDNA of the samples taken from nine (9) timepoints during the depilation treatment produced a total of 5,175,727 reads with an average of 191,694 reads per sample. For ITS rDNA amplicons there were 7,025,857 reads, with an average of 260,217 per sample. The number of reads remaining after DADA2 processing was 2,239,230 for the 16S rRNA gene region and 5,394,192 for the ITS gene region (Tables S8 and S9). A total of 325 amplicon sequence variants (ASVs) were identified for Bacteria and 307 for Fungi after read criteria filtering.

5.3.1 The microbial diversity in permeate during sheepskin depilation

Evaluation of the bacterial alpha diversity, *i.e.*, species diversity within each sample, was carried out initially by construction of rarefaction curves that represent the number of ASVs obtained from 10 sub-samplings of the total read

pool. Rarefaction curves showed that sampling depth for each sample reached saturation, meaning that no new ASVs would be discovered after 23,274 reads (Fig. S1a). The Shannon diversity index (H) is commonly used to characterise species diversity in a microbial community³². It considers both the richness (number of taxa observed in the community without regard to their frequencies) and evenness (distribution of frequencies of the taxa) to measure diversity. As a result, a larger number of taxa increases diversity, and similarly, an increase in the uniformity of taxa distribution also increases diversity³³.

Based on the Shannon index (H), the samples from different timepoints are clustered into three groups: (a) 0 - 16 hours, (b) 24- 32 hours, and (c) 40 - 64 hours, which shows there is a statistically significant successive increase in bacterial diversity during the depilation process (one-way ANOVA p -value < 0.01 , followed by a Tukey-Kramer post hoc test, $q_{\text{test}} > q_{\text{critical}}$; Fig. 1a, Table S10). However, to attribute the increase in alpha diversity to richness, or evenness, or both, observed ASVs and Pielou's evenness index were incorporated into this analysis. Similar to the results from the Shannon's diversity index, both of the observed ASVs and Pielou's evenness index suggested that as depilation progressed, the richness of the bacterial species increased (Fig. S1) and the abundances of the bacterial community became more even, *i.e.* the dominant bacteria at the beginning of the process became outnumbered by other species (Fig. S2).

Microbial taxonomic profiles obtained at the genus level were used to calculate the beta diversity analysis using the Bray-Curtis distance matrix as shown by a principal coordinate analysis (PCoA) plot (Fig. 1b). The PCoA plot showed clustering of samples based on incubation time, with the same grouping patterns as shown by the Shannon's diversity index; 0 - 16 hours, 24 - 32 hours, and 40 - 64 hours. Together, these results show that the microbial community composition experienced a significant shift between 16 hours and 24 hours, and again between 32 and 40 hours. Coincidentally, these three timespans were related to the change in pH of the depilation solution, where the pH dropped from 6.0 to 5.0 between 16 - 28 hours, and dropped again to 4.5 after 43 hours.

Contrary to the bacterial alpha biodiversity, there appeared to be no significant differences in the fungal diversity between the different timepoints with the Shannon's diversity index (Fig. 2a; one-way ANOVA p -value = 0.47, Table S11), also showing there were no significant changes in the ASV richness (Fig. S1b and Pielou's evenness index (Fig. S2b). The beta diversity analysis at the genus level, based on the Bray-Curtis index, represented in the PCoA plot showed no obvious

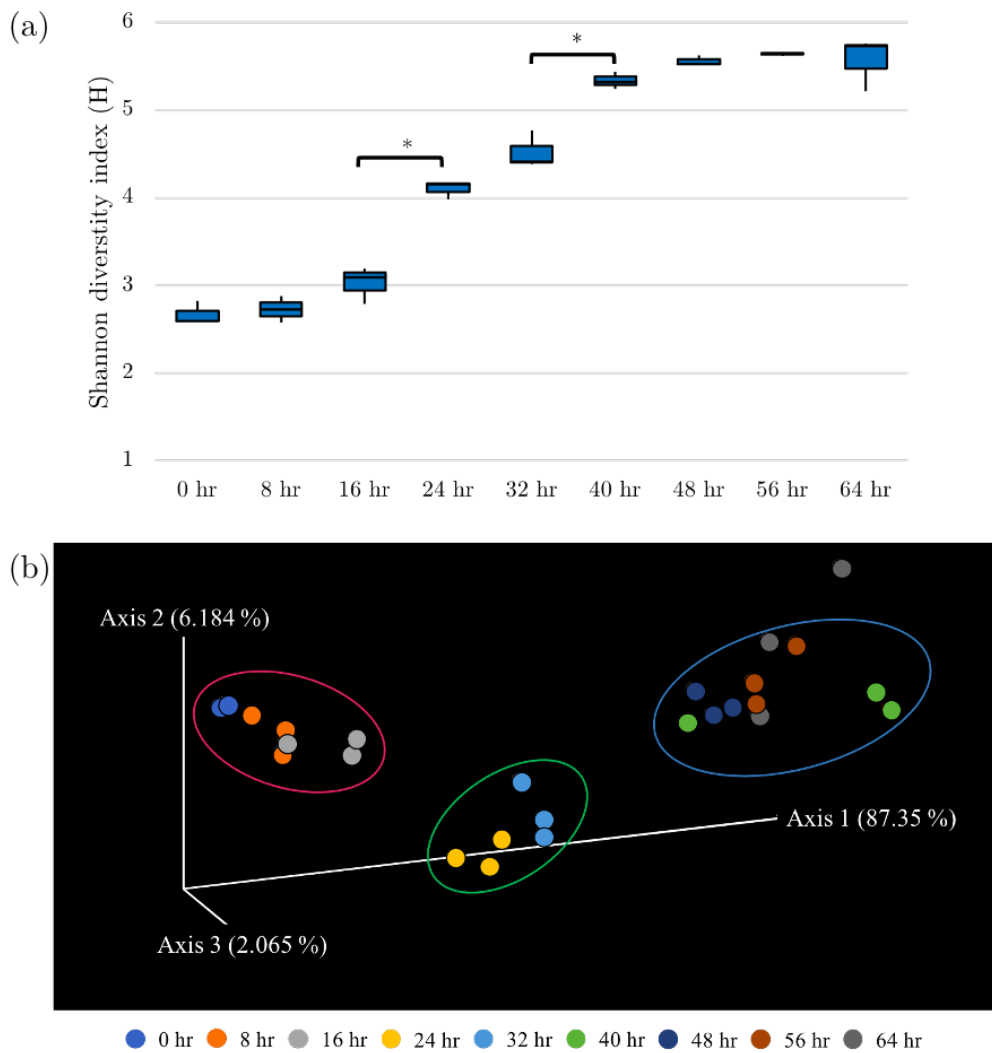


Figure 1: Alpha and beta diversity of bacteria from samples collected at different timepoints during permeate depilation of sheepskin. (a) The Shannon's diversity index obtained for each timepoint. (b) PCoA representation obtained using the Bray-Curtis index and the genus-level profiles. Samples are coloured based on incubation timepoints. *, p -value < 0.01.

clustering of samples according to timepoints (Fig. 2b). The results from the ITS alpha and beta diversity analysis suggested there was no clear association between the diversity of the fungi present during depilation and the different stages of the process.

5.3.2 Relative abundance of microbial taxa during permeate depilation

Analysis of the bacterial taxonomic profiles of the samples taken from various incubation timepoints showed the main phyla at all timepoints to be

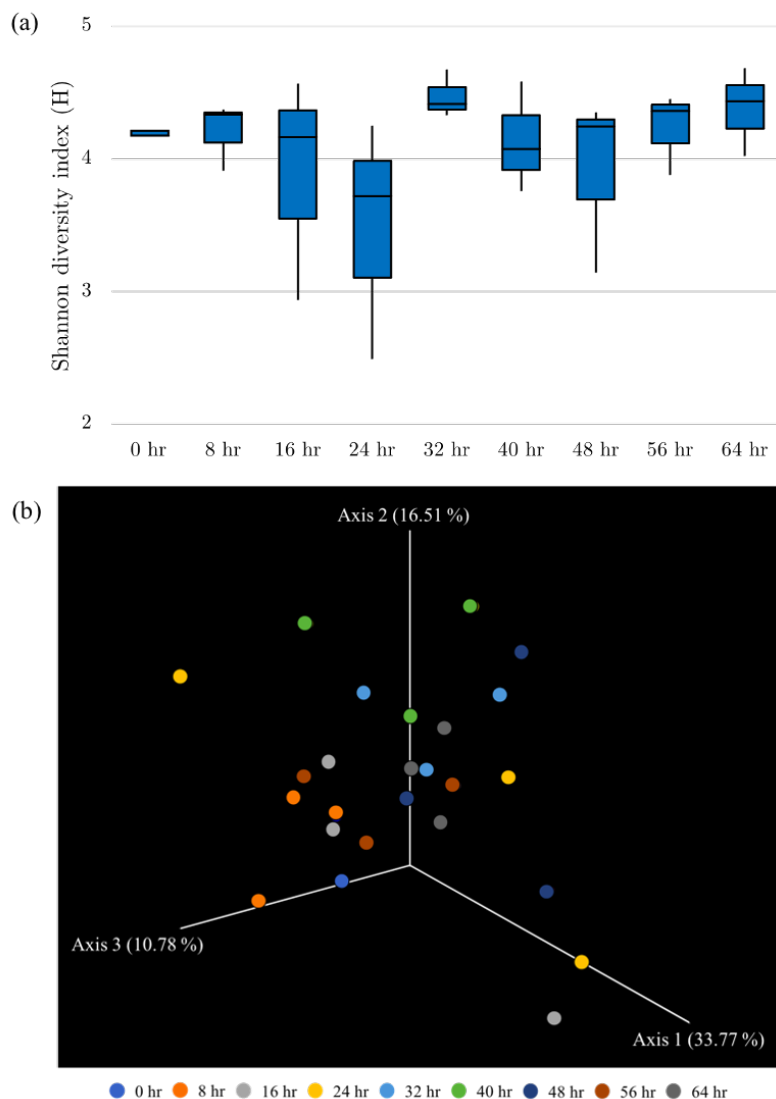


Figure 2: Alpha and beta diversity of fungi from samples collected at different timepoints during permeate depilation of sheepskin. (a) The Shannon's diversity index obtained for each timepoint. (b) PCoA representation obtained using the Bray-Curtis index and the genus level profiles. Samples are coloured based on incubation timepoints.

Proteobacteria, with relative abundance of 72 - 99 %, followed by Firmicutes, with relative abundance of 0.5 % - 24 % (Fig. S3a). The relative abundance of Proteobacteria was significantly depleted after 40 hours of incubation, and concurrently, the relative abundance of Firmicutes drastically increased 50-fold (Fig. S3a). At the genus level, the main Proteobacteria genera identified were *Acinetobacter*, *Aeromonas*, *Pseudomonas*, *Escherichia-Shigella*, and *Comamonas* (Fig. 3a), all commensal genera naturally found on sheepskin^{14,15,16}. Except for the genus *Acinetobacter*, the relative abundance of other genera identified increased overtime (Fig. 3a). *Aeromonas*, in particular, showed a steady increase in relative

abundance at the early stages of incubation (0 - 24 hours, 0.1 % - 25 %), as most species of this genera are able to utilise lactose as their carbon source³⁴.

Although the taxonomic resolution at the species level for *Acinetobacter* is challenging, and often requires information on other house-keeping genes (*e.g.* RNA polymerase subunit B, DNA gyrase subunit B), we managed to identify *Acinetobacter celticus* which is commonly found in the environment and *Acinetobacter lwoffii*, commonly found on skin (Fig. S4). As lactose is the main carbon source in permeate and *Acinetobacter* are non-lactose-fermenting bacteria, it was not unexpected that their relative abundance decreased from 90 % at the start of incubation to 25 % by the time the sheepskins were depilated. Although *Acinetobacter* can be cultured in TSB and LB media³⁵, they could not be cultured from the spent depilation media. It is therefore likely that none were viable at the completion of depilation. It should be remembered that the metagenomics analysis is based on DNA abundance and may originate from dead and lysed cells as well as live cells. Thus, although it is the best way to identify species that are or have been present in a sample, it does not measure viable cells. Several *Acinetobacter* species (*e.g.* *Acinetobacter baumannii*) are known to cause severe skin wound infections and have become antibiotic resistant³⁶, but there are no reports of them being involved in the putrefaction in animal skins, most likely due to lack of research in this area. They are, however, known dairy and meat spoilage microorganisms, due to their ability to produce proteolytic and lipolytic enzymes³⁷. Therefore, it is possible that the presence of *Acinetobacter* on wet or damp skins could result in enzymes secretion and the accompanying break down of the skin structure, although this was not observed in this study.

Bacterial species that are known to be involved in the putrefaction of animal skins and hides, those belonging to the *Escherichia*, *Hafnia*, *Proteus*, and *Shewanella* genera, were also identified in the depilation liquid^{12,15,17}. However, their relative abundances were low, and each accounted for less than 5 % of the total by the end of depilation (Fig. 3a). Unknown bacterial species of the *Pseudomonas* genus were found with a relative abundance of approximately 10 % by the end of the depilation treatment. Specific *Pseudomonas* species, such as *Pseudomonas fluorescens* and *Pseudomonas putida* are known to contribute to the degradation of animal skins¹⁷. Although the phylogeny analysis identified some *Pseudomonas* species, the partial 16S rRNA gene sequences do not provide enough resolution for reliable identification at the species level. A follow-up investigation of the bacteria present on the skins after depilation at 5-, 8- and 14-weeks post-incubation with permeate, when the skins

had rotted, showed *Pseudomonas* to be the most dominant bacteria present in the liquid with a relative abundance of 50 – 80 % (Fig. S5). This suggested that despite the presence of some skin putrefying bacteria in the permeate-skin 'environment', their low abundance (10 % *vs.* 50 %), did not cause observable degradation during the course of depilation (3 - 4 days).

Of the predominant Firmicutes genera identified, (*Lactococcus*, *Enterococcus*, and *Propionispira*), the relative abundance of *Lactococcus* substantially increased 5-fold after 40 hours compared to previous timepoints (3.5 % - 18.2 %, Fig. 3a). At the species level, *Lactococcus raffinolactis* and *Lactococcus lactis* were the most abundant lactococci identified, making up 25 % of the bacteria at the end of the depilation treatment. The fact that this population contained viable cells was confirmed by culture at the end of the depilation trial, which positively identified *Lactococcus lactis*, *Lactococcus lactis* subsp. *cremoris* and *Lactococcus lactis* subsp. *lactis* (Chapter 3, Table 4). Lactococci are lactose-fermenters that utilise lactose in their energy production pathway, produce lactate, and eventually lactic acid which increases the acidity of their environment. They are also known to secrete bacteriocins many of which act on a wide variety of bacteria, both gram-negative and gram-positive³⁸. We hypothesise that the reduction in the pH of the depilation liquid to pH 4.5 during depilation, inhibited the growth of species such as *Acinetobacter* and *Pseudomonas* and that the antimicrobial substances secreted by them contributed to controlling the microbial diversity. Nisin, is a bacteriocin produced by *Lactococcus lactis* that is widely used in the food industry to prevent microbial spoilage³⁸. However, an experiment in which nisin (in PBS) was added to the skins showed that this single bacteriocin cannot prevent skin putrefaction, indicating that the mechanism of preservation is more complex.

Analysis of Composition of Microbiomes (ANCOM) was carried out to identify genera/species that were differentially abundant between the nine timepoints. ANCOM analysis of the 16S rRNA gene-encoding sequences showed 11 genera (of 76) to be differentially abundant throughout depilation (Fig. 4). Using SILVA database taxonomy and manual annotation with NCBI blastn against nucleotide collection (nr/nt) databases identified eight genera. Except for *Lactococcus*, *Propionispira*, *Citrobacter*, *Escherichia-Shigella*, and U. m. of Enterobacteriaceae, all other genera that were differentially abundant had a relative abundance of less than 1 % throughout the whole depilation treatment (Fig. 3). The differential abundance of the genera *Corynebacterium*, and the U. m. of both the Rhizobiaceae and Arcobacteraceae families was significantly decreased, whereas the remaining eight genera increased in abundance by the end of depilation (Fig. S6). As

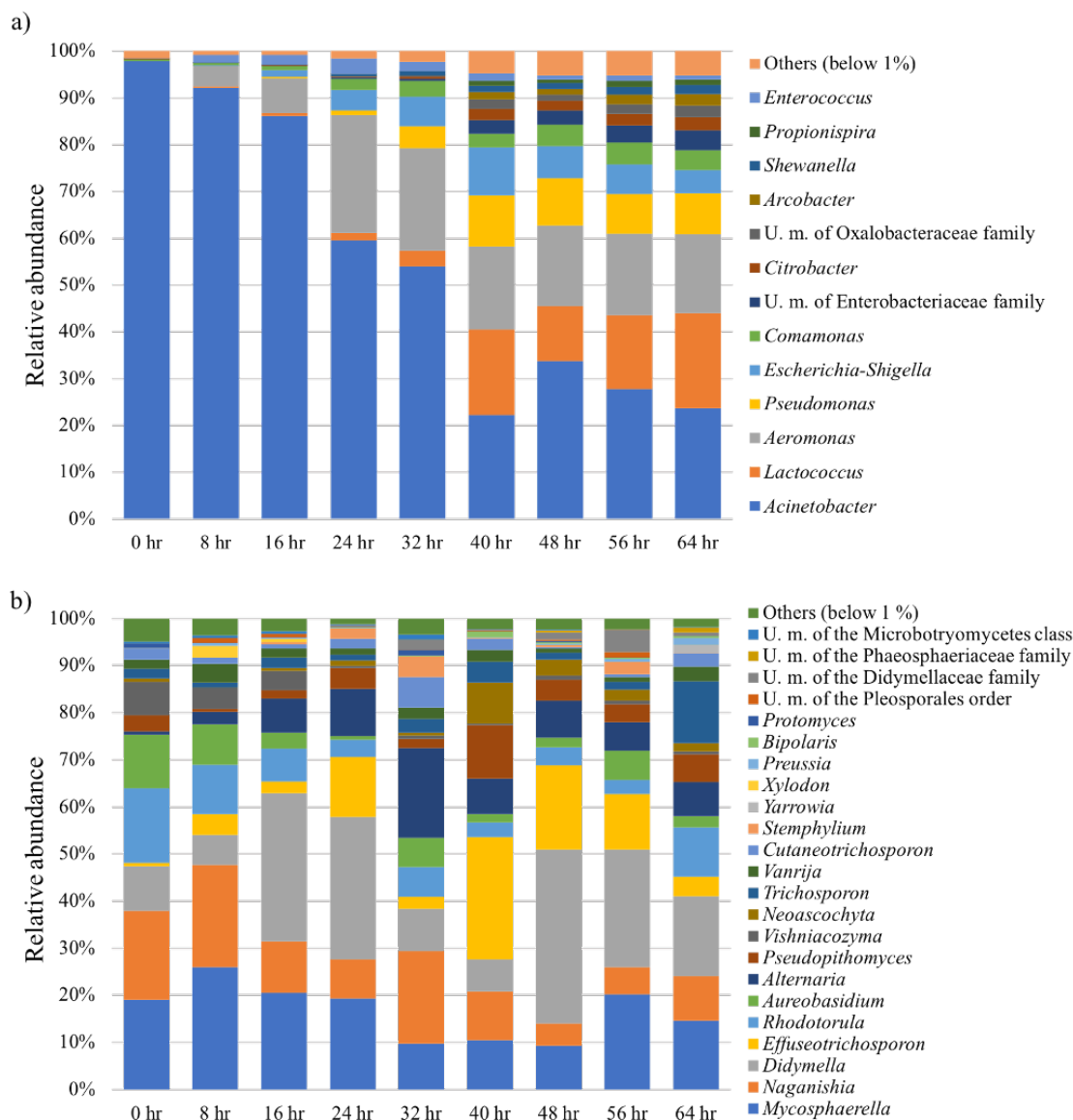


Figure 3: Bar plot showing the distribution of microbial genera over the time course of permeate depilation of sheepskin. (a) Distribution of bacterial genera. (b) Distribution of fungal genera. U. m., unclassified member. Others, genera with a relative abundance below 1 %. The others list can be found in Table S12

taxonomy assignments at the species level are not accurate when a part of a phylogenetic marker is used, we did not consider differences at the species level.

Analysis of the ITS encoding-gene taxonomic profile of the fungi microbiome at nine timepoints throughout permeate depilation of sheepskin showed that it consists of two main phyla, Ascomycota ($\sim 55\%$) and Basidiomycota ($\sim 45\%$) (Fig. S3b). There were 63 genera identified. Of these, *Mycosphaerella*, *Naganishia*, *Didymella*, *Effuseotrichosporon* and *Rhodotorula* were the most abundant. There were, however, no obvious trends in the relative abundance of either fungal genera over the course

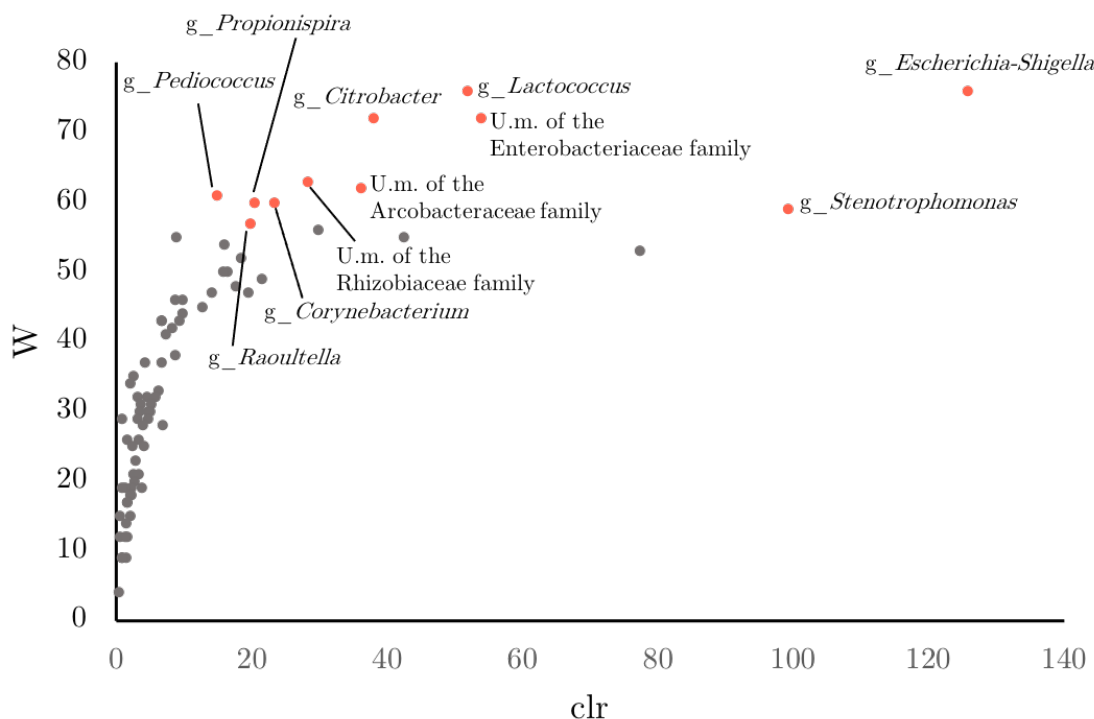


Figure 4: Volcano plots of differentially expressed bacterial ASVs over the different timepoints of permeate depilation at genus level. ANCOM analysis was performed to analyse statistical significance. Statistically significant ASVs are coloured in orange. W, W statistics; clr, centered log-ratio, F-statistics.

of depilation (Fig. 3b) and ANCOM analysis at the genus level showed there were no ASVs that showed significant changes in abundance (Fig. S7). Putrefaction of raw skins and hides is more commonly associated with bacteria, while fungi are more commonly involved in damage to leather products¹⁷. It has, however been shown that in salted and semi-processed leather products, such as pickled skins, fungal deteriogens do damage the skins. Examples of these include *Alternaria spp.*, *Aspergillus spp.*, *Aureobasidium spp.*, *Cladosporium spp.*, *Fusarium spp.*, *Penicillium spp.*, *Rhizopus spp.*, and *Trichoderma spp.*^{13,39}.

In this analysis, we identified only two of the fungi known to damage leather products: *Alternaria alternata* (increased in relative abundance, 1 % to 7.4 %) and *Aureobasidium pullans* (decreased in relative abundance, 11.4 % to 2.4 %). Metabarcoding analysis of the ITS gene region identified 63 genera, whereas only 5 were cultured from the depilation media, all of which were identified in the metabarcoding analysis except for *Pichia*. *Geotrichum candidum* and *Yarrowia lipolytica* were most frequently identified by culture (Chapter 3, Table 5), however, their relative abundance at 64 hours was less than 1 % for *G. candidum* and 2 %

for *Y. lipolytica*. To verify the presence of these two fungi, a proteomic experiment was done on permeate that was used to depilate sheepskin. Mass spectrometry peptide spectrum was searched against the NCBI protein database of the top 10 abundant fungi identified in the metagenomics analysis (*i.e.* *Alternaria alternata*, *Aureobasidium pullulans*, *Didymella exigua*, *Rhodotorula graminis*, *etc.*) along with the two (*G. candidum* and *Y. lipolytica*). Proteins of both *G. candidum* and *Y. lipolytica*, along with several other fungi were identified (Table S15) which substantiated the presence of these fungi in the depilation liquid. Similarly, the search against bacterial protein database also identified proteins belonging to the bacteria identified in both culture (Chapter 3) and metagenomics experiments (Tables S13 and S14). The differences in the dominant fungi from the culturing and metagenomics results are difficult to explain but may reflect the efficiency of DNA extraction from a solution or from a colony of these cells, as well as the presence of non-viable cells or spores. They also show the importance of using both culture and culture-independent methods in cases where a process is being investigated, rather than a study of diversity.

The concomitant changes in the dominant bacteria genera over the course of depilation could be the results of (a) the carbon source availability of the depilation media (*i.e.* lactose and lactic acid at the beginning of the process), (b) the rock-paper-scissors (RPS) model of the non-transitive competition dynamics of bacteria^{40,41}, (c) the reduction in pH caused by the release of lactic and other organic acids by the bacterial population and (d) macronutrient supplementation of the depilation media as skin depilated and skin proteins, lipids and complex carbohydrates leached into the liquid medium. At the beginning of the depilation treatment (0 - 16 hours), the skin bacteria *Acinetobacter* were the most abundant species detected. However, as lactose cannot be utilised by most *Acinetobacter* species, its relative abundance decreased. The inability to culture these bacteria suggests that either dead or viable but non-culturable (VBNC) *Acinetobacter* cells are present at the end of the process⁴²(Chapter 3, Table 4). At the same time, Firmicutes, including *Lactococcus*, *Lactobacillus* and *Enterococcus* increased in abundance from 24 - 40 hours.

The skin-permeate 'environment' together with microorganisms form a complex ecology. To survive, microorganisms secrete antimicrobial substances to compete for limited resources, in which the interaction network resembles the game of rock-paper-scissors^{40,41}. In this game - the antimicrobial substance-producing bacteria outcompete others that are sensitive to those substances (by bactericidal

and bacteriostatic effects); in turn the sensitive bacteria outcompete other species that are resistant to the antimicrobial compounds (by growth-rate advantage), and finally bacteriocin resistant species outcompete those producing the toxins through acquired immunity. It is estimated that 99 % of all bacteria produce antimicrobial compounds, whether they are bacteriocins or secondary metabolites⁴³. Lactic acid bacteria (LAB), in particular, are known to be bacteriocin producers and due to their involvement in food fermentation, many have been identified and characterised³⁸.

A proteomic analysis performed on permeate solution that depilated sheepskins identified peptides belonging to the bacteriocins lactococcin B, sakacin A (= curvacin A), and a few other bacteriocins (Table 2). Lactococcin B and sakacin A are produced by *Lactococcus lactis* subsp. *cremoris* and *Latilactobacillus sakei* (basonym: *Lactobacillus sakei*) or *Latilactobacillus curvatus* (basonym: *Lactobacillus curvatus*), respectively. These bacteria were identified both in the culture and metagenome analysis. It is not unexpected that nisin, produced by *Lactococcus lactis* subsp. *lactis* was not identified as it is highly modified and resistant to trypsin proteolysis. Furthermore, the intact molecule, MWt 3,354 Da, requires specific fragmentation conditions to produce identifiable fragmentation ions⁴⁴. Other lantibiotics and modified bacteriocins, of which there are many, would similarly not be identified in a general proteomic analysis as they are commonly resistant to proteolysis. As reported earlier, the addition of nisin to a skin sample incubating in PBS did not prevent or slow putrefaction of the skin, confirming that it is the complex interaction of many different factors that preserves the skin structure while promoting loosening of the hair fibre in the hair follicle. A preliminary metabolomic analysis was also conducted to identify the presence of antimicrobial secondary metabolites in the same permeate solution at the completion of depilation. Compounds identified that have been reported to have antimicrobial properties are listed in Table S16. Although a handful of these were detected, the studies were only preliminary and require validation with further analysis. An investigation into the production and secretion of these metabolites by the microbes identified in this study, and inhibition assays are needed to understand their real effects.

It was shown that as skin immersed in the permeate solution, small amounts of protein (*e.g.* collagens and keratin), water-soluble sugars (*e.g.* hyaluronic acid and sulfated-glycosaminoglycans), and lipids leaked into the solution⁴⁵. Those macromolecules act as nutrients for most bacterial species and it was therefore not

Table 2: Bacteriocin peptides identified in the proteomic analysis of permeate upon completion of depilation.

Bacteriocin	NCBI blastp top hit sequence ID	Producing microorganism	Antimicrobial action	# PSMs	# Unique peptides	Peptide sequence identified	Reference
Lactococcin-B	WP_015081788.1	<i>Lactococcus lactis subsp. cremoris</i>	<i>L. lactis</i> & <i>Lactobacilli</i>	15	2	TGKTICKQTID TASYTFGVMAE GWGKTFH	Parada <i>et al.</i> (2007), Venema <i>et al.</i> (1993)
Sakacin-A (=Curvacin-A)	WP_032488606.1 2A2B_A	<i>Latilactobacillus sakei/curvatus</i>	<i>Listeria monocytogenes</i> & <i>Enterococcus faecalis</i>	5	2	KCWVNRGEAT QSIHGGMISGWA SGLAGM	Parada <i>et al.</i> (2007), Tichaczek <i>et al.</i> (1993)
Colicin-Ib	MWL96891.1 SUJ17653.1	<i>Escherichia coli</i>	Other <i>E. coli</i> strains	3	2	NALTRAEQQLT QQKNTPDGK & ITTSVIDNRRAN LNYLLTHSGLD YK	Cascales <i>et al.</i> (2007)
Propionicin T1	AAG24829.1	<i>Propionibacterium thoenii</i>	<i>Propionibacterium</i> & <i>Lactobacillus sake</i>	3	1	LDCNNAPDKTS VWAKPKVMVS VHCLVGQPR	Faye <i>et al.</i> (2000)

unexpected that the relative abundance of almost all bacteria identified in the study, except for *Acinetobacter*, increased during depilation (Fig. 3a). The release of these of macromolecules was most likely due to the action of lipases and proteases secreted by microorganisms, and was responsible for loosening the wool in the follicle, allowing it to be removed. It is interesting that enzymes produced by *Pseudomonas fluorescens* have been used to enhance depilation and the removal of non-collagenous proteins in skins by the leather industry^{4,46}. In addition, although the fungi *Yarrowia lipolytica* and *Geotrichum candidum* were in very low relative abundances in the metagenomic study, they were the main fungal species identified in the culturing experiments (Chapter 3, Table 5). Both of these are commonly used in the food industry, specifically, for the cheese-making, due to their secretion of extracellular proteases and lipases^{47,48,49}. Even though, proteomic analysis on the depilation liquid did not identify any microbial extracellular enzymes, future experiments should include proteolytic and lipolytic activity assays with the supernatant of fungal cultures or a combination of bacterial and fungal cultures.

Conclusions and future perspectives.

Previous work on culture and the culture-independent methods used in this study have provided an understanding of the changes in microbial community for a novel sheepskin depilation process. The use of metabarcoding analysis complimented the findings from culture where only viable and culturable cells were identified. This metagenomic study showed the changes in the relative abundance of the microorganisms throughout the process and also identified microorganisms that were not cultured from previous experiments. The significant increase in the

relative abundance of *Lactococcus* species was highlighted suggesting the secretion of lactococcal antimicrobial substances could potentially be a mechanism to preserve skin. The proteomic analysis on the permeate that depilated sheepskin did not identify any wide-spectrum bacteriocin, possibly due to the limitations of the bacteriocin and traditional databases, and the difficulty in using bottom-up proteomics to identify small, heavily modified peptides that are resistant to proteolysis. Future experiments should include the use of an extended number of culture media and conditions to isolate all viable microorganisms during depilation experiments. To validate the results skin sterilised using gamma irradiation could then be incubated with pure cultures, or a mixture of cultures to narrow down the conditions needed for skin preservation. It may then be possible to isolate the molecules responsible for the preservation of the skin, as well as the enzymes responsible for its depilation.

Acknowledgements

This study is supported by the Massey University Agricultural and Life Sciences Trust (Project number RM3000028979) and New Zealand Leather and Shoe Research Association (LASRA) through the Ministry of Business, Innovation and Employment (MBIE) grant number LSRX1801. The funders had no role in study design, data collection and interpretation, or the decision to submit the work for publication. The authors thank LASRA (Palmerston North, New Zealand) for the supply of fresh sheepskins, and Mr. Lin Xiaoxiao from Massey Genome Service for the help with metagenomic sequencing, and New Zealand eScience Infrastructure (NeSI) for the use of high performance computing services for the analysis of metagenomic data.

Author contributions

GEN and DG designed the research and edited the manuscript. Y-HT conducted the experimental work, carried out the metagenomic analyses and wrote the manuscript. DG and MLP provided advice on metagenomic studies. TSL prepared the proteomic analysis samples of permeate and collected mass spectrometry data.

5.4 References

- [1] S. Dixit, A. Yadav, P. D. Dwivedi, and M. Das. Toxic hazards of leather industry and technologies to combat threat: a review. *J. Cleaner Prod.*, 87:39–49, 2015. ISSN 0959-6526. doi: <https://doi.org/10.1016/j.jclepro.2014.10.017>. URL <http://www.sciencedirect.com/science/article/pii/S0959652614010580>.
- [2] J. Kanagaraj, T. Senthivelan, R. C. Panda, and S. Kavitha. Eco-friendly waste management strategies for greener environment towards sustainable development in leather industry: a comprehensive review. *J. Cleaner Prod.*, 89:1–17, 2015. ISSN 0959-6526.
- [3] N. R. Kamini, C. Hemachander, J. G. S. Mala, and R. Puvanakrishnan. Microbial enzyme technology as an alternative to conventional chemicals in leather industry. *Curr. Sci. India*, 77(1):80–86, 1999. ISSN 00113891. URL <http://www.jstor.org/stable/24102916>.
- [4] N. Kandasamy, P. Velmurugan, Sundarvel A., R. J. Raghava, C. Bangaru, and T. Palanisamy. Eco-benign enzymatic dehairing of goatskins utilizing a protease from a *Pseudomonas fluorescens* species isolated from fish visceral waste. *J. Cleaner Prod.*, 25:27–33, 2012. ISSN 0959-6526. doi: <https://doi.org/10.1016/j.jclepro.2011.12.007>. URL <http://www.sciencedirect.com/science/article/pii/S0959652611005324>.
- [5] L. M. I. Lopéz, C. A. Viana, M. E. Errasti, M. L. Garro, J. E. Martegani, G. A. Mazzilli, C. D. T. Freitas, Í. M. S. Araújo, R. O. da Silva, and M. V. Ramos. Latex peptidases of *Calotropis procera* for dehairing of leather as an alternative to environmentally toxic sodium sulfide treatment. *Bioproc. Biosyst. Eng.*, 40(9): 1391–1398, 2017. ISSN 1615-7605. doi: 10.1007/s00449-017-1796-9. URL <https://doi.org/10.1007/s00449-017-1796-9>.
- [6] S. Sivasubramanian, B. Murali Manohar, A. Rajaram, and R. Puvanakrishnan. Ecofriendly lime and sulfide free enzymatic dehairing of skins and hides using a bacterial alkaline protease. *Chemosphere*, 70(6):1015–1024, 2008. ISSN 0045-6535. doi: <https://doi.org/10.1016/j.chemosphere.2007.09.036>. URL <http://www.sciencedirect.com/science/article/pii/S0045653507011605>.
- [7] P. Thanikaivelan, J. R. Rao, B. U. Nair, and T. Ramasami. Recent trends in leather making: processes, problems, and pathways. *Crit. Rev. Env. Sci. Tec.*, 35(1):37–79, 2005. ISSN 1064-3389. doi: 10.1080/10643380590521436. URL <https://doi.org/10.1080/10643380590521436>.
- [8] B. Wahyuntari and H. Hendrawati. Properties of an extracellular protease of *Bacillus megaterium* DSM 319 as depilating aid of hides. *Microbiology Indonesia*, 6(2):4–4, 2012. ISSN 2087-8575.

- [9] L. Schlosser, A. Hein, W. Keller, and E. Heidemann. Utilisation of a *Lactobacillus* culture in the beamhouse. *J. Soc. Leather Technol. Chem.*, 70:163–8, 1986. ISSN 0144-0322.
- [10] F. K. Lucke. Utilization of microbes to process and preserve meat. *Meat Sci.*, 56(2): 105–15, 2000. ISSN 0309-1740 (Print) 0309-1740.
- [11] R. Ramu, P. S. Shirahatti, A. T. Devi, and A. Prasad. Bacteriocins and their applications in food preservation. *Crit. Rev. Food Sci. Nutr.*, pages 00–00, 2015. ISSN 1040-8398. doi: 10.1080/10408398.2015.1020918. URL <https://doi.org/10.1080/10408398.2015.1020918>.
- [12] M. Falkiewicz-Dulík. *Leather and Leather Products*. ChemTec Publishing, 2015. ISBN 978-1-895198-87-4. doi: <https://doi.org/10.1016/B978-1-895198-87-4.50009-8>. URL <http://www.sciencedirect.com/science/article/pii/B9781895198874500098>.
- [13] A. Orlita. Microbial biodeterioration of leather and its control: a review. *Int. Biodeterior. Biodegrad.*, 53(3):157–163, 2004. ISSN 0964-8305. doi: [https://doi.org/10.1016/S0964-8305\(03\)00089-1](https://doi.org/10.1016/S0964-8305(03)00089-1). URL <https://www.sciencedirect.com/science/article/pii/S0964830503000891>.
- [14] T. A. Jackson, J. F. Pearson, S. D. Young, J. Armstrong, and M. O’Callaghan. Abundance and distribution of microbial populations in sheep fleece. *N. Z. J. Agric. Res.*, 45(1):49–55, 2002. ISSN 0028-8233.
- [15] H. A. A. Mohamed, G. M. Van Klink, and S. M. ElHassan. Damage caused by spoilage bacteria to the structure of cattle hides and sheep skins. *Int. J. Anim. Health Livestock Prod. Res.*, 2(1):39–56, 2016.
- [16] P. N. Shede, P. P. Kanekar, A. V. Polkade, P. K. Dhakephalkar, and S. S. Sarnaik. Bacterial succession on raw buffalo hide and their degradative activities during ambient storage. *Int. Biodeterior. Biodegrad.*, 62(1):65–74, 2008. ISSN 0964-8305. doi: <https://doi.org/10.1016/j.ibiod.2007.12.007>. URL <https://www.sciencedirect.com/science/article/pii/S0964830507001771>.
- [17] R. O. Oruko, J. O. Odiyo, and J. N. Edokpayi. The role of leather microbes in human health. In *Role of microbes in human health and diseases*. IntechOpen, 2019.
- [18] W. Frendrup. Hair-save unhairing methods in leather processing. Technical report, United Nations Industrial Development Organisation, 2000.
- [19] K. Wilson, A. A. Padhye, and J. W. Carmichael. Antifungal activity of *Walleimia ichthyophaga* (= *Hemispora stellata* Vuill. = *Torula epizoa* Corda). *Antonie van Leeuwenhoek*, 35(1):529–532, 1969. ISSN 1572-9699. doi: 10.1007/BF02219170. URL <https://doi.org/10.1007/BF02219170>.

- [20] P. C. R. Amplicon, P. C. R. Clean-Up, and P. C. R. Index. 16S Metagenomic Sequencing Library Preparation, 2013.
- [21] A. Klindworth, E. Pruesse, T. Schweer, J. Peplies, C. Quast, M. Horn, and F. O. Glockner. Evaluation of general 16S ribosomal RNA gene PCR primers for classical and next-generation sequencing-based diversity studies. *Nucleic Acids Res.*, 41(1):e1, 2013. ISSN 0305-1048. doi: 10.1093/nar/gks808.
- [22] D. L. Taylor, W. A. Walters, N. J. Lennon, J. Bochicchio, A. Krohn, J. G. Caporaso, and T. Pennanen. Accurate estimation of fungal diversity and abundance through improved lineage-specific primers optimized for Illumina amplicon sequencing. *Appl. Environ. Microbiol.*, 82(24):7217–7226, 2016. ISSN 0099-2240.
- [23] E. Bolyen, J. R. Rideout, M. R. Dillon, N. A. Bokulich, C. C. Abnet, G. A. Al-Ghalith, H. Alexander, E. J. Alm, M. Arumugam, F. Asnicar, Y. Bai, J. E. Bisanz, K. Bittinger, A. Brejnrod, C. J. Brislawn, C. T. Brown, B. J. Callahan, A. M. Caraballo-Rodríguez, J. Chase, E. K. Cope, R. Da Silva, C. Diener, P. C. Dorrestein, G. M. Douglas, D. M. Durall, C. Duvallet, C. F. Edwardson, M. Ernst, M. Estaki, J. Fouquier, J. M. Gauglitz, S. M. Gibbons, D. L. Gibson, A. Gonzalez, K. Gorlick, J. Guo, B. Hillmann, S. Holmes, H. Holste, C. Huttenhower, G. A. Huttley, S. Janssen, A. K. Jarmusch, L. Jiang, B. D. Kaehler, K. B. Kang, C. R. Keefe, P. Keim, S. T. Kelley, D. Knights, I. Koester, T. Kosciulek, J. Kreps, M. G. I. Langille, J. Lee, R. Ley, Y-X. Liu, E. Loftfield, C. Lozupone, M. Maher, C. Marotz, B. D. Martin, D. McDonald, L. J. McIver, A. V. Melnik, J. L. Metcalf, S. C. Morgan, J. T. Morton, A. T. Naimey, J. A. Navas-Molina, L. F. Nothias, S. B. Orchanian, T. Pearson, S. L. Peoples, D. Petras, M. L. Preuss, E. Pruesse, L. B. Rasmussen, A. Rivers, M. S. Robeson, P. Rosenthal, N. Segata, M. Shaffer, A. Shiffer, R. Sinha, S. J. Song, J. R. Spear, A. D. Swofford, L. R. Thompson, P. J. Torres, P. Trinh, A. Tripathi, P. J. Turnbaugh, S. Ul-Hasan, J. J. J. van der Hooft, F. Vargas, Y. Vázquez-Baeza, E. Vogtmann, M. von Hippel, W. Walters, et al. Reproducible, interactive, scalable and extensible microbiome data science using QIIME 2. *Nat. Biotechnol.*, 37(8):852–857, 2019. ISSN 1546-1696. doi: 10.1038/s41587-019-0209-9. URL <https://doi.org/10.1038/s41587-019-0209-9>.
- [24] M. Martin. Cutadapt removes adapter sequences from high-throughput sequencing reads. *EMBnet. journal*, 17(1):10–12, 2011. ISSN 2226-6089.
- [25] B. J. Callahan, P. J. McMurdie, M. J. Rosen, A. W. Han, A. J. Johnson, and S. P. Holmes. DADA2: high-resolution sample inference from Illumina amplicon data. *Nat. Methods*, 13(7):581–3, 2016. ISSN 1548-7091 (Print) 1548-7091. doi: 10.1038/nmeth.3869.
- [26] D. McDonald, J. C. Clemente, J. Kuczynski, J. R. Rideout, J. Stombaugh, D. Wendel, A. Wilke, S. Huse, J. Hufnagle, F. Meyer, R. Knight, and J. G. Caporaso. The biological observation matrix (BIOM) format or: how I learned to stop worrying

- and love the ome-ome. *GigaScience*, 1(1), 2012. ISSN 2047-217X. doi: 10.1186/2047-217X-1-7. URL <https://doi.org/10.1186/2047-217X-1-7>.
- [27] C. Quast, E. Pruesse, P. Yilmaz, J. Gerken, T. Schweer, P. Yarza, J. Peplies, and F. O. Glöckner. The SILVA ribosomal RNA gene database project: improved data processing and web-based tools. *Nucleic Acids Res.*, 41(D1):D590–D596, 2013. ISSN 0305-1048. doi: 10.1093/nar/gks1219. URL <https://doi.org/10.1093/nar/gks1219>.
- [28] K. Abarenkov, A. Zirk, T. Piirmann, R. Pöhönen, F. Ivanov, R. H. Nilsson, and U. Kõljalg. UNITE QIIME release for Fungi, 2020. URL <https://plutof.ut.ee/#/doi/10.15156/BIO/786385>.
- [29] K. Katoh and D. M. Standley. MAFFT multiple sequence alignment software version 7: improvements in performance and usability. *Mol. Biol. Evol.*, 30(4):772–780, 2013. ISSN 0737-4038. doi: 10.1093/molbev/mst010. URL <https://doi.org/10.1093/molbev/mst010>.
- [30] Y. Vázquez-Baeza, M. Pirrung, A. Gonzalez, and R. Knight. EMPeror: a tool for visualizing high-throughput microbial community data. *Gigascience*, 2(1):16, 2013. ISSN 2047-217X (Print) 2047-217x. doi: 10.1186/2047-217x-2-16.
- [31] S. Mandal, W. Van Treuren, R. A. White, M. Eggesbø, R. Knight, and S. D. Peddada. Analysis of composition of microbiomes: a novel method for studying microbial composition. *Microb. Ecol. Health Dis.*, 26(1):27663, 2015. ISSN null. doi: 10.3402/mehd.v26.27663. URL <https://www.tandfonline.com/doi/abs/10.3402/mehd.v26.27663>.
- [32] A. D. Willis. Rarefaction, alpha diversity, and statistics. *Front. Microbiol.*, 10(2407), 2019. ISSN 1664-302X. doi: 10.3389/fmicb.2019.02407. URL <https://www.frontiersin.org/article/10.3389/fmicb.2019.02407>.
- [33] B. D. Wagner, G. K. Grunwald, G. O. Zerbe, S. K. Mikulich-Gilbertson, C. E. Robertson, E. T. Zemanick, and J. K. Harris. On the use of diversity measures in longitudinal sequencing studies of microbial communities. *Front. Microbiol.*, 9(1037), 2018. ISSN 1664-302X. doi: 10.3389/fmicb.2018.01037. URL <https://www.frontiersin.org/article/10.3389/fmicb.2018.01037>.
- [34] S. L. Percival and D. W. Williams. *Aeromonas*, pages 49–64. Academic Press, London, 2014. ISBN 978-0-12-415846-7. doi: <https://doi.org/10.1016/B978-0-12-415846-7.00003-2>. URL <https://www.sciencedirect.com/science/article/pii/B9780124158467000032>.
- [35] A. C. Jacobs and D. V. Zurawski. Laboratory maintenance of *Acinetobacter baumannii*. *Curr. Protoc. Microbiol.*, 35:6g.1.1–6, 2014. ISSN 1934-8525. doi: 10.1002/9780471729259.mc06g01s35.

- [36] C-R. Lee, J. H. Lee, M. Park, K. S. Park, I. K. Bae, Y. B. Kim, C-J. Cha, B. C. Jeong, and S. H. Lee. Biology of *Acinetobacter baumannii*: pathogenesis, antibiotic resistance mechanisms, and prospective treatment options. *Front. Cell. Infect. Microbiol.*, 7 (55), 2017. ISSN 2235-2988. doi: 10.3389/fcimb.2017.00055. URL <https://www.frontiersin.org/article/10.3389/fcimb.2017.00055>.
- [37] E. A. Snellman and R. R. Colwell. *Acinetobacter* lipases: molecular biology, biochemical properties and biotechnological potential. *J. Ind. Microbiol. Biotechnol.*, 31(9):391–400, 2004. ISSN 1367-5435. doi: 10.1007/s10295-004-0167-0. URL <https://doi.org/10.1007/s10295-004-0167-0>.
- [38] B. Collins, P. D. Cotter, C. Hill, and P. Ross. *Applications of lactic acid bacteria-produced bacteriocins*, pages 89–109. Blackwell Publishing, 2010. doi: <https://doi.org/10.1002/9780813820866.ch5>. URL <https://onlinelibrary.wiley.com/doi/abs/10.1002/9780813820866.ch5>.
- [39] J. Fontoura and M. Gutterres. Damage of pickled hides, wet-blue leather and vegetable tanned leather due to biodeterioration. *J. Am. Leather Chem. Assoc.*, 110(05):138–144, 2015. ISSN 0002-9726.
- [40] T. L. Czárán, R. F. Hoekstra, and L. Pagie. Chemical warfare between microbes promotes biodiversity. *PNAS*, 99(2):786, 2002. doi: 10.1073/pnas.012399899. URL <http://www.pnas.org/content/99/2/786.abstract>.
- [41] B. Kerr, M. A. Riley, M. W. Feldman, and B. J. M. Bohannan. Local dispersal promotes biodiversity in a real-life game of rock-paper-scissors. *Nature*, 418(6894):171–174, 2002. ISSN 1476-4687.
- [42] L. Li, N. Mendis, H. Trigui, J. D. Oliver, and S. P. Faucher. The importance of the viable but non-culturable state in human bacterial pathogens. *Front. Microbiol.*, 5 (258), 2014. ISSN 1664-302X. doi: 10.3389/fmicb.2014.00258. URL <https://www.frontiersin.org/article/10.3389/fmicb.2014.00258>.
- [43] S-C. Yang, C-H. Lin, C. T. Sung, and J-Y. Fang. Antibacterial activities of bacteriocins: application in foods and pharmaceuticals. *Front. Microbiol.*, 5:241–241, 2014. ISSN 1664-302X. doi: 10.3389/fmicb.2014.00241. URL <https://pubmed.ncbi.nlm.nih.gov/24904554>.
- [44] N. Schneider, K. Werkmeister, and M. Pischetsrieder. Analysis of nisin A, nisin Z and their degradation products by LCMS/MS. *Food Chem.*, 127(2):847–854, 2011. ISSN 0308-8146.
- [45] R. Naffa. *Understanding the molecular basis of the strength differences in skins used in leather manufacture : a dissertation presented in partial fulfillment of the requirements for the degree of Doctor of Philosophy at Massey University, Palmerston North, New*

- Zealand*. Thesis, Massey University, 2017. URL <http://hdl.handle.net/10179/13154>.
- [46] A. Zago and S. Chugani. *Pseudomonas*, pages 245–260. Academic Press, Oxford, 2009. ISBN 978-0-12-373944-5. doi: <https://doi.org/10.1016/B978-012373944-5.00203-0>. URL <http://www.sciencedirect.com/science/article/pii/B9780123739445002030>.
- [47] R. Boutrou and M. Gueguen. Interests in *Geotrichum candidum* for cheese technology. *Int. J. Food Microbiol.*, 102(1):1–20, 2005. ISSN 0168-1605 (Print) 0168-1605. doi: [10.1016/j.ijfoodmicro.2004.12.028](https://doi.org/10.1016/j.ijfoodmicro.2004.12.028).
- [48] R. Boutrou, L. Kerriou, and J-Y. Gassi. Contribution of *Geotrichum candidum* to the proteolysis of soft cheese. *Int. Dairy J.*, 16(7):775–783, 2006. ISSN 0958-6946. doi: <https://doi.org/10.1016/j.idairyj.2005.07.007>. URL <http://www.sciencedirect.com/science/article/pii/S0958694605001470>.
- [49] C. I. Gonzalez-Lopez, R. Szabo, S. Blanchin-Roland, and C. Gaillardin. Genetic control of extracellular protease synthesis in the yeast *Yarrowia lipolytica*. *Genetics*, 160(2):417–27, 2002. ISSN 0016-6731 (Print) 0016-6731.

5.5 Supplementary information - Methods

Table S1: PCR conditions.

PCR using Phusion [®] high fidelity DNA polymerase		
Steps	Temperature (°C)	Duration (sec)
Initial denaturation	98	30
Amplification: (30 cycles)		
Denaturation	98	30
Annealing		
S-D-Bact-0341-b-S-17/S-D-Bact-0785-a-A-21	55	30
5.8S-FUN/ITS4-FUN	58	
Elongation	68	30
Final elongation	68	300

Table S2: Mass spectrometer configuration used for proteomic analysis

nanoLC system	Dionex UltiMate [™] 3000 Binary RSLCnano system (Thermo Fisher Scientific, USA)
Mass spectrometer	Q Exactive [™] Plus (Thermo Fisher Scientific, Bremen, Germany)
Ionisation source	Nanospray Flex [™] (Thermo Fisher Scientific, USA)
Trapping column	Acclaim [™] PepMap [™] 100 C ₁₈ , 3 µm particle size, 75 µm inner diameter, 1 cm length (Thermo Fisher Scientific, USA)
Analytical column	Acclaim [™] PepMap [™] C ₁₈ , 2 µm particle size, 75 µm inner diameter, 50 cm length (Thermo Fisher Scientific, USA)
Flow rates	Trap column: 15 µL/min Analytical column: 300 nL/min
Column oven temperature	50 °C
Gradient	3 - 30 % MeCN in 0.1 % formic acid over 60 minutes
Buffers	Trap loading: 0.1 % TFA/ 2 % MeCN/H ₂ O Analytical A: 0.1 % Formic acid/ 2 % MeCN/H ₂ O Analytical B: 0.1 % Formic acid/ 98 % MeCN/H ₂ O

Table S3: Parameter used for proteomic analysis

Capillary temperature (°C)	250
S-Lens RF level (%)	50
Polarity	Positive
Source voltage (kV)	1.6
AGC target	Full MS 3×10^6 , MS2 (HCD) 1×10^5
Maximum injection times (ms)	Full MS 150 ms, MS2 (HCD) 110 ms
Full MS mass range	375 - 1600 m/z
Resolution settings	Full MS 70,000, MS2 (HCD) 17,500
Number of micro-scans	1
Isolation width	1.4 m/z
Loop count (TopN)	10
MSX count	1
Normalised collision energy	28
Charge exclusion	Unassigned, 1, > 7
Peptide match	Preferred
Exclude isotopes	On
Dynamic exclusion	12 seconds
Spectrum data type	Centroid

Table S4: Parameters used for proteomic data analysis

Search engine	Proteome Discoverer™ v. 2.5
Databases	Non-redundant NCBI compiled on 29 th of April, 2021
Taxonomy	listed in Table S5
Enzyme	Trypsin
Maximum number of missed cleavages	2
Minimum peptide length	6
Precursor mass tolerance	10 ppm
Fragment mass tolerance	0.02 Da
Peptide charge	2 - 7
Protein mass	Unrestricted
Decoy database search	Enabled (default)
Significance threshold	0.01 %
Static modifications	Carbamidomethyl, + 57.021 (C)
Variable modifications	Oxidation, + 15.995 Da (M)
False discovery rate	≤ 1 %

Table S5: List of bacterial and fungal species from the NCBI protein database.

Taxonomy	
	<i>Acinetobacter celticus/lwoffii</i>
	<i>Arcobacter butzleri</i>
	<i>Bacteroides xyloxyticus</i>
	<i>Escherichia fergusonii</i>
	<i>Hafnia alvei</i>
	<i>Klebsiella aerogenes</i>
	<i>Kurthia gibsonii</i>
Bacteria	<i>Lactiplantibacillus plantarum</i>
	<i>Lactococcus lactis/raffinolactis</i>
	<i>Latilactobacillus curvatus</i>
	<i>Leuconostoc holzapfelii</i>
	<i>Lysinibacillus macroides</i>
	<i>Propionispira</i> genus
	<i>Pseudomonas</i> genus
	<i>Shewanella putrefaciens</i>
	<i>Alternaria alternata/metahromatica</i>
	<i>Aureobasidium pullulans</i>
	<i>Cutaneotrichosporon cutaneum</i>
	<i>Didymella exigua</i>
Fungi	<i>Geotrichum candidum</i>
	<i>Mycosphaerella tassiana</i>
	<i>Naganishia albida</i>
	<i>Rhodotorula graminis/mucilaginoso</i>
	<i>Trichosporon</i> genus
	<i>Yarrowia lipolytica</i>

Table S6: Mass spectrometry instrument configuration for metabolomic analysis

LC system	Dionex UltiMate™ 3000 Quaternary RSLCnano system (Thermo Fisher Scientific, USA)
Mass spectrometer	Q Exactive™ Focus (Thermo Fisher Scientific, Bremen, Germany)
Ionisation source	HESI-II (Thermo Fisher Scientific, USA)
Analytical column	Reverse phase: Phenomenex Gemini® C ₁₈ , 3 µm particle size, 2 × 100 mm, 110 Å
Analytical column	HILIC: Thermo Scientific Accucore™ HILIC, 2.6 µm particle size, 2.1 × 100 mm, 80 Å
Flow rate	0.35 mL/min
Column oven temperature	35 °C
C ₁₈ gradient	3 minutes hold on 2 % B, 2 - 42 % B for 40 minutes, 42 - 100 % B for 12 minutes
HILIC gradient	100 % B for 3 minutes, 100 - 60 % B for 40 minutes, 60 - 8 % B for 12 minutes
Positive mode buffers	A: 0.1 % Formic acid/ 5 mM NH ₄ HCO ₂ /H ₂ O B: 0.1 % Formic acid, 5 mM NH ₄ HCO ₂ / 80 % MeCN/H ₂ O
Negative mode buffers	A: 10 mM NH ₄ CH ₃ CO ₂ /H ₂ O, pH 9 B: 10 mM NH ₄ CH ₃ CO ₂ / 80 % MeCN/H ₂ O, pH 9

Table S7: Mass spectrometer settings for metabolomic analysis

Capillary temperature (°C)	330
S-Lens RF level (%)	85
Polarity	Positive/Negative
Source voltage (kV)	3.1
Sheath gas flow rate (L/min)	40
Aux gas flow rate (L/min)	8
Aux gas heater temperature (°C)	290
AGC target	Full MS 50 1×10^6 , MS2 1×10^5
Maximum injection times (ms)	Full MS 50 ms, MS2 70 ms
dd-MS ² mode	Discovery
Full MS mass range	50 - 750 m/z
Resolution settings	Full MS 70,000, MS2 17,500
Number of micro-scans	1
Isolation width	3 m/z
MSX count	1
Normalised collision energy	30, 40
Minimum AGC target	5×10^3
Exclude isotopes	On
Dynamic exclusion	7.5 seconds
Spectrum data type	Centroid

5.6 Supplementary information - Results

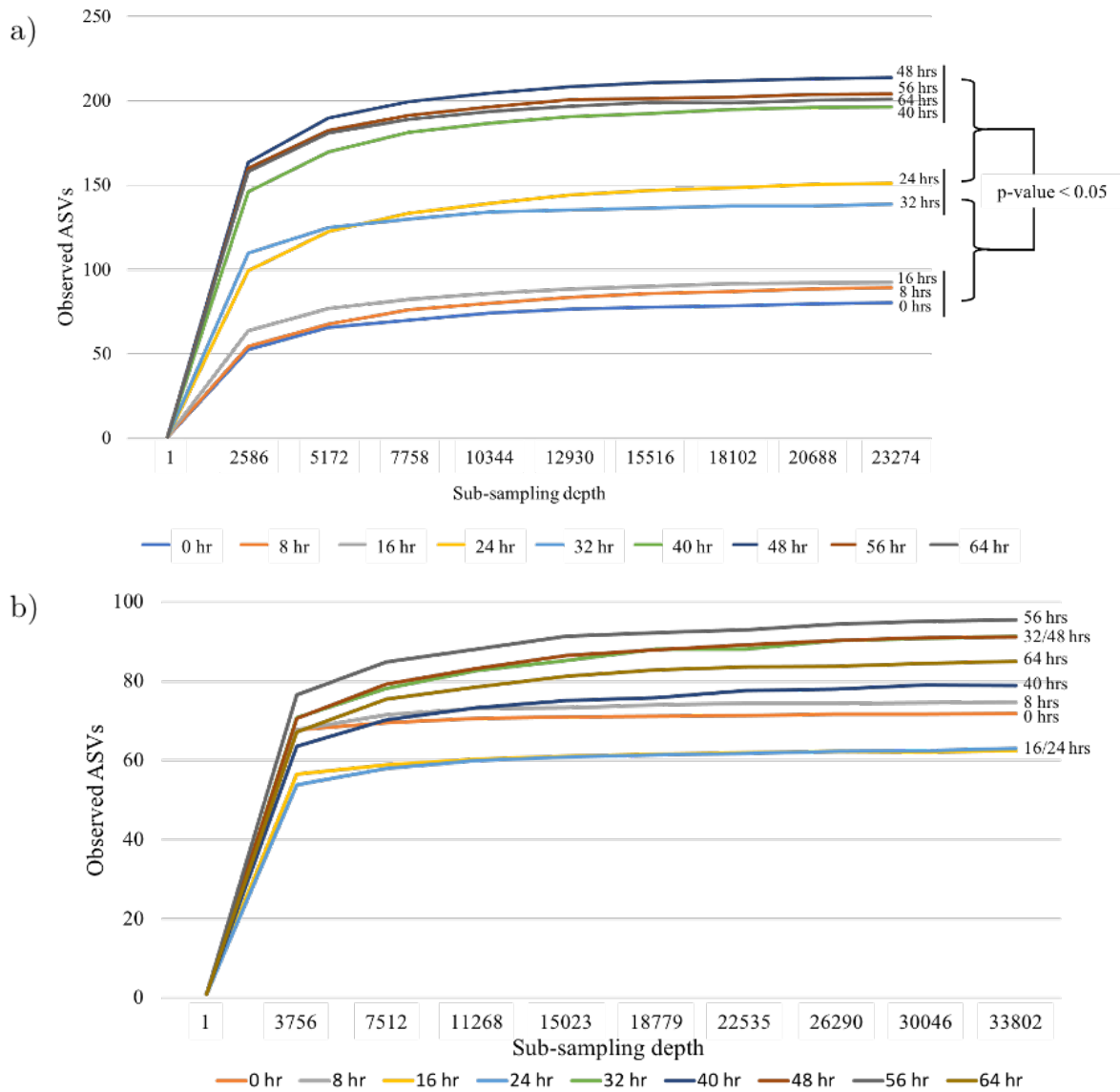


Figure S1: Average rarefaction curves obtained for each timepoint with the number of observed ASVs. (a) 16S rDNA samples rarefied to 23,271 reads. (b) ITS samples rarefied to 33,802 reads.

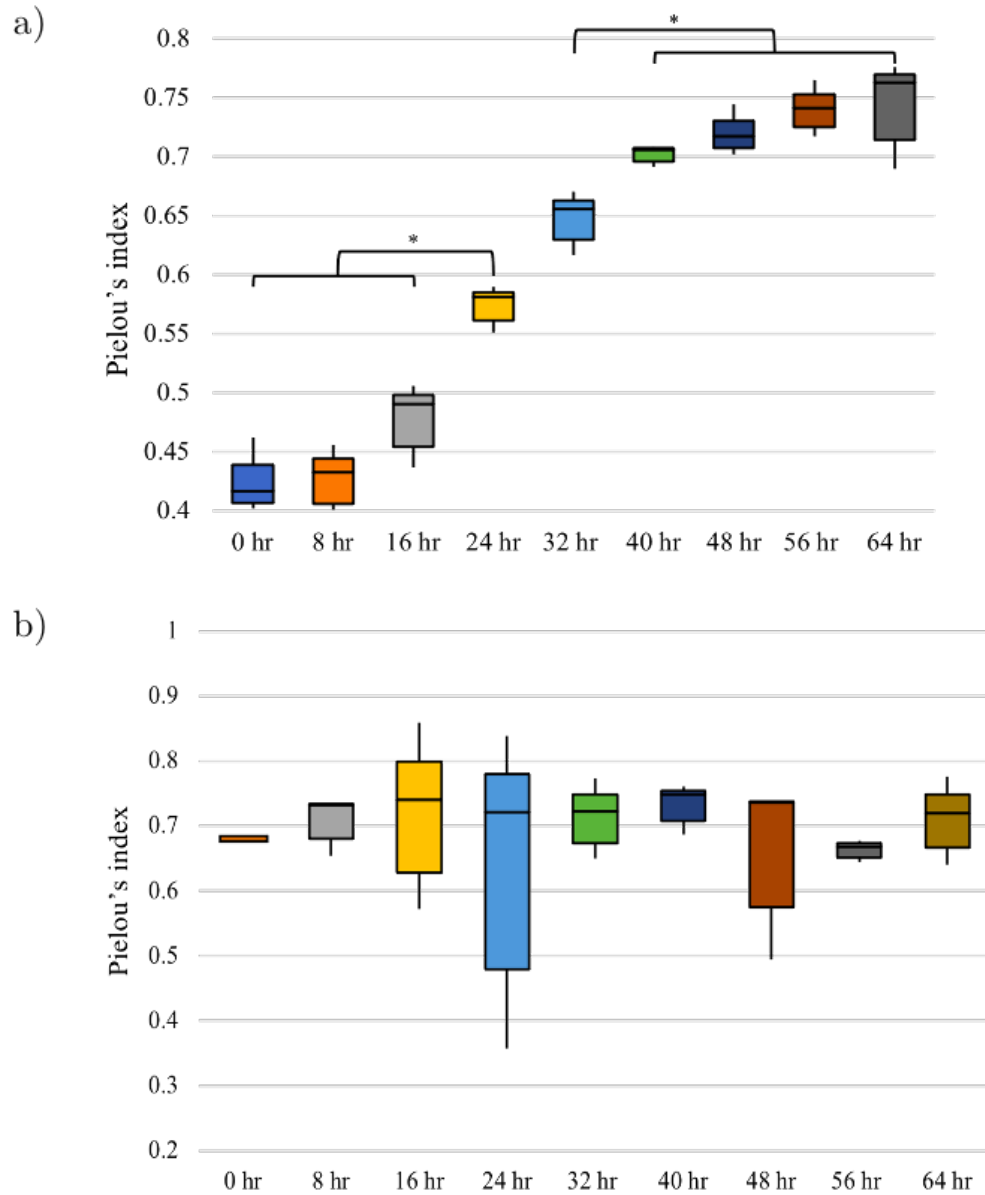


Figure S2: Pielou's evenness index for (a) 16S rDNA samples and (b) ITS samples.

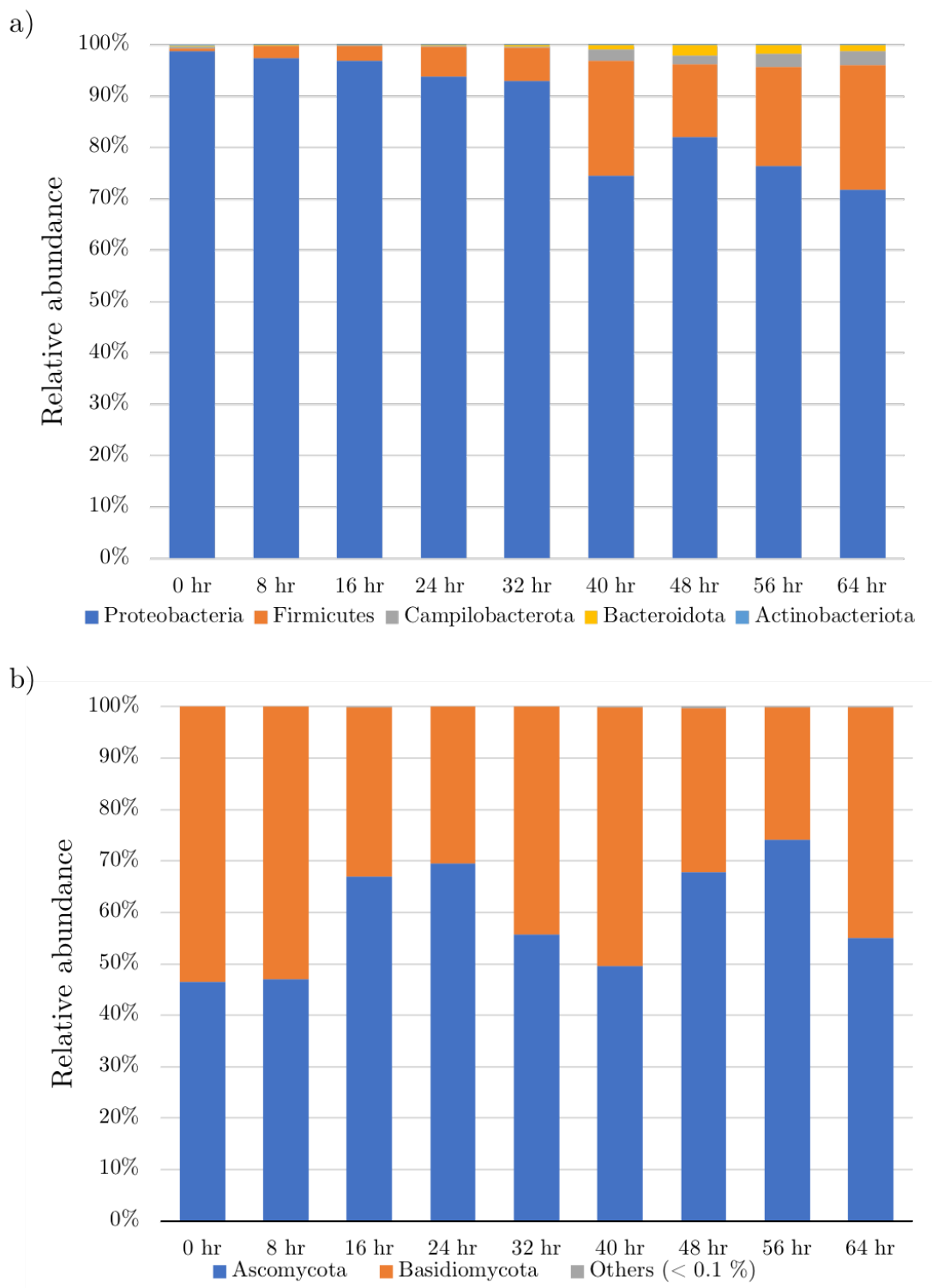


Figure S3: Bar plot showing the microbial phyla distributions over the time course of permeate depilation. (a) Bacterial phyla distributions. (b) Fungal phyla distributions. Others in (b) includes Chytridiomycota and Mucoromycota.

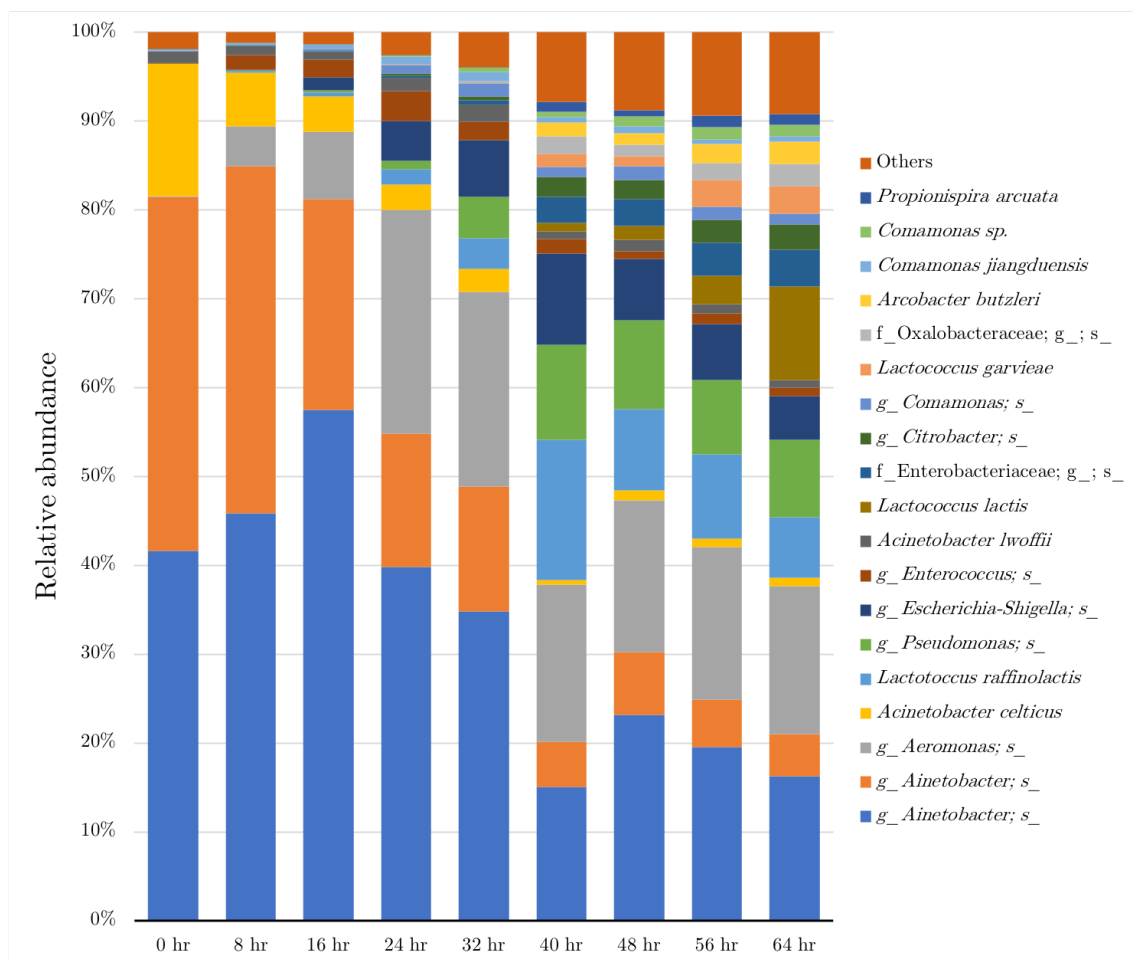


Figure S4: Bar plot showing the bacterial species distributions of permeate depilation. U. m., unclassified member. Others, species that are less than 1 % relative abundance.

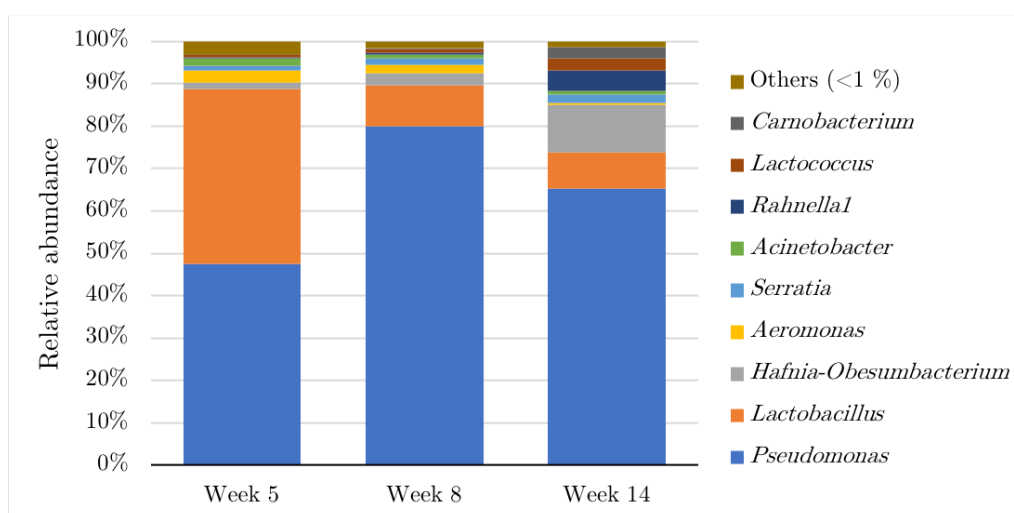


Figure S5: Bar plot showing the microbial genus distributions post permeate depilation at week 5, 8 and 14.

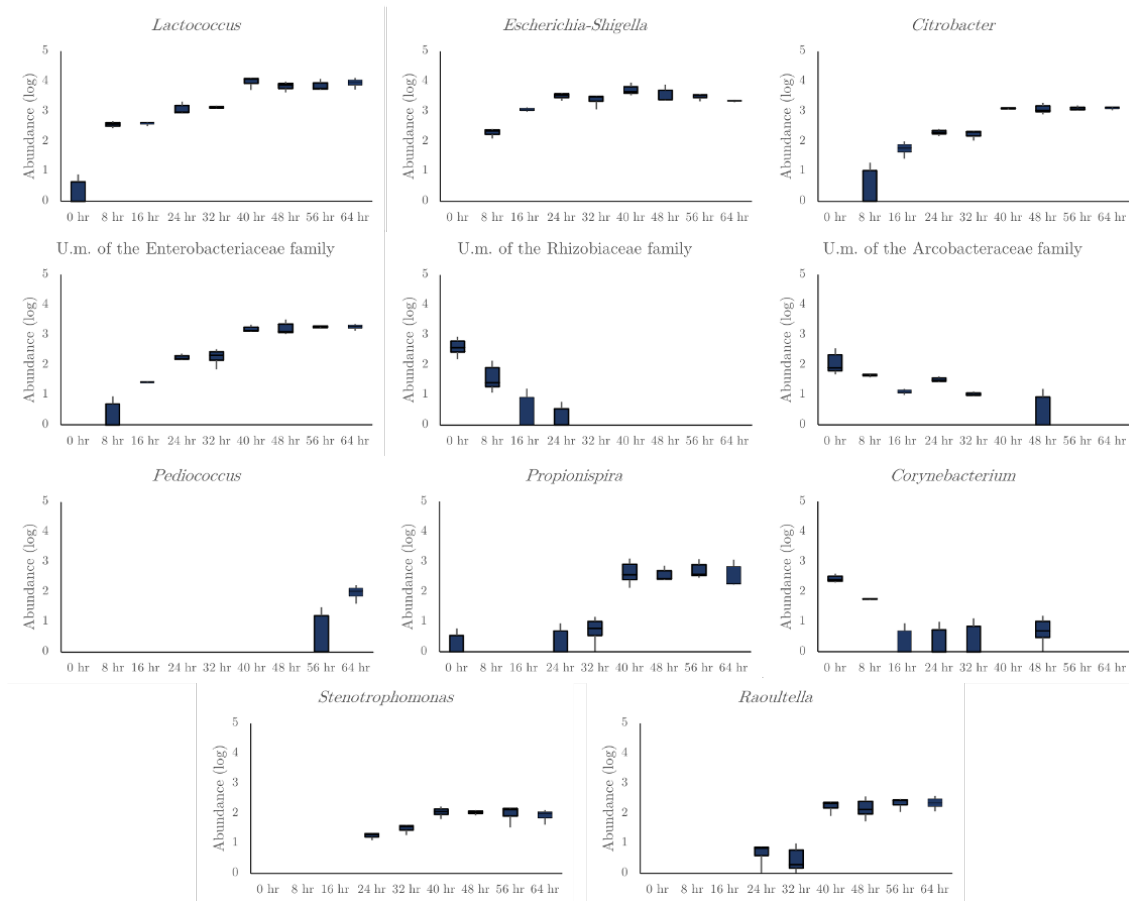


Figure S6: ANCOM analysis of the differentially abundant 16S rRNA ASVs at the genus level.

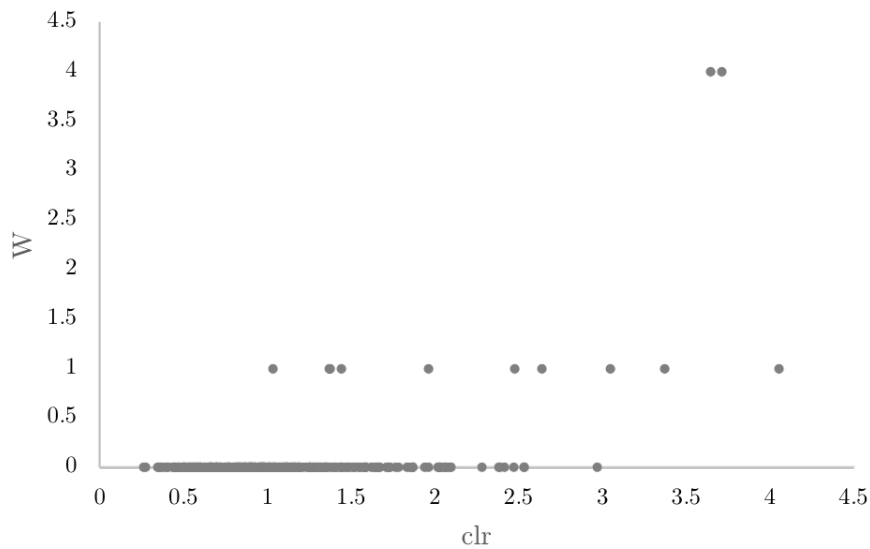


Figure S7: Volcano plots of differentially expressed fungal ASVs over the different timepoints of permeate depilation at genus level. ANCOM analysis was performed to analyse statistical significance. W, W statistics; clr, centered log-ratio, F-statistics.

Table S8: Quality-filtering of the 16S rRNA sequencing samples.

Sample name	Biological replicate	Sample collection timepoint (hr)	Input reads	Cutadapt adapter and primer sequence removed	Quality filtered reads	Denoised reads	Non-chimeric reads	% Non-chimeric reads
OSP1 0 hr	1	0	244621	244621	208671	208211	191922	78.5
OSP2 0 hr	2	0	230683	230683	202541	202407	183498	79.5
OSP3 0 hr	3	0	312237	312237	276265	275552	222514	71.3
OSP1 8 hr	1	8	182252	182252	158838	158349	132431	72.7
OSP2 8 hr	2	8	229435	229435	200734	200137	151412	66.0
OSP3 8 hr	3	8	210346	210346	183786	183107	142424	67.7
OSP1 16 hr	1	16	110400	110400	96364	95703	64555	58.5
OSP2 16 hr	2	16	109354	109354	94735	94086	62825	57.5
OSP3 16 hr	3	16	207117	207117	181599	180582	109650	52.9
OSP1 24 hr	1	24	232985	232985	203854	202373	90983	39.1
OSP2 24 hr	2	24	178510	178510	155871	154284	73865	41.4
OSP3 24 hr	3	24	165548	165548	139875	138596	59561	36.0
OSP1 32 hr	1	32	181574	181574	154778	153017	55384	30.5
OSP2 32 hr	2	32	107210	107210	59067	58108	23323	21.8
OSP3 32 hr	3	32	122763	122763	104333	102837	40293	32.8
OSP1 40 hr	1	40	198540	198540	171792	169500	55478	27.9
OSP2 40 hr	2	40	164242	164242	140509	137853	47878	29.2
OSP3 40 hr	3	40	188756	188756	163841	161764	61581	32.6
OSP1 48 hr	1	48	325034	325034	281737	278188	87760	27.0
OSP2 48 hr	2	48	196715	196715	167941	165050	54291	27.6
OSP3 48 hr	3	48	151152	151152	130847	128356	41047	27.2
OSP1 56 hr	1	56	123149	123149	104992	102739	31086	25.2
OSP2 56 hr	2	56	271299	271299	231203	227688	71363	26.3
OSP3 56 hr	3	56	171235	171235	147088	144525	46589	27.2
OSP1 64 hr	1	64	156368	156368	126327	124321	40349	25.8
OSP2 64 hr	2	64	220952	220952	189735	186636	57445	26.0
OSP3 64 hr	3	64	183250	183250	157475	154349	39723	21.7

Table S9: Quality-filtering of the ITS sequencing samples.

Sample name	Biological replicate	Sample collection timepoint (hr)	Input reads	Cutadapt adapter and primer sequence removed	Quality filtered reads	Denoised reads	Non-chimeric reads	% Non-chimeric reads
OSP1 0 hr	1	0	1018	1015	838	825	748	73.7
OSP2 0 hr	2	0	1127	1127	940	896	841	74.6
OSP3 0 hr	3	0	89300	89300	76179	76001	68816	77.1
OSP1 8 hr	1	8	58381	58381	50386	50163	46272	79.3
OSP2 8 hr	2	8	88372	88372	75884	75567	71952	81.4
OSP3 8 hr	3	8	1072056	1072056	930165	929182	852520	79.5
OSP1 16 hr	1	16	151907	151907	133134	133004	127591	84.0
OSP2 16 hr	2	16	138398	138398	115210	114914	109723	79.3
OSP3 16 hr	3	16	74504	74504	38804	38647	35638	47.8
OSP1 24 hr	1	24	132893	132893	112664	112495	108033	81.3
OSP2 24 hr	2	24	88391	88391	76824	76583	73822	83.5
OSP3 24 hr	3	24	93762	93762	80665	80431	77148	82.3
OSP1 32 hr	1	32	113016	113016	96185	95905	92512	81.9
OSP2 32 hr	2	32	87266	87266	72705	72307	70297	80.6
OSP3 32 hr	3	32	1962634	1962634	1663723	1661192	1546158	78.8
OSP1 40 hr	1	40	50228	50228	39758	39545	38567	76.8
OSP2 40 hr	2	40	91392	91392	77269	76413	74058	81.0
OSP3 40 hr	3	40	823947	823947	693233	692204	651967	79.1
OSP1 48 hr	1	48	149906	149906	132532	132090	125219	83.5
OSP2 48 hr	2	48	132264	132264	104297	103822	92317	69.8
OSP3 48 hr	3	48	717266	717266	579674	577683	423345	59.0
OSP1 56 hr	1	56	137114	137114	113903	113577	108049	78.8
OSP2 56 hr	2	56	175459	175459	150513	150064	139495	79.5
OSP3 56 hr	3	56	83947	83947	68216	67687	64485	76.8
OSP1 64 hr	1	64	50727	50727	42047	41758	38764	76.4
OSP2 64 hr	2	64	227166	227166	193168	192487	184643	81.3
OSP3 64 hr	3	64	233416	233416	186974	186418	171212	73.4

Table S10: Shannon’s diversity index statistical tests of the 16S metagenome.

Shannon’s diversity index (H)								
0 hr	8 hr	16 hr	24 hr	32 hr	40 hr	48 hr	56 hr	64 hr
2.82420169	2.57373568	3.19559789	3.98295981	4.76804866	5.43732674	5.52092534	5.65430685	5.21621067
2.58846748	2.73103628	3.0979531	4.15614226	4.38713116	5.32553341	5.53159235	5.61729696	5.75832814
2.59350877	2.88130622	2.79561656	4.16154857	4.41463549	5.23944409	5.62144975	5.64542184	5.72941624

one-way ANOVA: Single Factor				
Groups	Count	Sum	Average	Variance
0 hr	3	8.00617795	2.66872598	0.01813588
8 hr	3	8.18607818	2.72869273	0.02365403
16 hr	3	9.08916754	3.02972251	0.04348782
24 hr	3	12.3006506	4.10021688	0.01031922
32 hr	3	13.5698153	4.52327177	0.04512592
40 hr	3	16.0023042	5.33410141	0.00984444
48 hr	3	16.6739674	5.55798915	0.00304888
56 hr	3	16.9170257	5.63900855	0.00037328
64 hr	3	16.703955	5.56798502	0.09301787

Source of Variation	SS	df	MS	F	p-value	F crit
Between Groups	38.5907725	8	4.82384657	175.762464	1.7503E-15	2.5101579
Within Groups	0.49401469	18	0.02744526			
Total	39.0847872	26				

Tukey’s/Honest Significant Difference (HSD test)					HSD value	Q value from
Group 1	Group 2	Difference	MS _{within}	nh	Difference/Square-root(MSw/nh)	table = 4.955
0	8	0.05996675	0.02744526	3	0.62695653	NO
8	16	0.30102979	0.02744526	3	3.14728753	NO
16	24	1.07049437	0.02744526	3	11.1920937	YES
24	32	0.42305489	0.02744526	3	4.42306851	NO
32	40	0.81082965	0.02744526	3	8.47728081	YES
40	48	0.22388773	0.02744526	3	2.34076195	NO
48	56	0.0810194	0.02744526	3	0.84706356	NO
56	64	0.07102354	0.02744526	3	0.74255604	NO

Table S11: Shannon’s diversity index statistical tests of the ITS metagenome.

Shannon’s diversity index (H)								
0 hr	8 hr	16 hr	24 hr	32 hr	40 hr	48 hr	56 hr	64 hr
4.22345394	4.33713878	2.93662632	3.72094607	4.33279884	4.07847427	3.14467257	3.87784503	4.02339517
-	4.37116067	4.16637595	2.49093144	4.41536449	4.58553779	4.35064788	4.45308632	4.43665767
-	3.91333889	4.56906881	4.25191907	4.67240756	3.76030387	4.24386113	4.36318594	4.68502308

one-way ANOVA: Single Factor				
Groups	Count	Sum	Average	Variance
0 hr	1	4.22345394	4.22345394	-
8 hr	3	12.6216383	4.20721278	0.06506077
16 hr	3	11.6720711	3.89069036	0.72321903
24 hr	3	10.4637966	3.48793219	0.81599095
32 hr	3	13.4205709	4.47352363	0.03137039
40 hr	3	12.4243159	4.14143865	0.17322614
48 hr	3	11.7391816	3.91306053	0.44566589
56 hr	3	12.6941173	4.23137243	0.09575674
64 hr	3	13.1450759	4.38169197	0.1117038

Source of Variation	SS	df	MS	F	p-value	F crit
Between Groups	2.12304779	8	0.26538097	0.86232868	0.56584001	2.59109618
Within Groups	4.9239874	16	0.30774921			
Total	7.04703519	24				

Table S12: 'Others' genera list from the 16S rRNA genus level taxa bar plot.

Relative abundance (%)																									
	<i>Corynebacterium</i>	<i>Kocuria</i>	<i>Dysgonomonas</i>	<i>Maellibacteroides</i>	<i>Fluviicola</i>	<i>Flavobacterium</i>	<i>Myroides</i>	U. m. of Websloaceae family	<i>Chrysochlorobacterium</i>	<i>Empedobacter</i>	<i>Sphingobacterium</i>	U. m. of Aerobacteraceae family	<i>Pseudarcobacter</i>	<i>Kurtzia</i>	<i>Planomicrobium</i>	<i>Solibacillus</i>	<i>Erysipelothrix</i>	<i>Exigobacterium</i>	U. m. of Aerococcaceae family	<i>Alkalibacterium</i>	<i>Carnobacterium</i>	<i>Jeotgallibaca</i>	<i>Trichococcus</i>	<i>Lactobacillus</i>	<i>Pediococcus</i>
0 hr	0.145	0.013	0.000	0.000	0.000	0.026	0.019	0.117	0.040	0.005	0.014	0.081	0.032	0.000	0.048	0.028	0.056	0.001	0.042	0.016	0.057	0.016	0.079	0.000	0.000
8 hr	0.039	0.006	0.000	0.002	0.002	0.012	0.016	0.036	0.008	0.004	0.002	0.031	0.004	0.000	0.002	0.017	0.012	0.064	0.023	0.003	0.244	0.026	0.106	0.000	0.000
16 hr	0.003	0.000	0.006	0.000	0.000	0.003	0.003	0.036	0.000	0.003	0.005	0.015	0.000	0.000	0.000	0.038	0.002	0.034	0.003	0.000	0.176	0.034	0.115	0.000	0.000
24 hr	0.004	0.000	0.009	0.007	0.000	0.009	0.013	0.065	0.000	0.024	0.029	0.043	0.061	0.006	0.000	0.058	0.011	0.028	0.004	0.000	0.193	0.044	0.237	0.000	0.000
32 hr	0.010	0.000	0.034	0.000	0.000	0.003	0.039	0.147	0.008	0.075	0.055	0.024	0.128	0.056	0.000	0.028	0.003	0.016	0.008	0.000	0.344	0.019	0.308	0.000	0.000
40 hr	0.000	0.016	0.043	0.010	0.011	0.021	0.331	0.061	0.024	0.216	0.130	0.000	0.654	0.102	0.013	0.022	0.013	0.035	0.000	0.000	0.799	0.082	0.279	0.017	0.000
48 hr	0.010	0.026	0.047	0.028	0.013	0.052	0.596	0.215	0.061	0.564	0.378	0.008	0.480	0.078	0.000	0.015	0.002	0.017	0.000	0.000	0.270	0.031	0.265	0.006	0.000
56 hr	0.000	0.016	0.033	0.028	0.014	0.045	0.636	0.227	0.038	0.451	0.304	0.000	0.419	0.136	0.005	0.000	0.002	0.022	0.000	0.000	0.240	0.036	0.299	0.088	0.020
64 hr	0.000	0.020	0.024	0.008	0.019	0.077	0.444	0.197	0.032	0.298	0.144	0.000	0.216	0.125	0.000	0.006	0.009	0.017	0.007	0.000	0.170	0.024	0.255	0.344	0.227
Relative abundance (%)																									
	<i>Leuconostoc</i>	<i>Streptococcus</i>	<i>Jeotgallibacillus</i>	<i>Chlostridium</i>	<i>Proteocatella</i>	<i>Succinospira</i>	<i>Veillonella</i>	<i>Brevundimonas</i>	U. m. of Rhizobiaceae family	U. m. of Rhodobacteraceae family	<i>Candidatus</i>	<i>Sphingomonas</i>	<i>Sphingopyxis</i>	<i>Alishewanella</i>	<i>Rheinheimera</i>	<i>Achromobacter</i>	<i>Alcaligenaceae</i>	U. m. of Comamonadaceae family	<i>Delftia</i>	<i>Simplicispara</i>	<i>Vitreoscilla</i>	<i>Massilia</i>	U. m. of Enterobacterales order	<i>Enterobacter</i>	<i>Klebsiella</i>
0 hr	0.000	0.000	0.007	0.000	0.077	0.013	0.000	0.000	0.237	0.000	0.000	0.010	0.056	0.008	0.012	0.088	0.008	0.000	0.000	0.039	0.015	0.008	0.000	0.000	0.000
8 hr	0.000	0.000	0.017	0.000	0.005	0.000	0.000	0.000	0.040	0.000	0.000	0.000	0.013	0.000	0.000	0.002	0.001	0.000	0.000	0.006	0.001	0.000	0.014	0.004	0.000
16 hr	0.000	0.005	0.009	0.000	0.020	0.000	0.000	0.000	0.006	0.000	0.000	0.000	0.000	0.008	0.000	0.000	0.000	0.000	0.000	0.003	0.000	0.000	0.108	0.013	0.000
24 hr	0.000	0.024	0.008	0.014	0.023	0.003	0.000	0.000	0.002	0.000	0.002	0.000	0.000	0.007	0.028	0.000	0.001	0.009	0.015	0.000	0.000	0.025	0.142	0.035	0.000
32 hr	0.000	0.019	0.000	0.013	0.017	0.000	0.000	0.014	0.000	0.022	0.006	0.000	0.000	0.000	0.116	0.000	0.000	0.025	0.041	0.000	0.000	0.024	0.154	0.062	0.000
40 hr	0.004	0.037	0.009	0.050	0.017	0.003	0.021	0.014	0.000	0.026	0.017	0.000	0.000	0.000	0.381	0.000	0.000	0.058	0.110	0.000	0.000	0.036	0.087	0.199	0.033
48 hr	0.000	0.036	0.003	0.040	0.011	0.000	0.037	0.044	0.000	0.045	0.018	0.000	0.000	0.000	0.253	0.000	0.000	0.119	0.146	0.000	0.000	0.031	0.146	0.267	0.046
56 hr	0.031	0.030	0.000	0.104	0.008	0.000	0.039	0.046	0.000	0.031	0.018	0.000	0.000	0.000	0.151	0.000	0.000	0.093	0.162	0.000	0.001	0.020	0.105	0.318	0.068
64 hr	0.371	0.022	0.000	0.063	0.010	0.000	0.057	0.032	0.000	0.022	0.010	0.000	0.000	0.000	0.114	0.000	0.000	0.094	0.171	0.000	0.000	0.011	0.108	0.366	0.070
Relative abundance (%)																									
	<i>Raoultella</i>	<i>Pantoea</i>	<i>Hafnia- Obesumbacterium</i>	<i>Morganella</i>	<i>Proteus</i>	<i>Providencia</i>	<i>Pectobacterium</i>	<i>Serratia</i>	<i>Alkalinidiges</i>	<i>Psychrobacter</i>	<i>Stenotrophomonas</i>														
0 hr	0.000	0.011	0.000	0.000	0.000	0.000	0.000	0.000	0.022	0.074	0.000														
8 hr	0.000	0.009	0.000	0.000	0.008	0.011	0.000	0.012	0.012	0.036	0.000														
16 hr	0.000	0.018	0.000	0.014	0.039	0.099	0.000	0.063	0.000	0.007	0.000														
24 hr	0.006	0.051	0.001	0.025	0.057	0.081	0.000	0.073	0.003	0.007	0.024														
32 hr	0.008	0.044	0.003	0.019	0.066	0.088	0.000	0.099	0.003	0.008	0.079														
40 hr	0.333	0.041	0.026	0.021	0.058	0.048	0.008	0.087	0.000	0.000	0.213														
48 hr	0.310	0.089	0.019	0.012	0.047	0.044	0.007	0.101	0.002	0.004	0.179														
56 hr	0.464	0.086	0.029	0.000	0.041	0.049	0.000	0.078	0.000	0.000	0.218														
64 hr	0.534	0.088	0.023	0.018	0.035	0.064	0.018	0.085	0.000	0.000	0.196														

5.6. SUPPLEMENTARY INFORMATION - RESULTS

Table S13: Bacteria proteins identified in the permeate solution after depilation. The proteins listed are found with at least 2 unique peptides.

Species	Protein	NCBI accession	PSMs	# of unique peptides
<i>Acinetobacter</i>	50S ribosomal protein L11	ODA14486.1	94	2
	50S ribosomal protein L6	ODA11825.1	26	3
	co-chaperone GroES	WP_068888658.1	4	2
	DUF2147 domain-containing protein	WP_068885877.1	20	2
	inorganic pyrophosphatase	ODA12241.1	44	5
	NirD/YgiW/YdeI family stress tolerance protein	WP_078055429.1	5	3
	OmpA family protein	WP_068886036.1	60	5
	phosphonate ABC transporter substrate-binding protein	ODA13542.1	39	7
	polyisoprenoid-binding protein	WP_068888285.1	3	2
	thioredoxin	WP_068885391.1	87	3
	toluene tolerance protein	ODA11859.1	25	3
<i>Acinetobacter</i>	50S ribosomal protein L7/L12	RYJ49273.1	292	2
	antibiotic biosynthesis monooxygenase	RYJ48421.1	14	2
	molecular chaperone	BCD52722.1	13	2
	elongation factor Tu	ENW25616.1	15	3
	nitrogen regulatory protein P-II	EEY89141.1	20	2
<i>Enterobacter aerogenes</i>	type I glyceraldehyde-3-phosphate dehydrogenase	KZQ94805.1	15	2
	glutamate decarboxylase	QRX69407.1	9	2
<i>Escherichia coli</i>	fructose-bisphosphate aldolase	CAQ90350.1	21	3
<i>Lactiplantibacillus plantarum</i>	ubiquitin	TAR20416.1	320	2
	actin, cytoplasmic 2	KAF0950339.1	65	5
<i>Lactococcus lactis</i>	50S ribosomal protein L7/L12	TLQ15724.1	34	4
	cold shock domain-containing protein	QIW59349.1	19	3
	DNA starvation/stationary phase protection protein	WP_061773823.1	36	6
	fructose-1,6-bisphosphate aldolase	ATC60854.1	166	10
	integration host factor subunit α	QIW61055.1	15	3
	PDZ domain-containing protein	QIW59738.1	6	2
	peptidyl-prolyl cis-trans isomerase	PCS09494.1	4	3
	thioredoxin	QIW53577.1	2	2
	NAD-dependent glyceraldehyde -3-phosphate dehydrogenase	CCK20850.1	44	6
	phosphonate ABC transporter	CCK19796.1	3	2
	pyruvate kinase	CCK18800.1	7	2
	translation elongation factor Tu	CCK18662.1	6	2
	triosephosphate isomerase	CCK20178.1	4	2
<i>Pseudomonas sp.</i>	adenosylhomocysteinase	RZI83365.1	7	2
	polyamine ABC transporter substrate-binding protein	TXH94026.1	32	3
	thioredoxin TrxA	RZI90479.1	13	2
<i>Shewanella putrefaciens</i>	thioredoxin TrxA	QGS48504.1	34	2

Table S14: Bacterial proteins identified in the permeate solution after depilation. Proteins listed are found with 1 unique peptide.

Species	Protein	NCBI accession	PSMs	
<i>Acinetobacter</i>	30S ribosomal protein S15	WP_068885591.1	2	
	30S ribosomal protein S19	ODA11836.1	3	
	30S ribosomal protein S21	ODA13041.1	5	
	50S ribosomal protein L10	WP_068885623.1	6	
	50S ribosomal protein L24	ODA11829.1	5	
	alkyl hydroperoxide reductase subunit C	WP_171258089.1	16	
	ATP-binding protein	WP_068888984.1	2	
	<i>celticus</i>	F0F1 ATP synthase subunit δ	ODA14665.1	1
	HU family DNA-binding protein	WP_068889507.1	33	
	hypothetical protein:			
	BBP83_05670	ODA13847.1	1	
	BBP83_14495	ODA14074.1	3	
	NLPA lipoprotein	WP_068888136.1	5	
	nucleoside-diphosphate kinase	ODA14288.1	7	
<i>Acinetobacter</i>	30S ribosomal protein S16	AUC06747.1	1	
	50S ribosomal protein L11	TMS50648.1	88	
	acetamidase/formamidase family protein	RYJ50478.1	1	
	aspartate-semialdehyde dehydrogenase	AUC06114.1	2	
	cold-shock protein	AUC08149.1	9	
	dihydroliipoamide succinyl-transferase	VFQ37352.1	6	
	pyrimidine utilization protein C	QKU22125.1	1	
	RidA family protein	AUC06735.1	12	
	RidA family protein	TMS52165.1	8	
	50S ribosomal protein L10	ENW31343.1	10	
	50S ribosomal protein L27	ENW23850.1	3	
	50S ribosomal protein L30	ENW26159.1	4	
	<i>lwoffi</i>	acetyl-CoA carboxylase	ENW24327.1	2
	alkyl hydroperoxide reductase subunit C	ENW23528.1	21	
	ATP synthase subunit β	ENW26044.1	1	
	DNA-binding protein HU- β	ENW24282.1	52	
	isocitrate lyase	ENW23792.1	1	
	nucleoside diphosphate kinase	ENW29609.1	6	
	thioredoxin C-2	ENU61373.1	19	
	OmpA family protein	EEY90444.1	8	
	peptidoglycan-associated lipoprotein	EEY90963.1	2	
	phosphoribosylaminoimidazole carboxylase	EEY88540.1	3	
ribosomal protein S10	EEY88905.1	4		
ribosomal protein S8	EEY88890.1	6		
sulfate ABC transporter	EEY90922.1	3		
<i>Arcobacter butzleri</i>	hydroxymethylbilane synthase	WP_152058143.1	1	
	membrane protein	KLE04067.1	2	
<i>Enterobacter aerogenes</i>	sugar ABC transporter	KUQ11008.1	5	
	substrate-binding protein			

5.6. SUPPLEMENTARY INFORMATION - RESULTS

Table S14 continued from previous page

Species	Protein	NCBI accession	PSMs	
<i>Escherichia</i>	50S ribosomal protein L24	QMC79732.1	5	
	acid stress chaperone HdeB precursor	VUX05689.1	2	
<i>fergusonii</i>	acyl carrier protein	QKD65649.1	6	
	amino-acid transporter subunit	CAQ90739.1	1	
<i>Escherichia spp.</i>	acid-resistance protein	PSS41939.1	8	
<i>Hafnia</i>	cold-shock protein	KID04857.1	3	
	D-galactose/D-glucose-binding protein	STQ79521.1	21	
<i>alvei</i>	maltose/maltodextrin ABC transporter substrate-binding protein MalE	QIP54404.1	7	
<i>Hungatella xylinolytica</i>	AraC family transcriptional regulator	PPK83394.1	10	
<i>Klebsiella</i>	ABC-type amino acid transport/signal transduction system protein	STR14730.1	5	
	glutamine-binding periplasmic protein	VDZ69001.1	1	
	leucine-specific-binding protein	AML38136.1	2	
	murein lipoprotein	AWD05105.1	2	
<i>aerogenes</i>	pyrroloquinoline quinone biosynthesis protein PqqE	PMC22372.1	1	
	TPR domain protein	CCG33231.1	1	
	50S ribosomal protein L10	EUL47189.1	1	
<i>Lactococcus</i>	taurine ABC transporter ATP-binding protein	OSP87262.1	1	
<i>lactis</i>	HrcA family transcriptional regulator	QTP12279.1	1	
<i>Lactococcus</i>	50S ribosomal protein L30	QIW57081.1	4	
	BMP family ABC transporter substrate-binding protein	QIW55689.1	10	
	CHAP domain-containing protein	WP_061774202.1	3	
	CsbD family protein	QIW59867.1	1	
	DUF4097 family β strand repeat protein	WP_003138462.1	2	
	PASTA domain-containing protein	QIW54136.1	2	
	<i>raffinolactis</i>	peptide ABC transporter substrate-binding protein	QIW51618.1	15
	phosphocarrier protein HPr	QIW59245.1	2	
	transcription elongation factor GreA	TLQ13116.1	1	
	YneF family protein	QIW55906.1	6	
ribosome recycling factor	CCK20152.1	1		
<i>Pseudomonas</i>	50S ribosomal protein L1	RZI59624.1	1	
	alkyl hydroperoxide reductase subunit C	RZI71061.1	6	
	<i>spp.</i>	cold-shock protein	RZI74359.1	17
	cold-shock protein	RCL54467.1	2	
	nucleoside-diphosphate kinase	RZI54025.1	5	
	phosphate ABC transporter substrate-binding protein PstS	RZI89310.1	4	
	transcriptional regulator	PJI46836.1	2	

Table S14 continued from previous page

Species	Protein	NCBI accession	PSMs
<i>Shewanella</i>	acyl-CoA dehydrogenase	OUM09721.1	2
	C4-dicarboxylate ABC transporter	AVV86081.1	1
	elongation factor Tu	QSE49585.1	6
	malate dehydrogenase	GGN09766.1	7
<i>putrefaciens</i>	nitrogen regulatory protein P-II	VEE62836.1	1
	phosphate-binding protein	GGN13613.1	1
	tungsten ABC transporter		
	substrate-binding protein	GGN29504.1	1

Table S15: Fungi proteins identified in the permeate solution after depilation.

Species	Protein	NCBI accession	PSMs	# of unique peptides
<i>Alternaria alternata</i>	Actin, gamma	OWY50982.1	418	5
<i>Aureobasidium pullulans</i>	MFS transporter	TIA60903.1	1	1
<i>Cutaneotrichosporon oleaginosum</i>	hypothetical protein CC85DRAFT_197039	KLT39409.1	1	1
Didymella exigua	uncharacterised proteins:			
	M421DRAFT_418802	XP_033450740.1	1	1
	M421DRAFT_90003	XP_033452013.1	1	1
<i>Geotrichum</i>	hypothetical proteins:			
		CDO54370.1	3	1
		CDO55685.1	1	1
<i>candidum</i>	similar to <i>Saccharomyces cerevisiae</i> :			
	YLR167W RPS31	CDO51676.1	149	2
	YOR099W KTR1	CDO57638.1	1	1
<i>Pseudomicrostroma glucosiphilum</i>	thioredoxin H-type-like protein	XP_025348933.1	176	1
<i>Rhodotorula graminis</i>	uncharacterised protein RHOBADRAFT_66416	XP_018271446.1	6	1
<i>Trichosporon asahii</i>	hypothetical proteins:			
	A1Q1_00799	EJT52894.1	1	1
	A1Q1_02608	EJT48325.1	2	1
	A1Q1_03082	XP_014183647.1	1	1
<i>Yarrowia</i>	elongation factor Tu	QNP99396.1	5	1
	hypothetical protein YALI1_F15517g	AOW07013.1	2	1
<i>lipolytica</i>	YALIH222S03e22804g1_1	VBB85732.1	196	2

Table S16: List of potential antimicrobial secondary metabolites identified in the metabolomics analysis of permeate that depilated sheepskin. Sample, permeate after depilation. Control, sterilised permeate prior to incubation.

Name	Antimicrobial action	Relative abundance (%)	Abundance ratio (sample:control)	Reference
2-Hydroxycinnamic acid (o-Coumaric acid)	Active against <i>S. aureus</i> , <i>L. monocytogenes</i> , <i>Candida sp.</i> , and <i>E. coli</i>	0.78	825	Keman and Soyer (2019), Miyague <i>et al.</i> (2015), Martins <i>et al.</i> (2015), Parkar <i>et al.</i> (2008), Taofiq <i>et al.</i> (2017)
Indole-3-acrylic acid	Inhibits various Gram-negative bacteria	0.51	2529	Matsuda <i>et al.</i> (1990), Cadelis <i>et al.</i> (2020)
9-Oxo-10E,12E-octadecadienoic acid	Antifungal activity against <i>Phomopsis obscurans</i> (on strawberry plants)	0.42	8928	Bilikova <i>et al.</i> (2012), Cantrell <i>et al.</i> (2008)
5-Hydroxymethyl-2-furaldehyde	Active against <i>B. cereus</i> , <i>E. coli</i> , <i>Proteus sp.</i> , <i>Salmonella sp.</i> and <i>C. albicans</i>	0.26	5	Duru <i>et al.</i> (2012), Lee <i>et al.</i> (1995), Subramenium <i>et al.</i> (2018)
N-Acetylneuraminic acid	Inhibits <i>Helicobacter pylori</i>	0.05	44	Yamazaki (1993), Kim <i>et al.</i> (2016)
Coumarin (2H-1-benzopyran-2-one)	Active against <i>E. coli</i> , <i>P. aeruginosa</i> , and <i>S. aureus</i>	0.04	215	Abyshew <i>et al.</i> (2006), Behrami <i>et al.</i> (2011), Al-Majedy <i>et al.</i> (2017) Souza <i>et al.</i> (2005)
2-Hydroxycaproic acid (2-hydroxyhexanoic acid)	Destabilises and disintegrates the outer membrane of bacteria.	0.03	153	Alakomi <i>et al.</i> (2007)
Malic acid	Common additive for food preservation. Active against <i>Listeria</i> , <i>Salmonella</i> , and <i>Escherichia</i> species	0.02	124	Eswaranandam <i>et al.</i> (2006), Doyle (2019)
3-Hydroxybutyric acid	Polymer of this substance is antimicrobial	0.02	75	Ma <i>et al.</i> (2019)
2-Amino adipic acid	Precursor of beta-lactam antibiotics	0.02	19	Martin <i>et al.</i> (2010)
2-Aminoisobutyric acid (2-methylalanine)	Unusual amino acid used to make lantibiotics, also a common component of several antibiotic metabolites	0.02	248	Krause <i>et al.</i> (2006), Pushpanathan <i>et al.</i> (2013)
Didecyldimethylammonium	Inhibits <i>E. coli</i>	0.01	1	Li <i>et al.</i> (2015)
3-Phenyllactic acid	Broad antimicrobial spectrum. Active against a range of Gram-negative bacteria and fungi	0.01	46	Dieuleveus <i>et al.</i> (1998), Mu <i>et al.</i> (2012), Ohlira <i>et al.</i> (2004), Prema <i>et al.</i> (2010)
Hippuric acid	Potentially active against <i>E. coli</i>	0.007	196	Fellers <i>et al.</i> (1932), Jensen <i>et al.</i> (2017)
Azelaic acid	Active against various skin bacteria, including <i>Propionibacterium sp.</i> , <i>Bacillus</i> , <i>Enterococcus</i> , <i>Escherichia</i> , <i>S. aureus</i> , and <i>Acinetobacter</i> species	0.007	10	Blaskovich <i>et al.</i> (2019), Bojar <i>et al.</i> (1991)
Stearic acid	Active against <i>Mycobacteria</i> and <i>Streptococcus sp.</i> and <i>C. albicans</i>	0.003	25	Dantas das Silva <i>et al.</i> (2003), Choi <i>et al.</i> (2013)
Citric acid	Commonly added into food products for preservation. Inhibits <i>Salmonella</i> and <i>E. coli</i> species	0.002	2	Doyle (2019)
Phenylacetic acid	Active against <i>S. aureus</i> , <i>Micrococcus</i> , <i>Bacillus</i> , <i>Escherichia</i> , and <i>Pseudomonas sp.</i>	0.002	24	Kim <i>et al.</i> (2004)

The relative abundance of each compound was calculated as the percentage fraction of the chromatogram area over the sum of all.

The abundance ratio was calculated using permeate solution as baseline.

6 | Final conclusions and future directions

6.1 Overall conclusions and future direction

This investigation, undertaken to understand the molecular mechanism behind the ability of milk and milk by-products to both preserve and depilate sheepskin, lays the foundations for a shift away from the use of environmentally hazardous chemicals by the leather industry towards a more sustainable process.

We showed in this study, that leather made from sheepskin depilated using permeate had the same properties as that produced using the traditional beamhouse method and if anything had a better appearance. In contrast to the leather made the traditional way, no sodium sulfide or strong alkalis were used, and much less water was required during processing. Furthermore, skins could be preserved in the permeate solution for up to seven days, while depilation was occurring, reducing the use of salt and water. This process was tested on multiple pieces of sheepskin of different size (up to one quarter of a pelt) over three years, and regardless of biological differences or size, depilation was always successful. Another advantage to using this process is that after depilation, four pre-tanning steps, liming, deliming, bating and pickling could be skipped, and the skins taken straight to degreasing and tan.

These studies have resulted in partial explanations of some of the observations made during these experiments and provided some understanding of the complex mechanisms involved.

Firstly, it was established early on that restricting the carbon source of the skin microbiome to lactose was initially responsible for restricting the growth of many organisms that rapidly multiplied in water to cause putrefaction. This also promoted the growth of lactic acid bacteria resulting in a drop in pH that further controlled the species able to grow. On top of this, the complex balancing of the microbial community as shown by the metagenomics results, also played a part. Time restrictions did not allow a more thorough investigation of these changes, as to understand the process completely, an in-depth study of the viable organisms at each stages of the depilation is required. This is possibly something that could be achieved using flow cytometry.

Another factor in the preservation observed with this process was the production of metabolites by the microbial population during depilation. A preliminary metabolomic study produced some tantalising results, showing the antimicrobial

substances, such as indol-3-acrylic acid, a substance active against a number of gram-negative bacteria had an abundance more than 2000-fold higher than the control. Time did not allow this study to be done with the required number of replicates to make the findings statistically reliable, thus to confirm them, another study should be undertaken to optimise the extraction and repeat the analysis on a suitable number of biological and technical replicates.

Secondly, the results from the biochemical analyses showed why the skin had such a good appearance and could be converted into fine leather. However, a major unanswered question is what enzyme or enzymes are implementing the depilation and why is there an apparent protection of the molecules making up the basement membrane and the junction between it and the dermis? Unfortunately time did not allow an investigation into the identification of potential enzymes but strong circumstantial evidence suggests that they are either secreted by one or more of the microorganisms identified in these studies, or come from lysed cells. The fact that the wool was removed so cleanly from the follicle suggests that the activity is due to enzymes with relatively specific substrates. Once a more thorough analysis of the live/dead cell population has been made, it should be possible to incubate sterilised (gamma radiation) pieces of skin with combinations of the viable species identified to try and find those responsible for the activities observed. It should then be possible to isolate enzymes in the media and to identify them. Such a study proved to be beyond the scope of this project.

Although the tests carried out indicated there were no significant differences between the leathers produced using both these processes, there were minor differences between the skins depilated with permeate, and pickled skin produced by the beamhouse process, with permeate-depilated skin having a slightly better tear strength. TEM gives a very small snapshot of the collagen structure of skin. A better technique to obtain a picture of the organisation and architecture of the collagen fibres in skin is to use small angle x-ray scattering (SAXS) as shown by Naffa *et al.*, (2017)¹. A SAXS study comparing skins processed using both these processes would show if the small differences in the tear strength of the pre-tanned skins observed in this work have a structural basis, which disappears on tanning.

Finally, SEM showed the presence of bacteria on the skins depilated with permeate. Tests need to be done to see if these cells are viable, if they can be identified, and if they remain viable after the skin is tanned.

Whether or not this process is taken on board by the industry remains to be seen. One problem is the availability of whey or permeate. Fonterra processes most of its whey and further fractionates it into a lactose-rich permeate and a protein-rich retentate. The permeate is used for the production of lactose and is added back to milk to standardise protein content for the production of milk powder, or used to make lactose that is used as a filler in tablets by the pharmaceutical industry. The retentate is used for the production of whey protein that is used for the food and beverage industries. Therefore, the use of both these products may not be cost effective. Smaller dairy companies may have to get rid of whey or permeate, but whether they would be able to provide enough volume to the leather industry is not known. The provision of vats large enough to transport the skins should not be a problem, but in order to scale the process up research on the optimum volume of whey or permeate to skin would need to be assessed as well as the efficacy of the process on stacked skins.

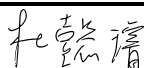
In conclusion, this preliminary study has paved the way for the development of a depilation process that is kind to the environment. More research is needed to investigate its potential use with other animal skins. It is possible that further work based on this study may be able to produce a cocktail of enzymes that does indeed 'depilate without damage'.

6.2 References

- [1] R. Naffa. *Understanding the molecular basis of the strength differences in skins used in leather manufacture : a dissertation presented in partial fulfillment of the requirements for the degree of Doctor of Philosophy at Massey University, Palmerston North, New Zealand*. Thesis, Massey University, 2017. URL <http://hdl.handle.net/10179/13154>.

STATEMENT OF CONTRIBUTION DOCTORATE WITH PUBLICATIONS/MANUSCRIPTS

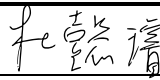
We, the candidate and the candidate's Primary Supervisor, certify that all co-authors have consented to their work being included in the thesis and they have accepted the candidate's contribution as indicated below in the *Statement of Originality*.

Name of candidate:	Yi-Hsuan Tu
Name/title of Primary Supervisor:	Associate Professor Gill Norris
In which chapter is the manuscript /published work: Chapter 3	
Please select one of the following three options:	
<input type="radio"/> The manuscript/published work is published or in press <ul style="list-style-type: none"> • Please provide the full reference of the Research Output: 	
<input type="radio"/> The manuscript is currently under review for publication – please indicate: <ul style="list-style-type: none"> • The name of the journal: • The percentage of the manuscript/published work that was contributed by the candidate: 90% • Describe the contribution that the candidate has made to the manuscript/published work: Conducted all experimental work and wrote the manuscript. 	
<input checked="" type="radio"/> It is intended that the manuscript will be published, but it has not yet been submitted to a journal	
Candidate's Signature:	
Date:	11/06/2021
Primary Supervisor's Signature:	Gill Norris <small>Digitally signed by Gill Norris Date: 2021.06.11 16:44:02 +12'00'</small>
Date:	11/06/2021

This form should appear at the end of each thesis chapter/section/appendix submitted as a manuscript/ publication or collected as an appendix at the end of the thesis.

STATEMENT OF CONTRIBUTION DOCTORATE WITH PUBLICATIONS/MANUSCRIPTS

We, the candidate and the candidate's Primary Supervisor, certify that all co-authors have consented to their work being included in the thesis and they have accepted the candidate's contribution as indicated below in the *Statement of Originality*.

Name of candidate:	Yi-Hsuan Tu
Name/title of Primary Supervisor:	Associate Professor Gill Norris
In which chapter is the manuscript /published work:	Chapter 4
<p>Please select one of the following three options:</p> <p><input type="radio"/> The manuscript/published work is published or in press</p> <ul style="list-style-type: none"> • Please provide the full reference of the Research Output: <p><input type="radio"/> The manuscript is currently under review for publication – please indicate:</p> <ul style="list-style-type: none"> • The name of the journal: • The percentage of the manuscript/published work that was contributed by the candidate: 90% • Describe the contribution that the candidate has made to the manuscript/published work: Conducted all experimental work and wrote the manuscript. <p><input checked="" type="radio"/> It is intended that the manuscript will be published, but it has not yet been submitted to a journal</p>	
Candidate's Signature:	
Date:	11/06/2021
Primary Supervisor's Signature:	Gill Norris <small>Digitally signed by Gill Norris Date: 2021.06.11 16:45:59 +12'00'</small>
Date:	11/06/2021

This form should appear at the end of each thesis chapter/section/appendix submitted as a manuscript/ publication or collected as an appendix at the end of the thesis.

